Assessment of Natural Ventilation Using Whole Building Simulation Methodological Framework

Frederico Martins de Barros

A Thesis

in the

Building Science Graduate Program

Presented in Partial Fulfillment of the Requirements for the

Degree of Master of Applied Science in Building Engineering/Building Science

at the

British Columbia Institute of Technology

Burnaby, British Columbia, Canada

September, 2017

BRITISH COLUMBIA INSTITUTE OF TECHNOLOGY

Building Science Graduate Program

This is to certify that the thesis prepared

By: Frederico Cezar Gonçalves Martins de Barros Student Number:

Entitled: Assessment of Natural Ventilation Using Whole Building Simulation – Challenges and Limitations

And submitted in partial fulfillment of the requirement for the degree of:

Master of Applied Science in Building Engineering/Building Science

Complies with the regulations of the Institute and meets the accepted standards with respect to originality and quality.

Signed by the final Examining Committee:

Dr. Fitsum Tariku, Chair

Dr. Cheney Chen, external to program

Mr. Bo Li, Examiner

Dr. Rodrigo Mora, Supervisor

Approved by:

Graduate Program Director

ABSTRACT

Natural ventilation is a passive alternative to provide both indoor air quality and thermal comfort for the building's occupants with low energy use. But at the same time, it is challenging for the building designers to implement natural ventilation strategies due to its complexity and highly dynamic behaviour, especially when it is compared with the mechanically ventilated buildings. Nevertheless, the use of naturally ventilated buildings is increasing along with the use of passive strategies, but depending on the complexity of the project, the designer still use rules of thumb for the implementation of natural ventilation strategies instead of a more comprehensive simulation-based approach.

In theory, whole building simulation models (WBSM) are becoming viable tools to support natural ventilation design, particularly in the early stages of the project where the impacts of measures to implement a natural ventilation strategy are magnified. However, the only "evidence" of such level of support comes from individual case-study projects. Nevertheless, there is a lack of validation through measurement of the effectiveness of natural ventilation design in real buildings. This research will shed light into the "inner-workings" of natural ventilation models in WBSM to answer fundamental questions such as the following: How is wind data processed? How are envelope openings characterized? How are internal openings modelled? When and how is air buoyancy modelled in spaces? How are the coupled thermal and fluid mass transfers modelled to reflect the dynamic thermal responses of constructions and airflows?

Therefore, a methodological framework is developed in order to provide the necessary knowledge for natural ventilation assessment. This framework is based on simulation (WBSM) and field testing. The proposed framework is tested in an existing landmark building in Vancouver. A WBSM of that building is developed, calibrated, and used to analyze how different factors that compose an integrated natural ventilation strategy (like the building shape, window shading, thermal mass, indoor spaces functionality and connectivity, and local climate) influence the thermal comfort of its occupants.

Keywords: Natural ventilation, thermal comfort, adaptive model, whole building simulation models (WBSM).

AKNOWLEDGEMENTS

First, I would like to thank my supervisor, Dr. Rodrigo Mora, for the tremendous support throughout my time at BCIT. Without his supervision and guidance the thesis would not be possible. I will take his example and lessons with me. I also want to thank Mr. Ron Kato for making this research possible by enabling access to the building and its documentation, as well as by giving me feedback and guidance from the very early stages of the study.

I would like to acknowledge Mr. Chris Flood, for the continuous support in creating, developing, updating and improving the IES-VE model, and for his patience and guidance given; his mentoring and supervision made the thesis possible.

Finally, I want to thank both the supervisory committee and the examining committee for the valuable comments that made this thesis better, and the Building Science department, Dr. Fitsum Tariku, Ellen Scobie, the whole Building Science staff, my colleague and friends, and in special for my family and girlfriend, for all the support given even with the distance.

TABLE OF CONTENTS

LIST OF TABLES

Table **Page**

LIST OF FIGURES

Figures **Page**

1. INTRODUCTION

Human activity is directly connected with different types of environmental damages. But nowadays, it has become well accepted that human activity it is also related to global warming. That knowledge acquired in recent years increases the environmental awareness around different subjects such as the use fossil fuels, greenhouse gases emission and sustainable development. Therefore, efforts have been made to decrease worldwide energy consumption in all energy sectors, such as transportation, commercial, residential, and industrial.

The International Energy Agency (2013) claims that buildings represent the largest energy-consuming sector in the economy, with over one-third of all final energy and half of global electricity consumed by this particular sector. As a result, they are responsible for approximately one-third of global carbon emissions. With an expected population increase of 2.5 billion people by 2050, and given improvements in economic development and living standards, energy use in the buildings sector is set to rise sharply, placing additional pressure on the energy system. Perez-Lombard *et al*. (2008) point out that residential energy subsectors include domestic hot water, lighting, food preparation, appliances, and others, but heating, ventilation, and air conditioning take up substantially more energy than any other subsector.

According to Price *et al*. (2005), global consumption of primary energy to provide heating, cooling, lighting and other building related energy services grew from 86 exajoules in 1971 to 165 exajoules in 2002. This is an average annual growth rate of 2.2% per year. Energy demand for commercial buildings, during the same period, grew about 50% faster than for residential buildings. The final global energy consumption by sector for the year of 2010 is represented by the figure 1.1. In the graph it is also presented the origin of the energy used in the building sector.

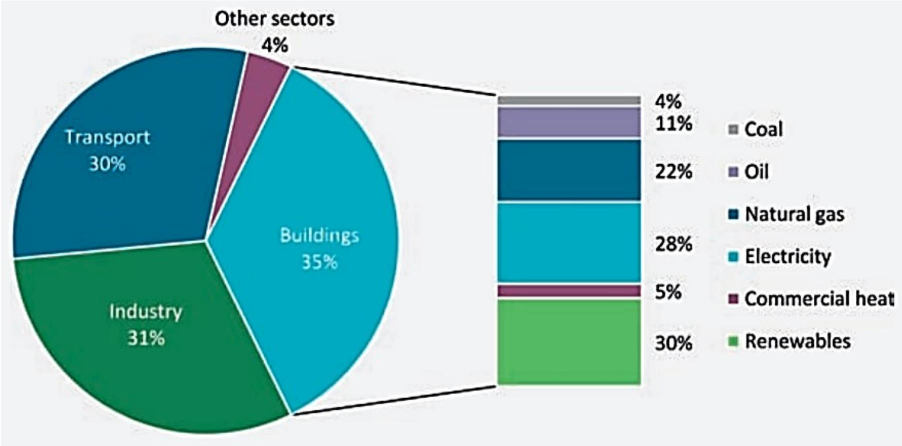

Figure 1.1 – Final energy consumption by sectors, 2010 (International Energy Agency, 2013)

In Canada, not differing from the world-wide average, the energy consumption used for residential and commercial is around 31% of total energy consumed. Figure 1.2 presents the energy consumption trends from 1990 to 2009 published by NRC (2015).

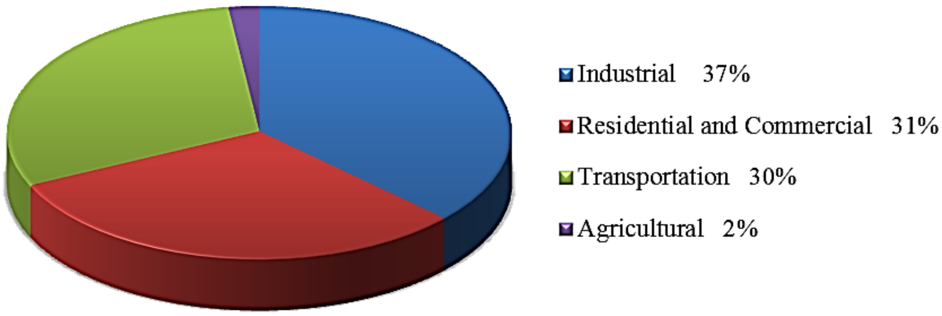

Figure 1.2 – Canadian energy consumption trends from 1990 to 2009 (NRC, 2015)

The construction sector is assimilating a kind of environmental consciousness which is leading to more efficient and sustainable buildings, which has raised interest on the use of natural ventilation. The potential benefits of natural ventilation are in terms of lower energy consumption, thermal comfort, indoor air quality and operating costs. In recent years, the development of natural ventilation technology was done especially in Europe. But there is still a lot work needed before this potential improvement can be realized in North America. Natural ventilation is slowing gaining acceptance as a viable strategy to deliver satisfactory indoor environmental quality and cooling for the spaces. However, the added complexity of having to consider uncertainties from natural forces and interactions with human occupancies still leads building stakeholders to prefer rely on mechanical ventilation.

Nevertheless, the use of naturally ventilated buildings are increasing but depending on the complexity of the project the designers still use rules of thumb in the implementation of natural ventilation strategy instead of a more comprehensive systematic strategy. The NatVent project (Kukadia, 1998) identified the lack of experience and know-how of the main stakeholders (such as architects, engineering consultant and building developers) as the main barrier to the use of natural ventilation. Moreover, they concluded that design tools and simulation codes were missing.

Nowadays, with modern energy software, whole building simulation model (WBSM) emerges as a viable tool to support natural ventilation design, particularly in the early stages of the project. However, there is a lack of validation through measurement of the effectiveness of natural ventilation design in real buildings (Ellis, 2016). This research will shed light into the "inner-workings" of natural ventilation models in WBSM. Whole Building Simulation Models (WBSM), also called Building Energy Models (BEM), are physics-based computer representations of buildings describing relevant abstractions of the geometry, properties, and behaviours of interrelated building systems and components through mathematical models of underlying physics heat, air, and moisture transport processes. WBSMs are used to simulate dynamic energy flows in buildings and estimate whole building performance under realistic dynamic boundary conditions defined by the local climate, occupancy, and processes. Until simulation models are validated with real life data, building simulations cannot give absolute answers about the performance of a building.

The use of WBSM is becoming mainstream to support design decisions. Several commercial software applications are available and in use by the industry, notably: eQUEST (2016), TRNSYS (2015), IES-VE (2016), DesignBuilder (2016), and OpenStudio (2016). The latter two tools are interfaces for the EnergyPlus energy modelling engine. All the applications above are well established, and their models have been extensively validated. However, the reliability of the results depend on two main factors: 1) the adequacy of the models embedded in the tools to accurately represent the intended building application, and 2) the accuracy of the input parameters and coefficients used by those models. Simulating building energy flows under natural ventilation operation involves increased complexities compared to pure mechanical operation. This research has chosen IES-VE software in order to achieve its goals. Several reasons led to this decision, the first is that this particular software is well-established in Europe to model natural ventilation and other passive strategies. In addition to that, a previous energy model of the case study building using IES-VE was given to the author of this work. Considering the software features regarding natural ventilation, its reputation along the literature on dealing with passive strategies, and the time consuming process to develop from the ground the building complex geometry, the IES-VE seems the best choice in terms of WBSM for this research.

Alongside with the inclusion of the WBSM as viable tool evaluate natural ventilation. It is found a lack of systematically approach to natural ventilation assessment using these simulation methods in association with field testing. Therefore, as a final outcome, this study aims to provide a methodological framework to natural ventilation assessment. The framework is composed by simulation, WBSM, field testing, and calibration and validation of the WBSM. Finally, the proposed framework is applied to case study building.

2. THEORETICAL BACKGROUND

2.1 Natural Ventilation

Natural ventilation is a strategy to supply and remove air through the building openings by natural means, without the use of fan or other mechanical system. The airflow is caused by pressure differences between the building and its surrounding, providing ventilation and cooling for the spaces. In a few climates, cooling strategies might also include pre-cooling building thermal mass by night-time ventilation to mitigate anticipated uncomfortably warm conditions during the coming day. But the main drawback to natural ventilation is that mechanically ventilated buildings are significantly easier to design, control and verify. Mechanical ventilation is meant to typically overpower any natural or human forces that may create uncertainties and performance unreliability. According to Schulze and Eicker (2013), the two main functions of natural ventilation are to provide fresh air to improve the indoor air quality without the use of energy and to provide thermal comfort by increased daytime air speed and high night ventilation rates. But according to Emmerich *et al.* (2001) natural ventilation may be used for:

- **Air quality control**: to control building air quality, by diluting internally-generated air contaminants with cleaner outdoor air;
- **Direct advective cooling**: to directly cool the interior of the building by replacing or diluting warm indoor air with cooler outdoor air when conditions are favourable;
- **Direct personal cooling**: to directly cool the building's occupants by directing cool outdoor air over building occupants at sufficient velocity to enhance convective transport of heat and moisture from the occupants;
- **Indirect night cooling**: to indirectly cool building interiors by pre-cooling thermally massive components of the building fabric or a thermal storage system with cool night-time outdoor air.

Schulze and Eicker (2013) concluded that the adaptive thermal comfort could be achieved by using natural ventilation but is strongly depended on the room thermal loads, which is a function of the building's heat losses and gains, sun shading performance, internal loads and etc. The higher the loads, the greater the needs for effective opening area to improve summer comfort in moderate climates. According to Atkinson *et al*. (2009), simulations show that a well-deigned natural system saves considerable amount energy used for cooling down the spaces, but it also reduces the amount of electrical energy that would be used in mechanical ventilation (fans). The natural ventilation airflow is created by natural pressure differences that occur along the building. The two main driving forces causing this pressure deferential are temperature differences and wind forces. In nearly all instances these forces work simultaneously, but their interaction might not always be positive in delivering effective natural ventilation airflow.

2.1.1 Thermal Buoyancy and Stack Pressure

Thermal buoyancy and stack pressure are intrinsically related but they are essential different. Thermal buoyancy is the upward or downward flow of an air mass caused by the heating or cooling of its molecules which change its properties. For gases, the density and the volume expansion coefficient are inversely proportional to the temperature: as temperature increases, density and volumetric expansion decrease. Similarly, the dynamic viscosity and the thermal conductivity are directly proportional to the temperature to the power of 0.65 ($T^{0.65}$). As temperature increases, so do the dynamic viscosity and thermal conductivity of the fluid, but the relation is not linear. Therefore, the airflow is intimately coupled to the temperature field (Etheridge and Sandberg, 1996). Stack pressure, on the other hand, is driven by the thermal buoyancy. It is caused by the hydrostatic pressure difference created between air masses in two different environments, normally indoors and outdoors. Stack effect leads to buoyancy (cold air enters from the bottom and warm air leaves from the top), and buoyancy leads to stack effect (as buoyant air leaves from the top, it drives more cold air into the space). However, when it comes to simulation, both phenomena are modelled differently.

Stack pressure is proportional to the difference between internal and external temperature and to the distance from the neutral pressure level. Neutral pressure level is the where the pressure difference is zero and therefore there is no air motion between indoor and outdoor environment. With the pressure difference, exchange of air between inside and outside happens through one or more openings in the outer wall. In contrast to the purely wind-driven cases, the presence of these buoyancy forces leads to temperature variations within the space. This stratification may lead to quite different flow configurations, but the natural tendency is for hot air to rise and accumulate toward the upper part of the space. The pressure at a single point at level H above the reference height (floor level) can be expressed by equation 2.1.

$$P = P_0 - \rho_0 \cdot g \cdot H \qquad \text{Equation 2.1}$$

where,

P_0: atmospheric pressure at $H=0$ [Pa];

ρ_0: air density at $H=0$ and at T temperature [kg/m³];

g: gravity acceleration [m/s²];

H: height [m].

If equation 2.1 is applied to the internal (i) and external (e) air, the equations 2.2 and 2.3 are derived. In these expressions the temperature distribution is regarded as uniform and the internal air density (ρ_i) and external air density (ρ_e) are constant.

$$P_i = P_{i,0} - \rho_i \cdot g \cdot H \qquad \text{Equation 2.2}$$

$$P_e = P_{e,0} - \rho_e \cdot g \cdot H \qquad \text{Equation 2.3}$$

where,

P_i: internal pressure [Pa];

P_e: external pressure [Pa];

$P_{i,0}$: pressure difference between internal and atmospheric pressure[Pa];

$P_{e,0}$: pressure difference between internal and atmospheric pressure[Pa].

Thereby, the pressure difference (ΔP) between internal and external air can then be found by the equation 2.4.

$$\Delta P = P_{e,0} - P_{i,0} - (\rho_e - \rho_i) \cdot g \cdot H \qquad \text{Equation 2.4}$$

At the neutral plane the pressure difference (ΔP) is zero. If internal temperature (T_i) is lower than external temperature (T_e), the pressures below the neutral plane are negative and will allow the air to flow into the building. Above the neutral plane the opposite happens, there is positive pressure across the envelope and the airflow tends to goes towards outside. Thus, the position of the opening compared to the neutral plane in the building is which determines whether the air enters or exits the building at a certain height (see figure 2.1).

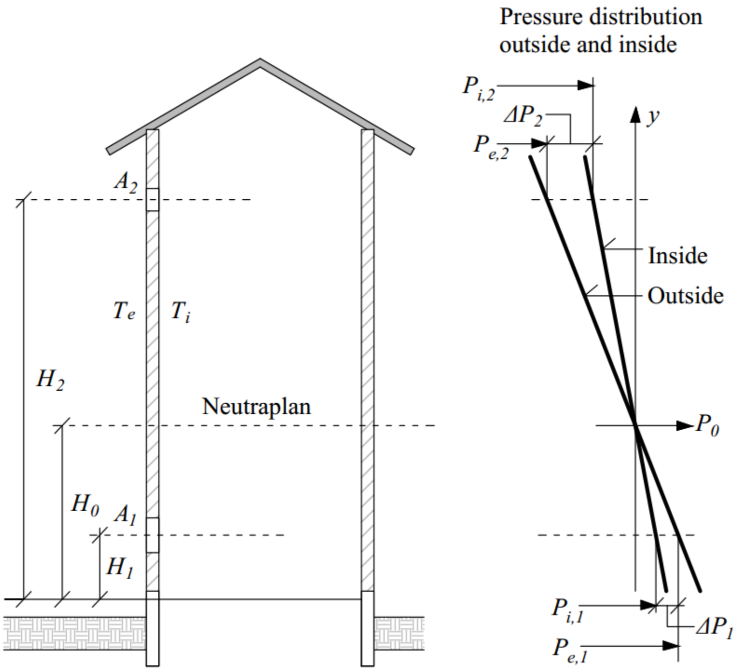

Figure 2.1 – Pressure difference around the neutral plane in a building ventilated considering only thermal buoyancy

At the neutral plane, where $H=H_0$ where $\Delta P=0$, the equation 2.4 turns into equation 2.5.

$$P_{e,0} - P_{i,0} = (\rho_e - \rho_i) \cdot g \cdot H_0 \qquad \text{Equation 2.5}$$

where,

ρ_e: exterior air density at external temperature (T_e) [kg/m³];

ρ_i: interior air density at internal temperature (T_i) [kg/m³];

Using the equation of state, equation 2.6 can be found.

$$\frac{\rho_e - \rho_i}{\rho_i} \cong \frac{T_i - T_e}{T_e} \therefore \frac{\rho_e - \rho_i}{\rho_i} \cong \frac{T_i - T_e}{T_i} \qquad \text{Equation 2.6}$$

Applying equation 2.6 into 2.5, equation 2.7 is obtained.

$$P_{e,0} - P_{i,0} = \rho_i \cdot g \cdot H_0 \cdot \frac{T_i - T_e}{T_e} \qquad \text{Equation 2.7}$$

Likewise, the pressure in the height H_1 (where $\Delta P \neq 0$) is described by the following equation 2.8.

$$\Delta P_{H=H_1} = P_{e,0} - P_{i,0} - \rho_i \cdot g \cdot H_1 \cdot \frac{T_i - T_e}{T_e} \qquad \text{Equation 2.8}$$

If equation 2.7 is inserted into equation 2.8 the pressure difference in H_1 can be expressed using only the internal and external temperatures, gravitational acceleration and density of air.

$$\begin{aligned} \Delta P_{H=H_1} &= \rho_i \cdot g \cdot H_0 \cdot \frac{T_i - T_e}{T_e} - \rho_i \cdot g \cdot H_1 \cdot \frac{T_i - T_e}{T_e} \\ &= \rho_i \cdot g \cdot (H_0 - H_1) \cdot \frac{T_i - T_e}{T_e} \end{aligned} \qquad \text{Equation 2.9}$$

From equation 2.9 it is observed that pressure is increased with the height difference or with the temperature difference. In absence of other driving forces, the neutral pressure level position depends on leakage area distribution and interior building layout.

2.1.2 Wind Pressure

A major driving force in natural ventilation is the wind; its nature is highly dynamic and uncertain. The wind on the building surfaces creates, simplistically, overpressure (positive pressure) on windward surfaces and depression (negative pressure) on leeward surfaces. But the actual wind pressure distribution across the building depends on the wind incidence angle, dimensions and slope of building surface, and the presence of obstructions in the surroundings. The wind pressure over the building envelope drives the airflow through openings and cracks. Figure 2.2 illustrate the pressure induced by the wind across the building.

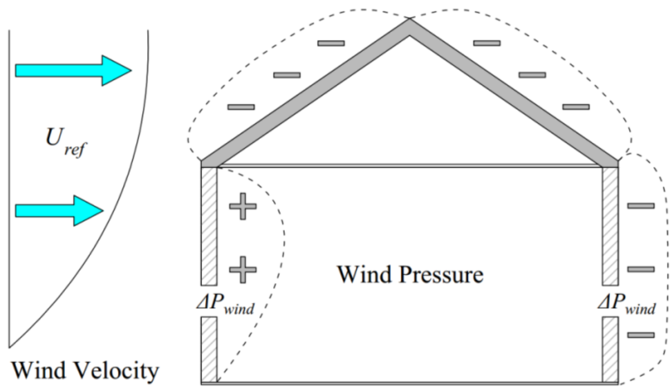

Figure 2.2 – Wind pressure across the building

The wind pressure is represented by equation 2.10.

$$P_{wind} = C_p \cdot \frac{1}{2} \cdot \rho_e \cdot U_{ref}^2 \qquad \text{Equation 2.10}$$

where,

P_{wind}: difference of pressure due to wind effect [Pa];

C_p: wind pressure coefficient;

ρ_e: outdoor air density [kg/m³];

U_{ref}: wind speed at reference point, usually the height of the building's roof [m/s].

The pressure difference between internal (P_i) and external air due to wind is given by equation 2.11 and 2.12.

$$\Delta P_{wind} = C_p \cdot \frac{1}{2} \cdot \rho_e \cdot U_{ref}^2 - P_i \qquad \text{Equation 2.11}$$

$$\Delta P_{wind} = (C_{p,windward} - C_{p,leeward}) \cdot \frac{1}{2} \cdot \rho_e \cdot U_{ref}^2 = \Delta C_p \cdot \frac{1}{2} \cdot \rho_e \cdot U_{ref}^2 \qquad \text{Equation 2.12}$$

The wind pressure coefficient (C_p) is influenced by a wide range of parameters, including building geometry, façade detailing, position of openings on the façade, degree of exposure/sheltering, and wind speed and direction. It is hard to consider the full complexity of the pressure coefficient variation, and programs like building energy simulation (BES) or airflow network (AFN) generally incorporate this factor in a simplified way. Wind pressure coefficients may be obtained by a variety of means, including *in situ* measurements, Computational Fluid Dynamics (CFD) studies and wind tunnel experiments. Figure 2.3 illustrates an example of C_p values on a building surface.

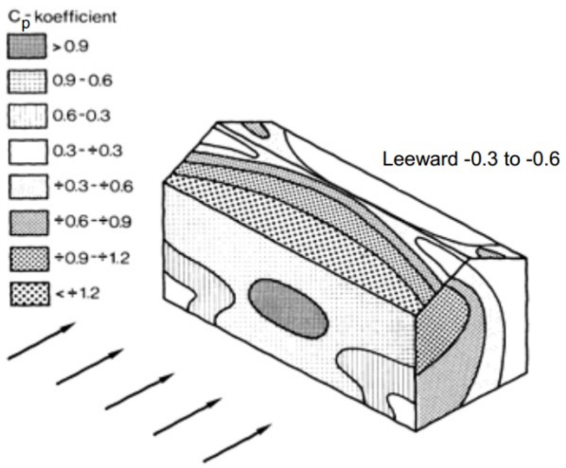

Figure 2.3 – Example of C_p values on a building (Larsen, 2006)

Knoll *et al.* (1996) created the *CpGenerator*, which is a web-based simulation program, developed by TNO, based on systematic wind tunnel tests (Phaff, 1977 and 1979), and on published measured data. The program provides C_p data for a wide range of isolated and non-isolated block-shaped buildings with flat roof, and for either high-rise or low-rise buildings. For low-rise buildings, a surface-averaged pressure coefficient (C_p) is proposed by Swami and Chandra (1988) and Walton (1982) illustrated by figure 2.4. According to the models, the coefficient depends on the wind angle of incidence (θ) and the building geometry characteristic. The building's aspect ratio is represented by the letter S, which is a result of the ratio between the buildings outside surfaces (L_1 and L_2).

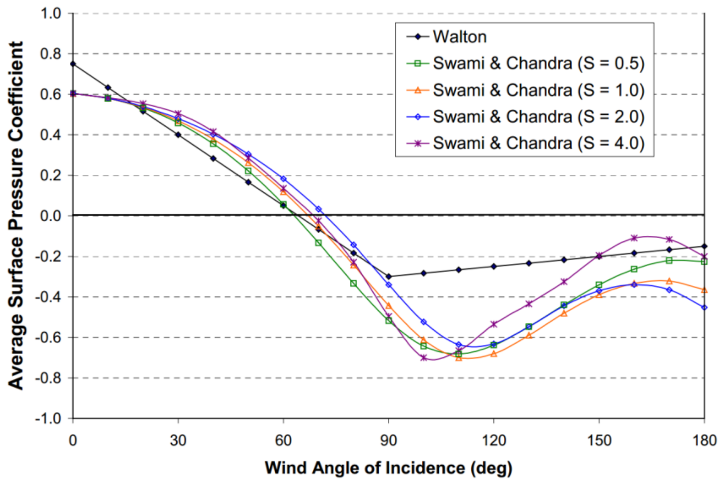

Figure 2.4 – Surface pressure coefficient as a function of wind incident angle for the Walton model and the Swami and Chandra model for side ratios $S=L_1/L_2$

The wind speed also needs to be estimated. Correction factors relate the wind speed recorded by the weather station to the local wind speed, depending on type of terrain and height where the speed is estimated. Wind velocity is usually taken from meteorological data, which is often measured in large open spaces and a recalculation is therefore necessary to find the level of the wind velocity (*e.g.* in the middle of an urban area). The calculation of the velocity profile is made by the equation 2.13 and table 2.1.

$$U_h = U_{10} \cdot k \cdot h^{\alpha} \qquad \text{Equation 2.13}$$

where,

U_{10}: wind speeds at 10 meter of height [m/s];

k: terrain correction factor;

α: terrain correction factor;

h: height of the wind speed [m].

The parameters k and α depend on the terrain as the following table 2.1.

Table 2.1 – Wind speed correction factors related to the terrain

Location	k	α
Open, Flat terrain	0.68	0.17
Terrain with scattered growth	0.52	0.20
Suburban area	0.35	0.25
Urban area	0.21	0.33

Figure 2.5 illustrate the variation of the wind speeds due to roughness of the terrain.

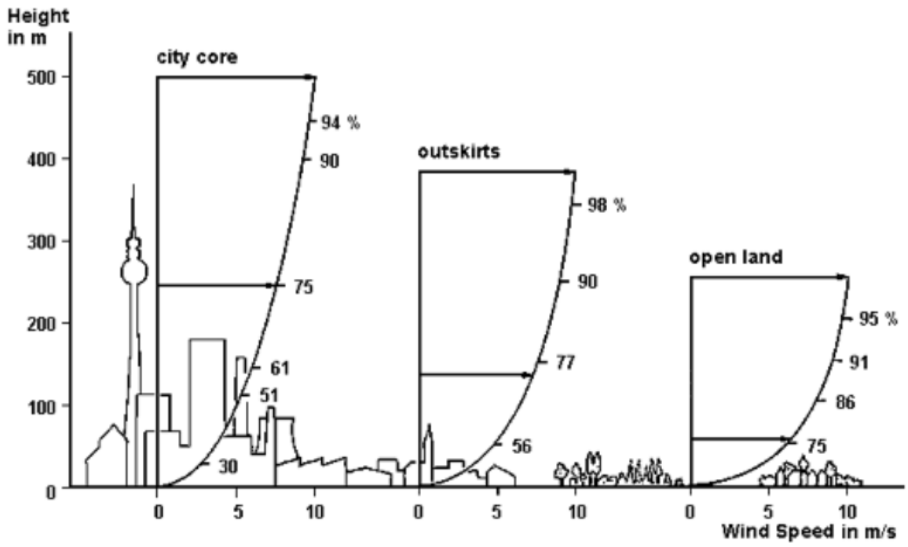

Figure 2.5 – Decrease in wind speed as influenced by varieties of terrain roughness (Baumbach, 1990)

2.1.3 Combination of Stack Effect and Wind Pressure

In real applications, building airflows are driven from a combination of wind and thermal effects. In nearly all instances these forces work in parallel, with the resulting flow being the combination of the two. This combination depends on the weather conditions, building operations, wind forces and etc. The wind could be prevalent against buoyancy effects and vice versa. The total pressure across an opening (*ΔP*), shown by equation 2.14, is found by the addition of the pressure created by buoyancy (equation 2.9) and wind (equation 2.11).

$$\Delta P = \Delta P_{wind} + \Delta P_{bouyancy}$$

$$= \left(C_p \cdot \frac{1}{2} \cdot \rho_e \cdot U_{ref}^2 - P_i\right) + \left(\rho_e \cdot g \cdot (H_0 - H_1) \cdot \frac{T_i - T_e}{T_e}\right) \quad \text{Equation 2.14}$$

The wind effect might not necessarily lead to increased ventilation in association with buoyancy forces. Actually, this is may be an undesirable feature in many situations, as the objective of the design is to provide an adequate level of ventilation and cooling over a wide range of wind and stack-driven conditions.

2.1.4 Strategies for Natural Ventilation in Buildings

Using the driving forces described earlier, the architects and building's designers use a combination of strategies to achieve an effective and desirable natural ventilation performance. These strategies aim to maximize and/or control the dynamic effects of natural ventilation driving forces and at the same time provide the proper thermal comfort and ventilation for the building. The strategies use a combination of buildings characteristics, such as: building orientation, building geometry, openings' size and positions, proper shading system, thermal mass to moderate indoor temperatures by smoothing dynamic climate effects, connectivity and geometry of spaces, an etc. This section divides these strategies in:

- Wind-driven ventilation;
- Buoyance-driven and stack ventilation;
- Single-sided ventilation;
- Night ventilation.

Many buildings employ different technologies using the basic natural ventilation driving forces, creating different technologies to support natural ventilation strategies. Mora (2016) numbers these strategies in table 2.2, enumerating the main driving forces for each one. Some of the strategies will not be explored during this section.

Table 2.2 – Main natural ventilation strategies (Mora, 2016)

Strategy	Main Driving Force
Central Atrium	1) Thermal buoyancy, 2) Wind
Solar Chimney	1) Thermal buoyancy, 2) Wind
Buffer spaces*	1) Thermal buoyancy
Cross-ventilation	1) Wind
Single-sided (least effective)	1) Momentum, instantaneous, turbulence

* Solar wall, double-skin façade, sun-space and others.

2.1.4.1 Wind-Driven Ventilation

The main challenge of wind-driven natural ventilation strategies is that wind tends to be unpredictable. Thereby, to use that strategy the building designers need to take into consideration the location of the building and the immediate surroundings. In case of buildings surrounded by other structures, the characteristics of the wind may be altered depending on the wind direction and position of adjacent structures; this might reduce or enhance the airflow potential and building's surface pressures created by the wind.

The wind-driven cross-ventilation occurs by designing ventilation openings on opposite sides of the building. There is also a need to make ventilation openings across the building's interior, providing a path for the airflow through the building. Figure 2.6 illustrates a schematic cross-ventilation strategy in a multi-room building. According to Emmerich *et al.* (2001), the wind pressure difference across the outlet and inlet openings must be design to ensure a sufficient ventilation flow to effectively remove heat and pollutants from the spaces.

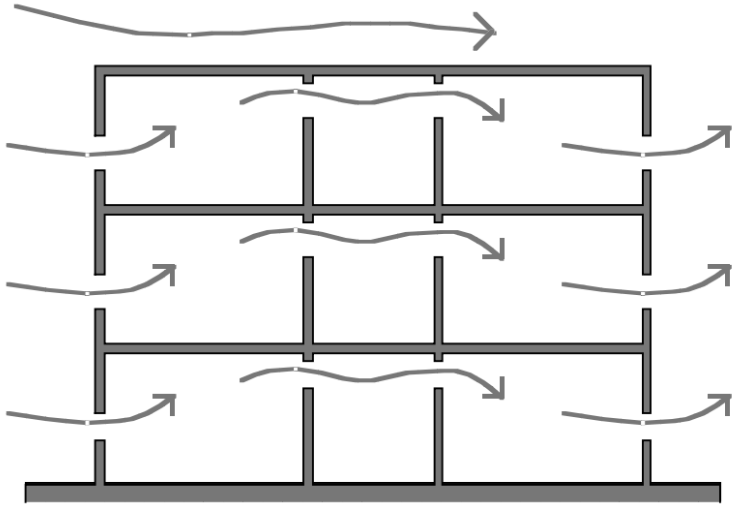

Figure 2.6 – Schematic of wind-driven ventilation strategy (Emmerich *et al.*, 2001)

According to Larsen (2006), in cases of cross-ventilation the expressions are rather well defined, but the difficulty lies within the definition of the discharge coefficient that describes the characteristics of the opening, since it fluctuate depending on the incidence angle of the wind.

2.1.4.2 Buoyance-driven and Stack Ventilation

Buoyancy-driven and stack ventilation relies on air density differences. Buoyancy-driven is a strategy that is often included in natural ventilation designs when considering central atria, a solar chimney or buffer spaces (table 2.2). Other spaces where buoyancy effects are important are large spaces such as: auditoriums or multi-function spaces. The stack ventilation, on the other hand, uses cooler outdoor air in lower ventilation openings and exhaust warmer indoor air by upper openings. The connection between spaces it is also important to guarantee the airflow through the building. Figure 2.7 pictures a schematic of stack ventilation for a multi-room building. An atrium is usually used to generate sufficient buoyancy forces to achieve an acceptable airflow.

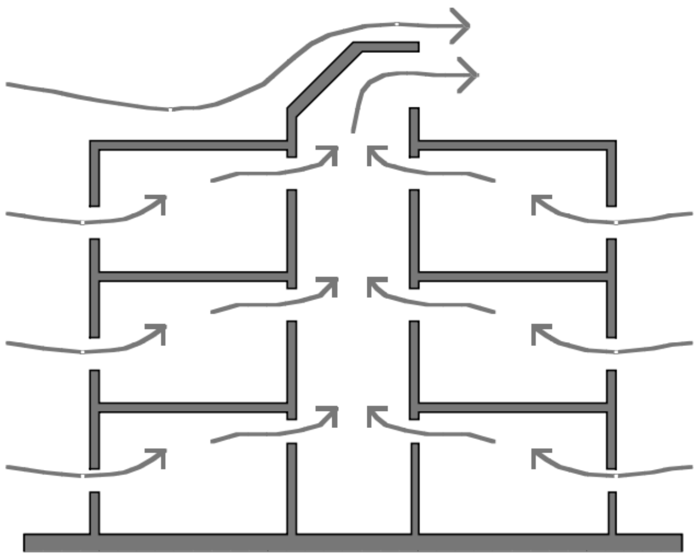

Figure 2.7 – Schematic of buoyancy-driven stack ventilation strategy (Emmerich *et al.*, 2001)

Even if the focus of stack ventilation is to work independently of the wind forces, in real life scenarios the wind induces pressure distributions across the envelope and actually has a big influence on the airflow distribution. Furthermore, according to Emmerich *et al.* (2001), the wind effects may well be more important than buoyancy effects in stack ventilation schemes. Therefore, successful designs will seek ways to make full advantage of both driving forces.

2.1.4.3 Single-Sided Ventilation

Single-sided ventilation typically serves single rooms and thus provides a local ventilation solution. For this case, the ventilation airflow is caused by room-scale buoyancy effects, small differences in envelope wind pressures, and/or turbulence. Consequently, driving forces for single-sided ventilation is generally relatively smaller and highly variable than the previous strategies presented. According to Emmerich *et al.* (2001), compared to the other alternatives, single-sided ventilation offers the least attractive natural ventilation solution but, nevertheless, a solution that can serve individual offices. Figure 2.8 shows a schematic of single-sided ventilation in a multi-room building.

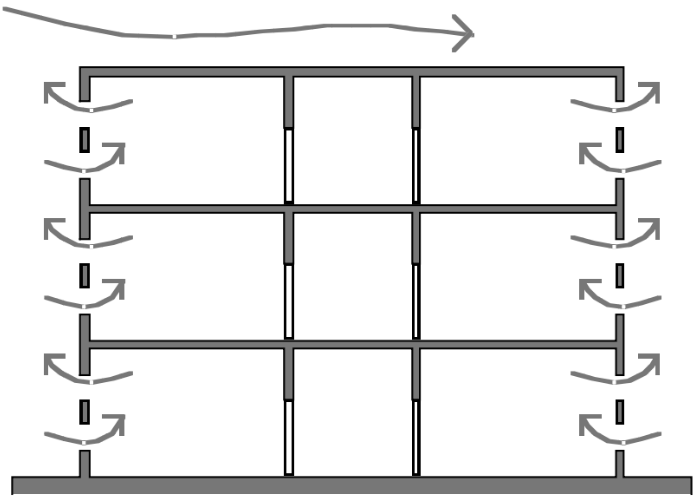

Figure 2.8 – Schematic of single-sided ventilation strategy (Emmerich *et al.*, 2001)

To be more effective, this strategies needs to have openings located at different heights or a large openings to allow the airflow in and out of the space. According to Larsen (2006), in single-sided ventilation the flow through the opening is harder to predict because the turbulence in the wind and the pulsating flow near the opening also affect the flow through the opening.

2.1.4.4 Night Ventilation

Direct natural ventilation is no longer useful when daytime outdoor temperatures exceed the upper thermal comfort limit. Night ventilation comes as an alternative for such cases. Night ventilation works well in climates with large diurnal temperature differences, making it possible to offset daytime internal gains by cooling the building's thermal mass using outdoor air during the previous night. When properly designed, night ventilation might have big impacts for cooling saving, especially for office buildings with higher internal gains. The night ventilation strategy takes advantage of the lower external night-time temperature to pre-cool the building structure, and thereby lower the mean radiant temperature. By lowering the mean radiant temperature, comfort can be maintained even though air temperatures in the space might rise. By increasing thermal capacity (thermal mass), the amount of heat the structure can absorb per degree rise in mean radiant temperature increases, thereby increasing the ability of the space to maintain reasonable comfort conditions through the day. Figure 2.9 illustrates the effect of thermal mass and natural ventilation on summer peak indoor temperature.

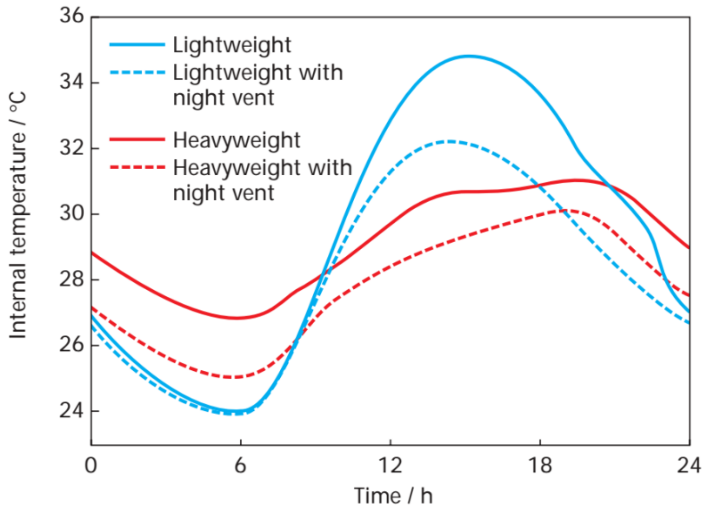

Figure 2.9 – Effect of thermal mass and night ventilation on peak indoor temperatures (CIBSE AM10, 2005)

A number of studies evaluating the night ventilation indicate considerable cooling potential in comparison to similar spaces that do not use night ventilation. Pfafferott *et al.* (2003) showed that the night ventilation reduced the mean room temperature by 1.2 °C during working hours for an office building in Freiburg, Germany. In La Rochelle, France, Blondeau *et al.* (1997) identified a decrease in temperature between 1.5 and 2°C using night ventilation. Geros *et al.* (1999) concluded that the night ventilation imposed a temperature reduction between 1.8 and 3°C for an office building in Greece. Schulze and Eicker (2013), via simulation, showed that natural night ventilation is only suitable in buildings with sufficient and accessible thermal mass of about 75-100 kg/m² of floor space. The internal gains also have to be limited to 30 W/m² of floor area.

2.1.5 Adaptive Thermal Comfort to Assess Natural Ventilation Effectiveness

The goal of a design for natural ventilation is to maintain thermally comfortable indoor conditions for all spaces in a building without relying on mechanical cooling. Therefore, the most suitable metric to assess natural ventilation effectiveness is a thermal comfort metric. Adaptive thermal comfort has been widely accepted as the most suitable thermal comfort model for naturally ventilated buildings. The adaptive model has been incorporated in the most widely used thermal comfort standards in the world: ASHRAE Standard 55 (2013) and EN15251 (2007). The adaptive model has been developed based on numerous field studies in USA, Europe, and Asia. The model has suffered from two major criticisms:

- It is based on field data from mostly milder climates of Europe, North America and Asia, and therefore excludes data from hot and hot-humid climates. However, this limitation is currently being overcome with ongoing research on adaptive thermal comfort in hot and hot-humid climates in Asia, South America, and Africa. Countries like China, India, Japan, and Brazil have developed their own adaptive comfort models that apply to hot and humid climates. For the Canadian climate, however, the current adaptive model is applicable.
- It aggregates many factors into a single operative comfort temperature, but does not explain the factors or underlying processes participating in achieving comfort (*i.e.* a black-box model). Ongoing research is underway to disaggregate the adaptive processes (*i.e.* behavioral, psychological, and physiological), and investigate how different factors participate in achieving thermal comfort. One particular aspect that couples psychology and physiology is the influence of the perceived level of control over the environment, *i.e.* occupants accept warmer temperatures when they perceive that they are in-control of their environment (Paciuk, 1990). The influence of perceived control on thermal comfort is an active subject of ongoing research. A review of the literature in this subject is out of the scope of this research. However, the aspect of perceived control will be considered in the final analyses of this project.

According to Humphreys *et al.* (2001), the occupants of naturally ventilated buildings have a large range of tolerances to thermal comfort when compared to occupant in mechanically ventilated building. Adaptive thermal comfort is a theory that suggests a human connection to the outdoors and the control over the immediate environment that allow them to adapt to a wider range of thermal conditions than is generally considered comfortable. The fundamental assumption of the adaptive approach is expressed by the adaptive principle: if a change occurs such as to produce discomfort, people react in ways which tend to restore their comfort. The development of the adaptive thermal comfort relies on the findings from thermal comfort surveys conducted by a number of researchers across the globe. It was founded that, for naturally ventilated buildings, the comfort temperatures is a function of outdoor air temperature. ASHRAE Standard 55 (2013) presents the adaptive thermal comfort approach, but in order to be properly used the following criteria need to be met:

- There is no mechanical cooling system (*e.g.* refrigerated air conditioning, radiant cooling, or desiccant cooling) installed. No heating system is in operation;
- Occupants have metabolic rates ranging from 1.0 to 1.3 *met* (*met* is unit to indicate the metabolic rate of an individual, 1 *met* indicate a sitting person doing light insensitive activity);
- Representative occupants are free to adapt their clothing to the indoor and/or outdoor thermal conditions within a range at least as wide as 0.5 to 1.0 *clo* (*clo* is a unit used to represent the amount of insulation provide by the occupant clothing);
- The prevailing mean outdoor temperature is greater than 10°C and less than 33.5°C.

Figure 2.10 presents the graph that represents the adaptive thermal comfort depending on the indoor operative temperature (t_o) and the prevailing mean daily outdoor air temperature ($\overline{t_{pma(out)}}$). The dark grey area in the graph represents the region where temperatures provide a thermal comfort for 90% of the occupants of the space, also known as the upper limit for thermal comfort. The light grey area (lower limit) represents the area where 80% of the occupants are comfortable with the conditions of the spaces.

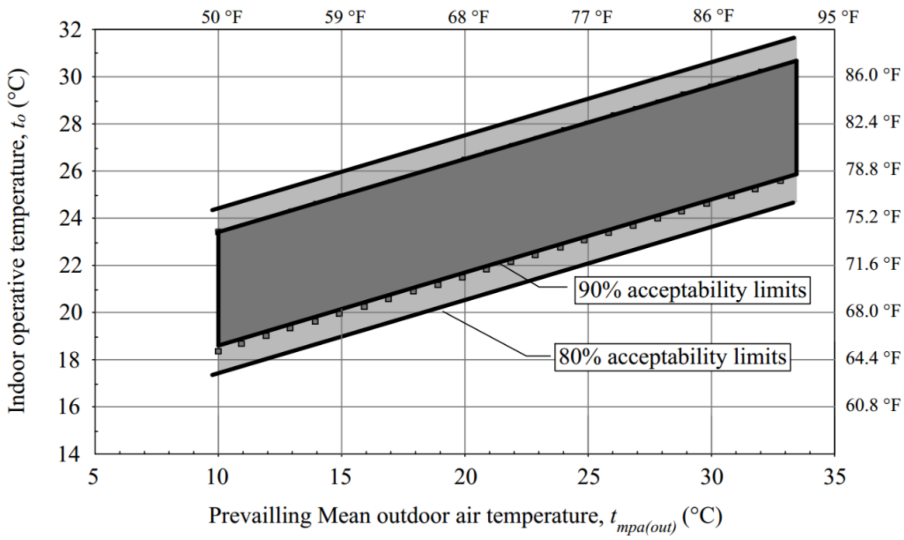

Figure 2.10 – Acceptable operative temperature (t_o) ranges for natural conditioned spaces (ASHRAE Standard 55, 2013)

Equation 2.15 and 2.16 mathematically represents the thermal comfort limits for 80 and 90%, respectively.

$$Upper\ Limit = 0.31 \cdot \overline{t_{pma(out)}} + 21.3\ [°C] \qquad \text{Equation 2.15}$$

$$Lower\ Limit = 0.31 \cdot \overline{t_{pma(out)}} + 14.3\ [°C] \qquad \text{Equation 2.16}$$

According to ASHRAE Standard 55 (2013), the prevailing mean outdoor air temperature ($\overline{t_{pma(out)}}$) shall be determined in accordance with all of the following:

- It shall be based on no fewer than seven and no more than 30 sequential days prior to the day in question;
- It shall be a simple arithmetic mean of all of the mean daily outdoor air temperature of all the sequential days in the previous point.

A tool that can be used for predicting natural indoor operative temperatures (t_o) for adaptive thermal comfort is whole building simulation model (WBSM). However, the capability and accuracy of the model to simulate natural ventilation has some limitations; those limitations are further discussed.

3. LITERATURE REVIEW

3.1 Whole Building Simulation Model Supporting Natural Ventilation

Normally, the whole building simulation model (WBSM) uses the Airflow Network (AFN) approach to characterize the airflow through the building. However, modern energy software is usually fully coupled with a Computational Fluid Dynamics (CFD) module. CFD could be used to describe the airflow behaviour within a particular internal space or though whole building. But the inclusion of a CFD analysis in WBSM is a decision that is taken by the designer to accomplished clear objective. Furthermore, the appropriate use of CFD requires a number of special attentions to details and model validation. Figure 3.1 illustrates a schematic example of air flow modeling in whole building simulation model (WBSM). In that example, AFN is used to model the airflow through the entire building. But for the atrium (red circle) the airflow is better detailed using CFD or a zonal model (section 3.3 for more information about zonal models).

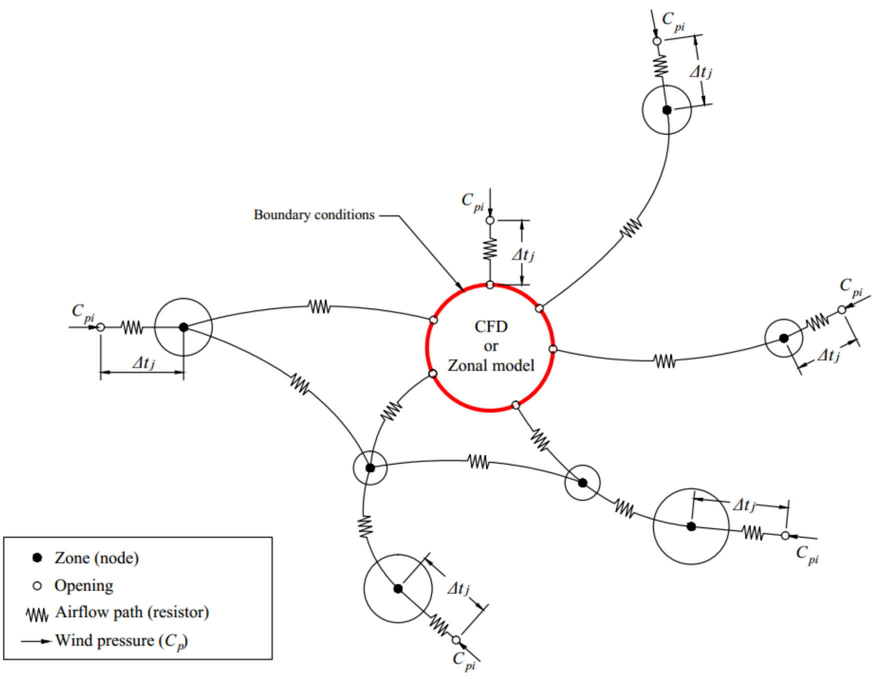

Figure 3.1 – Schematic example of whole building simulation model (WBSM)

3.2 Airflow Network (AFN) Approach in Whole Building Simulation Model

The airflow network (AFN) model is based on the assumption that the building and mechanical system are considered as being composed by nodes or zones. The airflow paths (*e.g.* openings, cracks, doors and etc.) are represented by electrical resistance (see figure 3.2). Airflow network (AFN) calculates the mass flow balance of a space, combining the wind and buoyancy forces to capture pressure differences across zones connecting the spaces. The building envelope pressure boundary conditions are derived from the wind velocity profile. The flows through the openings are usually assumed to be driven by static-pressure differences. The main assumption in AFN is that the air within a (zone) is considered fully-mixed; this approach is called mixed-model. Moreover, Bradly and Utzinger (2007) points out another three important assumptions in AFN. First, it is assumed that the resistance to airflow of a flow-limiting path between building zones is much greater than the resistance to airflow of the zones themselves. Second, the pressure varies hydrostatically within a building zone is only true when airflow within the zone (and, thus, airflow in and out of paths connecting zones) is zero. Lastly, it is assumed that temperatures within a given zone are uniform.

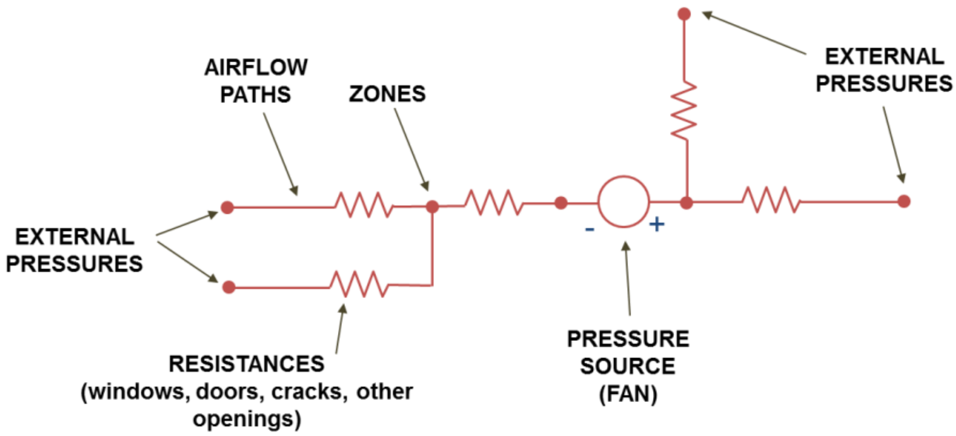

Figure 3.2 – Schematic representation of relationship between zones and air paths

The spaces, characterized as nodes, are usually represented by a name, fluid type, node type, height, and temperature. The nodes represent either internal or external boundary pressures.

The difference is that only internal nodes are subjected to the mass balance approach. The reference height is assigned to each node; this is used as part of stack forces calculations.

Every external surface considered in the AFN has to be associated to an external node which defines environmental conditions. These conditions include wind pressure coefficients (C_p) and are highly dependent on the building geometry. External nodes play an essential role in the modelling of stack effect where ventilation rates are also driven by pressure differences due to height difference between inlet and outlet.

Time-averaged and space-averaged variables are associated with the nodes and specific pressure-airflow relations are assigned to each airflow element (doors, windows, or structural leakages). Governing equations are formed by mass conservation at each node and hydrostatic pressure conditions at each of the modeling zones. Conservation of mass at the nodes is imposed by assuming the difference between the inlet and outlet mass flow rate as equal to the mass accumulated in the zone (equation 3.1).

$$\sum_{in} \dot{m}_i - \sum_{out} \dot{m}_j - \frac{dm}{dt} = 0 \qquad \text{Equation 3.1}$$

where,

$m_{i,j}$: mass flow rate through the airflow i or j [kg/s];

dm/dt: accumulation term [kg/s].

If the flow is assumed to be at steady state, the accumulation term (dm/dt) is equal to zero. However, accumulation can be considered in the case of smoke generation and dispersal analyses. Specific pressure-airflow relations are defined for each airflow element to relate the pressure difference between two adjacent zones ($\Delta P_{1,2}$) with the airflow m_i (mass flow rate). The general form of pressure-airflow relation is reported below (equation 3.2).

$$\dot{m}_i = f(\Delta P_{1,2}) \qquad \text{Equation 3.2}$$

where,

f: generic pressure-airflow relation characteristic of the airflow element;

$\Delta P_{1,2}$: pressure difference between two adjacent zones1 and 2 [Pa];

The calculation procedure consists of three sequential steps:

- Pressure and airflow calculations;
- Node temperature and humidity calculations;
- Sensible and latent load calculations.

The pressure and airflow calculations determine pressure at each node and airflow through each linkage given wind pressures and forced airflows. Based on the airflow calculated for each linkage, the model calculates node temperatures and humidity ratios given zone air temperatures and humidity ratios. Using these node's temperatures and humidity ratios, the sensible and latent loads from duct system conduction and leakage are summed for each zone. Convergence is reached when the sum of all mass flow rates through all components approaches zero within the tolerance band specified.

Zhai *et al*. (2010) performed airflow models evaluations by comparing predicted airflow from EnergyPlus, CONTAM and ESP-r AFN models with measured airflow in laboratory experiments across 8 defined scenarios at steady conditions. They concluded that all the models yielded similar predictions, which are within 30% error for the simple cases evaluated. The worst results were obtained for buoyancy driven single-sided ventilation, wind-driven cross-ventilation and combined buoyancy and wind-driven natural ventilation configuration (whereas buoyancy-driven cross-ventilation error is less than 10%). Emmerich *et al*. (2003) remembers that numerous studies carried out over the past few decades have shown that AFN analyses in fact provide quite accurate estimates of wind-driven infiltration and natural ventilation for buildings with façade porosities up to 20% and accurate estimates the airflow for higher porosities. Porosity is a commonly used terminology to define the ration between the areas of openings by the total area of the building external walls. Belleri (2013) claims that within the existing natural ventilation modelling techniques, airflow network (AFN) models seem the most promising tool to support the natural ventilation design as they are coupled with the most widely used building energy simulation tools used nowadays. However, AFN is not suitable for all natural ventilation strategies. According to Zhaia *et al*. (2015), wind-driven single-sided ventilation cannot be modeled with the current AFN models available in the market and usually found on WBSM.

3.2.1 The Wind Pressure Coefficients and AFN Modelling

According to Cóstola *et al*. (2009), wind pressure coefficients (C_p) are influenced by a wide range of parameters, including building geometry, façade detailing, position on the facade, the degree of exposure/sheltering, wind speed and wind direction. The authors state that it is extremely difficult to take into account the full complexity of C_p variation. Hensen (1991) already described the difficulty to perform an accurate evaluation of C_p. Whole building simulation model (WBSM) and airflow network (AFN) programs generally incorporate C_p in a simplified way.

Cóstola *et al*. (2009) made a distinction between primary sources of C_p data, composed by full-scale measurements, reduced-scale measurements in wind tunnels and CFD simulations, and secondary sources, composed by databases and analytical models. According to the author, primary sources are considered to be the most reliable C_p data sources. Secondary sources are generated based on primary sources (*e.g.* databases and analytical models derived from wind-tunnel and full-scale experiments) are not as reliable as C_p originated from preliminary source.

According to Cóstola *et al*. (2009), on-site full-scale measurements at real building façades provide the most representative description of C_p. In those measurements, there is no need to reproduce boundary conditions, no scaling issues, and no physical models needs to be adopted. However, full-scale measurements are complex and expensive, and are mainly used for validation purposes. Not to mention the uncertainty in dealing with highly sensible sensors, such as manometers and cup anemometers for the wind speeds.

But at design stage, wind-tunnel experiments are generally considered the most reliable source of pressure data for buildings. Cóstola *et al*. (2009) concluded that wind-tunnel experiments present specific challenges, such as the quality of wind-tunnel results is directly affected by the history of calibration in the wind tunnel, quality assurance procedures, and the know-how of the personnel involved in the test setup and execution.

CFD simulation is an option to determine the C_p values across the building surfaces. In recent years, the application of CFD strongly increased due to improvements in computer performance, price reduction, and the availability of commercial CFD software. However, results from Cóstola and Alucci (2007) showed differences on the C_p values generated by CFD simulation and the values found in the literature. The authors claimed that validation is necessary to assess which of the two C_p sources is the best input for AFN models. According to Cóstola *et al*. (2009), despite the vast increase in the application of CFD to study the wind flow around buildings, it is not common practice to use CFD as source of custom C_p data for WBSM. The main reasons are the required level of expertise and the high cost of these simulations, both in terms of computational resources and user time, when compared to the WBSM simulation itself.

As secondary sources of C_p, databases are compilations of C_p data from one or more sources, where the data is classified according to some parameters, such as building shape and orientation to the incident wind. Cóstola and Alucci (2007) point out the limitation of the estimation of C_p using database, which is the small number of building and surrounding shapes available. In general, only very simple forms, like cubes and parallelepipeds with flat or slope roof can be found in these database. However, real buildings have complex geometries, architectural elements in the façade, balconies, overhangs and other geometrical features that make them divergent from those presented in the database.

Analytical models consist of a set of equations to calculate C_p for a specific building configuration. Analytical models are developed based on wind-tunnel and full-scale experiments. According to Cóstola *et al*. (2009), they aim to provide C_p data for a broader range of building configurations, considering obstructions, the effect of different wind profiles and the C_p variation across the façade.

According to Cóstola *et al*. (2009), most of the modern WBSMs use database to estimate C_p values, but they rarely used analytical tools. The authors concluded that pressure coefficients from different data sources, for the same building in the same conditions, show large variations, even for simple configurations like fully exposed cubic buildings. Large variation also applies to complex building geometries, which are not included in existing databases. In addition, Tuomaala (2002) stated that there is no reliable and effective method for evaluating the value of C_p for complex cases. Cóstola *et al*. (2009), also highlighted the lack of information about the uncertainty associated with the values provided by each data source, which raises questions about the accuracy of WBSM. Figure 3.3 illustrate an example of C_p values assumed along the building surfaces on a typical WBSM simulation case.

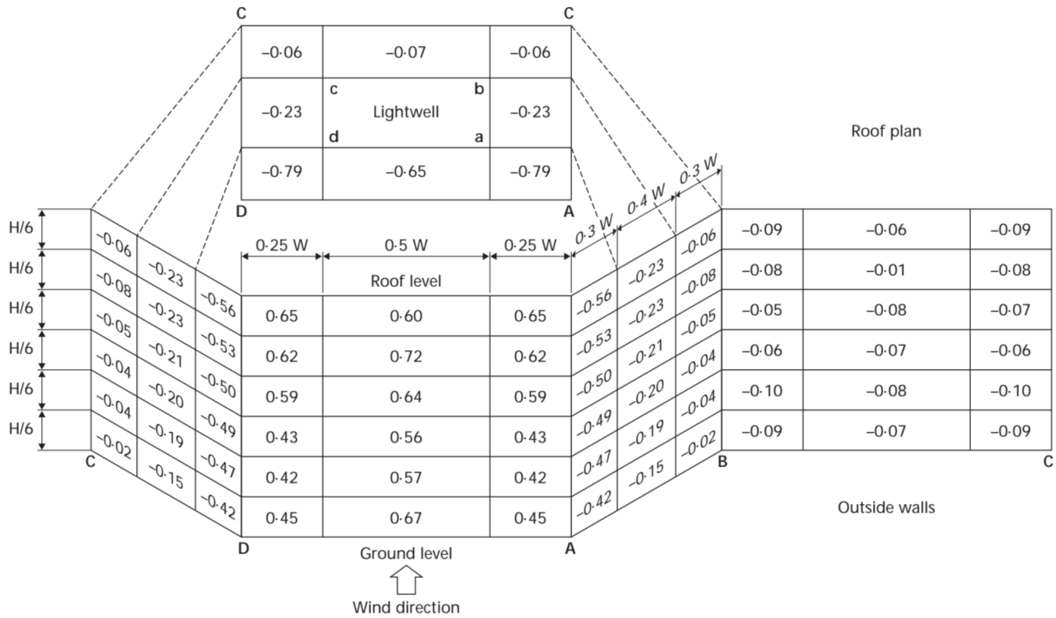

Figure 3.3 – Example of a distribution of C_p across the building surfaces

3.2.2 Characterization of the Openings

A number of studies shown that a poor characterization of the openings generates a big source of uncertainty in terms of airflow simulation (Dascalaki *et al*., 1999; Furbringer *et al*, 1999; Wachenfeldt, 2003; Heiselberg, 2004). Commonly, the equation used to describe the airflow through an opening is the orifice equation. Equation 3.3 is based on Bernoulli's assumption for steady incompressible flow and can be used for a relatively large opening area. For the flow characteristics through cracks, the orifice equation needs some adjustments in order to be representative.

$$q_{window} = C_D \cdot A \cdot \sqrt{\frac{2}{\rho} \cdot \Delta P} \qquad \text{Equation 3.3}$$

where,

C_D: discharge coefficient;

q_{window}: airflow through the window [l/s];

A: opening area [m²];

ρ: air density in the opening [kg/m³];

ΔP: pressure difference across the opening [Pa].

The discharge coefficient (C_D) is the ratio between the actual flow rate measured under specified conditions and the theoretical flow rate through the opening. For wind-driven cross-ventilation, Karava *et al*. (2004) say that the orifice equation is valid under the following assumptions:

- Fully-developed turbulent flow;
- The pressure distribution on the building envelope is not affected by the presence of openings;
- The pressure drop across the inflow and outflow opening is equal to the static pressure difference*, i.e.* the dynamic pressure in the room can be neglected. In other words, the orifice equation can be a realistic model when the kinetic energy is dissipated downstream of the opening (Sandberg, 2004).

For real cases, the use of the orifice equation presents a lack of accuracy when compared with real measured data. The simplicity of the equation neglects important aspects that influence the flow through the openings. According to Karava *et al*. (2004), there are different alternative theories that tried to fill the gap left by the orifice equation, but yet none of them can be established as a potential replacement of the conventional equation. Therefore, the selection of an appropriate simple equation to represent the flow characteristics of openings is still problematic.

However, Karava *et al*. (2011) found that the orifice equation predicts the ventilation flow rate with reasonable accuracy for configurations with openings located in the middle or upper section of a building façade and with wall porosity lower than 10%, while it underestimates the flow rate if any of the inlet or outlet openings cover more than 10% of the wall area. Porosity is the ratio between the openings and total external wall area. For configurations with openings below the mid-height of the building, the author claims that the orifice model overestimates the ventilation flow rate, except for configurations with large inlets and outlets (20% wall porosity). The study showed that the internal airflow pattern has a significant impact on induced airflow rate and internal pressure distribution; this effect is more pronounced for configurations with large wall porosities (higher than 10%) and cannot be predicted by simplified macroscopic models such as the orifice equation.

The discharge coefficient (C_D) is one of the problematic parameters to be determined; it depends on the type of the opening, geometry of the opening, the Reynolds number (*Re*) of the flow and etc. Through laboratory measurement, Heiselberg and Sandberg (2006) demonstrated that the discharge coefficient (C_D) for a window opening depended on the window type, opening area and geometrical relation between the window and façade, temperature and pressure differences across the opening, and the control strategy. Karava *et al*. (2003) also found from a literature review that the C_D of openings for wind-driven cross ventilation varied considerably with opening area, porosity, configuration (shape and location in the façade) and wind velocity. According to ASHRAE Fundamentals (2009) typical discharge coefficients (C_D) vary between 0.6 and 0.65 for small square-edged openings, and between 0.9 and 0.95 for round edge openings (Andersen, 2002). Recently, newly developed methods such as coupled CFD with energy and airflow analysis have been used for the airflow calculation through large internal or external openings (Yuan and Srebric, 2004; Wang and Chen, 2004).

When dealing with WBSM, the simulation programs present a simplified calculation using adjustments and modifications to the orifice equation to estimate the flow through the opening. The method used for the calculation and further presented is based on IES-VE (2012) approach, a similar method used by other simulation software.

One of the main concerns in characterizing the opening is to correctly describe the area of the opening (A) and the discharge coefficient (C_D). WBSM normally uses a simplified semi-empirical model based on experimental data and wind tunnel tests to calculate these factors. To calculate the airflow through the opening, the approach used by IES-VE uses the equivalent opening area (A_{ef}). The equivalent opening area (A_{ef}) is an idealized sharp edge orifice that air would flow under the same volume airflow rate and identical applied pressure difference (ΔP) as the opening under consideration. In other words, the A_{ef} is an idealized sharp edge opening with the same airflow rate and ΔP as the window that is being analyzed. The advantage of using an idealized sharp edge orifice is that the discharge coefficient (C_D) is considered to be constant (C_D=0.62) throughout the opening surface. The conversion is made using window's manufacturer data in conjunction with empirical data from wind tunnel tests for different types of openings. The software automatically calculates the equivalent sharp edge orifice area (A_{ef}) based on: the type of opening, degree of opening, and opening geometry. Equation 3.4 is adjusted version of orifice equation (equivalent to equation 3.1), which calculates the airflow rate across the openings according to IES-VE (2012).

$$q_{window} = C_D \cdot A_{ef} \cdot \sqrt{\frac{2}{\rho} \cdot \Delta P} \qquad \text{Equation 3.4}$$

where,

C_D: discharge coefficient, it assumes the value 0.62 for sharp edge orifices;

q_{window}: airflow through the window [l/s];

A_{ef}: effective opening area [m²];

ρ: air density in the opening [kg/m³];

ΔP: pressure difference across the opening [Pa].

The effective opening area (A_{ef}) is calculated according equation 3.5.

$$A_{ef} = f \cdot A \qquad \text{Equation 3.5}$$

where,

f: equivalent area fraction;

A: rough area of the opening [m²].

The equivalent area fraction (f) is the factor that makes the adjustments needed to properly estimate the A_{ef}. This coefficient varies with the window type; see figure 3.4 different window types normally used.

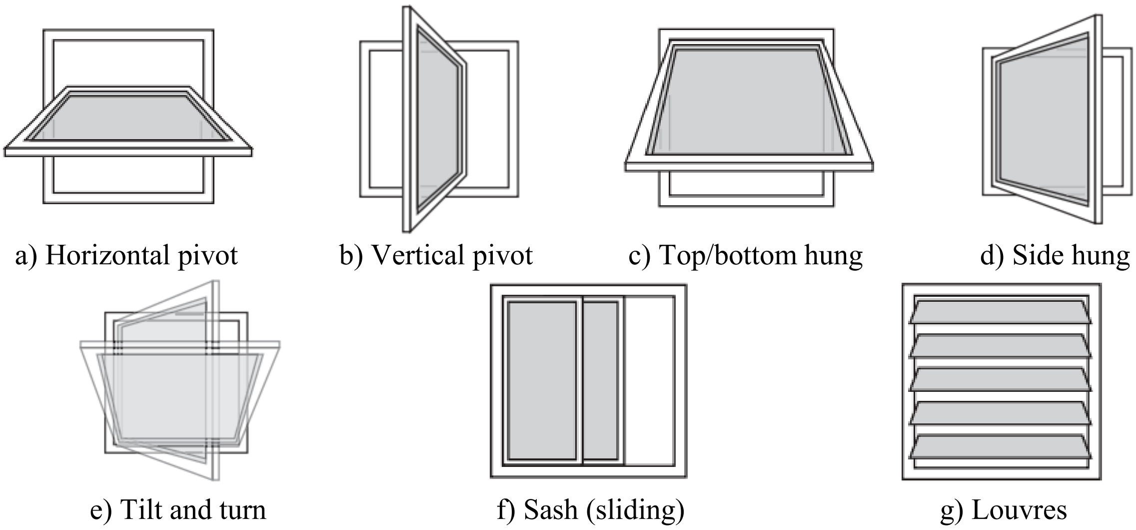

Figure 3.4 – Mainly window types used for natural ventilation

For all hung window (figure 3.4, a, c and d) the equivalent area fraction (f) is represented by equation 3.6.

$$f_{hung} = C_v \cdot \frac{f_a}{100} \qquad \text{Equation 3.6}$$

where,

C_v: coefficient interpolated from the table 3.1;

f_a: operable area [%].

The operable area (f_a) represents the amount of window that actually opens, not considering the window frame area or any existing fixed part on the window. Depending on the opening degree angle, the length (L) and height (h) of the hung window, the coefficient C_v assumes a determined value. Table 3.1 presents the values adopted for all hung windows.

Table 3.1 – Coefficient (C_v) for all hung window (IES-VE, 2012) [1]

Side hung window/door	Proportions of the window			
	L/h<0.5	*0.5<=L/h<1*	*1<=L/h<2*	*L/h>2*
Opening angle (°)	C_v	C_v	C_v	C_v
10	0.10	0.17	0.24	0.34
20	0.22	0.31	0.39	0.51
30	0.36	0.43	0.50	0.60
45	0.50	0.54	0.64	0.65
60	0.58	0.60	0.63	0.67
90	0.64	0.65	0.65	0.67

Centre hung window/Horizontal pivot	Proportions of the window	
	L/h=1	*L/h>2*
Opening angle (°)	C_v	C_v
10	0.15	0.13
30	0.30	0.27
45	0.44	0.39
60	0.56	0.56
90	0.64	0.61

Top hung window	Proportions of the window			
	L/h<0.5	*0.5≤L/h<1*	*1≤L/h<2*	*L/h>2*
Opening angle (°)	C_v	C_v	C_v	C_v
10	0.34	0.24	0.17	0.10
20	0.52	0.39	0.30	0.23
30	0.60	0.50	0.43	0.36
45	0.65	0.58	0.54	0.50
60	0.67	0.63	0.60	0.58
90	0.68	0.65	0.65	0.64

Table 3.1 – Coefficient (C_v) for all hung window (IES-VE, 2012) [2]

Bottom hung window	Proportions of the window			
	L/h<0.5	*0.5≤L/h<1*	*1≤L/h<2*	*L/h>2*
Opening angle (°)	C_v	C_v	C_v	C_v
10	0.27	0.23	0.15	0.09
20	0.53	0.42	0.26	0.16
30	0.62	0.52	0.37	0.26
45	0.67	0.62	0.53	0.46
60	0.69	0.66	0.61	0.57
90	0.72	0.69	0.67	0.64

Parallel hung window	Proportions of the window		
	L/h=1	*L/h=2*	*L/h>2*
Opening angle (°)	C_v	C_v	C_v
15	0.23	0.15	0.13
30	0.40	0.30	0.24
45	0.51	0.41	0.34
60	0.57	0.50	0.43
90	0.65	0.60	0.60

For sash (sliding) windows (figure 3.4, f) and rollers doors the equation 3.7 calculates the equivalent area fraction.

$$f_{sliding} = C_v \cdot \frac{f_a}{100} \qquad \text{Equation 3.7}$$

where,

C_v: coefficient fixed at 0.65 for a fully open window;

For louvres and grilles (figure 3.4, g) the equivalent area fraction is expressed by equation 3.8. The discharge coefficient (C_D) of louvres and grilles are widely available from manufacturers.

$$f_{louvres} = \frac{C_x}{0.62} \cdot \frac{f_a}{100} \qquad \text{Equation 3.8}$$

where,

C_x: discharge coefficient according to manufacture information.

To consider the difference in pressure with the height of the opening (h) due to buoyancy forces, equation 3.9 is presented. Each series of infinitesimal narrow horizontal slices of the opening are calculated using this approach. The total volume airflow in the opening is calculated when equation 3.9 is integrated over the total height (h) of the opening, generating equation 3.10.

$$dq_{window} = C_D \cdot \sqrt{\frac{2}{\rho} \cdot \Delta P(h)} \cdot dA_{ef} \qquad \text{Equation 3.9}$$

$$q_{window} = C_D \cdot A_{ef} \cdot \sqrt{\frac{2}{\rho}} \int_0^h \sqrt{\Delta P(h)} \qquad \text{Equation 3.10}$$

The method earlier described is called decoupled approach (figure 3.5, a), this is the standard approach used in AFN and incorporated in WBSM. In this method the outdoor and indoor airflow are solved separately. The results of the outdoor wind flow and pressure fields on the building surfaces are used as boundary conditions for solving the indoor airflow (figure 3.5, a). However, a number of studies (Murakami *et al.*, 1991; Kato *et al.*, 1992; Etheridge and Sandberg, 1996; Seifert *et al*., 2006; Karava *et al*., 2007, 2011; Kobayashi *et al*., 2010) claim that decoupled approach can introduce relevant errors, since it assumes that: the pressure distribution on the building envelope is not affected by the presence of the openings, the turbulent kinetic energy is dissipated at the windward opening, and that the effect of the dynamic pressure on the airflow passing through the opening is negligible. Notwithstanding, the application of a coupled approach is still quite limited and specific guidelines for this case have not yet been fully developed.

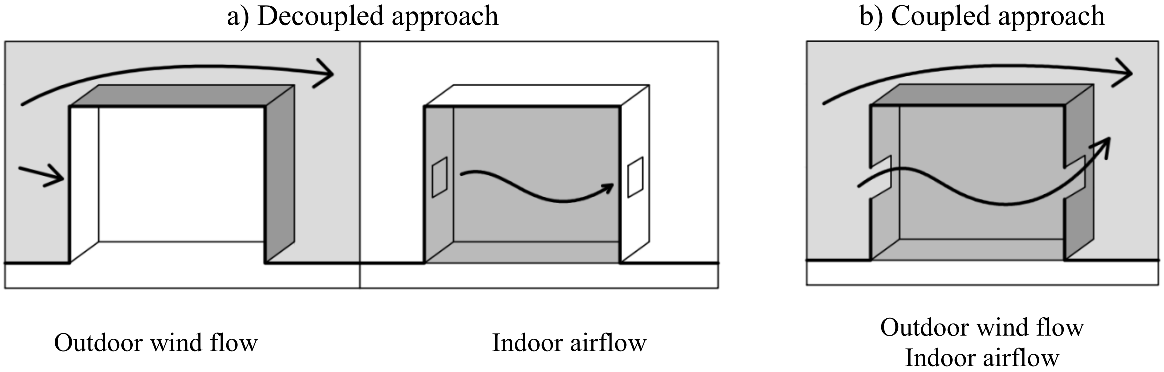

Figure 3.5 – Approaches of coupling outdoor and indoor airflow (Ramponi, 2014)

3.2.3 Buoyancy Forces and Stack Effect in AFN Simulation

Buoyance forces and stack pressure are interconnected but different phenomena. In AFN, the stack effect is fairly well described by the simulation. Section 2.1.1 presents how this pressure is normally calculated by AFN, following equations 2.1 to 2.9. Buoyancy forces, on the other hand, are not explicitly modelled within a node/space in AFN simulation. However, when the calculation methods of EnergyPlus (2015) are analyzed, buoyancy flows between zones are modelled if they are on the top of each other, functioning as zonal model (see section 3.3). Given the limitation of AFN of not modelling buoyancy forces within a space, three alternatives are left for designers to choose: simplified analyses (CIBSE, 2005), zonal models (section 3.3), and CFD simulations (section 3.5). But on the one hand, simplified analyses generally cannot be coupled with WBSMs.

3.2.4 Thermal-airflow Coupling

The WBSM uses the airflow network (AFN) coupled with the dynamic thermal simulation model (already used for the building's energy simulation) to evaluate the building thermal performance. The AFN is integrated with the thermal model; both modules converge to results that combine both models. Figure 3.6 illustrates the thermal-airflow coupling schematically.

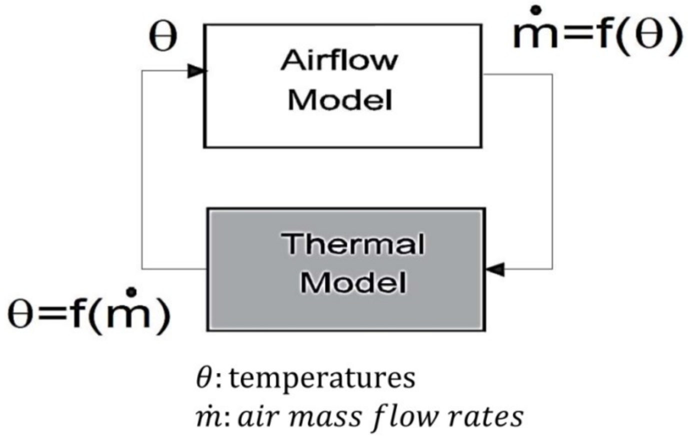

Figure 3.6 – Thermal-airflow coupling (Mora, 2016)

The coupling of these two elements is a result of the airflow energy balance for each zone. This energy balance involves the sum of all the energy gain or losses due to energy stored in the zone, convective internal loads, heat transfer due to air movement between zones, heat transfer expected form natural ventilation, and the energy output from the mechanical system (heating or cooling). After the energy balance, it is possible to calculate the temperature within a zone. This temperature is representative to the zone node. Equation 3.11 shows a standard airflow heat balance for a singular zone (EnergyPlus, 2015).

$$C_z \frac{dT_z}{dt} = \sum_{i=1}^{N_{sl}} \dot{Q}_i + \sum_{i=1}^{N_{surfaces}} h_i A_i \cdot (T_{si} - T_z) + \sum_{i=1}^{N_{zones}} \dot{m}_i C_p \cdot (T_{zi} - T_z) + \dot{m}_{inf} C_p \cdot (T_\infty - T_z) + \dot{m}_{vent} C_p \cdot (T_\infty - T_z) + \dot{Q}_{sys} \qquad \text{Equation 3.11}$$

where,

$C_z \frac{dT_z}{dt}$: energy stored in zone air [W];

$\sum_{i=1}^{N_{sl}} \dot{Q}_i$: sum of convective internal loads [W];

$\sum_{i=1}^{N_{surfaces}} h_i A_i \cdot (T_{si} - T_z)$: convective heat transfer from the zone surfaces [W];

h_i: heat transfer coefficient [W/m²·K];

A_i: surface area [m²];

T_{si}: temperature of internal surface [°C];

T_z: temperature of zone air [°C];

$\sum_{i=1}^{N_{zones}} \dot{m}_i \, C_p \cdot (T_{zi} - T_z)$: heat transfer due to interzone air mixing [W];

$\dot{m}_i$: airflow rate between zones [kg/s];

C_p: zone air specific heat [J/kg·K];

T_{zi}: temperature of zone air exchange [°C];

$\dot{m}_{inf} C_p \cdot (T_\infty - T_z)$: heat transfer due to infiltration of outside air [W];

$\dot{m}_{inf}$: airflow rate due to infiltration [kg/s];

T_∞: temperature of outside air [°C].

$\dot{m}_{vent} C_p \cdot (T_\infty - T_z)$: heat transfer due to natural ventilation [W];

$\dot{Q}_{sys}$: air system output [W];

For naturally ventilated buildings without the use of any type of mechanical ventilation is possible to assume that air system output ($\dot{Q}_{sys}$) term in the equation is equal to zero. The building thermal mass is indirect calculated by this approach; its characteristics are inferred on several terms from equation 3.11 (*e.g.* temperature of internal surface, energy stored in zone air, and etc.).

3.3 Zonal Model in Whole Building Simulation Model

The zonal model uses the similar physical background as the airflow network (AFN), but instead of considering a room/space as a single node, the zonal model divides that one space in subzones. The use of zonal model is suitable when the assumptions adopted by the AFN do not represent the space being modeled (*e.g.* fully-mixed air in the space, single temperature and pressure). Rooms where buoyancy forces are preponderant are not proper represented by AFN. For those cases, zonal models are used by dividing a room/space, represented in AFN as a node, into a number of nodes, better representing the buoyancy forces that occur in those spaces. According to Belleri (2013), zonal models are considered intermediate models between airflow networks (AFN) and computational fluid dynamics (CFD), as they divide the bounded space into a number of smaller volumes to calculate velocity and temperature field within the zone. The relatively coarse grid leads to advantages in terms of simulation speed when compared to a computational fluid dynamics (CFD) simulation. According to Mitterhofer *et al*. (2016), zonal model provides accurate and detailed information about the thermodynamic of indoor air behaviour within a space.

Zonal models are a common approach used in WBSM. To represent a large space using a zonal model, the space is represented as vertical zones stacked on top of each other. Even though, one limitation on that approach is in calculating solar distribution for a high number of zones. Beam solar radiation is transmitted as diffuse radiation only to the first zone, neighbouring the zone with glazing on its external surfaces. Thermal analysis of the sub-zones is highly affected by the way solar radiation is distributed in the indoor environment (D'Aquilio *et al*., 2016).

3.4 Empirical and Semi-Empirical Models

Modern WBSM commonly use a number of empirical and semi-empirical models in order to represent a part of the simulated airflow in the building. These models try to fill the gap left by the AFN simulation, such as the mixed-model consideration of fully-mixed air within a space, which is unsuited for some cases (*e.g.* under-floor ventilation, cross-ventilation and etc.). Moreover, these models are usually based on experimental data, analytical and numerical models. Belleri (2013) states that empirical models are generally limited by the number of case studies that the model is based on or to more detailed model simplifications based on specific assumptions. But on the other hand, empirical models allow simplified calculation avoiding the need of detailed and time-consuming simulation. EnergyPlus (2015) describes a number of different empirical and semi-empirical calculations used to characterize the internal space's airflow configuration, thermal stratification, buoyancy-driven airflow, single-sided ventilation, and etc.

3.4.1 Empirical Model for Single-Sided Ventilation

Single-sided ventilation produces complicated and fluctuating airflow patterns at the buildings openings, which the normal AFN approach cannot fully appreciate. Thus, empirical and analytical model are the alternative to model these spaces. There are a number of analytical and empirical model that describe the airflow through a single-sided ventilation opening (Yamanaka *et al*., 2006; Phaff *et al*., 1980; BS 5925, 1991). A review of single-sided ventilation analysis is presented by Allocca (2001). However, for the widely used multi-zone AFN, normally found on WBSM, there is a lack of accuracy in modeling single-side ventilation (Caciolo, 2009). CFD also comes as an alternative tool for fully characterize this kind of ventilation.

3.5 Computational Fluid Dynamics (CFD) Approach in Whole Building Simulation Model

CFD models, although complex, are becoming more accessible due to the rapid increase in computer capacity and user friendly options in the market. CFD solves the fundamental equations of motion for individual elements of a fluid at all points within a specific space. It numerically solves a set of partial differential equations for the conservation of mass, momentum, energy and turbulence quantities. Equation 3.12, 3.13, 3.14, and 3.15 express the instantaneous three-dimensional mass and momentum conservation for an incompressible, viscous, isothermal flow of a Newtonian fluid, in Cartesian co-ordinates, in partial differential equation form and in conservation form. Equation 3.16 is the transport equation for a passive scalar. In these following equations "*div*" is the divergence operator and "*grad*" is the gradient operator.

$$div\,\vec{v} = 0 \qquad \text{Equation 3.12}$$

$$\rho\frac{\partial u}{\partial t} + \rho \cdot div(u\,\vec{v}) = -\frac{\partial p}{\partial x} + div(\mu\, grad\, u) \qquad \text{Equation 3.13}$$

$$\rho\frac{\partial v}{\partial t} + \rho \cdot div(v\,\vec{v}) = -\frac{\partial p}{\partial y} + div(\mu\, grad\, v) \qquad \text{Equation 3.14}$$

$$\rho\frac{\partial w}{\partial t} + \rho \cdot div(w\,\vec{v}) = -\frac{\partial p}{\partial z} + div(\mu\, grad\, w) \qquad \text{Equation 3.15}$$

$$\rho\frac{\partial \phi}{\partial t} + \rho \cdot div(\phi\,\vec{v}) = div(\Gamma\, grad\, \phi) + S_{\Phi} \qquad \text{Equation 3.16}$$

where,

v, u and w: is the instantaneous velocity vector for the coordinate x, y and z;

t: is the time coordinate;

p: is the instantaneous pressure;

μ: is the dynamic viscosity;

ρ: density of the fluid;

ϕ: scalar quantity;

Γ: diffusion coefficient for the quantity ϕ;

S_{Φ}: is the scalar source term.

In order to be useful, CFD models need validation; otherwise they can only be used for flow visualizations. Validation of CFD airflow models can be done by two approaches, wind tunnel testing and field measurements. Furthermore, CFD could be used to model the thermo-fluid characteristics of one particular space (room) or the whole building thermo-airflow pattern.

The use of CFD in WBSM is becoming accessible in modern WBSM. The WBSM allows an easier integration between the CFD model and the data provided by the thermal and AFN models. AFN is more appropriate for investigating spatially averaged airflow rates, but when detailed airflow and temperatures within a room are needed, CFD is more suited for this application. The data provided by the AFN analysis from the adjacent spaces could be used as boundary condition for the CFD investigation.

3.5.1 Turbulence Modeling

When modeling the airflow in naturally ventilated buildings the nature of the flow is almost certainly turbulent. Furthermore, virtually almost all engineering applications of fluid dynamics are turbulent and hence require a turbulence model (McDonough, 2013) .Currently, there are two approaches normally used by the industry to model turbulence effects in building application. The first one adopts a statistical approach to represent turbulence effects by solving Reynolds Averaged Navier Stokes (RANS) equations (for a review of RANS turbulence modelling see Pope, 2000). The second approach is called Large Eddy Simulation (LES) (for a review of LES model see Sagaut, 2006); this form of turbulence calculation lays between direct numerical simulation (DNS) and the Reynolds Averaged Navier Stokes (RANS) method. According to Durrani *et al.* (2015), the RANS turbulence modelling is currently the “industry-standard” approach regarding turbulence model, essentially due to its considerably lower computational expense compared to LES (at least 2 orders of magnitude smaller than LES).

The RANS with standard $k - \varepsilon$ model is valid only for fully turbulent flows. This assumption is valid when dealing with building airflows. This model is based on the characteristic quantities of turbulence represented by the turbulent kinetic energy (k) and its dissipation rate (ε). Their values are presented by equations 3.17 and 3.18 respectively, which are functions of instantaneous velocity (u), and position (x).

$$k = \frac{1}{2} \cdot \overline{u_l' u_l'} \qquad \text{Equation 3.17}$$

$$\varepsilon = v \cdot \frac{\partial \overline{u_l'}}{\partial x_J} \cdot \frac{\partial \overline{u_l'}}{\partial x_J} \qquad \text{Equation 3.18}$$

Another assumption in turbulence models is that fluid is incompressible (*i.e.* the density remains relatively constant). According to CRADLE-CFD (n.d.), a fluid is considered incompressible if it has low velocity flows (<100 m/s), low temperature variation (under several hundred °C), it is single phase, and non-combusting. This scenario is fully achieved in natural ventilation. Thus, the balance equations governing flow for incompressible fluids are functions of the turbulent kinetic energy, dissipation rate, eddy viscosity (μ_t), density (ρ), thermal expansion coefficient (β), and Prandtl Number (P_{rt}), as well as some other constants. These balance equations are presented below (equation 3.19 to 3.24).

$$\frac{\partial \rho k}{\partial t} + \frac{\partial u_i \rho k}{\partial x_i} = \frac{\partial}{\partial x_i}\left(\frac{\mu_t}{\sigma_k} \cdot \frac{\partial k}{\partial x_i}\right) + G_S + G_T - \rho\varepsilon \qquad \text{Equation 3.19}$$

$$\frac{\partial \rho \varepsilon}{\partial t} + \frac{\partial u_i \rho \varepsilon}{\partial x_i} = \frac{\partial}{\partial x_i}\left(\frac{\mu_t}{\sigma_\varepsilon} \cdot \frac{\partial \varepsilon}{\partial x_i}\right) + C_1 \frac{\varepsilon}{k} \cdot (G_S + G_T) \cdot \left(1 + C_3 R_f\right) - C_2 \frac{\rho \varepsilon^2}{k} \qquad \text{Equation 3.20}$$

where,

$$G_S = \mu_t \cdot \left(\frac{\partial u_i}{\partial x_j} + \frac{\partial u_j}{\partial x_i}\right) \cdot \frac{\partial u_i}{\partial x_j} \qquad \text{Equation 3.21}$$

$$G_T = g_i \beta \cdot \frac{\mu_t}{P_{rt}} \cdot \frac{\partial T}{\partial x_i} \qquad \text{Equation 3.22}$$

$$R_f = -\frac{G_T}{G_S + G_T} \qquad \text{Equation 3.23}$$

$$u_t = C_u \rho \cdot \frac{k^2}{\varepsilon} \qquad \text{Equation 3.24}$$

The constants σ_k, σ_ε, σ_t, C_1, C_2, C_3, and C_μ are obtained experimentally and are expressed in Table 3.2.

Table 3.2 – Constants used in standard and RNG $k - \varepsilon$ turbulent model

	σ_k	σ_ε	C_1	C_2	C_3	C_μ	σ_t
Standard $k - \varepsilon$ model	1.000	1.300	1.440	1.920	0.000	0.090	0.900
RNG $k - \varepsilon$ model	0.719	0.719	$C_1(\eta)$	1.680	0.000	0.085	n/a

$C_1(\eta)$ is calculated using equation 3.25 and 3.26.

$$C_1(\eta) = 1.42 - \frac{\eta \cdot \left(1 - \frac{\eta}{4.38}\right)}{1 + 0.012 \cdot \eta^3} \qquad \text{Equation 3.25}$$

$$\eta = \frac{k}{\varepsilon} \cdot \sqrt{\frac{1}{2} \cdot \left(\frac{\partial u_i}{\partial x_j} + \frac{\partial u_j}{\partial x_i}\right) \cdot \left(\frac{\partial u_i}{\partial x_j} + \frac{\partial u_j}{\partial x_i}\right)} \qquad \text{Equation 3.26}$$

The Re-Normalization Group (RNG) $k - \varepsilon$ model (presented in table 3.2) presents some improvements compared with the standard $k - \varepsilon$ model. This turbulence model differs from the standard $k - \varepsilon$ model due to the methods which the constants are obtained. Instead of using a constant value for C_1, the model uses the Fourier analysis. Others $k - \varepsilon$ models have been developed over time. However, the standard and RNG $k - \varepsilon$ models are the most widely used $k - \varepsilon$ turbulence models in buildings. The standard $k - \varepsilon$ model typically gives satisfactory results, but the RNG $k - \varepsilon$ model is more widely used by researchers.

Iqbal *et al*. (2012, 2015) found that the standard $k - \varepsilon$ turbulence model was sufficiently accurate, while they found it was less precise for pressures under 0.5 Pa. Similar results were found by other researchers, though they directly compared the results to the RNG $k - \varepsilon$ model. Cook *et al*. (2003) concluded that the standard $k - \varepsilon$ model over-predicted the rate of entrainment into a buoyant plume, whereas the RNG model was closer with the experimental and analytical results. Evola and Popov (2006) found that the s standard $k - \varepsilon$ model was poor at predicting the air velocity around horizontal surfaces, but was a good model for cross-ventilating flows. Chen (1995) did a comparison of five different $k - \varepsilon$ models, showing inaccuracies in predicting penetration depth among the 2S and standard $k - \varepsilon$ models. A general analysis of the five models is presented in table 3.3. The author claims that the RNG model is the best suited for indoor airflows. Similar conclusions are expressed by Tan and Glicksman (2005), Seifert *et al*. (2006), and Yang *et al*. (2010).

Table 3.3 – Summary of the performance of the $k - \varepsilon$ models for predicting indoor airflow (Chen, 1995)

Flow Type	Parameters	$k - \varepsilon$	LB $k - \varepsilon$	2L $k - \varepsilon$	2S $k - \varepsilon$	RNG $k - \varepsilon$
Natural convection	Mean velocity	B	A	B	B	B
	Turbulence	C	C	D	D	C
	Temperature	B	D	B	B	B
	Heat transfer	C	B	A	C	C
Forced convection	Mean velocity	C	C	C	E	C
	Turbulence	D	D	D	D	D
Mixed convection	Temperature	A	A	C	A	A
	x_e	C	B	B	D	A
Impinging jet	Mean velocity	C	C	C	A	A
	Turbulence	D	D	D	C	C

A=excellent; B=good; C=fair; D=poor; E=unacceptable.

Another commonly used turbulence model is Large Eddy Simulation (LES). The LES model uses "filtered" Navier Stokes equations and as a result the dynamics of large eddies are modeled only. According to Cable (2009), LES models require much finer mesh densities and thus can take 20 times longer to converge on a solution than the RANS models. While LES has been shown accurate results, $k - \varepsilon$ models have proved to be sufficiently accurate using short computational time and is currently established as the standard approach to CFD simulations.

3.5.2 Buoyancy on Computational Fluid Dynamic (CFD)

Differently than the AFN simulation, the buoyancy forces within a room/space can be well-described using CFD. According to Nielsen *et al*. (2007), in CFD the Boussinesq approximation for buoyancy is used. It consists of the following approximation (Etheridge and Sandberg, 1996):

- Density is constant except when it is directly caused by buoyancy forces;
- A linear relation between temperature and density is adopted;
- All other fluid properties as constant.

According to Allocca *et al*. (2003), for buoyancy-driven ventilation, the CFD model is sensitive to how the boundary conditions are set up (see section 3.5.3 for boundary conditions). Teodosiu *et al*. (2014) claims that along the literature it is established that, in order to improve the prediction of CFD modeling buoyancy-driven airflow, is recommended to revise or enhance the following issues: discretization, turbulence modeling, treatment of airflow near wall, radiation modeling, thermal boundary conditions and heat source description.

3.5.3 Computational Domain and Boundary Conditions in CFD

The computational domain and the determination of boundary conditions in CFD are dependent on the type of environment being analyzed. Three types of environments can be identified: a) a fully enclosed space, b) a semi-enclosed or semi-open space, and c) a whole building.

a) Fully enclosed space – the boundary conditions are defined as the spaces surfaces, interior obstructions, air diffusers and returns, and type of connection with adjacent rooms or spaces. Normally, the boundary condition between the room connections is described as a fixed pressure differential or derived from AFN. The computational domain is defined as the as the room/space walls.
b) Semi-open/enclose space – The semi-enclosed space has a connection between the internal and the outdoor space. Therefore, a part of the boundary condition is subjected to wind forces and wind flow momentum. Regarding the computational domain, the domain is defined as the space walls and openings.

c) Whole building – In that category the building's surrounding are a part of the boundary conditions and elements such as the terrain, topography and adjacent buildings are taken into consideration. The boundary conditions for those cases are related with wind conditions as well as the building surfaces modeling. According to Cook et al. (2003), some studies may model the wind around a building, giving input conditions for a second set of simulations performed on the interior, specifying conditions directly at the inlet of the building. However, this method can limit the detail of the flow through the openings, and may also neglect the contribution of natural ventilation by buoyancy if the inlet velocity or flow rate is specified instead of the pressure across the opening. Define the computational domain for whole building approach is not as simple as when just one zone is being modeled. The definition of the minimum size of the computational domain is dependent on the investigated building and if not properly determined could be a source of uncertainty. According to Tan and Glicksman (2005), the computational domains should be 2.5 times the height of the building, 4 times the width wide, and 4 times the length long. Evola and Popov (2006) suggest using 4 times the height of the building and 8 times the length in the leeward direction. While there is some ambiguity in the exact size, the general consensus is to model the computational domain with 4 to 8 times each dimension of the building.

3.6 Calibration and Validation of Whole Building Simulation Model for Natural Ventilation

Model calibration aims to validate the accuracy of WBSM to represent actual building operational behaviors. The most common approach for WBSM nowadays is "trials and error" (Fabrizio and Monetti, 2015). However, more systematic approaches are emerging. A comprehensive review of WBSM calibration methods is out of the scope of this research. This section is therefore limited to uncover the main challenges in calibrating WBSM for natural ventilation. Coakley *et al*. (2014) provide an extensive review of the methods used across the literature. In general, all methods use energy metrics for calibration. In addition to energy metrics, Coakley *et al*. (2014) proposes using average zone temperatures. Common knowledge indicates that a successful WBSM model calibration involves major components: an adequate amount of high-quality building information and operational data, and a carefully built and verified WBSM. Table 3.4 shows calibration levels based on building information available (Fabrizio and Monetti, 2015). However, not only the type and quantity of data available, but most importantly, its quality and resolution needs to be considered for a successful WBSM calibration (Coakley *et al*., 2014).

Table 3.4 – Levels of calibration based on building information available (Fabrizio and Monetti, 2015)

Calibration Levels	Building Input Data Available					
	Utility Bills	As-Built Data	Site Visit or Inspection	Detailed Audit	Short-Term Monitoring	Long-Term Monitoring
Level 1	X	X				
Level 2	X	X	X			
Level 3	X	X	X	X		
Level 4	X	X	X	X	X	
Level 5	X	X	X	X	X	X

Coakley *et al*. (2014) state that the problem with WBSM calibration is over-specify, by having too many inputs, and under-determine, by having few validation points. Therefore, obtaining a unique calibrated model and simulation result is not reasonable. To address this problem, Coakley *et al*. (2014) proposed a methodology for uncertainty characterization of the calibration process that enable risk and uncertainty quantification of the final model predictions.

There is a clear gap in the literature regarding calibration of WBSM for natural ventilation. In general, case study papers are not validated. Only Coakley *et al*. (2014) proposes adding the average air temperature metric to the calibration, and presents a case study of a naturally ventilated building. However, the case study building is not a fully naturally ventilated but a mixed-mode building that does not eliminate the needs for mechanical cooling. Therefore, the building is still air conditioned in the summer.

The complexity in calibrating WBSM for natural ventilation comes from an increased uncertainty level. Such uncertainty originates from the close coupling between indoor and outdoor environments, the stochastic nature of wind, the increased influence of occupants' behaviors in operating windows and doors, and the use of personal comfort devices such as portable fans. Table 3.5 groups the sources of uncertainty in WBSM (Heo, 2011). Furthermore, a truly naturally ventilated building is expected to maintain occupants' thermal comfort during warm periods of the year without relying on mechanical cooling. Therefore, energy data is not suitable for such model calibration under natural ventilation mode of operation. As a consequence, calibrating WBSM for natural ventilation involves compounded uncertainties in each group in table 3.5.

Table 3.5 – Sources of uncertainty in WBSM (Heo, 2011)

Category	Factors
Scenario uncertainty	Outdoor weather conditions Building usage/occupancy schedule
Building physical/operational uncertainty	Building envelope properties Internal gains HVAC systems Operation and control settings
Model inadequacy	Modeling assumptions Simplification in the model algorithm Ignored phenomena in the algorithm
Observation error	Metered data accuracy

The currently criteria used to determine if a building energy simulation model is considered "calibrated" is set out by ASHRAE Guideline 14 (2014). Being generic, the criteria can be applied to any metric that could be suitable for natural ventilation. ASHRAE Guideline 14 (2014) uses two methods to represent how well the WBSM describes the variability in measured data. The first is named coefficient of variation of the Normalized Mean Bias Error (NMBE), which is a non-dimensional bias measure (sum of errors), between measured and simulated data. The NMBE is a good indicator of the overall bias in the model. It captures the mean difference between measured and simulated data points. However, positive bias compensates for negative bias, creating a cancellation effect. Hence, a further measure of model error is used. The second factor is the Coefficient of Variation of Root Mean Square Error (CVRMSE). This index allows one to determine how well a model fits the data by capturing offsetting errors between measured and simulated data. It does not suffer from the cancellation effect, like the previous factor. The NMBE and CVRMSE are calculated according to equation 3.27 and 3.28, respectively.

$$NMBE = \frac{\sum(y_i - \hat{y}_i)}{(n-1) \cdot \bar{y}} \cdot 100 \qquad \text{Equation 3.27}$$

$$CVRMSE = 100 \cdot \sqrt{\frac{\sum(y_i - \hat{y}_i)^2}{(n-1)}} \cdot \frac{1}{\bar{y}} \qquad \text{Equation 3.28}$$

where,

y_i: real measured data at hourly time i;

$\hat{y}_i$: simulation-predicted data;

$\bar{y}$: real measured data average.

According to ASHRAE Guideline 14 (2014), the simulation is considered validated if the value of NMBE is lower than 10% and the CVRMSE is lower than 30%, for hourly calibrated data. For monthly data, the guideline suggests that the NMBE and CVRMSE should assume the maximum value of 5 and 15%, respectively.

3.7 Limitations in Whole Building Simulation Model for Natural Ventilation

From the literature and the knowledge on the underlying physics-based models, the following limitations can be outlined on WBSM for supporting natural ventilation.

- Due to the mixed-model assumption (*i.e.* fully-mixed air in a space) in AFN, the airflow patterns, temperature stratification and the velocity fields within a room are not modelled, which imposes imprecisions to the simulation. Especially for naturally ventilated spaces that are subject of drafts, thermal stratification and non-uniform flows. Though, zonal models applied to those types of spaces can reduce those errors.

- The inability of AFN to represent the coupled approach for outdoor and indoor airflows (*i.e.* neglect the momentum of the outdoor airflow) affects the predictions of airflows and draft discomfort, from wind turbulence and gustiness, nearby windows and other large envelope openings (Murakami *et al.*, 1991; Kato *et al.*, 1992; Etheridge and Sandberg, 1996; Seifert *et al*., 2006; Karava *et al*., 2007, 2011; Kobayashi *et al*., 2010). Therefore, even though the simulations may be accurate from a thermal balance point of view, they may completely misrepresent the thermal discomfort/comfort in naturally ventilated spaces.
- Wind speed is variable and gusty in nature and its direction changes every second. Wind pressure coefficients (C_p) are surface averaged and typically derived from wind-tunnel tests or parametric analyses. Cóstola *et al*. (2010) compared calculations of airflow rate using local and surface-averaged C_p and results indicated large uncertainty in the calculated flow rate using the surface-averaged pressure coefficient. The weather data used to estimate the C_p are limited for each time step. Hence, the coefficients adopted are not representing the wind dynamic behaviour that occurs in that time step, but is restricted to singular value.
- Characterization models for all types of envelope openings are lacking. Furthermore, airflow characteristics change with the degree of opening, and the incidence angle of the wind. These changes are often not fully-reflected in the models.
- According to Caciolo (2009), the AFN models cannot represent single-sided ventilation, as it is mainly driven by turbulent fluctuations of wind pressures are neglected in nodal models. Furthermore, Balaras *et al*. (1999) determined that there were significant errors in assessing single-sided ventilation with high wind speeds.
- CFD simulations, coupled with AFN can address the limitations above. However, CFD involves limitations of its own that reduce the analyses to very specific aspects or areas, and often reduce the use of CFD to steady-state simulations on two-dimensional flows.
- From the literature, it is observed a lack of research in model calibration methods to validate WBSMs for natural ventilation. Due to the increased level of uncertainties in

the natural driving forces and the effects of human behaviour, different levels of measurements are required, which are not typically available through the building automation system.

Belleri (2013) summarizes the WBSM limitations in supporting natural ventilation as follows:

- Temperature distribution within air volumes (*e.g.* stratification) cannot be determined;
- Air speed in rooms cannot be calculated;
- Heavily dependency on coefficients like wind profile exponent, wind pressure (C_p) and discharge coefficient (C_v);
- Local surface convection determination is limited by the insufficient resolution;
- Turbulent fluctuations of wind pressures are neglected;

In general, due to the increased complexities involving in natural ventilation (compared to pure mechanical ventilation) the whole reliability of using WBSM to accurately represent building airflows under natural ventilation regime can be questioned. To overcome this concern, researchers often rely on uncertainty analyses. Breesch and Janssens (2007) have chosen the Monte Carlo Analysis (MCA) to assess this uncertainties; this approach performs multiple evaluations with randomly selected model input factors and can deal with correlated input parameters. The authors carried out the following steps: (1) selection of a range and distribution for each input parameter, (2) sample generation from these distributions, (3) evaluation of the model for each element of this sample, (4) uncertainty analysis and (5) sensitivity analysis. The determination of the uncertainty analysis is straightforward, as the expected average value and variance of the output are estimated. This is done using the global sensitivity indicator Standardized Regression Coefficient (SRC) (based on regression analysis). This coefficient measures the effect of the variation of an input parameter with a fixed fraction of its standard deviation on the variation of the output, while all other input parameters equalize their expected value. However, conducting a comprehensive uncertainty analysis is out of the scope of this research. To deal with this issue, this research will rely on sensitivity analyses to help understand the relative relevance of the factors affecting natural ventilation airflows.

4. PROBLEM STATEMENT

Recently, the use of natural ventilation is being promoted as a sustainable, “green”, and a passive cooling alternative; but designers and architects still use rules of thumbs in order the implement natural ventilation strategies. Consequently, natural ventilation is being not rigorously analyzed. In addition, there is a lack of consistency in the literature in assessing natural ventilation using simulation and field testing. Thus, one premise of this research is that natural ventilation assessment can be better supported by using dynamic tool, based in suitable models, and field testing.

According to Belleri (2013), available building simulation tools allow users to integrate energy models with AFN models providing quantitative information on natural ventilation performance both in terms of energy use and indoor environmental comfort. These tools can be used to support early design decisions, which have the highest influence on building energy performance. Due to the complexity of the simulation and the lack of knowledge and measured data, the natural ventilation simulations in practice often have no engineering analysis base: modellers are not aware of the type and processing of the climate data required for the analyses, the airflow models and their capabilities, the boundary conditions needed according to the types of flows, the complexities in characterizing the openings, the process of calibration and validation for the simulation, and the uncertainties of all the factors involved. As a consequence, modellers use these tools as “black boxes” that with sufficient care in the inputs provide “sufficiently reliable” results.

As expected, the standards that establish the calibration and validation approaches for the WBSM exclusively focus on the energy consumption data. There is no pre-defined approach to the validation of models of naturally ventilated buildings, as the main focus. In the calibration and validation process, the relevance of the energy data for naturally ventilated buildings are lower than for normal cases. After all, the building under natural ventilation, apart for the equipment loads and lighting system, almost operates as a free-running building.

Moreover, it is important to understand how different factors that compose the natural ventilation strategy work in conjunction. Architects and engineers often know that a specific building feature or a juxtaposition of different elements support a more effective natural ventilation strategy in providing cooling for the building. But it is extremely hard for designers to quantify how much each factor that composes the natural ventilation strategy is actually effective in order deliver thermal comfort for the occupants.

5. RESEARCH APPROACH

5.1 Research Objectives

Firstly, this study aims to provide a systematic framework to natural ventilation assessment. The proposed framework is divided in simulation and field testing. In the simulation part, it is provided the necessary instructions for the development, calibration and validation of the WBSM for naturally ventilated buildings. A detailed flowchart for field testing is presented in parallel. Finally, the proposed framework is applied for the assessment of natural ventilation in the case study building.

Moreover, this research aims to evaluate whole building simulation models (WBSM) in supporting natural ventilation. It is identified the challenges and limitations involved in using this tools to assess natural ventilation. A number of limitations in using WBSM regarding natural ventilation are already exposed along the literature review, but a more in depth evaluation of those challenges, and how the industry is dealing with natural ventilation in WBSM, is shown throughout the thesis.

The validated WBSM for VanDusen case study is later used in order to analyze the factors that compose the natural ventilation of that particular building. Consequently, it is investigated the impact of each individual parameter to the whole effectiveness of the natural ventilation in that building. The parameters that compose the natural ventilation strategy are: solar shading system, building thermal mass, the building's solar chimney and indoor spaces connectivity. To limit the scope, the effectiveness of the natural ventilation is focused on the thermal comfort provided by this passive technology on the warmer season.

Through the completion of the research, it is expected to contribute to the knowledge on the assessment of natural ventilation using WBSM and field testing, and in the identification of critical aspects that compose natural ventilation strategy in a building.

5.2 Scope and Limitations

The assessment of natural ventilation may focus on different areas, such as the ventilation effectiveness, indoor air quality (IAQ), pollutant dispersion, energy performance, and thermal comfort. To limit the scope and make the research feasible in terms of time and resources, the effectiveness of the natural ventilation is focused on the thermal comfort provided during the summer period. Due to limitations imposed by the building owners, surveys were not applied to occupants' of the case study building in order to evaluate the occupant's thermal comfort or how they interact with the environment to achieve thermal comfort (*i.e.* windows opening, personal fans, clothing options, and etc.). The thermal comfort is evaluated by using the adaptive thermal comfort provided by ASHRAE Standard 55 (2013). Furthermore, the field testing and monitoring applied to the case study was limited to avoid extra intrusion to the building occupants. To narrow down the scope, it is chosen to not use computational fluid dynamics (CFD) to model key spaces in the case study building, like the building's solar chimney and the external wind pressure coefficient (C_p) across the building surfaces.

As calibration is not the main focus of the research, the calibration/validation methodology suggested to WBSM for natural ventilation is not presented in depth. But notwithstanding, the presented methodology should serve as foundation for future research. It is also excluded critical aspects of natural ventilation that could be left for future research, such as: developing integrative methods to help designers optimize natural ventilation, optimizing control strategies for natural and mixed-mode ventilation, and developing occupant-behaviour and occupant-technology interactions models to be incorporated in naturally ventilated buildings.

Other important topics were left out of this study to make the project tractable. These are: 1) models and methods to support a comprehensive climate and micro-climate analysis, 2) the study of algorithms to predict and assess occupants' behaviours and interactions with the building which are critical for natural ventilation performance, 3) incorporating uncertainty in natural ventilation assessments.

6. RESEARCH METHODOLOGY

The research methodology is centered on the development of a methodological framework for natural ventilation assessment. The framework will help to develop a better understanding of the capabilities and limitations of WBSM and field testing to support natural ventilation. Thus, the research methodology is divided as the following:

1. Conduct a review of the literature on the assessment of natural ventilation using Whole Building Simulation Models (WBSM) with the goal of finding the challenges and limitations in using such detailed building models to support natural ventilation design.
2. Development of the methodological framework for natural ventilation assessment. The framework is one of the main contributions of this research, as it carefully synthesizes knowledge from the literature and by the lessons learned from the case study.
3. Apply the framework to conceive the whole building simulation model (WBSM) of VanDusen case study.
4. Develop a WBSM of the case study building. WBSM development will pay special attention and apply more rigour to details that will affect natural ventilation simulation. The WBSM software used is IES-VE for the following reasons:
    - A model of the case study building developed in IES-VE by the mechanical design company was made available for this study. The model was particularly valuable given the complex geometry of the case study building.
    - The software IES-VE, developed in the UK, is a well-known software and recognized in the industry for its improved capabilities to support passive designs.
5. Monitoring the case study building during the summer operation.
6. Calibrate and validate the WSBM by using data from: field testing, local weather, and energy consumption data.
7. Analyse the importance of each individual parameter that composes the whole natural ventilation strategy in VanDusen.

6.1 Case Study Building

Using the framework proposed for natural ventilation assessment, the VanDusen case study is analyzed. The assessment of the naturally ventilated building involves: the development of the WBSM, its validation, and field testing and monitoring under natural ventilation.

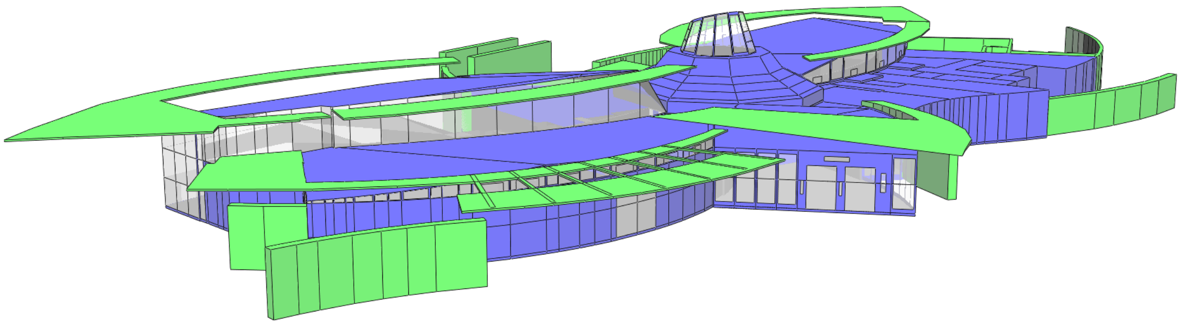

Figure 6.1 – VanDusen's WBSM using IES-VE

The details of the field testing are further presented (section 8.4) together with results (section 8.4.1). This data will serve to calibrate and validate the WBSM (section 8.6) but also to make a thermal comfort analysis using the recorded data (section 8.4.1.3). Later, the main design features that compose the case study's natural ventilation strategy are analyzed, with a sensitivity analysis (section 8.7). The factors to be analyzed are: solar shading system, solar chimney, building's green roof, and the connectivity between the spaces. The effectiveness of each element is assessed using the ASHRAE Standard 55 (2013) adaptive thermal comfort.

7. METHODOLOGICAL FRAMEWORK FOR NATURAL VENTILATION ASSESSMENT

It was observed a deficiency across the literature regarding the assessment of natural ventilation in buildings. Normally, this subject is presented in an inconsistent and fragmented way. This research tries to suppress that deficiency by introducing how the natural ventilation should be systematically assessed in a building. Furthermore, the framework is developed using the knowledge and the lessons learned during the assessment of natural ventilation in the case study building. The development of the framework comes as an effort to answer questions such as: how to develop a WBSM to support natural ventilation? What are the key components in a WBSM of a naturally ventilated building? How to model these components in the WBSM? How to calibrate/validate a WBSM for natural ventilation? How to assess natural ventilation in an existing building? What tools and sensors are needed? Is it possible (feasible) to monitor the building under these conditions? How intrusive the experiments could be done in the building? In case of possible limitations in the monitoring plan, what are the possible options?

There are usually two common paths usually taken when assess a naturally ventilated building is necessary: simulation and field testing. The framework illustrated by figure 7.1 introduces both processes and how they should interact in order to fully assess natural ventilation considering the limitation and constrains normally found in real cases.

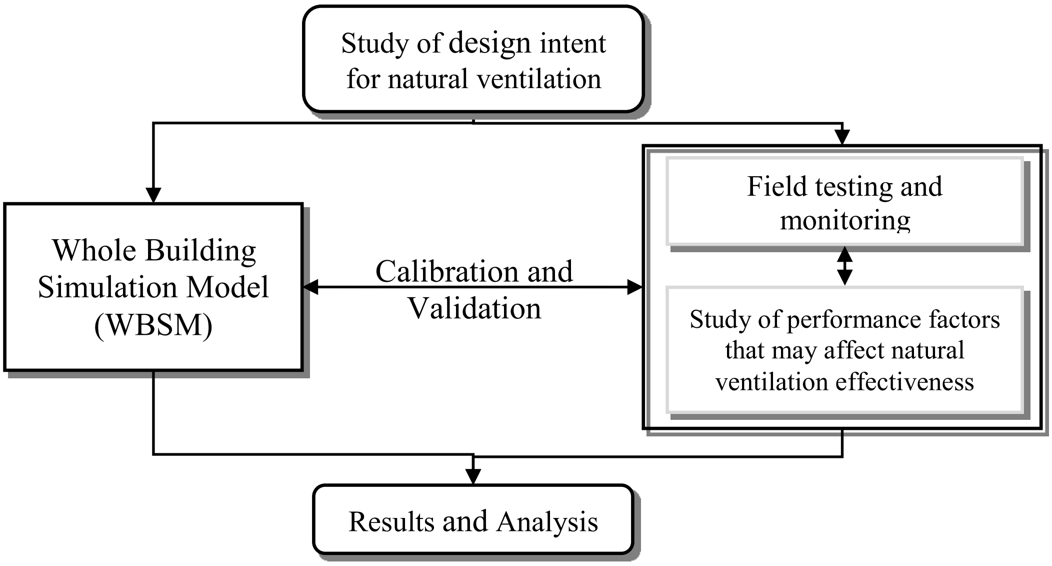

Figure 7.1 –Framework of natural ventilation assessment

Subsequently in the thesis, each aspect (simulation in section 7.2, field testing in section 7.3, study of building performance in section 7.4, and validation/calibration in section 7.5) is further detailed with more depth.

7.1 Study of Design Intent of Natural Ventilation

The design intent serves as the benchmark against which the natural ventilation performance is assessed. However, for practical reasons, the natural ventilation design intent is often not materialized. Thus, the study of the design intent should strive to answer the following questions: is the design intent properly documented in design reports? Are any changes to the design intent documented? How do changes to the design intent affect building performance under natural ventilation? If design documentation is not available, is it possible to interview the designers? What lessons can be learned from the design and construction process that could be improved in future designs?

7.2 WBSM Development for Natural Ventilation

Six different elements that compose the WBSM were established as foundation of having an optimal thermal/airflow model to support natural ventilation. They are: weather and climate, site and terrain, geometry and building orientation, building construction, building internal spaces, and connectivity. Between these factors, when dealing with natural ventilation simulation, there are two key elements: the building spaces (section 7.2.5) and the connectivity (section 7.2.6). For that reason, both factors are highlighted in figure 7.2. Figure 7.2 also illustrates how all elements interact and shows the ramifications and procedures to be done for each one in the WBSM.

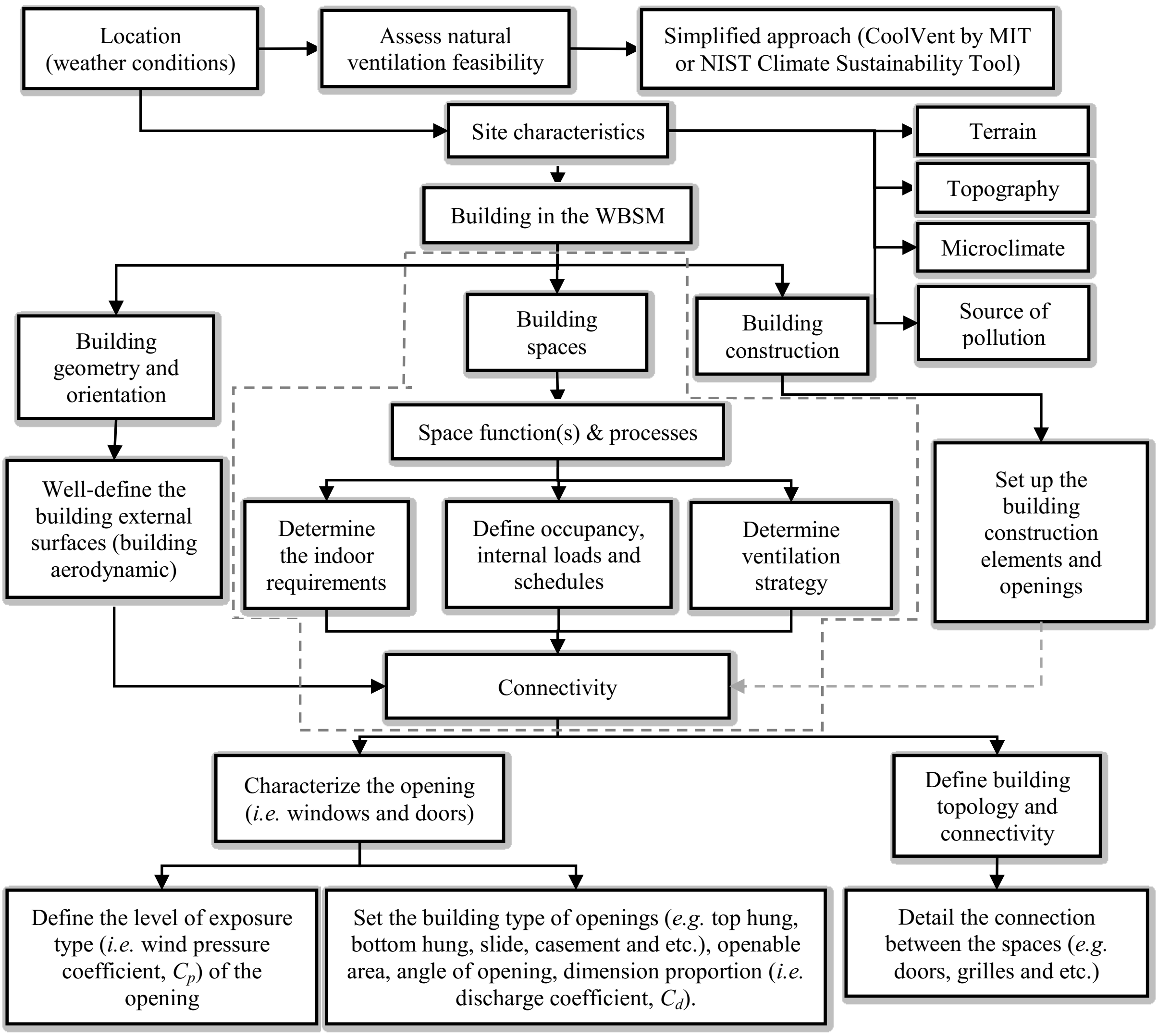

Figure 7.2 – WBSM flowchart development for natural ventilation

Regarding preliminary analysis on the use of natural ventilation, simplified approaches such as CoolVent (2017) and Climate Suitability Tool (2017) have been developed and are available for building practitioners. Further explanation for each element presented in figure 7.2 is explained on the following sections of this chapter.

7.2.1 Weather and Climate

There are two types of weather data formats normally used in WBSM: Design Day Weather, used for building loads calculations and equipment selection, and Hourly Weather Data, used for whole year energy analysis. The first consists of a typical hot summer day and a typical cold winter day and is referred to as design weather. The second consists of 8760 hours (365 days x 24 hours/day) of weather data for a full year. For whole year data, the source of weather data for WBSM usually can be broken into two major classes: historical data and typical weather years. Historical data is just "real" data measured from a particular location for a given period of time. Typical years, normally called as Test Reference Year (TRY), are artificial years assembled to match the long term data for a particular location using a particular statistical measure. The TRY is composed of 12 separate months of data each chosen to be the most average month from the collected data based on the last 30 previous years. Each software uses a specific format and source of the weather data, so it is important for the designer to be aware of the data that is being used. There are some weather files that take into consideration the climate change (warmer summers) in order to estimate futuristic weather data. Therefore, this might be a decision to be considered by the designers and building owners in order to have an effective natural ventilated building in a climate change scenario.

However, for the use of WBSM for existing naturally ventilated buildings, it is strongly suggested to use local weather data in the simulation. Prior results by Zhai *et al*. (2010) indicated that simulated building performance is significantly impacted by the use of locally measured weather, as compared to data available in the nearest weather station. The authors recommend the use of local weather data if possible, particularly for buildings with high solar gains. Belleri (2013) indicates that the wind speed profile is the main source of uncertainty for modelling natural ventilation. Notwithstanding, knowing the impact of the microclimate, variability of wind speed and direction, and influence of the surrounding's topography to the natural ventilation effectiveness, it is recommended the use of an on-site weather station.

For cases where installing a local weather station is considered unfeasible or impractical, it is recommended the use of weather data from a nearby weather station. This approach is not ideal but is more appropriate than to use weather data from a station that does not represent the building's microclimate. It is not guaranteed that the data from a nearby weather station is the best representation of the local weather conditions, but is possible infer that this data is fairly more precise than the data from a distant weather station.

7.2.2 Site and Terrain

Naturally ventilated buildings are highly sensible to external conditions (*i.e.* obstructions and topography), in specific to wind speeds and direction. For that reason, ASHRAE Fundamentals (2009) suggests using topography, landscaping, and surrounding buildings to redirect airflow and give maximum exposure to breezes to the building. Aware of the effect of the surrounding structures and obstruction on the building airflow, it is important to consider adjacent obstructions around the building simulation. However, it is necessary to observe if this option is available in the WBSM. For some cases, the software considers the obstructions and estimates how this factor influences the wind pressure coefficient (C_p) on the building surfaces. Notwithstanding, understanding the inner-works of the software is important in order to correctly consider external structures. Taking IES-VE for example, the software allows to model nearby structures and it takes this obstruction into consideration when calculating the solar and thermal gains. Nonetheless, adjacent structures have no direct influence on the wind characteristics across the building façade.

In summary, the site and terrain influence the simulation of natural ventilation and special care should be taken if it is observed severe restrictions (obstructions) to the building airflow openings and paths. However, if the building is localized in a flat area and its surrounding is composed by low-rise buildings with no significant obstruction to the airflow, the WBSM's surrounding could be modelled without the use of adjacent structures without major concerns.

7.2.3 Building Geometry and Orientation

The building geometries influence how the wind pressure coefficients (C_p) are considered on the building surfaces. The wind profile is critical to model to natural ventilation on WBSM (see section 2.1.2 and 3.2.1). The walls proportion, geometry and inclinations are what define the C_p across the surfaces. Remembering that WBSM uses database to estimate the C_p values (Cóstola *et al.*, 2009). The building orientation, on the other hand, has a special influence in the solar gains calculations, which is important for the thermal comfort provide by natural ventilation during summer usage. Along with the correct building orientation comes the shading system applied to the WBSM.

7.2.4 Building Construction

Building construction refers to the construction materials and assemblies that form mainly the envelope of the building, but also the interior floors and partition walls. They play a role in natural ventilation effectiveness by reducing heat gains and loses into and from spaces, and also in providing a thermal mass for reducing peak load gains in spaces and shifting peak indoor temperatures to unoccupied periods of the day. Air tightness is also a characteristic of building constructions; however, it is not expected to be a critical one because the air passing through unintended air leaks is over-powered by the ventilation air. For naturally ventilated building, the airtightness does not affect the precision of the WBSM (CIBSE AM10, 2005).

7.2.5 Building Spaces

The characterization of internal spaces for natural ventilation needs to consider the following: space function and processes, indoor environment requirements, internal loads, occupancy and schedule, consider ventilation strategy and buoyancy.

7.2.5.1 Space Function & Processes

The function of a space determines its occupancy, shape, dimensions, location, character, requirements, and the impact of the ventilation in the thermal environmental performance. Therefore, the function of a space dictates its natural ventilation performance requirements.

7.2.5.1.1 Indoor environmental requirements

Four categories of, interacting and often conflicting, requirements are typically considered for characterizing the acceptability of an indoor environment: indoor air quality (IAQ), thermal environmental, acoustic, and visual quality (ASHRAE Guideline 10, 2016). Meeting and exceeding those environmental requirements can lead to optimized environments that maximize well-being and performance, such as to: help workers be productive, minimize distractions, promote alertness, be suitable for learning, be pleasant, stimulate healing, etc. However, these requirements are often conflicting. For example cross-ventilation requires air circulation across open spaces, which often results in to noise and lack of privacy problems. Also, opening windows for natural ventilation may bring outdoor noise and air pollution into the building. Therefore, a careful assessment of these interactions between indoor environmental requirements is needed for natural ventilation designs.

7.2.5.1.2 Occupancy, Internal Loads, and Schedules

By their own nature, naturally ventilated buildings are particularly sensitive to occupancy dynamics and internal loads. As such, compared to mechanically ventilated buildings, extra-effort needs to be devoted to quantify and predict the building internal gains and schedules. A particular challenge in building performance simulation is considering building occupants because both their presence and behaviours affect the environment and are stochastic in nature. Occupants can be considered in WBSM as: a) generators of thermal loads, b) receivers and approvers of the indoor environment, and c) modifiers of the indoor environment. The accuracy of these three considerations depends on the proper quantification of the occupancy and the activities in the different spaces during typical days. However, consideration c) adds another level of complexity and increased uncertainty. For natural ventilation in particular, occupants operate portable fans, open windows, remove clothing, etc. All of which affect their satisfaction with the thermal environment. Occupants' behaviours/interactions with buildings are an active area of research nowadays (IEA-EBC, 2017). Several occupant behaviour/interaction algorithms have been proposed for window operation (Page, *et al.*, 2007; Tuohy *et al.*, 2007; Rijal *et al.*, 2014). However, these have not yet been incorporated in WBSM.

7.2.5.1.3 Consider Ventilation Strategy for the Space

At the space (room) level, natural ventilation can be divided in three types: a) cross-ventilation, b) buoyancy-driven ventilation, and c) single-sided ventilation. The ventilation strategy dictates the types of models that can be used, and that can be supported by the WBSM software. As discussed in the literature review, cross-ventilation is inherently supported by AFN (section 3.2), single-sided ventilation relies on empirical models (section 3.4.1), and buoyancy-driven ventilation requires improved characterization of airflows within a space, like zonal (section 3.3) or CFD model (section 3.5 and 3.5.2). Furthermore, the type of model used in the spaces is coupled with the rest of the building using the space's inter-connectivity.

7.2.5.1.3.1 Buoyancy Forces

When dealing with buoyancy forces in natural ventilation modeling, answering the following questions should be considered: are buoyancy forces an important component of the natural ventilation strategy for this building? In what spaces or zones should buoyancy forces be considered? How does the available software support buoyancy modelling? Would zonal modeling be sufficient to model the buoyancy forces? If not, CFD would be required? Does the WBSM incorporate CFD modelling? If not, how can I determine the boundary conditions for my CFD simulations? Is it possible to validate the CFD model by realizing field testing?

Furthermore, the importance of buoyancy in the design/operation of the building internal spaces should also be considered in selecting the level of field testing presented by section 7.3.

7.2.6 Connectivity

Connectivity was the term chosen to describe the airflow path between spaces, including internal and external air movement. The connectivity is divided in building topology (section 7.2.6.1) and characterization of the opening (section 7.2.6.2).

7.2.6.1 Building Topology

Apart from single-sided ventilation, the importance of the building topology is dependent of the strategy used in the building (*i.e.* wind-driven and cross-ventilation, buoyancy-driven stack ventilation, or the night ventilation). Furthermore, a number of times in the industry not enough care is taken to proper define the elements responsible to connect the internal spaces, such elements are composed by doors, grilles, louvers, ducts, holes, internal leakage area and etc. Even if properly applied to the internal spaces, a proper characterization of these openings is extremely important (section 7.2.6.2).

7.2.6.2 Characterization of the Openings

The literature review (see section 3.2.2) describes openings characterization and how WBSM normally characterizes the openings (windows, doors, grilles and etc.). Modern WMBS are facilitating the characterization of the openings by calculating the airflow using empirical and analytical models based on: the type of window, degree of opening, openings dimensions and proportions, wind exposure level and etc. However, the literature review and the case study building reveal that rigor is lacking in properly characterizing openings in WBSM for natural ventilation.

7.3 Natural Ventilation Field Testing and Monitoring

The field testing and monitoring is divided in 5 different levels (see figure 7.4 and table 7.2). This division is based on level of refinement in the analysis and in the level of intrusion that the experiments impose to the building occupants. The first level uses the building's building automation system (BAS) as the main source of data. The second level is relative to localized measurements made on-site, it consists of: pressure difference between spaces, measurements of temperatures and air speeds inside spaces to assess thermal stratification, and localized airflows. Third and fourth level correspond to building monitoring, but the level of intervention, number and types of sensors are different. In particular, if buoyancy forces are important, then microclimate monitoring (Level 4) is suggested. Level 5 analyzes the microclimate of the interior space by conducting a comfort study. This comfort study is composed by installing a microclimatic comfort station close to occupants (ASHRAE Standard 55, 2013) and conducting thermal comfort surveys for the building occupants. Independent of level of analysis, a local weather station positioned on-site provides the necessary data to the assessment of natural ventilation. After all, the weather is the main driving force in naturally ventilated building.

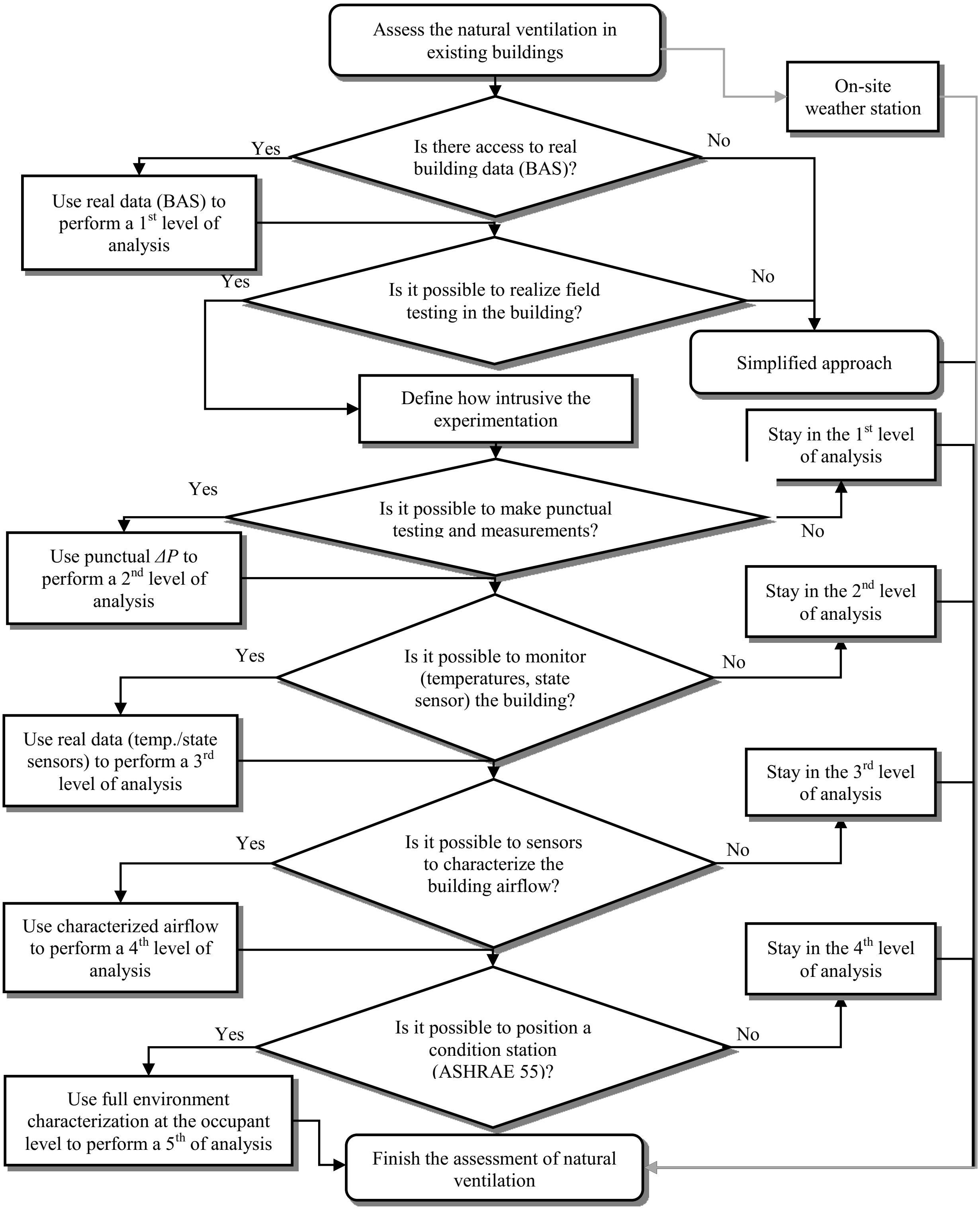

Figure 7.4 – Field Testing and Monitoring Flowchart

Table 7.2 details, depending on the levels of analysis, the factors analyzed through the building monitoring plan, and the outcomes of that data in relation with the modeling opportunities. The purpose of each level of analysis is also presented; it goes from model calibration to full environment characterization depending on the level chosen.

Table 7.2 – Level analysis used to assess natural ventilation in an existing building

Level of Analysis	Factors analyzed	Measurement detail			Indoor modeling			Outdoor modeling		Purpose
		Space	Topology	Micro climate	Multi zone	Zonal	CFD	Stack and wind profiles	CFD	
Level 1: BAS data	RH; Temp.; and CO_2	√			√			√		Calibrate models based on indoor space conditions
Level 2: Localized testing and measurements	ΔP Air speeds temperature	√	√		√			√		Calibrate models based on spaces connectivity and improved room thermo-fluid characterization
Level 3: Monitoring 1	RH; Temp.; CO_2; Operative Temp.; and Opening state	√	√		√			√		Improve detail on data for models calibration from levels 1 and 2
Level 4: Monitoring 2	Air speeds, temperature and ΔP		√	√		√	√	√	√	Enable thermal and airflow characterization at the microclimate and opening levels
Level 5: Comfortable study (ASHRAE 55)	RH; Temp.; CO_2; Operative Temp.; and Air speeds			√		√	√	√	√	Enable full environment characterization at the occupant level

Surveys in association with comfortable studies are the ultimate method to evaluate if natural ventilation is delivering the proper thermal comfort for its occupants. However, as this is not the focus of the research, this is not presented with the depth.

7.4 Study of the Performance Factors that may Affect Natural Ventilation Effectiveness

Buildings are complex and there are multiple interrelated factors that may impact natural ventilation effectiveness. These factors may be caused by unintended design and operational anomalies that may impact the year-round building performance; for example, changes in occupancy or use of spaces, mechanical heating or cooling that operate in parallel with natural ventilation, night-time ventilation, and etc. Furthermore, the impacts of these anomalies may be "visible" during heating mode operation, due to heating energy impacts, but may also impact natural ventilation effectiveness. Historic trend-log data from the building automation system (BAS), along with utility bills are the main tools to study the actual building performance and uncover apparent "anomalies" that may impact natural ventilation effectiveness. Last but not least, feedback from occupants may also leads into issues that may otherwise remain unnoticed (*e.g.* excessive solar gains, localized air drafts, glare, lack of control over the thermal environment, and etc.) but ultimately affect their satisfaction with a space that may be deemed comfortable from simulations.

7.5 WBSM Calibration and Validation for Natural Ventilation

Given the lack of a methodology for calibrating WBSM for natural ventilation, this research proposes a generic methodology. Further research is needed to develop a comprehensive methodology to calibrate WBSM for natural ventilation. The proposed methodology is driven by the considerations on the increased level of uncertainty involved in naturally ventilated buildings. The methodology, and the accuracy of the calibration, depends on the quality of the field testing data described in section 7.3. The methodology is applied to buildings that rely entirely on natural ventilation for cooling. Therefore, mixed-mode ventilation buildings are not included. The compounded sources of uncertainty in WBSM for natural ventilation is presented in table 7.3, the table is derived from table 3.5 by Heo (2011).

Table 7.3 – Compounded sources of uncertainty in WBSM for natural ventilation

Category	Factors	Example
1. Driving forces	Outdoor weather conditions	Stochastic nature wind as ventilation forces
	Human factors	Window's operation, personal fans, internal blinds, and etc.
2. Building physical/operational uncertainty	Building envelope properties	Assigning wrong envelope characteristics
	Internal gains	Incorrectly applying the internal loads; equipment and lighting
	HVAC systems	Assigning the wrong HVAC characteristics, efficiency and etc.
	Operation and control settings	Operation and control of automated windows
3. Model inadequacy	Modeling assumptions	Characterization of the openings; Single-side ventilation
	Simplification in the model algorithm	Modelling connectivity; fully mixed air characterization
	Ignored phenomena in the algorithm	Granularity of room air characterization
4. Observation error	Metered data accuracy	Lack of indoor occupancy data, indoor operative temperature, air speed and etc.

In table 7.3, the name "scenario uncertainty" in the first group has been changed to "driving forces". The reason for this change is that the driving forces for natural ventilation are inherently different from those in mechanically ventilated buildings; these are: the outdoor weather and the human factors, both directly affecting the building usage and operation. Figure 7.5 illustrates, for mechanically conditioned buildings, that weather and human factors have the greatest variability, and represent the lowest ability to influence the energy use.

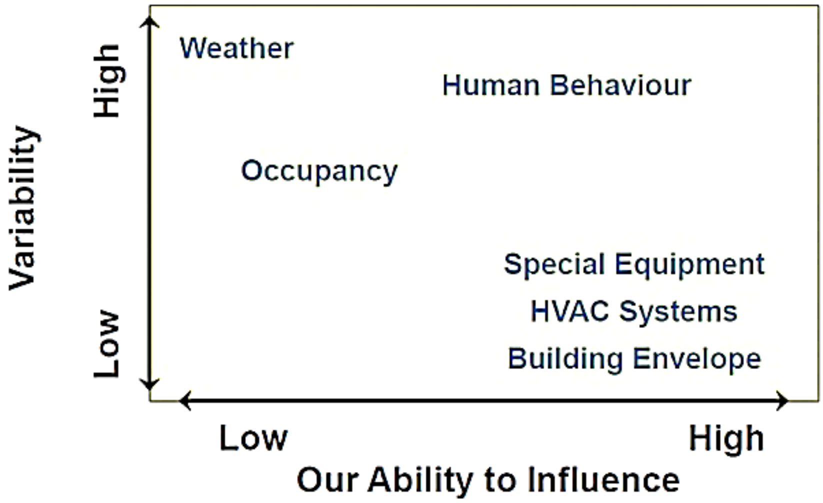

Figure 7.5 – Energy usage dependence

Therefore, weather and human factor need to be given careful consideration in WBSM calibration, even more than for mechanically conditioned buildings. Furthermore, again, unlike mechanically conditioned buildings, the measurement of these factors is crucial to reduce the observation error/uncertainty (group 4 at table 7.3).

Thus, it is suggested the following calibration process for WBSM under natural ventilation:

- Use of year-round simulation data with heating/cooling energy consumption. This is because cooling may be selectively used even in parallel natural ventilation, especially in mixed-mode ventilated buildings. For purely natural ventilation cooling, the year-round energy consumption makes it possible validate the internal loads applied to the building.
- Use of field testing data described in section 7.3. Including internal spaces and operative temperatures.
- Conduct occupant recurrent surveys to analyze how the occupants interact with the building. Identifying how the occupants operate the windows, use personal fans, and other thermal adaptive approaches.
- Realize an uncertainty model; similar to the one suggested by Coakley *et al*. (2014).

Figure 7.6 illustrates the methodology suggested. The quality of data serves as the base for the whole calibration process. The ultimate level of calibration is achieved through the use of the uncertainty analysis. The year-round energy consumption is put in parallel with the building data from the field testing (section 7.3). The survey complements both, and serves to complete the necessary information to the uncertainty analysis.

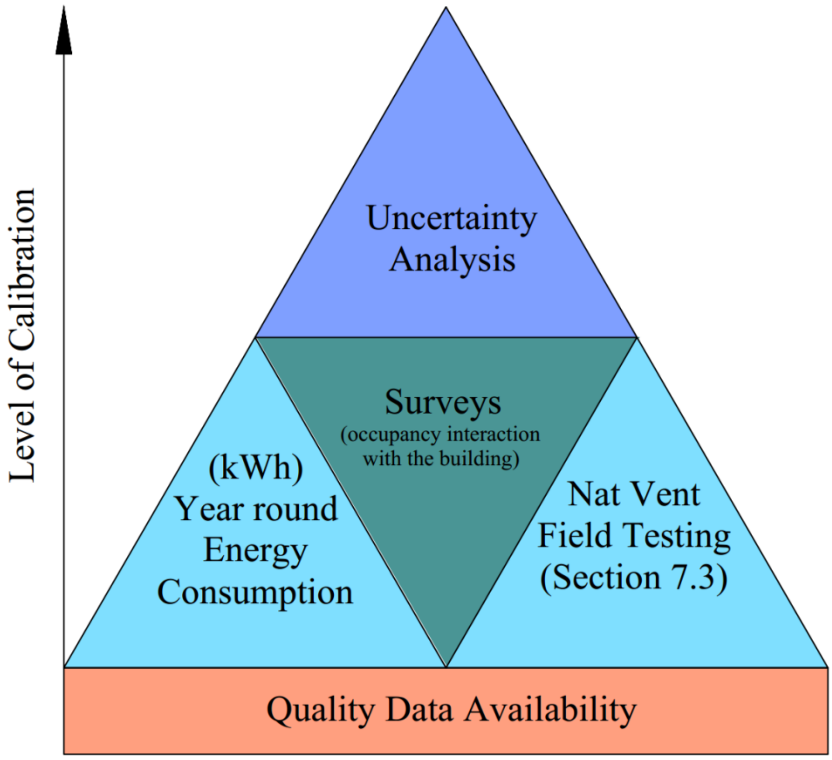

Figure 7.6 – Methodology for calibration of WBSM under natural ventilation

8. VANDUSEN CASE STUDY

8.1 VanDusen Botanical Garden

The VanDusen Botanical Garden is a landmark building that is being used as a case study. VanDusen's design aimed to achieve net-zero energy through a variety of technologies including solar hot water, photovoltaic panels, geothermal boreholes and natural ventilation. The main motivation for using VanDusen as a relevant case study building to the assessment of natural ventilation is that the building relies exclusively on natural ventilation to provide thermal comfort for its occupants during the summer.

Figure 8.1 – VanDusen Botanical Garden (http://www.ledcor.com/our-projects/environmental/sustainable-building/vandusen-botanical-gardens-visitor-centre)

According to VanDusen Gardens Sustainable Design Report (Cobalt, 2009), VanDusen's design followed an integrated passive design approach, focusing first on the climate and in the passive behaviour of the architecture before considering any active mechanical features. These architectures features incorporated in the natural ventilation design and are represented in the building as: solar shading system, building's thermal mass and green roof, and the solar chimney.

Figure 8.2 – Solar chimney in VanDusen (http://www.archdaily.com/215855/vandusen-botanical-garden-visitor-centre-perkinswill)

VanDusen's natural ventilation strategy relies on the combination of cross-ventilation and buoyancy-driven ventilation. The buoyancy-driven ventilation is generated by the spaces' high ceiling, plenum space at the top of the rooms, and a central atrium in association with a solar chimney. VanDusen's solar chimney (illustrated by figure 8.2) is designed to implement a more reliable buoyancy-driven natural ventilation strategy than just wind-driven ventilation. The solar chimney captures the solar radiation creating a pressure differential across the atrium where the solar chimney is positioned. Then, the upper openings exhaust the air from the atrium and other parts of the building, getting rid of the warmer air and letting the colder outside air comes from the other openings across the building. Moreover, buoyancy forces are especially evident in the atrium space, due to the association of the radiant floor (mechanical system), solar chimney and the large height of the space itself. Considering natural ventilation, Cobalt (2009) delineates the strategies utilized in VanDusen's design as illustrated in Figure 8.3.

Figure 8.3 – Natural ventilation design intent for Van Dusen (Cobalt, 2009)

VanDusen is operated to rely on natural ventilation from, approximately, May 1st through October 31st when the weather conditions are appropriate. According to the building control system, the windows shall be opened when outdoor air temperatures are higher than 14 °C and the space temperatures are higher than a predefined set point.

8.2 Study of the Design Intent of Natural Ventilation

In the case study, the building designers were not available for interview. However, an extensive documentation of the building design was available, which allowed to identify the initial natural ventilation intent. The VanDusen's natural ventilation strategy is composed of a number of design features, such as: solar chimney, green roof and high thermal mass, solar shading system, internal grilles, and a plenum space.

However, some of these initial features were not implemented to the actual building. The internal grilles and the plenum at the top of the internal spaces were not applied. The reason behind this decision is because those features would likely impose acoustical problems to some spaces. Hence, internal partitions were positioned separating key rooms such as the rental spaces (great hall, flex 1 and 2), library, classroom and volunteer room. For the rest of the spaces (garden shop, atrium, arrival hall, and restaurant), there is no internal division over a certain internal wall height. So, the plenum space is still partially present in the building. For the same acoustical reason, the internal grilles would were not applied to the actual building. The intent of these grilles was to connect these separated spaces with the rest of the building, allowing the air to flow to the plenum and then to be exhausted by the solar chimney, increasing the spaces connectivity.

The other design features (*i.e.* solar chimney, green roof and high thermal mass) that compose the natural ventilation design were successfully applied to VanDusen. The influence of each feature to the natural ventilation effectiveness is further analyzed (section 8.7 and 8.8).

8.3 WBSM Development for the Case Study

This section describes how the flowchart, earlier descried at section 7.2, is used in the development of the WBSM of the case of the study building. A previous whole building simulation model was given to the authors of this research. This first model was developed by Integral Group (2013) and it was used to obtain building loads to develop the net-zero analysis to the building. Throughout this section, a comparison between this previous model and the developed WBSM is made. With this comparison, it is traced a parallel between how the industry normally deals with natural ventilation and how natural ventilation should be addressed using WBSM.

The main effort in the development of the model was put in two factors represented in WBSM's flowchart (illustrated by figure 7.2) as the core of the natural ventilation simulation. The factors were: the building internal spaces (section 8.3.5) and the connectivity (section 8.3.6). Rigor in describing these key factors is often missing by designers and modellers. For the case study, a building that is relying in natural ventilation as the only source of cooling for the spaces, the original model lacked a careful modeling of the internal spaces loads, and most importantly, a detailed modelling of spaces' connectivity. Considering connectivity, the characterization of the openings was the feature that showed the biggest gap between the initial and the developed WBSM. It is hoped that this research demystifies the use of modern WBSM in the proper the characterization of the openings.

Notwithstanding, it is important to highlight the meticulous effort invested in modeling the building's geometry and construction characteristics by the designers and modellers. This shows the focus of the industry in the performance of the building envelope, which is understandable and desirable for climates with cold/mild winters, such as the one in Vancouver. Lastly, the section is divided similarly as the section 7.2, but one extra section is added showing the mechanical system applied to the model.

8.3.1 Weather and Climate

The WBSM uses a standard TRY weather file for Vancouver. Figure 8.4 shows the temperature for all the hours of the year. It is observed that the mild temperatures between May and September are suitable for natural ventilation. From March to October the temperature drops below 13 °C, which make makes natural ventilation for cooling impractical for most cases. For these range of temperatures, mechanical or hybrid ventilation become a more suitable option.

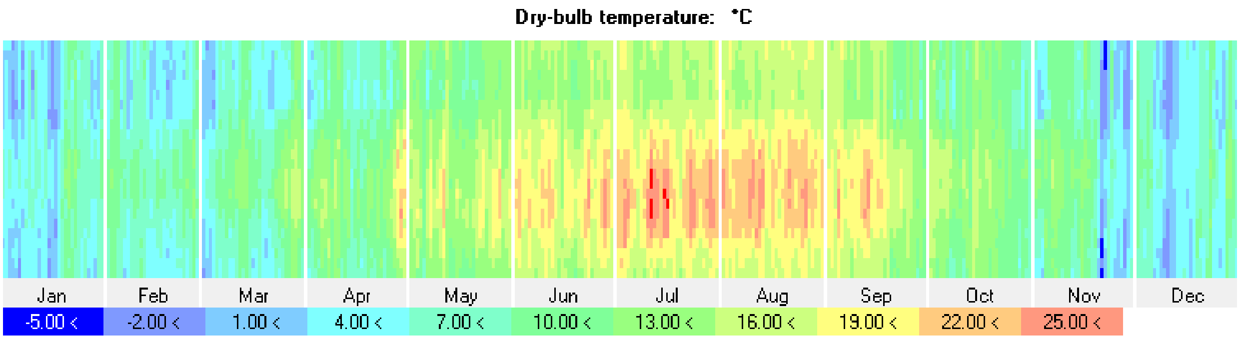

Figure 8.4 – Vancouver whole-year hourly temperatures

To isolate the suitable temperatures for natural ventilation figure 8.5 is presented. In the picture, the red points represent temperatures above 14 °C and the blue points temperatures below 14°C. This specific threshold of was chosen because according to VanDusen's controls design the windows that provide natural ventilation for the internal spaces should be open only when outdoor temperatures are higher than 14 °C and the spaces temperatures are above a certain specified setpoint.

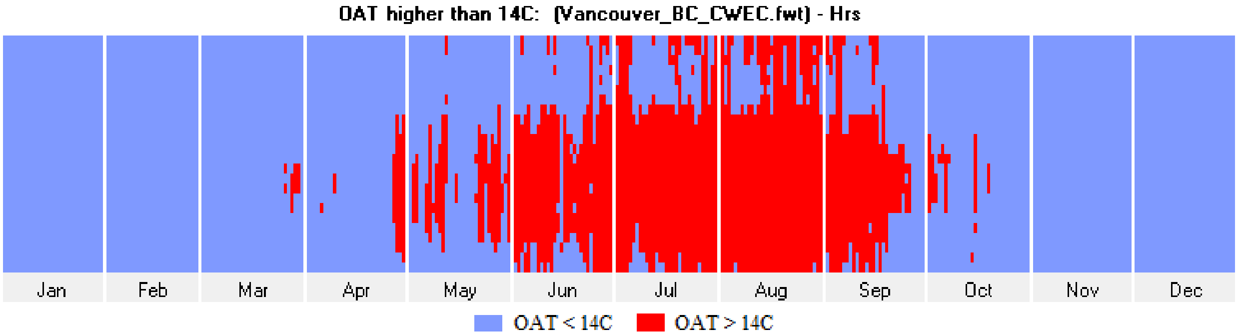

Figure 8.5 – Vancouver hourly temperatures above and below 14°C

During the whole year, 25.8% (2260 hours) of the total amount of hours the outdoor air temperatures are higher than 14 °C. When only the occupied hours are analyzed (between 9AM and 9PM), 35.9% (1572 hours) of the time the temperatures are that range. Those numbers show the potential of the use of natural ventilation for Vancouver's climate.

According to Mora (2015), the wind patterns in Vancouver are often modified due to "channelling" of winds by the local topography. The author claims that south-easterly winds are dominant all year, but in summer months there is an increase in their frequency, together with an increase in the winds from the west. The weather data used in the simulation endorses that statement, by indicating that the prevailing wind during the summer comes from east. Figure 8.6 illustrate distribution wind direction for the summer months.

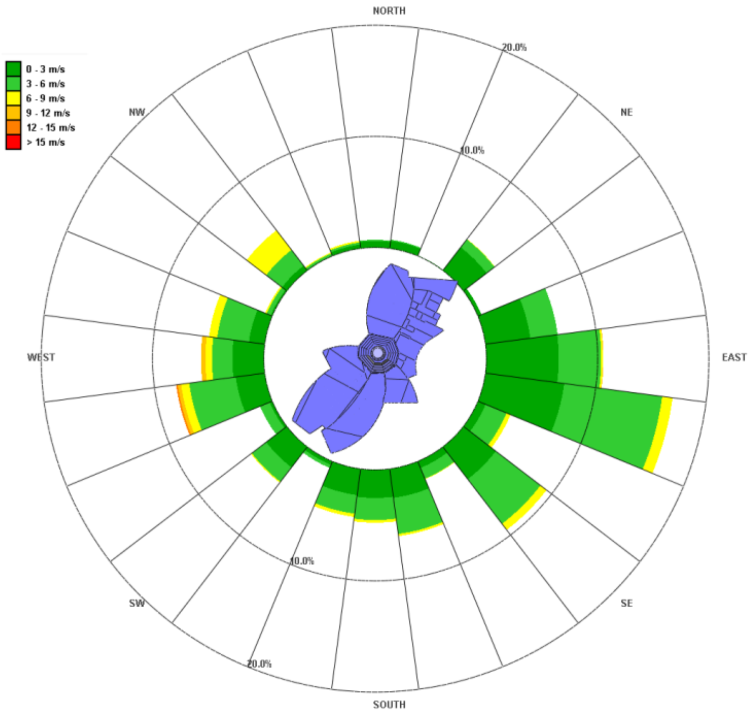

Figure 8.6 – Average wind speed and direction for VanDusen (June to August)

8.3.2 Site and Terrain

The case study building is surrounded mostly by green landscape: the botanical garden, trees, a small lake, low-rise residential buildings, and a park. The building's neighbourhood is not composed by high-rise buildings or any major obstruction to the airflow paths. For that reason, no obstruction or surrounding structure was positioned in the simulation space of the WBSM. Figure 8.7 shows a satellite photo the building's surrounding.

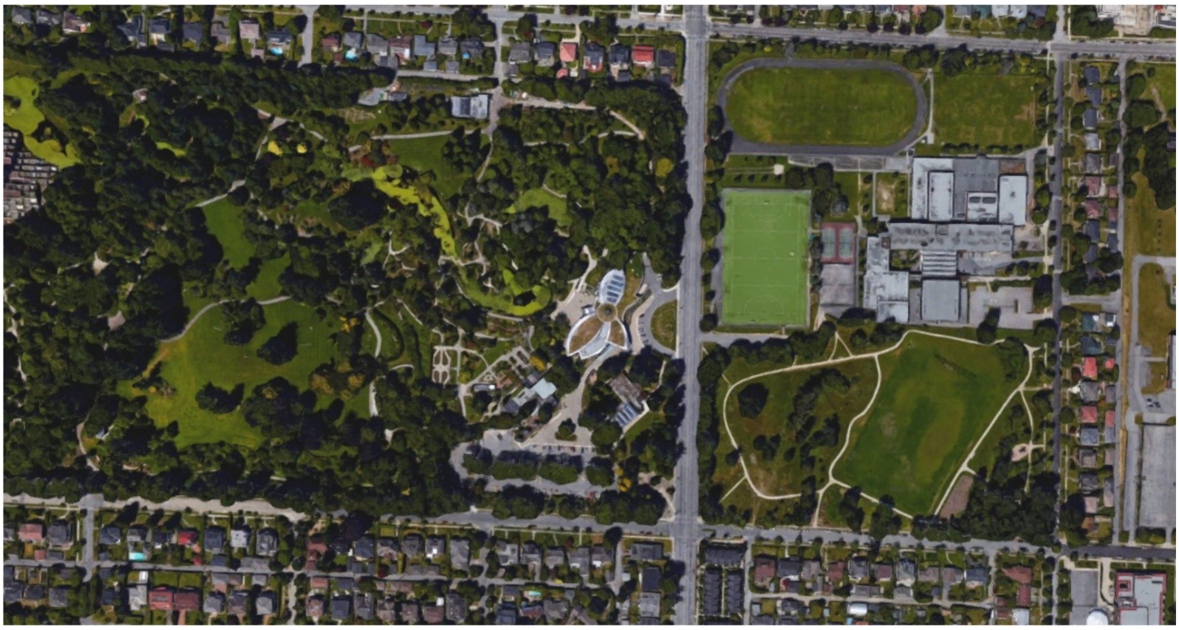

Figure 8.7 – VanDusen's site and terrain (Google Maps)

8.3.3 Geometry and Building Orientation

One of the main challenges in that specific simulation is the overall complexity of the building geometry. No changes were done in this feature from the original WBSM. Initially, the building geometry together with the shading system generated uncertainty in the process to estimate the building external pressure coefficients (C_p). One option earlier considered in the research was to use CFD in order to characterize the external pressures across the building surfaces. However, due to time and resource constrains it was chosen to use the standard approach of using the C_ps to calculate the wind pressure across the building surfaces and openings. Figure 8.8 illustrates how the building is oriented in the WBSM.

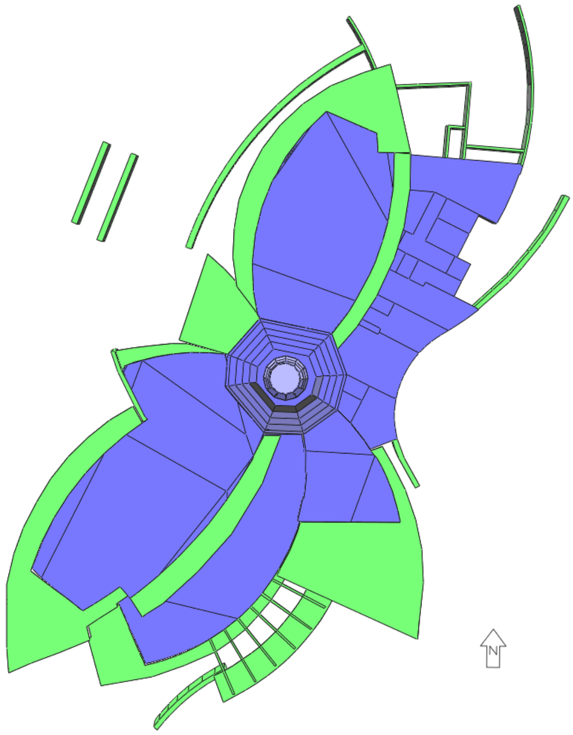

Figure 8.8 – VanDusen's orientation

The design of the Van Dusen includes a well-planned solar shading system. As observed in figure 8.9, b and c, special attention was given to south and east elevation in terms of high shading area and lower window-to-wall ratio.

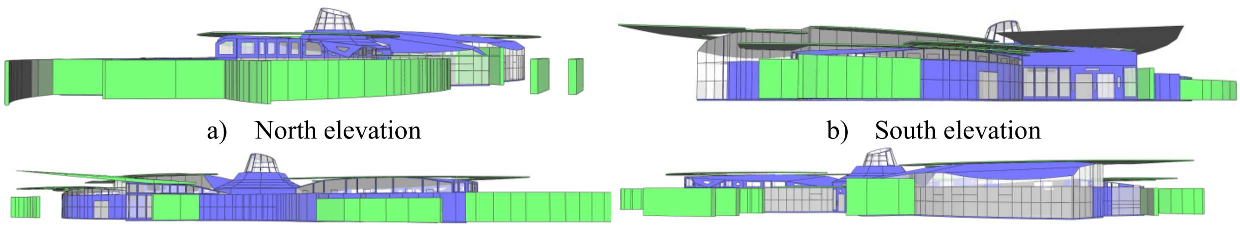

a) North elevation

b) South elevation

c) East elevation

d) West elevation

Figure 8.9 – VanDusen's elevations

8.3.4 Building Construction

Not differing from the building's geometry, VanDusen's envelope is complex; it uses a number of different materials in different configurations. The envelope is composed of a green roof, concrete walls, a high performance fenestration system, and concrete floor slabs. Apart from punctual small adjustments, the original WBSM properly represents the building construction. Figure 8.10 shows all the constructions setting applied to the model. Appendix A extensively details the envelope used at the WBSM.

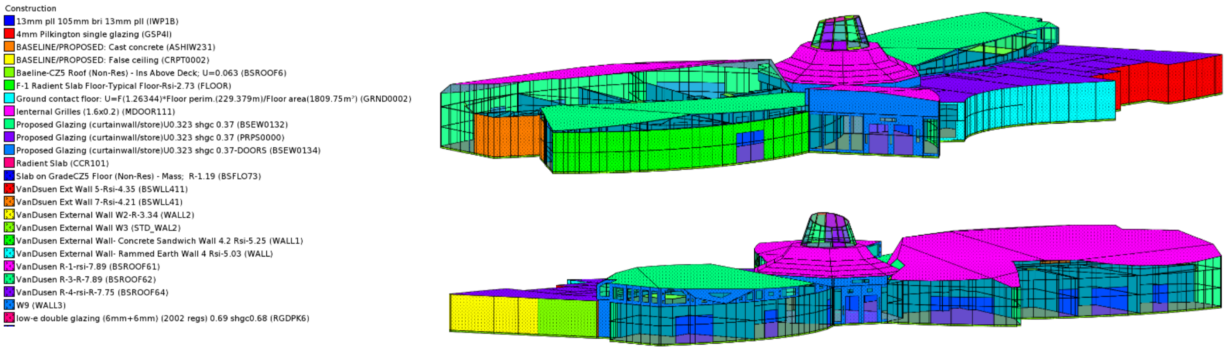

Figure 8.10 – Building constriction characteristics on the WBSM

The high thermal mass of the building is guaranteed by the presence of the building's green roof, external concrete and rammed earth walls, and the concrete floor slabs. This feature makes part of one of the elements that enhance the natural ventilation effectiveness for the building. In terms of airtightness, the WBSM followed the report by Integral Group (2013) that estimates the building's infiltration rate as 0.1 ACH (air changes per hour), a relative low value that represent the building higher airtightness. However, as explained earlier, for natural ventilation performance the airtightness does not have considerable influence on the final results.

8.3.5 Building Spaces

8.3.5.1 Space Function & Processes

The case study building is a multi-purpose single story building. The building consists of education and administration building comprising a library, visitors lounge, Garden shop, flexible spaces that may be rented out for meetings, a classroom and volunteer room. Figure 8.11 illustrates the building internal layout configuration.

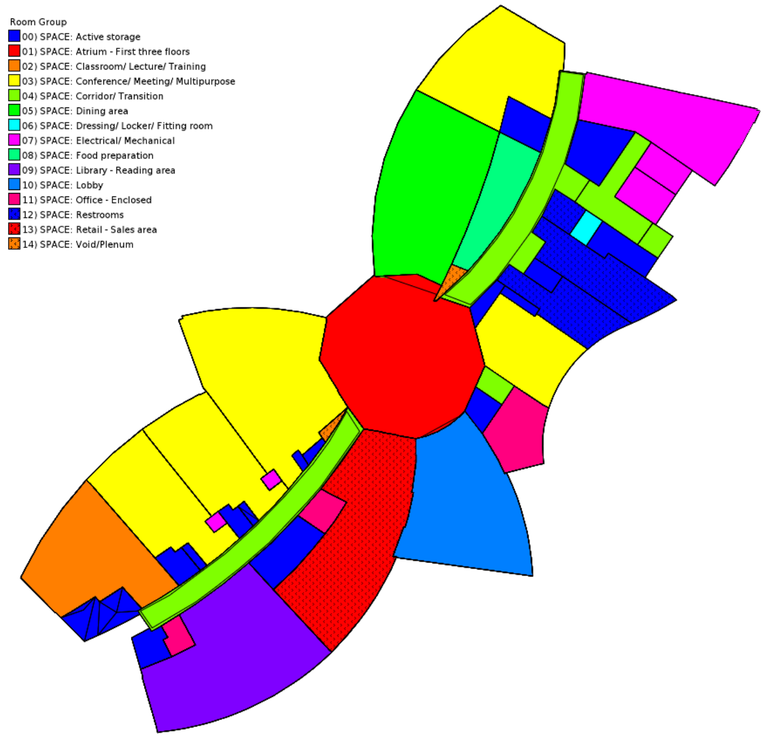

Figure 8.11 – Building internal spaces layout

Table 8.1 shows the function of each space according to the ASHRAE 90.1 (2010) parameters.

Table 8.1 – VanDusen's space functions

Room name	Space function
Arrival hall, Flex 1 and 2, Great hall, Volunteer room, Interpretative centre	Multipurpose
Atrium	Atrium
Garden shop	Retail
Garden shop office, Office, Library copy room	Office
Library	Library
Classroom	Classroom
Classroom storage, Flex 1 and 2 storage, South corridor storage, Main storage, Bike room, Shop storage, Library storage, Volunteer room storage, Janitor, Office storage, Locker	Active Storage
South corridor and North corridor	Corridor
Food service and Food preparation/servery	Food preparation
Men's and Woman's W/C	WC
Electrical and Mechanical room	Mechanical or Electrical Room

8.3.5.1.1 Occupancy, Internal Loads and Schedules

VanDusen's occupants are composed by visitors, people who work at the building and use the rental spaces. Due to limitations imposed by the building owners, no surveys were applied to the building's occupants. However, through informal conversation with the occupants, it is possible to trace some previous observations on the how they interact with the building to reach thermal comfort during the summer when natural ventilation is being used. Firstly, the occupants claim some thermal discomfort during the hot season. During that period is normal to find personal fans positioned across the building. As expected, the occupants also open the doors to increase the airflow. However, the building occupants do not have control on the mechanically operated windows. In general, a part of the building occupants are not fully able to interact with the building to achieve the thermal comfort. This raises the question if the adaptive thermal comfort model is the most suitable to analyse the thermal comfort for the case study. Notwithstanding, the adaptive model is further used to evaluate the effectiveness of natural ventilation in VanDusen because occupants still have some level of environmental control by being able to maintain open the exterior doors of all main spaces when needed (as intended for the summer), by being able to open some windows in the library, and by using personal fans, as noticed in four spaces.

However, one alternative to the adaptive model, Fanger's model is demonstrated by Beizaee *et al*. (2012) to not accurately predict the thermal comfort in naturally ventilated buildings. The authors concluded that the Fanger's PMV is not accurate enough in predicting people's thermal sensation in naturally ventilated homes and offices in the UK during the summer and in both homes and offices the PMV model under predicts the actual thermal comfort conditions and consequently predicts higher neutral temperatures.

In terms of the equipment and lighting loads, the initial WBSM used predefined values suggested by ASHRAE Fundamentals (2009) and ASHRAE 90.1 (2010), respectively. Notwithstanding, the developed WBSM used equipment loads estimated by Integral Group (2013) in their net-zero building analysis, and the lighting loads are based on the original lighting design provided by Bridge Electric Corp. The tables with all data applied to the

WBSM for equipment and lighting loads, for each space, are presented in the appendixes B and C, respectively.

The schedules adopted in the WBSM follow table 8.2 and based on the report developed by Integral Group (2013).

Table 8.2 – VanDusen's operation hours (Integral Group, 2013)

Garden and Gift shop hours	
January and February	10:00 AM to 4:00 PM
March	10:00 AM to 5:00 PM
April	10:00 AM to 6:00 PM
May	10:00 AM to 8:00 PM
June, July and August	10:00 AM to 9:00 PM
September	10:00 AM to 7:00 PM
October	10:00 AM to 5:00 PM
November and December	10:00 AM to 4:00 PM
Library Hours	
Tuesday through Friday	10:00 AM to 3:00 PM
Wednesday evenings	7:00 PM to 9:00 PM
Sunday	1:00 PM to 4:00 PM
Monday and Saturday	Closed

8.3.5.1.2 Ventilation Strategy for the Space

At the space level, the initial design intent considered, for most of spaces, a buoyancy-driven and cross-ventilation strategy. However, due to the modifications made in the building (section 8.2), these ventilation strategies were not followed for the following spaces: great hall, flex 1 and 2, classroom and volunteer room. For theses rooms, due to mainly acoustic reasons, natural ventilation is mainly provided via single-sided ventilation. For the rest of spaces the initial design strategy was applied in the real building. Notwithstanding, there were rooms that even in the initial design intent did not explicitly have a natural ventilation strategy applied, such as: the garden shop office and the library copy room. Table 8.3 summarizes the design and applied natural ventilation strategy for the different spaces.

Table 8.3 – Design and applied natural ventilation strategy for VanDusen

Room name	Design Natural Ventilation Strategy	Applied Natural Ventilation Strategy
Great Hall, Flex 1 and 2, Classroom and Volunteer room	Buoyancy-Driven and Cross-Ventilation	Single-Sided Ventilation
Atrium, Arrival Hall and Interpretative centre	Buoyancy-Driven (Solar Chimney) and Cross-Ventilation	Buoyancy-Driven (Solar Chimney) and Cross-Ventilation
Garden Shop, Library	Buoyancy-Driven and Cross-Ventilation	Buoyancy-Driven and Cross-Ventilation
Garden shop office and Library copy room	None	None
Food service and Food preparation/servery	Buoyancy-Driven and Cross-Ventilation	Buoyancy-Driven and Cross-Ventilation
South corridor and North corridor	Buoyancy-Driven and Cross-Ventilation	Buoyancy-Driven and Cross-Ventilation

VanDusen's solar chimney is one of the main natural ventilation strategies applied to the building (see table 2.2 for the main natural ventilation strategies). The following observations can be made on the design of the solar chimney. Its height does not seem to be tall enough to create a considerable temperature and pressure difference to allow a stable and constant airflow. The solar chimney needs to have a considerable length and height to collect heat from the sun in order to have an optimum performance. Moreover, it was observed that the atrium, where the solar chimney is located, is directly connected to the arrival hall. Both spaces have doors that are kept open during the summer. This creates cross-ventilation between these two spaces that seem to bypass the rest of the building. Even if only the atrium door is maintained open during the summer, the buoyancy current created by the solar chimney is likely to draw air from this "least-effort-path" nearby door, instead of drawing it from the rest of the building.

8.3.5.1.2.1 Buoyancy Forces

Regarding the buoyancy force, the initial WBSM divided each internal space in three zones stacked vertically (see figure 8.12). No explanation in the design documentation was found on the reason for such division of spaces. The main reasons for such configuration could be: a) to handle the complexity of the roof shape, b) to account for buoyancy in each space, as all the spaces have high ceilings. However, this approach successfully represents the buoyancy forces in the spaces and end up working similarly as a zonal model.

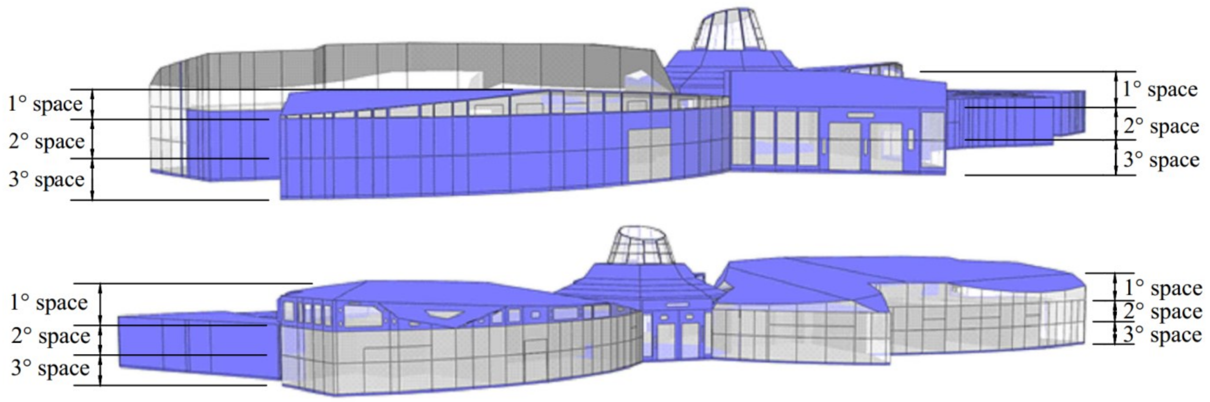

Figure 8.12 – Building internal spaces configuration

Similarly, especial attention was given to the buoyancy forces in the atrium in association with the solar chimney. For that space, the approximated zonal approach was used. That space was divided in four intermediate spaces, as illustrated by figure 8.13.

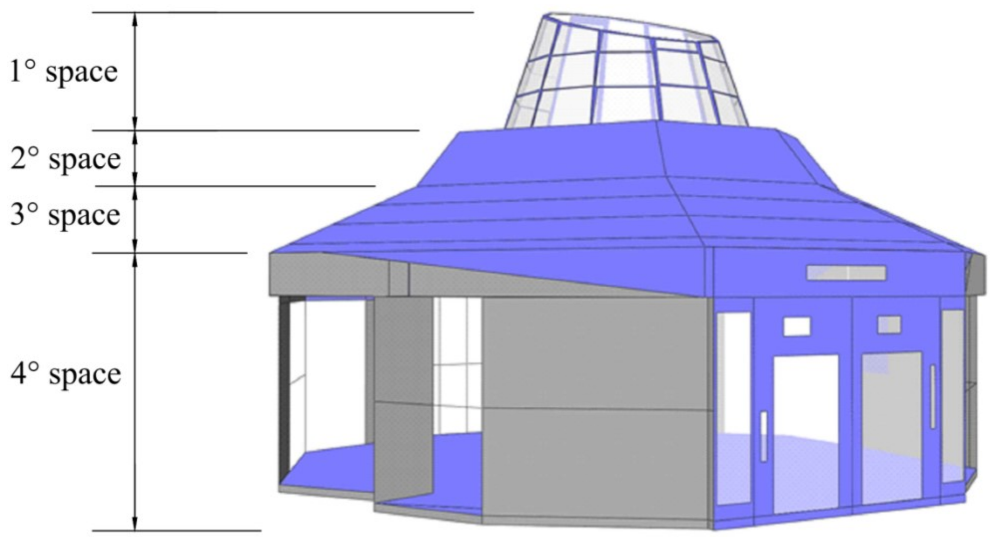

Figure 8.13 – Atrium representation at the WBSM

8.3.6 Connectivity

8.3.6.1 Topology

The initial design intent for the building was to use a plenum space to capture the warm air throughout the building and then exhaust it through the solar chimney (section 8.2). The initial WBSM was modelled using that approach (see figure 8.14). However, in the developed WBSM the plenum (in blue) was partitioned at: great hall, flex 1 and 2, classroom and volunteer room.

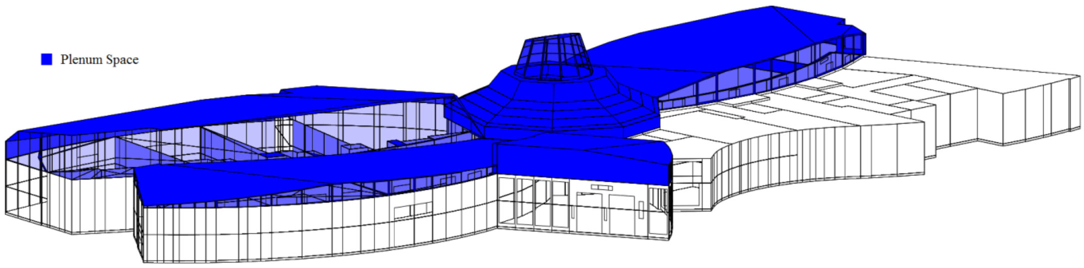

Figure 8.14 – Plenum space at the WBSM

Moreover, the initial design intent also considers the presence of grilles between the spaces that have of openings, generating the airflow paths that, in theory, would flow through both corridors and then to be exhausted by the solar chimney. However, those grilles were not installed in the building.

8.3.6.2 Characterization of the Openings

The initial WBSM did not characterize the openings with enough level of detail. Instead, it only applied over-sized custom sharp edge orifices for all windows/doors, and did not specify the type and degree of opening, dimensions, and etc. Regarding the real openings, VanDusen's openings are composed by top hung windows and side hung doors. The majority of the windows are automatically open following certain control logic. But there are manually operated windows positioned at the lower part of the library (4 windows) and at the office (2 windows), when the building occupants feel uncomfortable they have the freedom to change and adapt the environment by opening those windows. The automatic windows are open when the outside temperature is higher than 14 °C and the spaces temperatures are above a specific setpoint. When these conditions are met, the windows are open providing cooling for the spaces. However, if the internal spaces temperature drops below the setpoint (plus the dead band) the windows are closed. When the outdoor air temperature goes below 14 °C the windows should be closed, as well. In VanDusen's WBSM types of openings were set up as the following:

- Natural ventilation openings: describes the top hung windows;
- Oculus solar chimney openings: describes the windows at the solar chimney;
- Doors natural ventilation openings: describes the doors used for natural ventilation;
- Internal grilles: represents the grilles (not installed) connecting the internal spaces.

Apart from the internal grilles that are always open or close depending on the simulation, all the openings used the same logic behind its operation: they open when outdoor air temperatures are above 14°C and the internal space temperature is higher than 24°C. Figure 8.15 shows the position of all type of openings throughout the building. Each colour represents a different opening type.

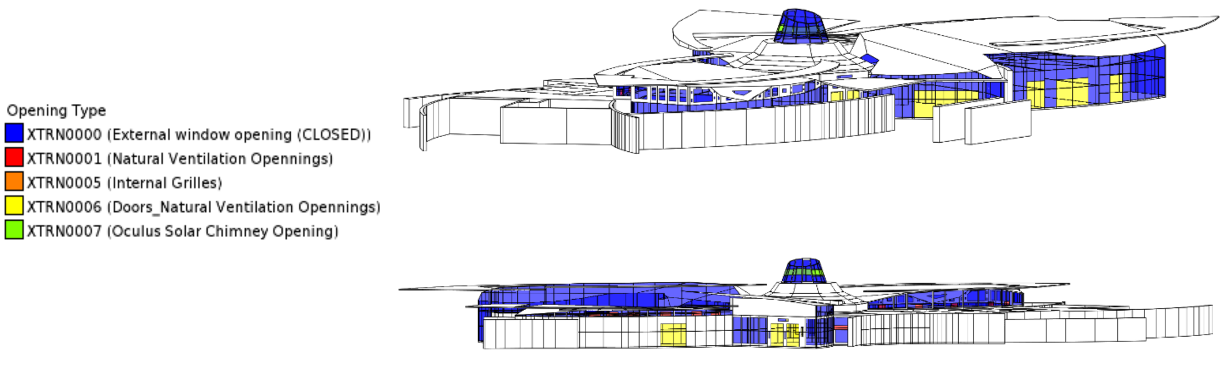

Figure 8.15 – Opening types on the WBSM

Table 8.4 shows all the characteristics of the openings existing at the building and applied to the WBSM.

Table 8.4 – Opening characteristics on the WBSM

Kind of opening	Position of the opening	# of openings	L (mm)	h (mm)	Opening category	Max angle (°)	Opening area (m^2)	Proportion (L/h)	Modulation profile
Windows (Automatic)	Solar Chimney	8	600	350	Top Hung	45	0.21	1.71	Ta>24
	North corridor	5	1000	500	Top Hung	25	0.50	2.00	Ta>24
	Library	4	1400	500	Top Hung	25	0.70	2.80	Ta>24
	Garden shop	2	1400	500	Top Hung	25	0.70	2.80	Ta>24
Windows (Manual)	Office	2	1380	500	Top Hung	25	0.69	2.76	Ta>24
	Library	4	1400	500	Top Hung	25	0.70	2.80	Ta>24
Doors (Manual)	Flex 1	1	1935	2750	Side Hung	90	5.32	0.70	Ta>24
	Flex 2	2	1935	2750	Side Hung	90	5.32	0.70	Ta>24
Doors (Manual)	Classroom	1	1935	2750	Side Hung	90	5.32	0.70	Ta>24
	Atrium	2	1935	2750	Side Hung	90	5.32	0.70	Ta>24
	Great hall	3	2030	2750	Side Hung	90	5.58	0.74	Ta>24
	Food service	2	1935	2750	Side Hung	90	5.32	0.70	Ta>24
	Volunteer	2	1935	2750	Side Hung	90	5.32	0.70	Ta>24
	Arrival hall	2	1935	2750	Side Hung	90	5.32	0.70	Ta>24
Grilles	Internal spaces	8	1600	200	Internal grilles	0	0.32	8.00	Always open/close

8.3.7 Mechanical System

The original model obtained from the designers did not have the mechanical system. Therefore, the original WBSM was used to obtain the internal loads on the building, which were used to estimate the building's energy consumption through external calculation methods. Even though modeling the mechanical system was not the main concern in this research, the mechanical system was fully developed by the author of this thesis and later used for the year-round model validation/calibration (section 8.6). The mechanical system is composed by displacement ventilation system, radiant floor slabs, solar thermal panels, ground source heat pump (GSHP), heat recovery ventilator (HRV), domestic hot water (DHW), and etc. Figure 8.16 illustrates the mechanical system at the WBSM.

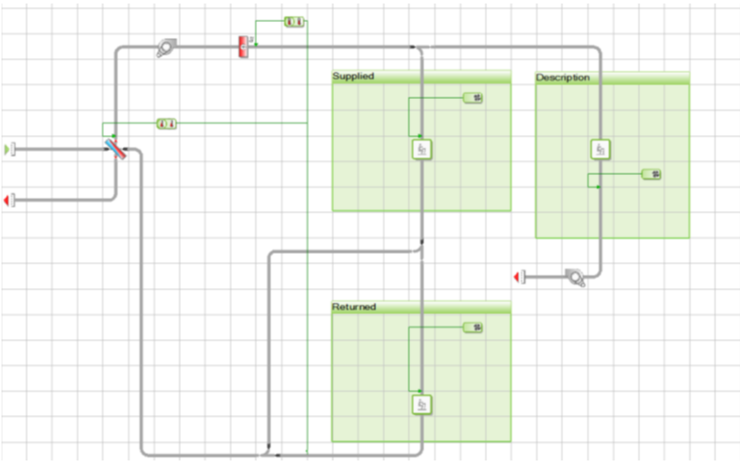

a) air side

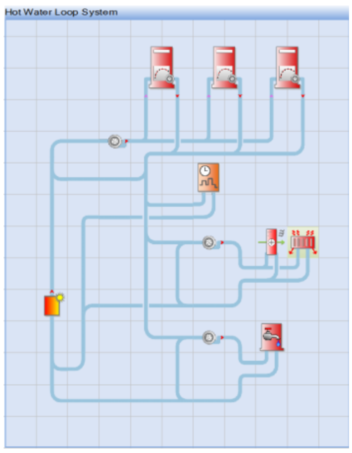

b) water side

Figure 8.16 – Mechanical system at VanDusen (IES-VE)

8.4 VanDusen Field Testing and Monitoring

According to the levels of analysis described in the previous section and from the project constraints and the instrumentation available, VanDusen's field testing and monitoring is characterized as level 3. In this level, sensors are positioned in the building to monitor its performance for a certain period of operation. The factors analyzed in the building monitoring are: internal spaces air temperatures, relative humidity, CO_2 concentration rates, and open/close status of openings. In addition to that, in order to monitor the outdoor environment, a weather station was positioned on the building's roof.

Two kinds of sensors was positioned at the indoor, the first is a data logger (Hobo® MX1102 data logger) responsible to measure air temperature, relative humidity, and CO_2 concentration. The time step adopted to measure those factors was every 5 minutes. The second sensor used is a state sensor (E-348-UX90-001) responsible to record the opening and closed status of the openings. Differently than the previous one, this sensor records any change that occurs in the opening status, without the need to establish a fixed time step. To monitor the outdoor environment, a weather station was installed on the building's roof. Table 8.5 sums up all the sensors used in the case study building.

Table 8.5 – Equipment used for monitoring VanDusen under natural ventilation

Sensor types	Measurement	Number of sensors
Hobo® data logger	Air temperature, relative humidity and CO_2 concentration	11
Sate sensor	Open and close status of the openings	16
Weather station	Outdoor air temperature, relative humidity, solar radiation, rain precipitation, wind speed and direction	1

Figure 8.17 illustrates the building's layout and the position of each sensor throughout the building.

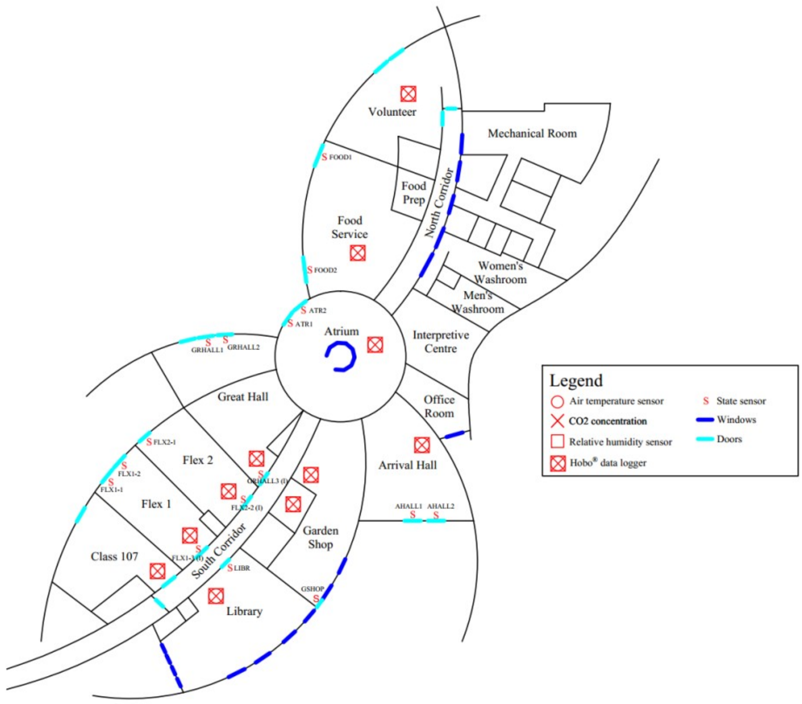

Figure 8.17 – Indoor monitoring plan for VanDusen under natural ventilation

Table 8.6 presents the label used to identify each sensor across the building.

Table 8.6 – Sensors' label and position [1]

Sensor types	Location	Label name	Serial number
State sensor (open/close)	Atrium	ATR1	10544884
		ATR2	10544885
	Food service	FOOD1	10458642
		FOOD2	10492460
	Arrival Hall	AHALL 1	10529486
		AHALL 2	10529487
	Great hall	GRHALL1	20153629
		GRHALL2	20153630
		GRHALL3 (I)	20153631
	Flex 1	FLX1-1	20153632
		FLX1-2 (I)	20153633
	Flex 2	FLX2-1	20153634
		FLX2-2	20153635
		FLX2-3 (I)	20153636
	Library	LIBR	20153637
	Garden Shop	GSHOP	20153628

Table 8.6 – Sensors' label and position [2]

Sensor types	Location	Label name	Serial number
Hobo data logger (CO_2, Temp., RH)	Atrium	ATR	10889680
	Volunteer Room	VOL	10889681
	Food Service	FOOD	10889682
	Garden shop office	GSHOFF	10889683
	Arrival hall	AHALL	10889684
	Great hall	GRHALL	20083066
	Garden shop	GSHOP	20083067
	Flex 1	FLX-1	20083068
	Flex 2	FLX-2	20083069
	Library	LIBR	20083070
	Class	CLASS	20083071

At first, the data loggers responsible to monitor the indoor spaces were strategically attached directly on the internal walls (see figure 8.18, b). But for safety reasons, all the sensors were repositioned on the top of stable surfaces, like is shown by figure 8.18, a.

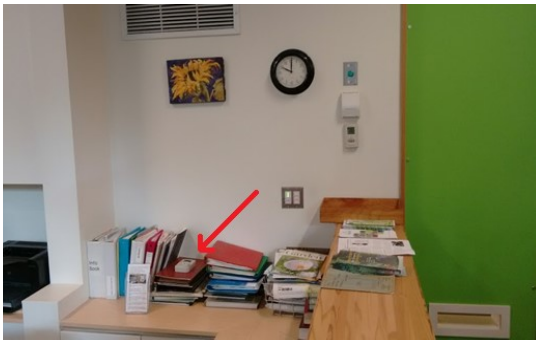

a) Data logger at the Library

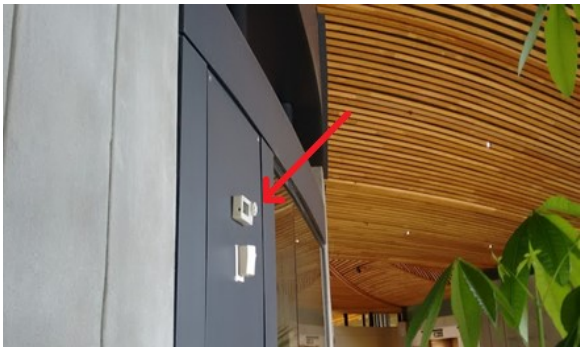

b) Data logger at the Arrival Hall

Figure 8.18 – Position of the data loggers in VanDusen under natural ventilation

The state sensors were installed at the top corner of 16 doors. From these 16 doors, 4 were internal and 12 were external. During the summer period, the external doors, besides the entrance use, are kept open to allow fresh cooler air into the internal spaces. The internal doors are also monitored in order to observe their influence in the overall natural ventilation performance. After all, with the opening of the internal doors the connectivity between spaces is enhanced, creating larger airflow paths across the building by magnifying the cross-ventilation. The airflow through the solar chimney might also be increased due to the improvement in the internal connectivity. Figure 8.19, a and b illustrate the position of the state sensors on external and internal door, respectively.

a) State sensor at external door b) State sensor at internal door

Figure 8.19 – Position of the state sensors at VanDusen's doors

The weather station positioned on the building roof is responsible to the record the outdoor air temperature, relativity humidity, solar radiation, rain precipitation, and the wind speed and direction. Figure 8.20 shows the weather station installed at VanDusen's roof.

Figure 8.20 – Weather station at VanDusen

8.4.1 Field Testing Results and Discussion

This section introduces the data gathered from the monitoring plan previously described. The field testing was conducted from August 10th to August 25th. The section is divided in: outdoor environment, indoor environment and thermal comfort analysis.

8.4.1.1 Outdoor Environment

This section describes the results taken from the weather station positioned on the building's roof. Due to problem in the installation of the station, the data was recorded from August 16th to August 25th of 2017. The experiments were done during the summer in Vancouver, Canada. The maximum temperature recorded was 29.5 °C and the minimum was 11.9 °C, during the night-time. During the monitoring, the average outdoor air temperature in the occupied hours (from 10 AM to 9PM) was 21.8 °C. Figure 8.21 shows the air temperature measured by the local weather station and also the weather data from the International Airport (YVR) to corroborate the data recorded. It is possible to observe that both curves follow a similar pattern except for a few days where VanDusen's peak temperatures are few degrees higher when compared with the data recorded by the weather station.

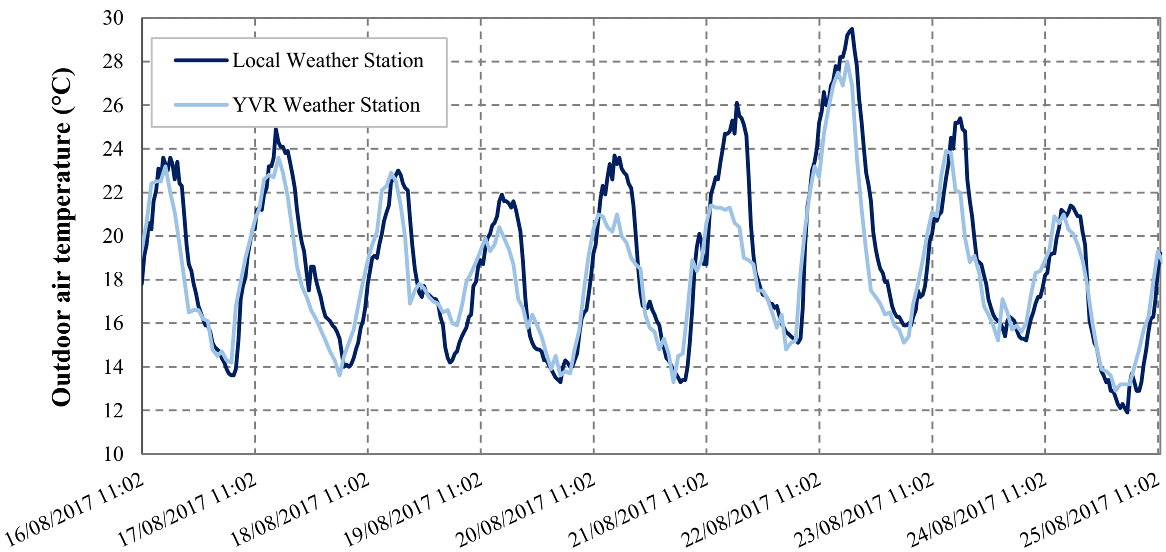

Figure 8.21 – Outdoor air temperature recorded by the local weather station

In terms of solar gains, the recorded days presented considerable solar radiation. The peak value was 909 W/m² at 2 PM on August 24th. During the daily peak, solar radiation values were around 800 W/m². Figure 8.22 illustrate both solar radiation and outdoor air temperature. As expected, it is possible to observe a certain relation between these two factors, with an increase of air temperature together with the solar incidence.

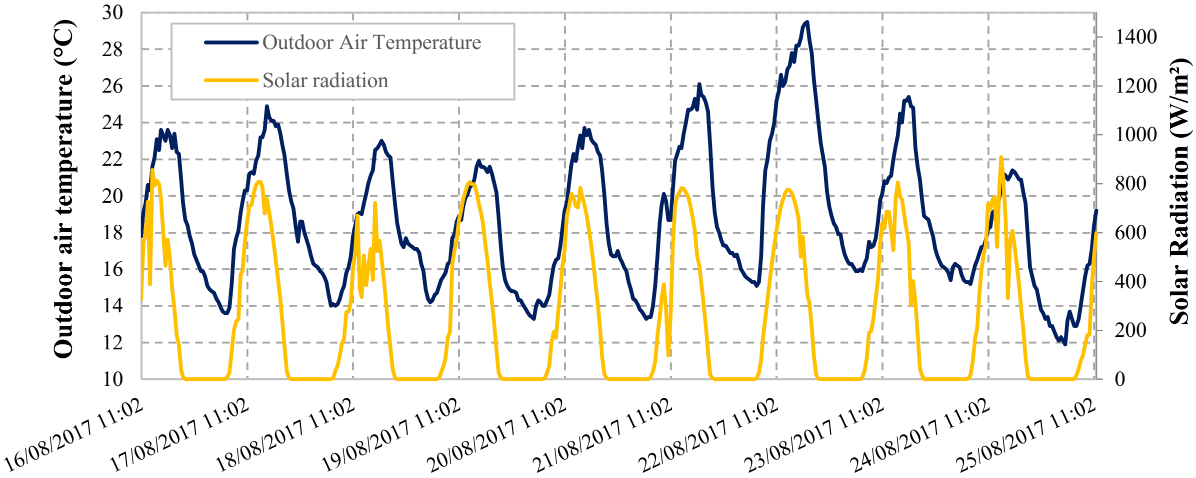

Figure 8.22 – Solar radiation recorded by the local weather station

A key aspect to natural ventilation is the wind. It is not possible to say that the recorded wind data is representative for the year-round wind behaviour on-site. Notwithstanding, this data indicates wind speeds and direction during the monitoring. For the majority of time the wind direction was south-east, but north-west wind occasionally occurred. Figure 8.23 illustrates the wind frequency for the monitoring period.

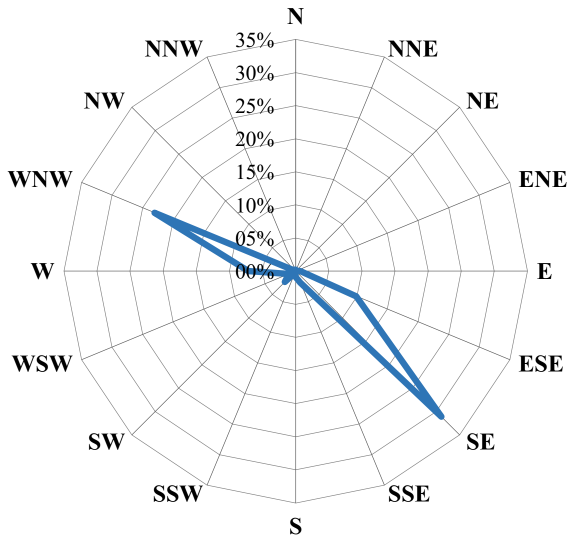

Figure 8.23 – Wind-rose frequency from August 16th to August 25th

Regarding the wind speed, for the majority of time the wind speed were inexitent or below 0.5 m/s. Only 1% of the data reported wind speeds above 2 m/s. The local climate, terrain condition, and height of the weather staton localized on the building's roof may explain the relatively lower wind speeds and limited wind direction. The whole wind speed distribution recorded by the local weather data is illsuatrted by figure 8.24.

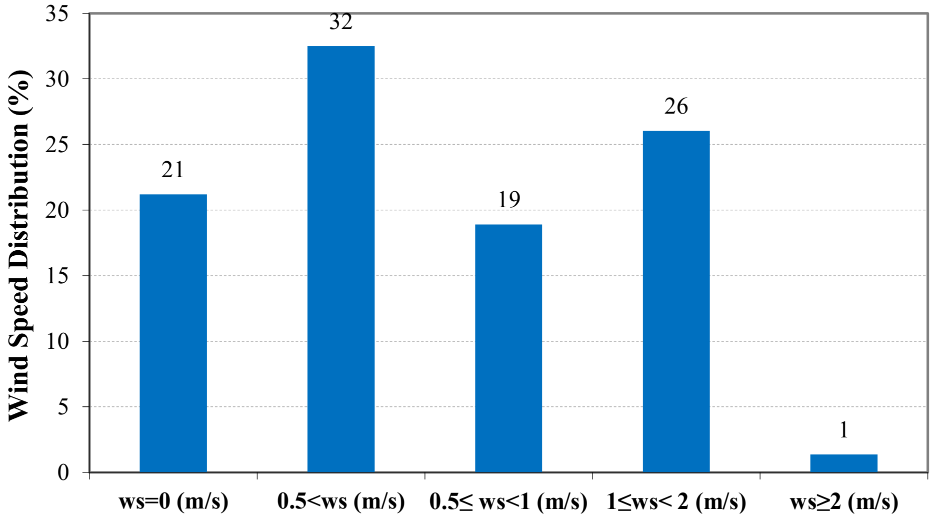

Figure 8.24 – Wind speed distribution

8.4.1.2 Indoor Environment

All the data recorded inside the building is presented in this section. As a part of the indoor environment, internal temperatures, CO_2 concentration rates, relative humidity, and windows and doors status (open and closed) were recorded. The sensors and equipment used in the monitoring are presented in section 8.4. No sensors were directly positioned on the windows openings; instead, the data related to the window status was gathered from the building automation system (BAS) during the experiments. However, some technical problems happened in a few sensors. More specifically, both states sensor installed in the food service's door presented problems and did not record any data during the monitoring period. The sensor positioned at the library stopped recording the CO_2 concentration after a certain time, and the Garden shop state sensor recorded that door was kept open for the majority of monitoring time, probably indicating a sensor's malfunction. The rest of the sensors functioned as expected.

VanDusen is a multifunction building; therefore, each monitored space has its own specific operation characteristics, usage and even schedule. In order to efficiently present the experiments results, this section introduces the data for each room with its peculiarities. Firstly, the atrium is a key space for the performance of the overall indoor environment, the presence of the solar chimney and the external doors are crucial airflow paths within the building. Figure 8.25 shows the atrium temperature, CO_2 concentration, and open and close status of the windows (solar chimney) and doors during the experiments.

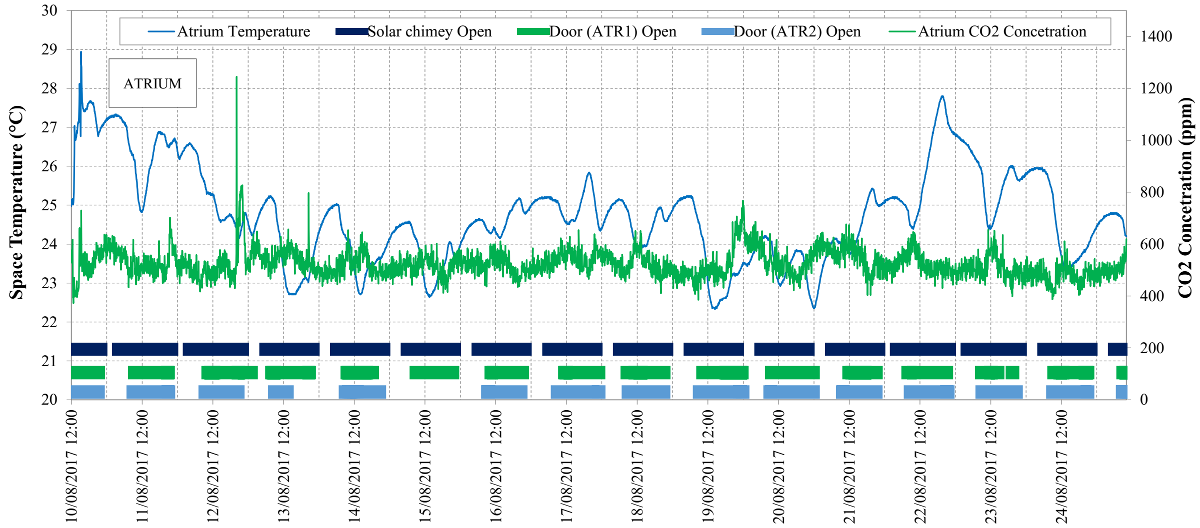

Figure 8.25 – Atrium indoor environment characteristics

With a similarly function as the atrium, the arrival hall indoor conditions are illustrated by figure 8.26. Notwithstanding the temperatures at the arrival hall are higher than the one recorded at the atrium.

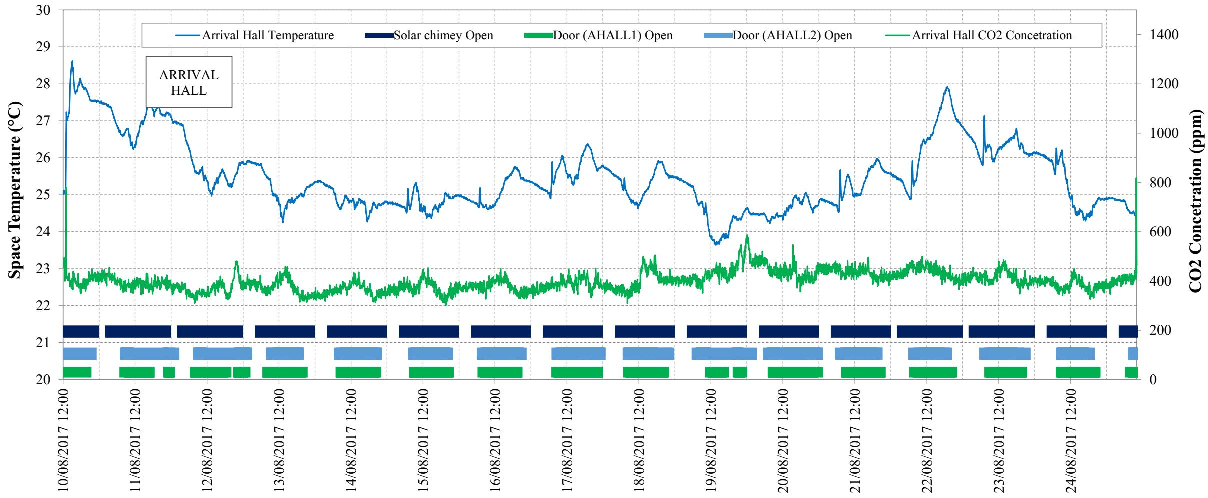

Figure 8.26 – Arrival Hall indoor environment characteristics

The classroom is located at the south part of the building. During the summer, this room is usually used for activities from 10 AM to 7 PM. Figure 8.27 illustrates the data recorded in that room.

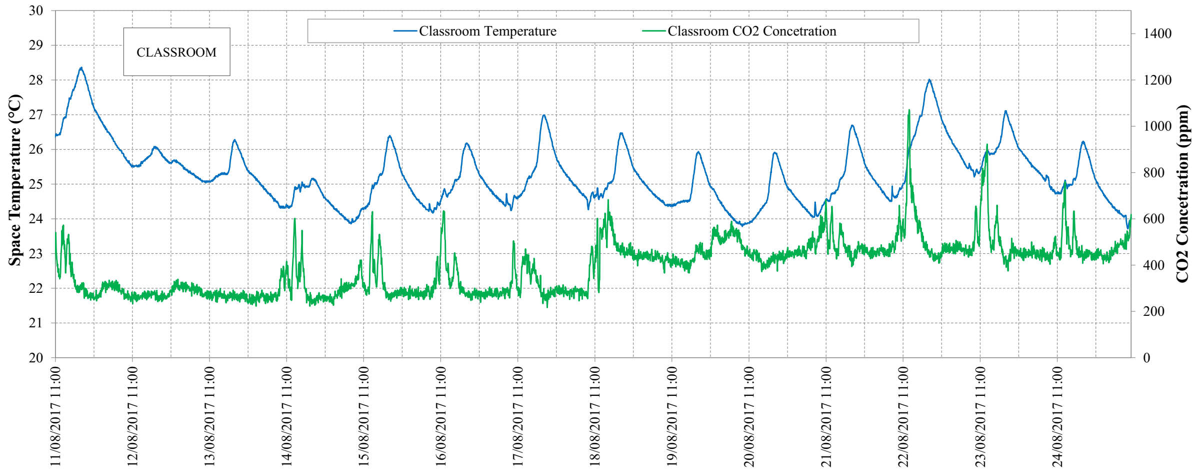

Figure 8.27 – Classroom indoor environment characteristics

The volunteer room is located at extreme north part of the building. That space has a function and hours of operation similar as the classroom. However, the temperatures recorded in that rooms were lower than the classroom. Both rooms have external doors, and during the summer the occupants usually open them to provide natural ventilation to the rooms. Sensors were not positioned in those doors due to limited number of sensors available for the monitoring plan.

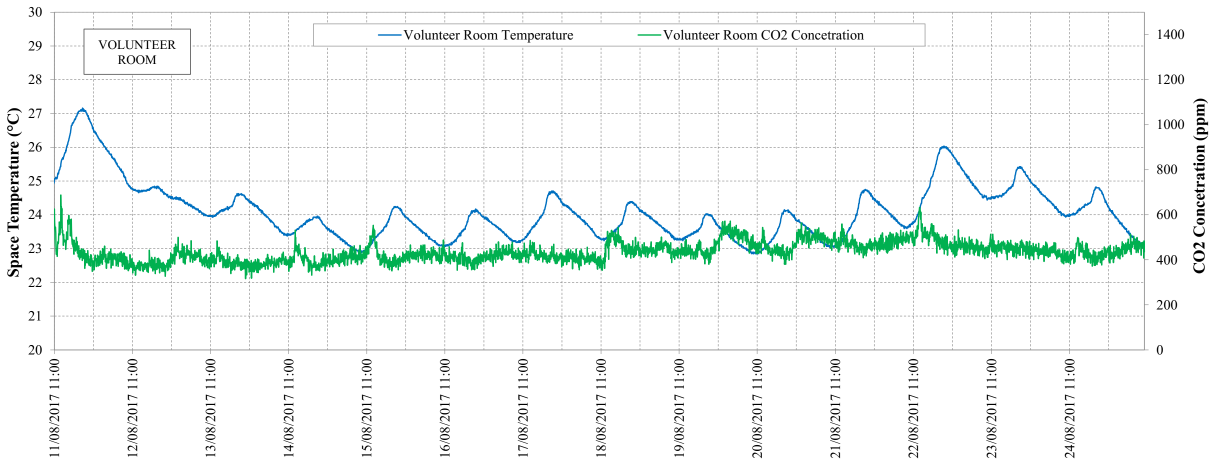

Figure 8.28 – Volunteer Room indoor environment characteristics

VanDusen's rental spaces are composed by 3 spaces, named Flex 1 and 2 and Great Hall. Occasionally, these spaces are used in conjunction by opening movable internal walls that separate those spaces if needed. Figure 8.29 illustrates the rental spaces and how these rooms are used as one big space.

Figure 8.29 – Rental spaces (Flex 1, 2 and Great Hall)

During the monitoring, the CO_2 concentration in Flex 1 indicates that this space was used and received a large amount of occupant, at least 7 times. That occupancy rate affected the temperatures and is also reflected by the doors operation. It is also observed that the occupants normally open both doors of the room at the same time.

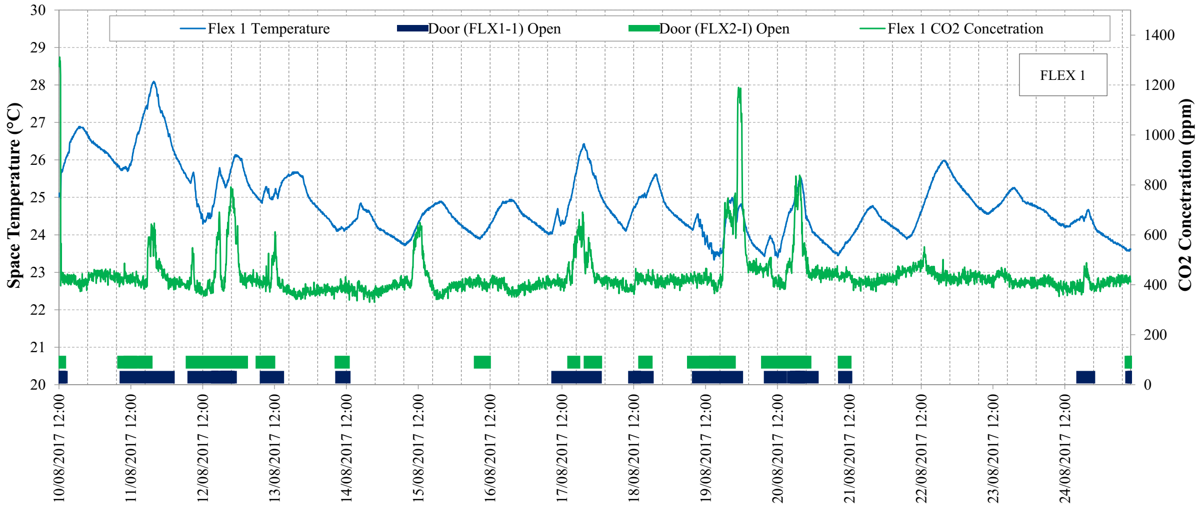

Figure 8.30 – Flex 1 indoor environment characteristics

Flex 2 is also a rental space and during the monitoring period followed a similar pattern than the one showed in the Flex 1 and Great Hall, indicating that these spaces might have been used in conjunction. The temperatures fluctuated between 23 and 28 °C and the CO_2 concentration got to peak of more than 1000 ppm, indicating the space was highly occupied. Figure 8.31 shows the Flex 2 temperature, CO_2 and door opening status.

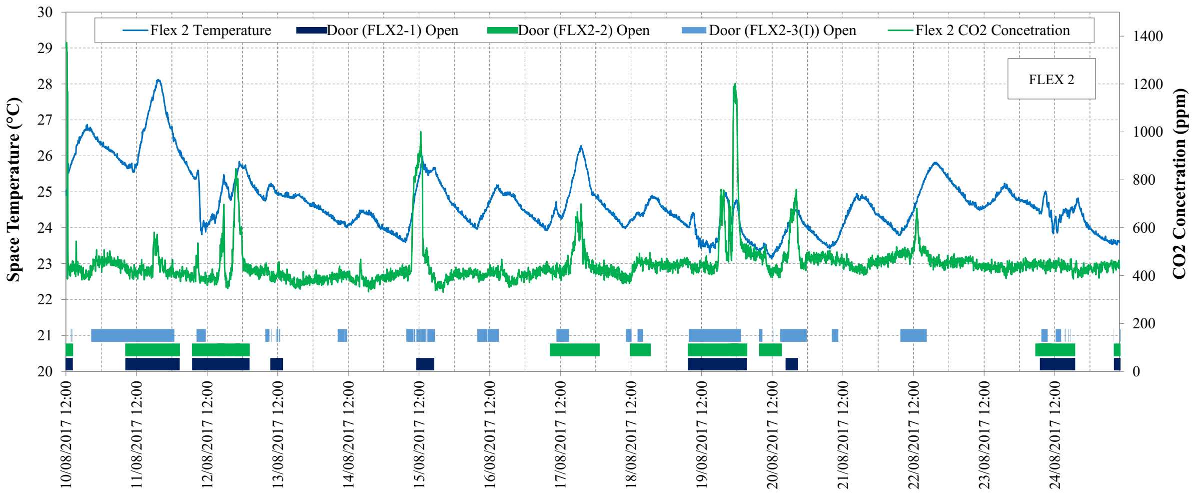

Figure 8.31 – Flex 2 indoor environment characteristics

Between all the rentals spaces, the Great Hall is the bigger one and is located closer to the atrium space. The indoor environment at the Great Hall is illustrated by figure 8.32.

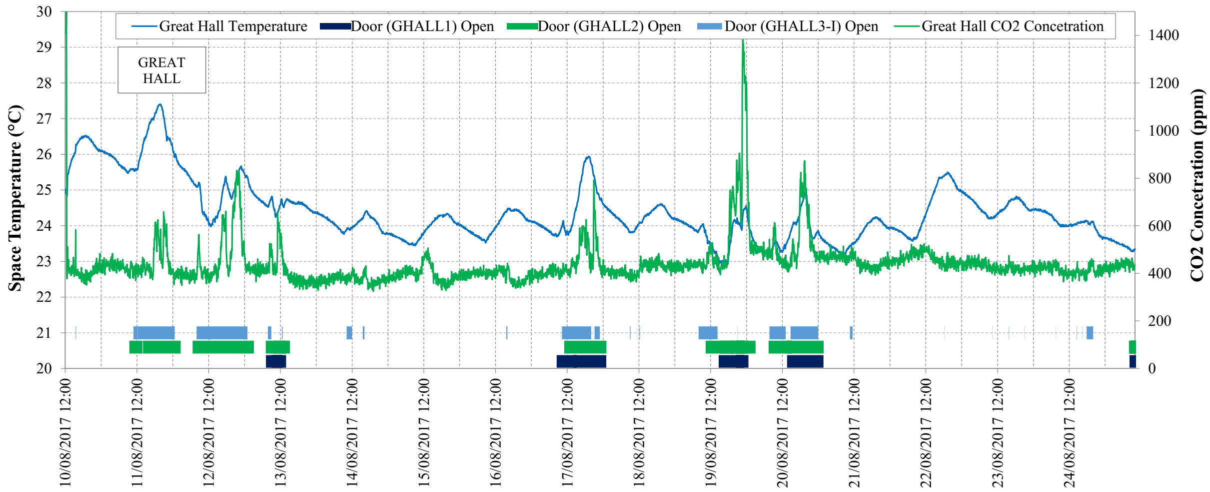

Figure 8.32 – Great Hall indoor environment characteristics

To show the interaction between Flex 1, Flex 2 and Great hall, figure 8.33 illustrates all the factors monitored in these rooms put in parallel. The doors usage also indicates that those spaces are mostly used in conjunction as one larger space.

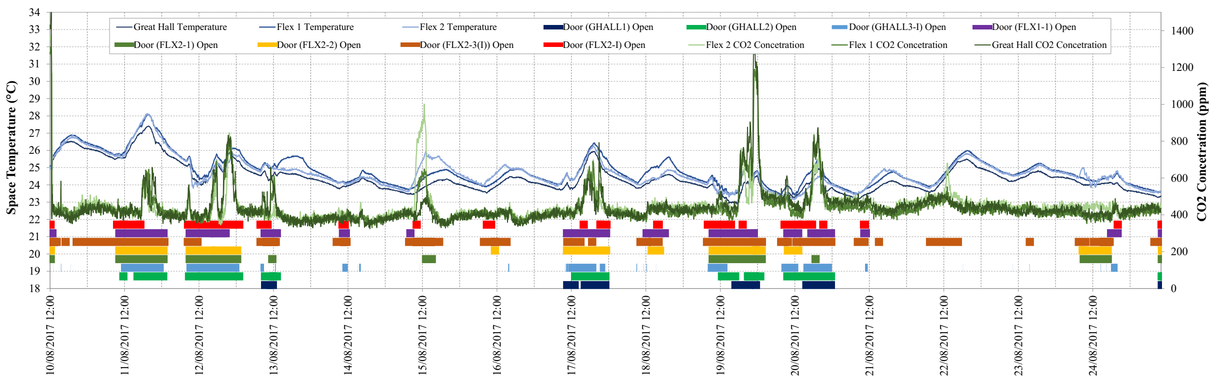

Figure 8.33 – Rental spaces indoor environment characteristics

Regarding the food service, the sensor was positioned relatively close to the kitchen, next to where the attendants work. The temperatures in that space reached 30°C at one point. The heat generated by the kitchen equipment is the main reason for the high temperatures recorded. Apart from the usage hours, there is a significant temperature drop when the kitchen is not being used. That space has external two doors that are kept open for the most time during the occupied hours. Two sensors were positioned at these doors, but due to technical problems both of them did not register any relevant data during that period.

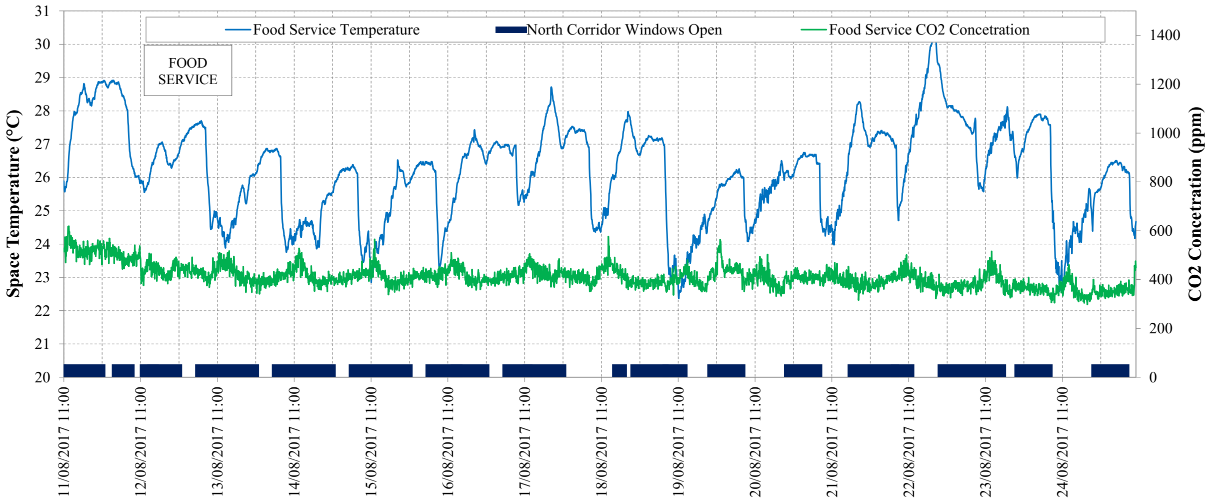

Figure 8.34 – Food Service indoor environment characteristics

During the monitoring, portable fans were observed in the following rooms: the garden shop (two fans), the garden shop office, the library, and the volunteer room. This kind of adaptive approach shows that the spaces temperatures during that period gets to a point that make occupants to feel uncomfortable. Figure 8.35 shows the fans installed at the Garden Shop.

Figure 8.35 – Fans used at the Garden Shop

During the monitoring, high temperatures were recorded at the Garden shop. The sensor positioned at the door indicates the door was kept open all the time. This is likely to be untrue, and product of some technical error in the sensor. However, the room has mechanically operated windows that periodically were open over that monitoring time. The Garden shop indoor environment is illustrated by figure 8.36.

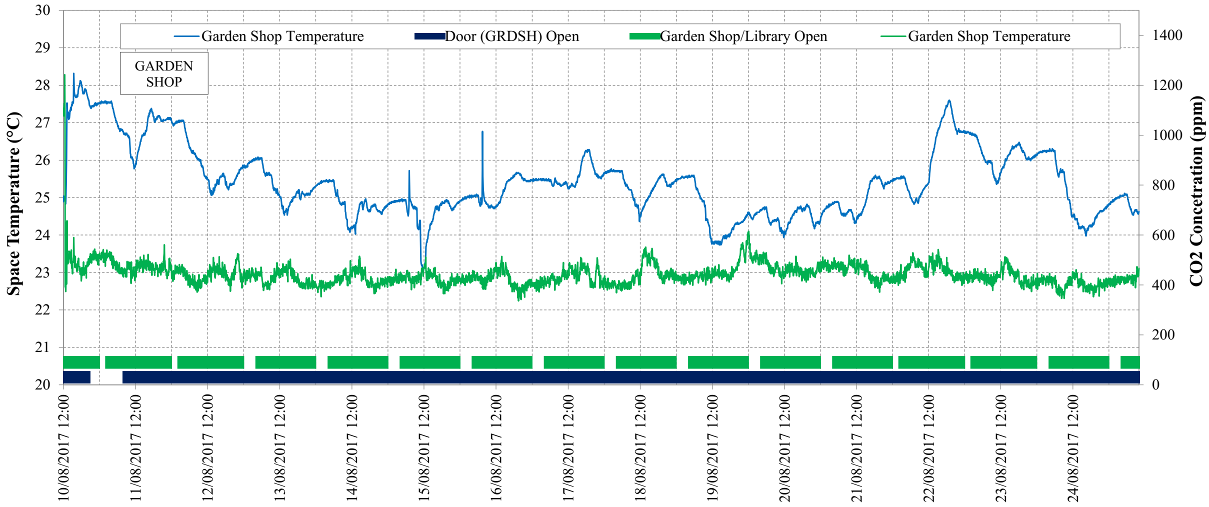

Figure 8.36 – Garden Shop indoor environment characteristics

The Garden shop has a small office at the back part (see figure 8.37). Initially, this room was not considered to be monitored, but due to concerns that the space was not performing as intended, a sensor was positioned in the room. The office is normally occupied by one occupant and has a computer, printer and copy machine. There is no ventilation system applied to the room, but a small personal fan used by the occupant. The door is kept open to avoid even higher temperatures.

Figure 8.37 – Garden Shop Office at VanDusen

During the monitoring period the temperature recorded were substantially high, fluctuating above 26°C for most of the time and getting up to 29°C. The CO_2 levels, however, stayed at reasonable lower levels. Figure 8.38 shows the indoor environment of that space.

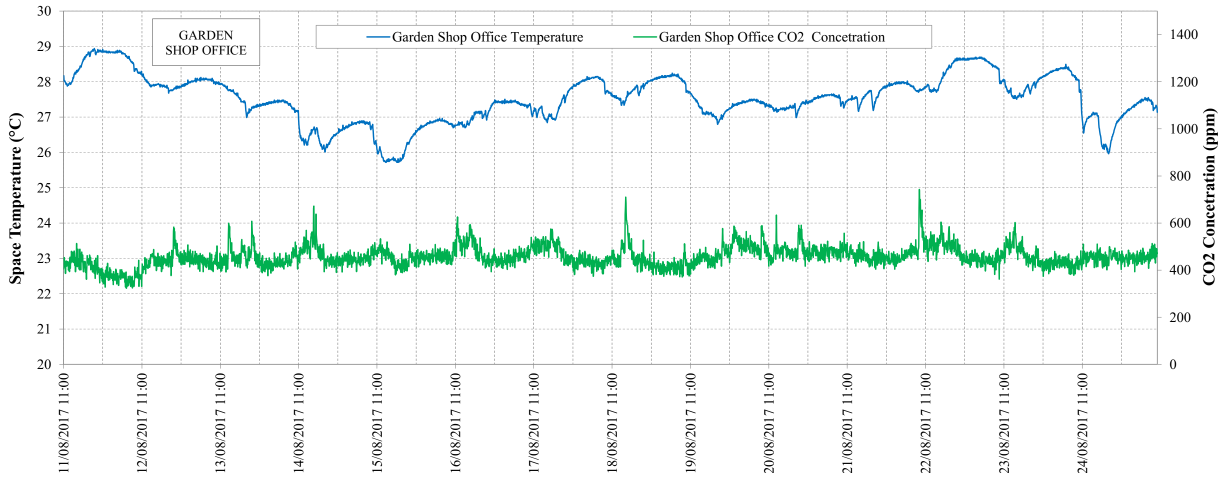

Figure 8.38 – Garden Shop Office indoor environment characteristics

When comparing with all the rooms monitored, the library was the one with the lower temperatures. This is explained by the amount of openings positioned in that the room in association with the good solar shading, lower occupancy rates and low window-to-wall ration. Remembering that the library have mechanically operating windows periodically open around 4 AM and also manually operated windows, normally open during the occupied hours. Figure 8.39 illustrates the indoor environment recorded at that space.

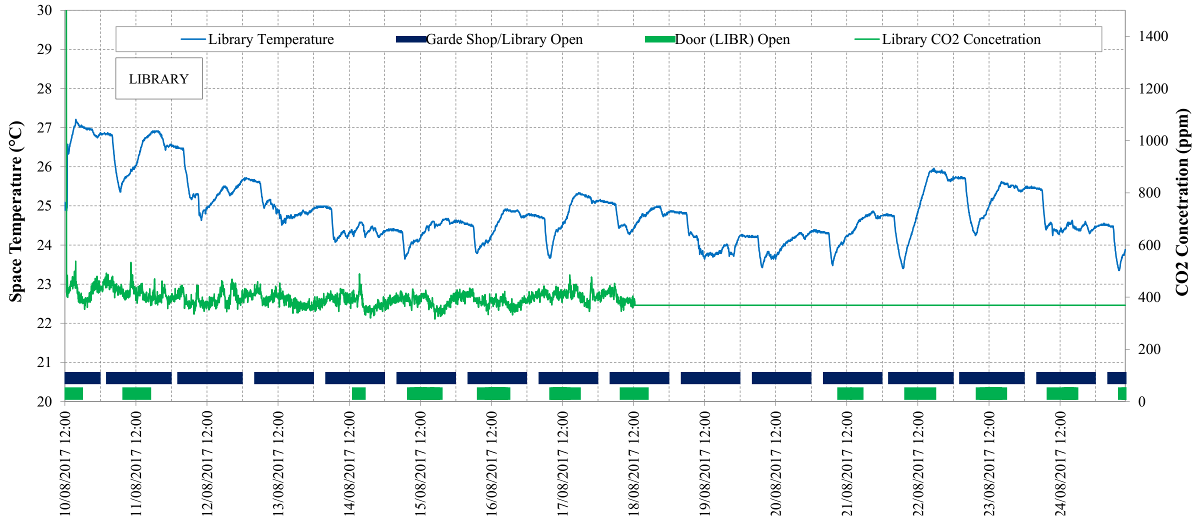

Figure 8.39 – Library space indoor environment characteristics

Table 8.7 summarizes the maximum, minimum and average temperatures recorded by the field testing for the different spaces.

Table 8.7 – Recorded temperatures at the field testing

	Maximum Temperature (°C)	Minimum Temperature (°C)	Average Temperature (°C)
Atrium	28.9	22.3	24.8
Arrival Hall	28.6	23.1	25.5
Classroom	28.4	23.7	25.4
Great Hall	27.4	22.9	24.4
Flex 1	28.1	23.3	24.8
Flex 2	28.1	23.1	24.7
Food Service	30.2	22.4	26.2
Garden Shop	28.3	23.1	25.4
Garden Shop Office	28.9	25.7	27.5
Library	27.2	23.4	24.9
Volunteer room	28.0	22.8	24.3

8.4.1.3 Adaptive Thermal Comfort Analysis

The metrics used to assess the thermal comfort are the aforementioned adaptive thermal comfort suggested by ASHRAE Standard 55 (2013) in association with the exceedance hours, also presented by the same standard. The exceedance hours method (*EH* method) allows the quantification of the number of hours in which environmental conditions are outside the comfort zone requirements during the occupied hours in the period of interest. To this end, the calculation of the *EH* follows equation 8.1

$$EH = \sum (H_{>upper} + H_{<lower}) \qquad \text{Equation 8.1}$$

where,

$H_{>upper} = 1$ if $t_{op} > t_{upper}$ and 0 otherwise;

$H_{<lower} = 1$ if $t_{op} < t_{lower}$ and 0 otherwise;

t_{upper}: upper comfort range;

t_{lower}: lower comfort range.

$H_{>upper}$ and $H_{<lower}$ are discomfort hours outside the zone boundaries and the units are in hours. Although, the method proposed on the standard only quantify the total of discomfort hours, which were separated in cold discomfort hours and hot discomfort hours by the author. The reason behind that choice is that since natural ventilation is being evaluated in providing cooling for the spaces, the analysis of hot discomfort range exclusively is more suitable for that application. So, with that approach is possible to isolate the $H_{>upper}$ factor to serve as a comparative factor later to be used.

The prevailing mean outside temperature was calculated using a linear average of the last 15 days temperatures, following the directions proposed by ASHRAE Standard 55 (2013). As the time steps used in the monitoring was every 5 minutes, for each time step minutes there is a dot (reading) representing the space temperature for a given prevailing outside temperature in the graph. Evidently, the data used in the analysis is only related to the building occupied hours, which is from 10 AM to 9 PM at summer time. The same concept applies to the *EH* calculation. Differently from what is recommended by ASHARE 55 (2013), which uses the operative temperatures (t_{op}) in the adaptive thermal comfort approach, the spaces air temperatures were used in the analysis instead.

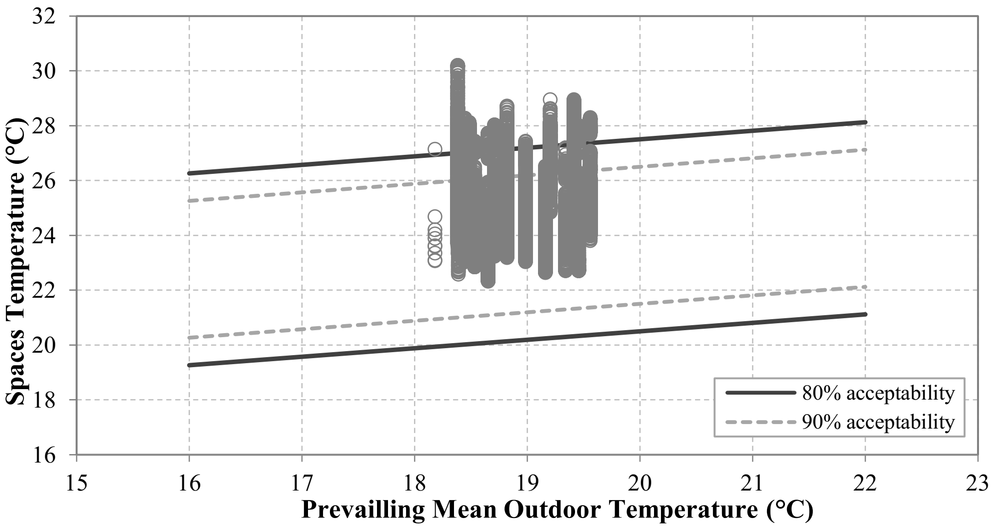

Figure 8.40 – Adaptive thermal comfort analysis for VanDusen

Figure 8.40 shows that for most of the time the temperatures are within the thermal comfort range. However, there are points outside the comfort range. To see what is happening in each space, the data illustrated in 8.40 is broken down to show the comfort analysis for each individual room. The spaces are grouped based on their similarity and space function.

Figure 8.41 shows the adaptive thermal comfort applied to the atrium and arrival hall. Both spaces have transient characteristics in terms occupancy and a similar usage. For the atrium, during 6% of the time the space is not under comfort temperature, according the adaptive thermal comfort. In the arrival hall, 10% of exceedance hours (*EH*) were observed during the experiments. The higher thermal discomfort of the arrival hall is possibly explained by the higher solar gains by the south face envelope, the doors located at the space are not always kept open, like both doors in the atrium. Moreover, the atrium also has the presence of the solar chimney.

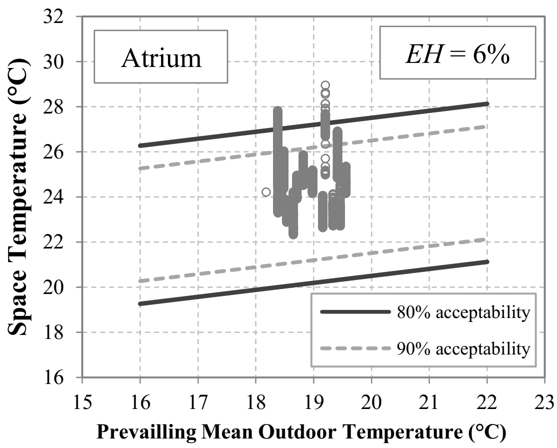

a) Atrium

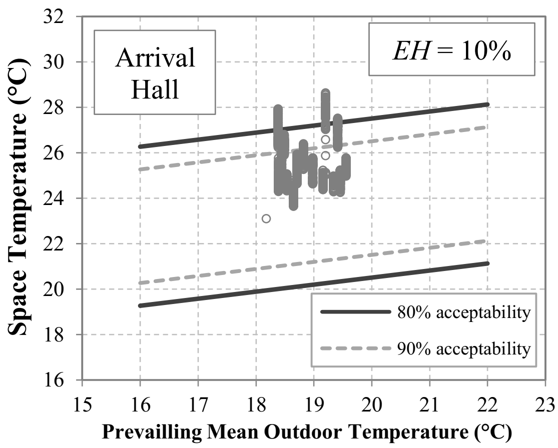

b) Arrival Hall

Figure 8.41 – Adaptive thermal comfort applied to the Atrium and Arrival Hall

The adaptive thermal comfort applied to the rental spaces are illustrated by figure 8.42. For most of the time, the spaces are on the comfortable range of temperatures. The great hall shows the better performance in terms of thermal comfort in comparison with the other spaces. The 1% of *EH* in the great hall and the 3% in the flex 1 and 2, is relative to only 1 and 5 hours, respectively. For that time, based on the CO_2 readings, there were no events happening on those spaces. Then, it is possible to assume that the rental spaces had comfortable temperatures during all the events held during the building testing and monitoring.

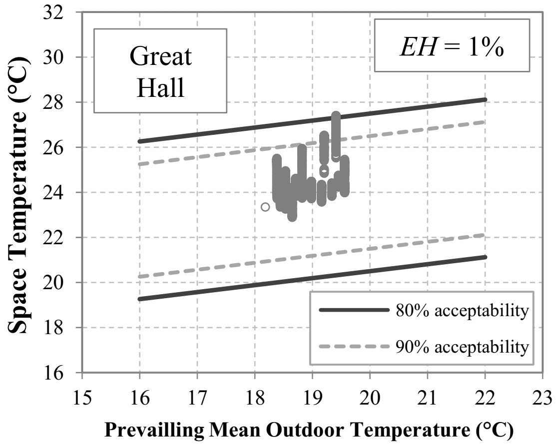

a) Great Hall

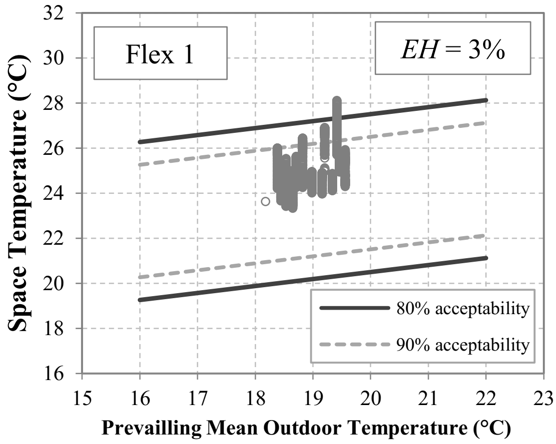

b) Flex 1

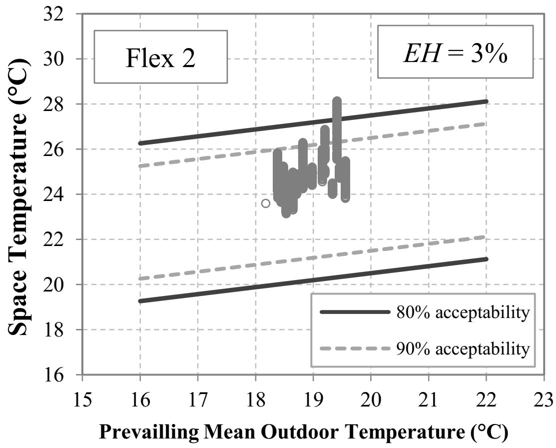

c) Flex 2

Figure 8.42 – Thermal comfort analysis for the rental spaces

Regarding the food service, figure 8.43 shows the adaptive thermal comfort applied for that space. Differently from the previous spaces, the food service presented uncomfortable temperatures for a substantial period of time, with *EH* of 23%. This numbers are resulted from the high thermal gains generated by the kitchen.

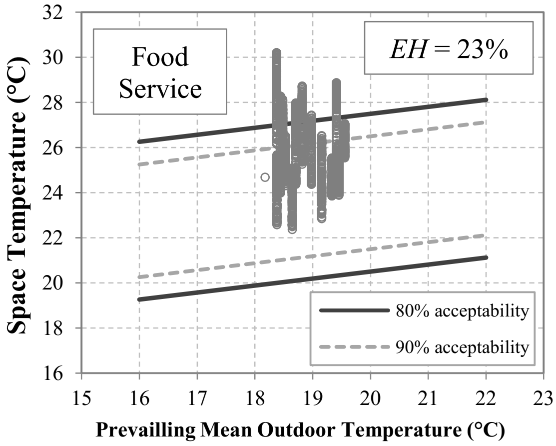

Figure 8.43 – Adaptive thermal comfort applied for the Food Service

Figure 8.44 illustrates the adaptive thermal comfort applied for both Garden shop and its office. The Garden Shop presents a reasonable *EH* value of 7%, but the garden shop office shows a *EH* of 62%. The high value of the thermal discomfort at the office is caused by the lack of proper ventilation and ways to extract the heat from that space.

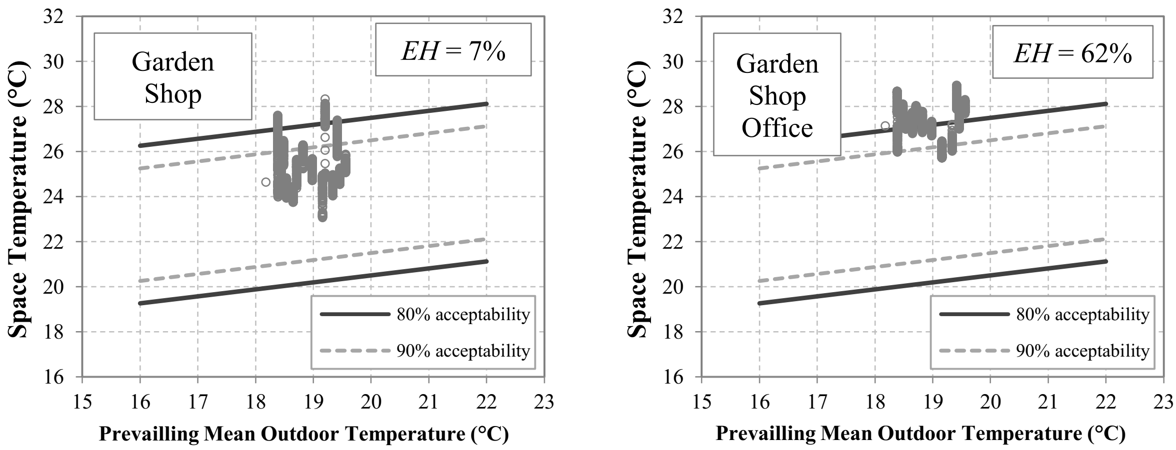

a) Garden Shop b) Garden Shop Office

Figure 8.44 – Adaptive thermal comfort applied for the Garden Shop and Office

Both volunteer and classroom are spaces with similar usage, but they are positioned at opposite sides in the building. Volunteer room is located at the south part of the building, and the classroom in the north part. The more exposure to the solar radiation in the south façade of the classroom may explain the higher thermal discomfort of that space in comparison with the volunteer room. The value of *EH* was 12% for the classroom and 3% for the volunteer room. Figure 8.45 shows the final results for both spaces.

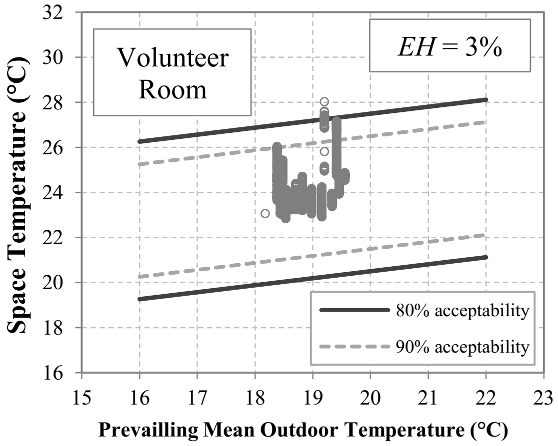

a) Volunteer room

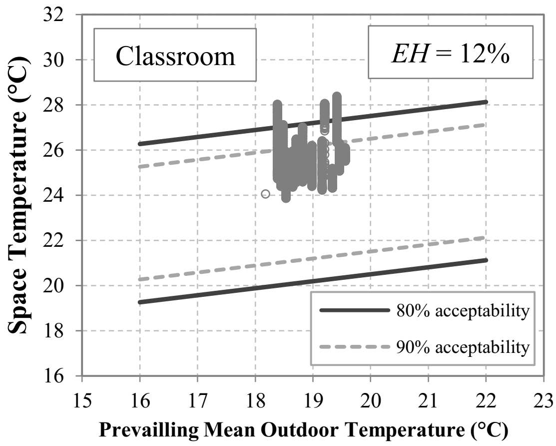

b) Classroom

Figure 8.45 – Adaptive thermal comfort applied for the Volunteer Rom and Classroom

During the monitoring, the library was the most comfortable space in the building. During the occupied time, the space temperatures were always within the comfortable temperature range. Figure 8.46 illustrates the final results for the adaptive comfort for the library.

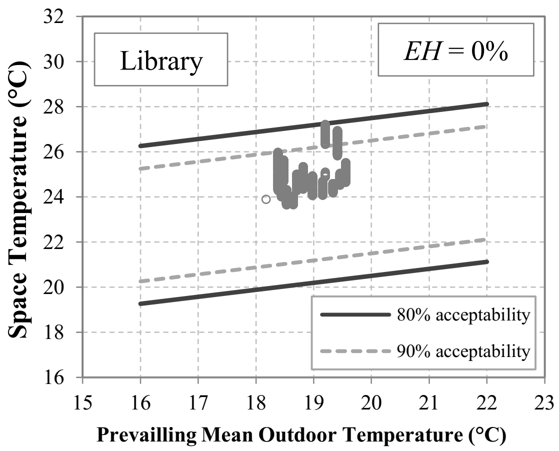

Figure 8.46 – Adaptive thermal comfort applied for the Library

Table 8.8 summarizes the exceedance hours (*EH*) for the different spaces analyzed.

Table 8.8 – Exceedance hours (*EH*) recorded at the field testing

	Exceedance Hours, *EH* (%)	Number of Exceedance Hours, *EH* (hrs)
Atrium	5.9	11
Arrival Hall	9.8	18
Classroom	11.7	21
Great Hall	0.8	1
Flex 1	2.9	5
Flex 2	3.0	5
Food Service	22.9	41
Garden Shop	7.4	13
Garden Shop Office	62.1	111
Library	0.0	0
Volunteer room	2.8	5
Average Space Temperature	5.8	10

Apart from a couple of rooms that are clearly are overheating in the summer, such as the food service and the office at the garden shop, it is possible to say that the natural ventilation is effectively delivering a thermal comfort for the indoor environment for the period when the monitoring was realized. Notwithstanding, the thermal comfort is sensible to the building anomalies further presented in section 8.5.

8.5 Study of Performance Factors that may Affect Natural Ventilation Effectiveness

During the field testing (section 8.4.1.2), it is observed a sensible decrease in the internal temperature when the windows or doors were open. The mechanically operated windows were open at 4 AM, before the building opening hours. From that moment, it is possible to notice a gradual decrease in temperature, especially if that one space is directly connected with those openings. A more drastic temperature drop is observed when the building opens and the occupants manually open the doors. The temperatures keep dropping until 10 AM when they start to rise, throughout most of spaces, together with the outdoor temperature. From then, the temperatures keep rising until the building closure, around 9 PM. The windows are closed at 10 PM, and from that moment the room temperatures are usually at the highest level. The temperatures start to drop only when the windows are open again at 4 AM. To illustrate a normal operational day, figure 8.47 shows the temperature, CO_2 levels and the solar chimney openings status for the atrium space during a day.

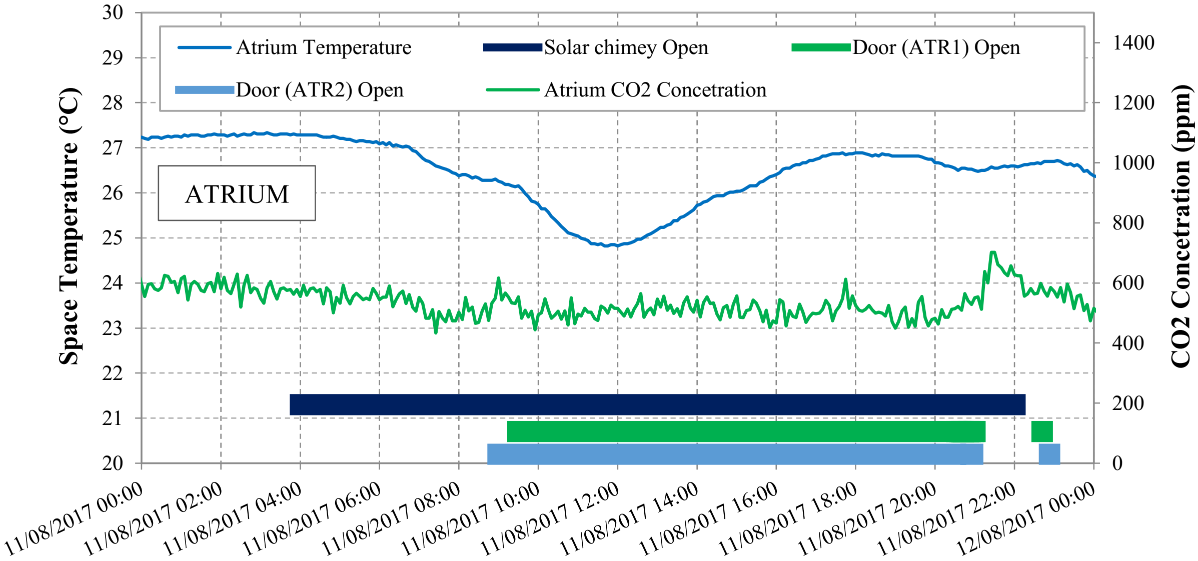

Figure 8.47 – Usual daily operation of the atrium

Persistently, the space's temperatures at unoccupied hour are higher than the temperature at occupied hours. This undesirable behaviour seems mainly caused by the lack of proper ventilation during the nigh-time. This anomaly is observed through the building's BAS during the field testing. Accordingly, the building's thermal mass is trapping the heat accumulated through the whole day and does not dissipate that heat by the use of mechanical or natural ventilation. If the intention behind this apparent anomaly was to save energy, the night-time natural ventilation would achieve the same effect without the use of any energy.

A mechanical design anomaly was identified related to the water to air heat pump, named HP4, which provides cooling for the electrical room exclusively for the whole year (the only room in the building that uses mechanical cooling). The heat pump is connected to the hydronic water loop, where it dumps the heat extracted from the electrical room. In other words, the heat pump uses the radiant slabs to dissipate heat year round. That configuration might be useful in winter operation but it is counterproductive with natural ventilation. However, the heat pump has total cooling capacity of 8 kW, an expected leaving water temperature of 35.5 °C, and a design water flow of 0.5 l/s. Therefore, it is expected that this anomaly is not able to substantially influence the overall radiant slab temperatures and consequently the operative temperatures.

After the examination of the mechanical system in the BAS during the monitoring, a mechanical operational anomaly was found. The anomaly is related with the geo-source heat pump (GSHP), the main source of heat for the whole building. The GSHP are responsible to warm up the water distributed to the radiant floor slabs. The GSHP was enabled, in heating mode, every day during the building monitoring, usually from 10 AM to 2 PM. This operation is clearly an operational anomaly. The access to the real building controls logic is not available, so it is not possible to assertively point out the reason behind that anomaly. However, initially, it is possible to trace a parallel between the building internal temperatures and the GSHP operation. The GSHP is turned on around the time when the building temperatures reached the lowest points throughout the day. Figure 8.48 illustrates the temperature average of measured internal spaces in combination with the solar chimney and the GSHP operation.

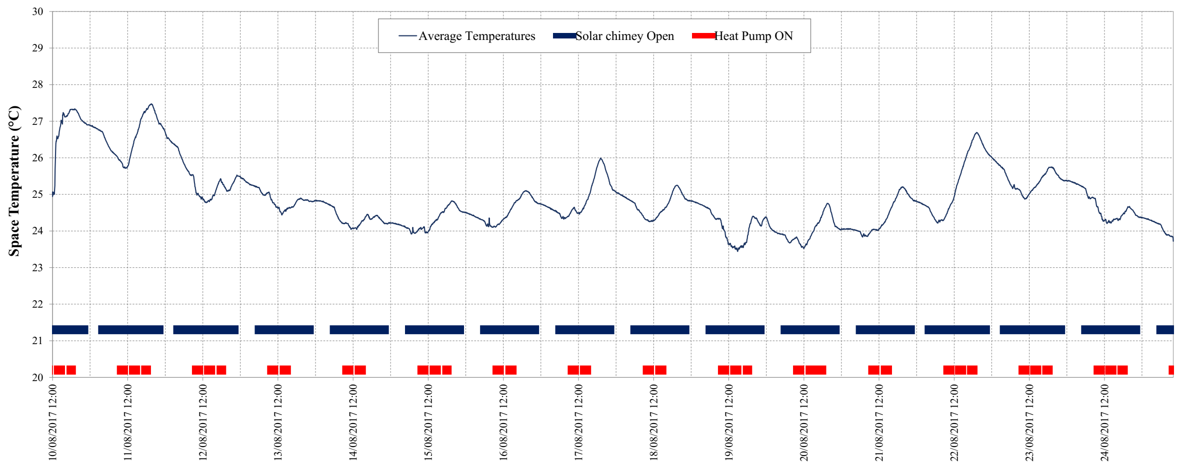

Figure 8.48 – Internal spaces average temperatures and GSHP operation

When the BAS is analyzed, it is traced some conclusions regarding the GSHP's supply water temperatures and operation hours. On the operation hours, the daily longest use of the GSHP was 118 minutes, and the lowest use was 78 minutes. On the supply water temperatures, when the GSHP is turned on is observed an increase in 2°C in comparison with when the GSHP is disabled and only recirculating the water. If the GSHP is enabled, the supply water temperature is around 32°C and 30°C when the GSHP is disabled. Therefore, knowing that small temperature increase when the GSHP is turned on, and the complexity of VanDusen's radiant floor system in association with the thermal mass of the concrete floor where this system is positioned, it is expected that this operation anomaly does not substantially affect the indoor environment and consequently the whole building natural ventilation effectiveness.

Even with the presented anomalies, after observing the temperature curves in parallel with the windows and doors opening status, it is possible to conclude that natural ventilation is providing a big source of cooling to the indoor environment. Even without the adjustments on the building operation, it is possible to infer that if the natural ventilation strategy was extended to the use of night ventilation the thermal comfort of the building occupants would increase substantially. The solutions for the anomalies involve adjusting the operation of the GSHP, and adding a by-pass to the HP4 water side, to be used exclusively during the summer.

8.6 Calibration and Validation of VanDusen's WBSM

Following the concepts previously presented in section 7.5, this section shows the calibration and validation performed on VanDusen's WBSM. The lack of historical data from the BAS made it necessary to position sensors inside the building (see section 8.4 for the whole field testing adopted). The outdoor environment was recorded by a local weather station positioned on the building's roof. The main drawback to the validation process is regarding the lower quality of energy data. The energy consumption available is inconsistent and presents a number of gaps. An extra obstacle in the case study was due to anomalies in the operation of the mechanical system, earlier presented in section 8.5. The calibration/validation was done using the spaces temperature and year-round energy data. No surveys and uncertainty analysis were performed. Figure 8.49 shows the level of calibration achieved in the case study, which is based on the monitoring realized on the case study (section 8.4) and the year-round energy consumption data.

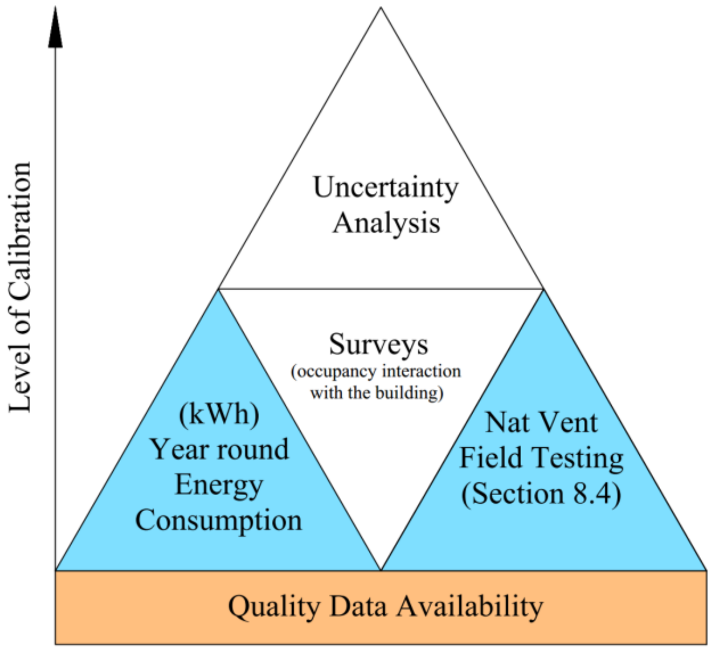

Figure 8.49 – Level of calibration achieved in the case study

Figure 8.50 illustrates the comparison between the measured and simulated energy consumption throughout the year. The values of CVRMSE and NMBE are higher than expected for monthly data. ASHRAE Guideline (2014) suggests that the values of CVRMSE and NMBE should be below 15% and 5%, respectively, for monthly energy consumption. However, the lower quality of energy data compromises the reliability of the energy data. Notwithstanding, the values or measured and simulated energy data fairly correlate.

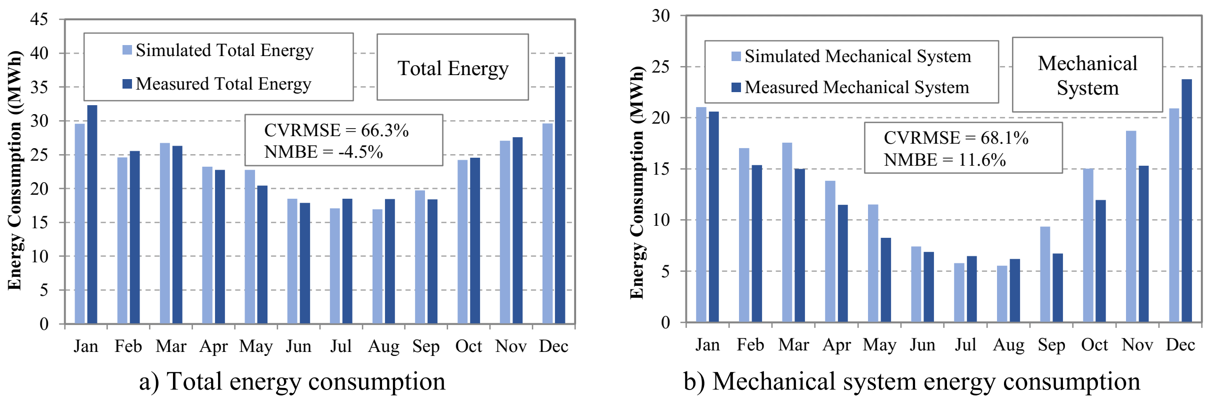

a) Total energy consumption

b) Mechanical system energy consumption

Figure 8.50 – Comparison between measured and simulated energy consumption [1]

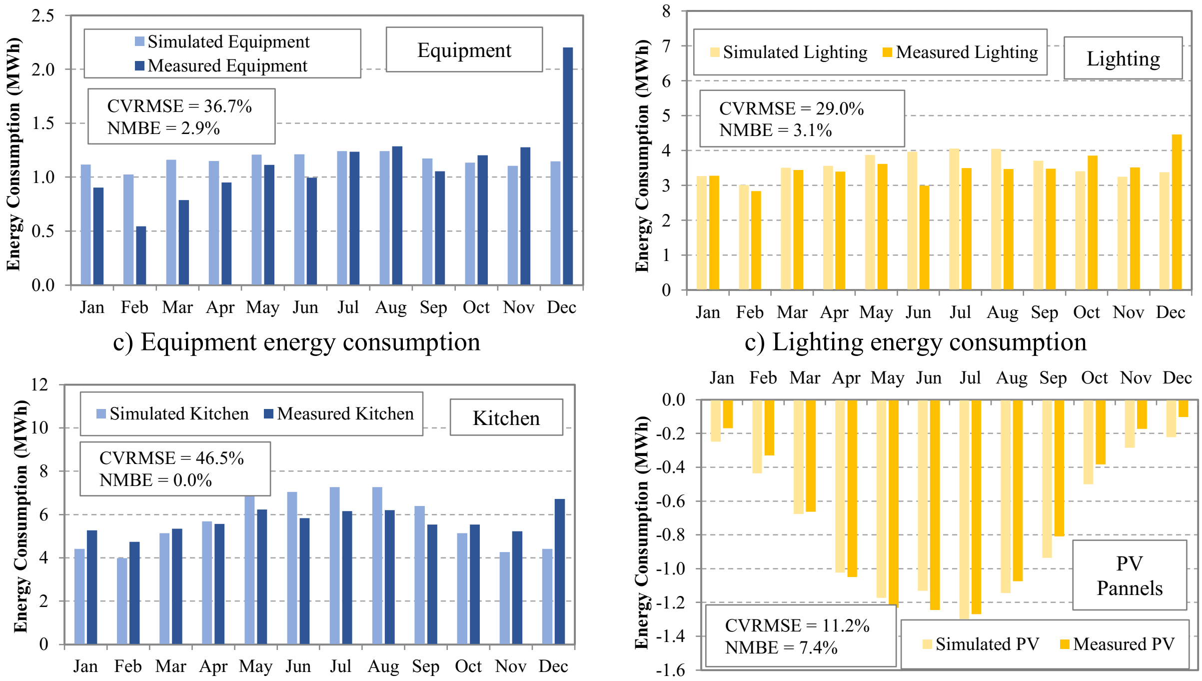

c) Equipment energy consumption

c) Lighting energy consumption

c) Kitchen energy consumption

d) PV panels energy generation

Figure 8.50 – Comparison between measured and simulated energy consumption [2]

Furthermore, the on-site weather data is not directly applied to the simulation. Instead, the weather data is used to compare real with simulation weather data. By comparing the simulation and real weather data, days with similar weather profile are compared. Then, the daily internal spaces temperatures for each space are compared. This approach is used extensively throughout different days. Not just one, but 10 days are analyzed and compared with the simulated data. Appendix D shows the daily results of CVRMSE and NMBE for all days and spaces analyzed; the NMBE and CVRMSE are calculated for each space.

The anomalies previously presented in section 8.5 involve the lack of night-time ventilation and the design and operational anomalies of the mechanical heating system. From the analysis of these anomalies and simulations with night-time ventilation (Appendix F) it appears that ventilation overpowers the mechanical anomalies. In other words, as long as there is some sort of ventilation, the effect of the mechanical anomalies seems negligible.

Thus, in order to validate the WBSM and accurately represent the actual indoor conditions, the lack of ventilation during the nigh-time, as is in the real building, is applied to the model. However, as explained in section 8.5, the heating system anomalies (*i.e.* HP4 and GSHP operation) are not considered to have a substantial influence in the indoor temperatures during the building operation hours. Therefore, these anomalies were not applied to the calibration of the WBSM. Figure 8.51 illustrates one typical day used in the validation of the VanDusen's WBSM.

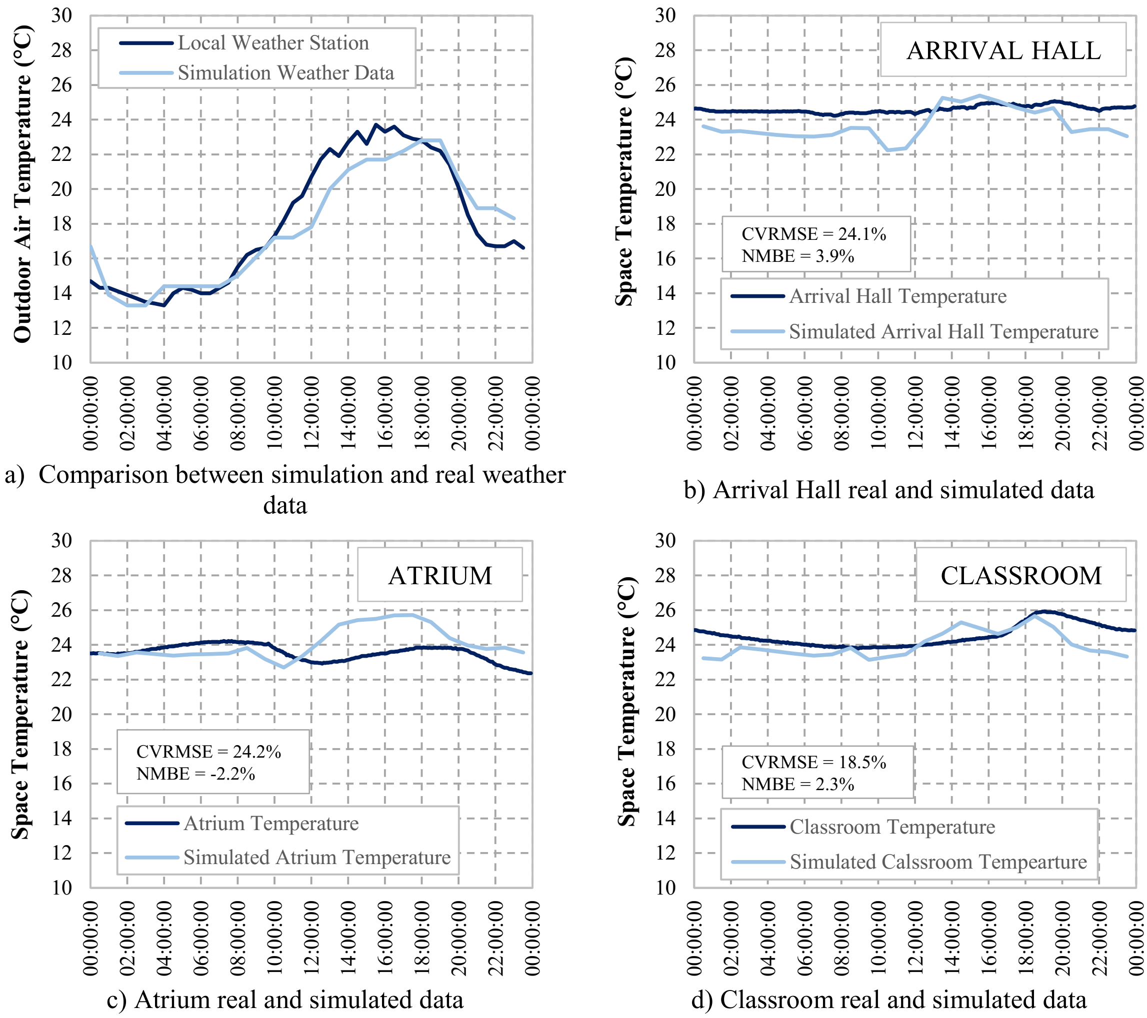

a) Comparison between simulation and real weather data

b) Arrival Hall real and simulated data

c) Atrium real and simulated data

d) Classroom real and simulated data

Figure 8.51 – Comparison of simulated and real data for a typical day [1]

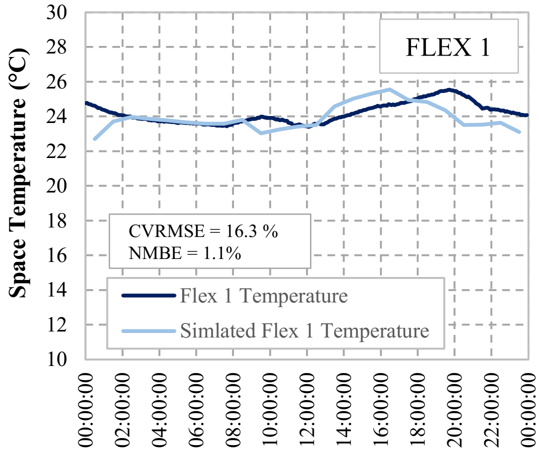

e) Flex 1 real and simulated data

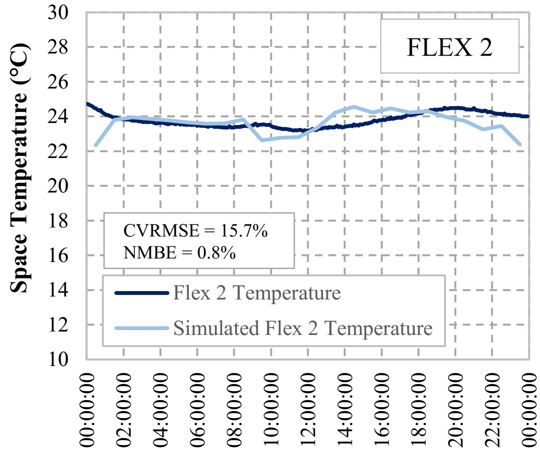

f) Flex 2 real and simulated data

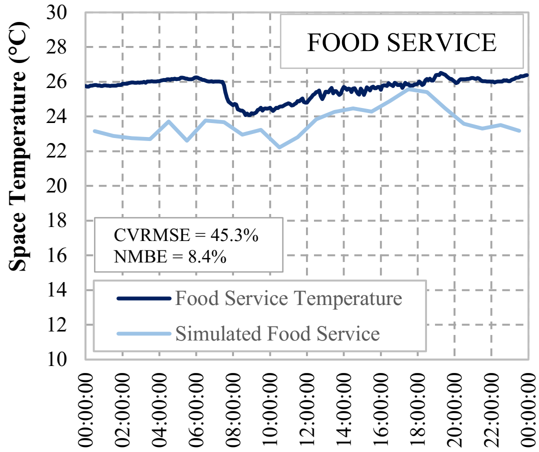

g) Food Service real and simulated data

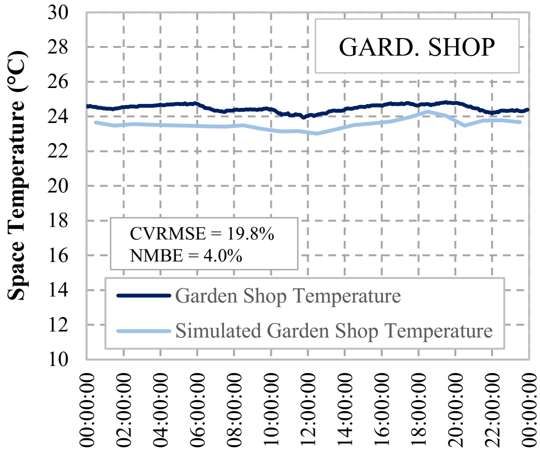

h) Garden Shop real and simulated data

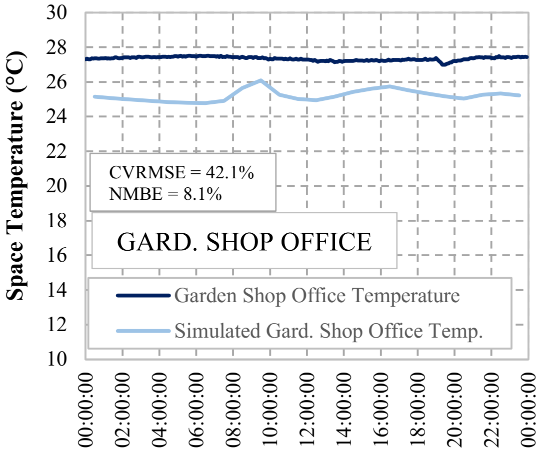

i) Garden Shop Office real and simulated data

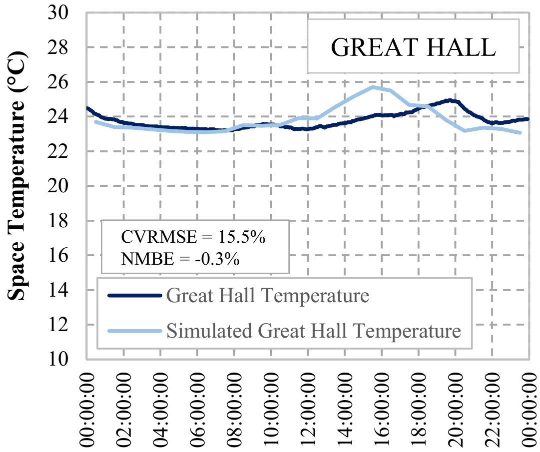

j) Great Hall real and simulated data

Figure 8.51 – Comparison of simulated and real data for a typical day [2]

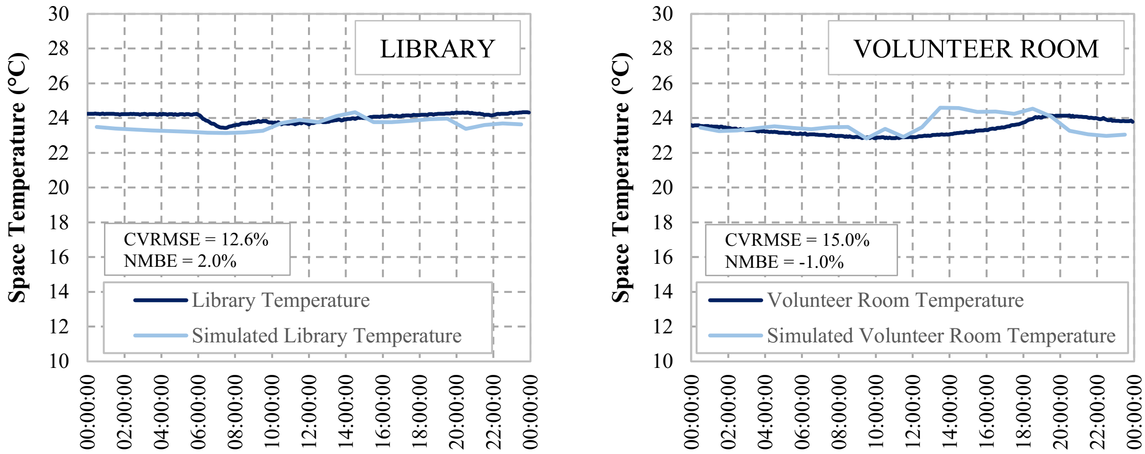

k) Library real and simulated data   l) Volunteer Room real and simulated data

Figure 8.51 – Comparison of simulated and real data for a typical day [3]

Figure 8.51 shows an unusual flat temperature pattern for all spaces. The main suspects for this unusual pattern are: 1) a lack of night-time ventilation, 2) the HP4 mechanical design anomaly that for cooling-down the electrical room dissipates heat into the radiant slabs. Appendix F demonstrates that night-time ventilation lowers-down temperatures at night and produces a more typical almost sinusoidal daily indoor temperature pattern. As explained in section 8.5, the mechanical anomalies were not included in the model calibration. In particular, given its small capacity, the amount of heat produced by HP4 is not expected to produce a big impact on the space temperatures of such a large and massive building, particularly at night when the need for cooling of the electrical room is significantly decreased.

Table 8.9 summarizes the values of CVRMSE and NMBE for all the 10 days used in WBSM validation, and presents the values for all the spaces used in the validation.

Table 8.9 – Final results on the WBSM validation

	CVRMSE (%)	NMBE (%)
Atrium	33.1	1.8
Classroom	38.0	6.0
Arrival Hall	38.9	4.8
Flex 1	24.6	2.9
Flex 2	26.2	3.5
Food Service	49.3	7.6
Great Hall	23.9	2.1
Garden Shop Office	60.8	11.1
Garden Shop	36.3	5.7
Library	36.6	6.1
Volunteer	23.5	2.3

From figure 8.51 and table 8.9, it is possible observe that the simulation is fairly representative. The values of the CVRMSE and NMBE are equal or below 30% and 15%, respectively, for most spaces. However, two spaces are not in that range of accuracy of CVRMSE: the garden shop office and food service. These slightly inaccuracies are explained by the position of the sensors at those spaces.

The data logger positioned at the food service was near the kitchen and the heat gains generated in that space. Thus, the measured temperatures in that space are normally higher than the simulated data, generating the inaccuracies observed in the validation process. The garden shop office sensor was positioned in a shelf, not well representing the room temperature, which affected the accuracy of the validation for that space. For the rest of the spaces the values are within the expected level of accuracy, thus it is considered that the WBSM is accurately representing the building.

8.7 VanDusen’s Natural Ventilation Sensitivity Analysis

This section uses the WBSM of the Van Dusen and conducts a sensitivity analysis on key design features that compose the natural ventilation strategy. The chosen design features are:

solar shading system, internal spaces connectivity, green roof, and solar chimney. The analyses consist of a baseline simulation, which represents the optimum design for natural ventilation, in comparison with the simulation that has a modification on a specific design feature that composes the natural ventilation strategy.

Two metrics were used to evaluate those factors, the exceedance hours method (*EH* method), previously presented in section 8.4.1.3, and an extended version of the *EH* method. The extended version uses the number of *EH* in conjunction with the temperature difference between the operative temperature and the upper temperature limit ($EH{\cdot}\Delta T$). This factor introduces not only the amount of hours where a space is in thermal discomfort, but it gives relevance to the actual space temperature in comparison with the thermal comfort threshold. For example, if the operative temperature of a space is 27°C for 2 hours, and say that number is above the comfort threshold, the *EH* is equal to 2. If the temperature was 30°C for the same 2 hour, the values would be the same $EH = 2$. By introducing the $EH{\cdot}\Delta T$ factor is possible to avoid distortions like that in the analysis.

The analysis uses only operative temperatures, as suggested by ASHRAE Standard 55 (2013). The *EH* is calculated for operative temperatures that are higher than the upper limit threshold. Temperatures below the lower limit of thermal discomfort are not considered in the analysis. In other words, when the room is colder than the adaptive thermal comfort suggests, that value was not considered in the final *EH* calculation. After all, the natural ventilation is being evaluated in its capacity to provide cooling for the spaces. The simulations were all relative to the months of July and August, the warmest period in Vancouver.

The baseline model is a representation of the optimum design for natural ventilation, with all the features that could be considered as good design practices, in theory. In that optimum design the building has an improved spaces connectivity, solar shading system, green roof, and solar chimney. The alternative simulation is a model with a certain feature removed. The current building has all the design strategies applied apart from the improved spaces connectivity. Table 8.10 summarizes the how the simulations are distributed.

Table 8.10 – Sensitivity analysis simulations

Factor Analyzed	Baseline	Alternative Simulation
Solar Shading	Optimum Design	No Shading System
Spaces Connectivity	Optimum Design	Actual Building (Poor Connectivity)
Green Roof	Optimum Design	No Green Roof (Roof from ASHRAE 90.1)
Solar Chimney	Optimum Design	No Solar Chimney

For the each design features analyzed, appendix E presents a comparison between the internal temperatures for the baseline and alternative simulation during the hottest day in the model.

8.7.1 Solar Shading System

VanDusen has a robust solar shading system applied to its envelope. In the sensitivity analysis, the baseline model represents the current status of the building and the other simulation represents the building with no shading system at all. Figure 8.52 and 8.53 illustrate the values found for percentage of *EH* and $EH \cdot \Delta T$, respectively.

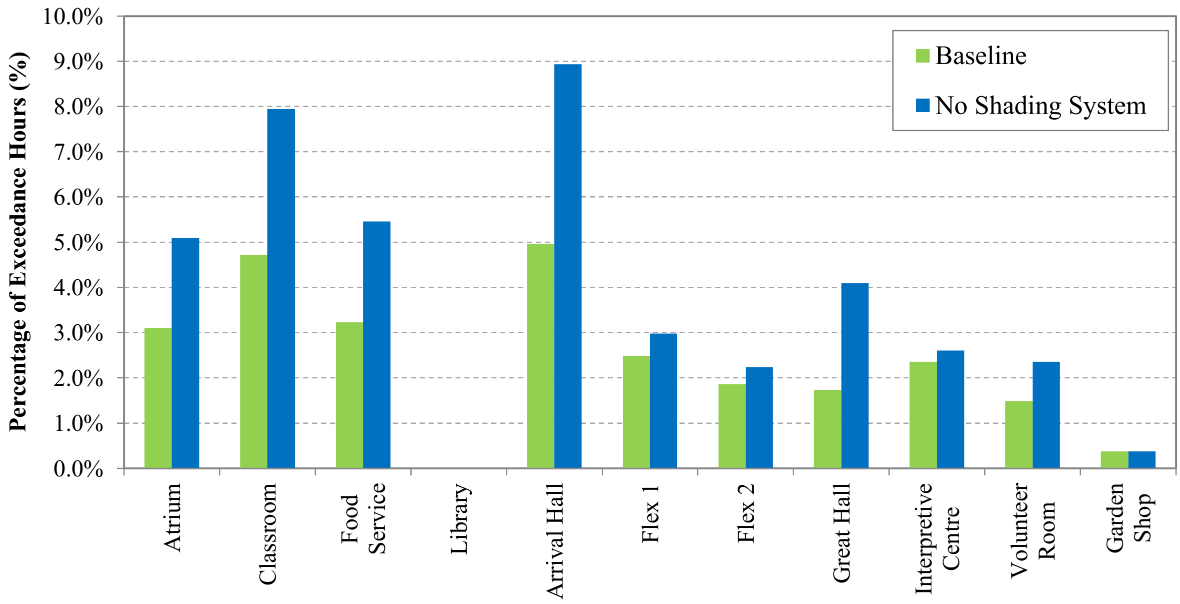

Figure 8.52 – Sensitivity analysis on the VanDusen's solar shading system (*EH* method)

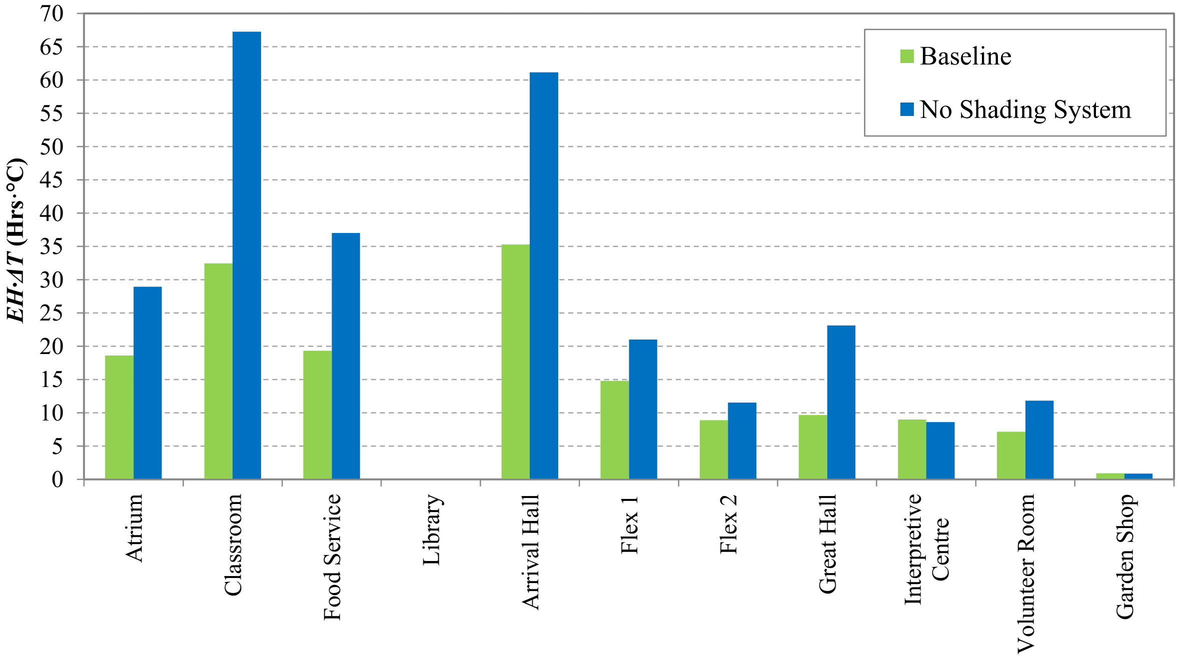

Figure 8.53 – Sensitivity analysis on the VanDusen's solar shading system (*EH·ΔT* method)

As expected, the spaces exposed to the south, like the arrival hall and the classroom, were the one with the drastic drop in the thermal comfort. The arrival hall was the space with the highest *EH*, but when considering the temperatures the classroom was the more sensible to the presence of the solar shading system. Considering the whole building, the baseline simulation has a *EH* of 2.39% and the simulation without the solar shading has 3.82%.

8.7.2 Internal Space Connectivity

Regards the internal spaces connectivity, the baseline WBSM presented the optimum configuration, with internal grilles connecting the spaces that have openings to the north and south corridors, and the walls limited to certain height, above that height the rooms are all connected in a great plenum space that allows the warm air to flow across the building until being exhausted by the solar chimney. In the other simulation, which represents the current building, the key spaces (great hall, flex 1 and 2, classroom and volunteer room) have no connection between each other. There are no grilles or flow paths that allow the air to flow from these spaces to the rest of the building and then to the solar chimney. Figure 8.54 and 8.55 shows the values found for percentage of *EH* and *EH·ΔT*, respectively.

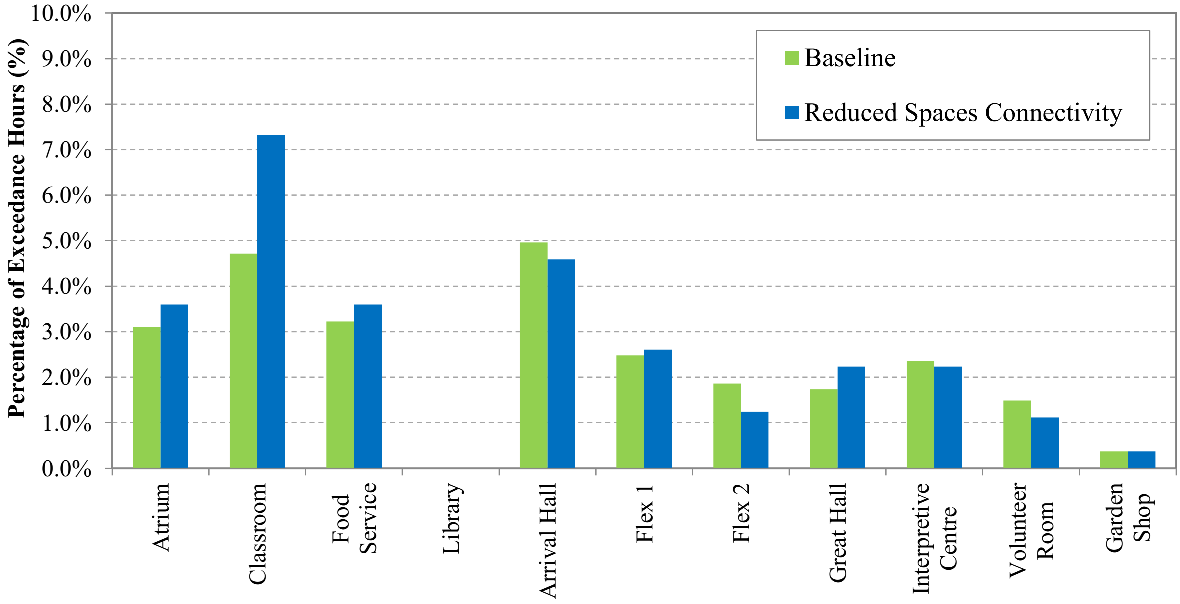

Figure 8.54 – Sensitivity analysis on the VanDusen's internal spaces connectivity (*EH* method)

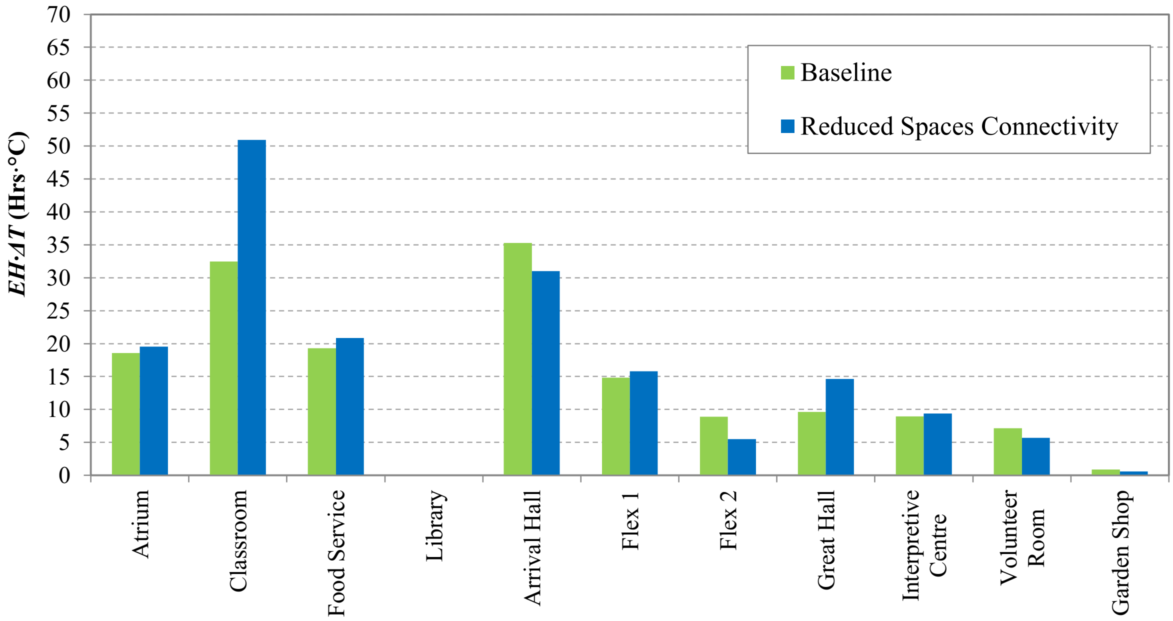

Figure 8.55 – Sensitivity analysis on the VanDusen's internal spaces connectivity (*EH·ΔT* method)

The spaces that still are connected with the plenum space at the core of the building, like the arrival hall, the atrium, the interpretative centre and the food service did not suffer big impacts with that modification. As expected, the more sensible spaces were the classroom and the rental spaces (flex 1 and great hall). The classroom is a south facing room, and receives more solar radiation than the volunteer room. This explains why its connectivity has a greater impact on room temperature variations, since dissipates the heat through the rest of the building more effectively than the single-sided ventilation. For the overall building, the *EH* is 2.63% for the model with reduced spaces connectivity and 2.39% for the baseline has.

8.7.3 Green Roof

The baseline WBSM presents the building with the green roof. The simulation with no green roof uses a standard roof assembly as suggested by ASHRAE 90.1 (2010) for Vancouver's climate zone 5. This roof assembly's thermal performance and thermal mass are lower than those of the original green roof. Figure 8.56 and 8.57 shows the percentage of *EH* and $EH{\cdot}\Delta T$, respectively.

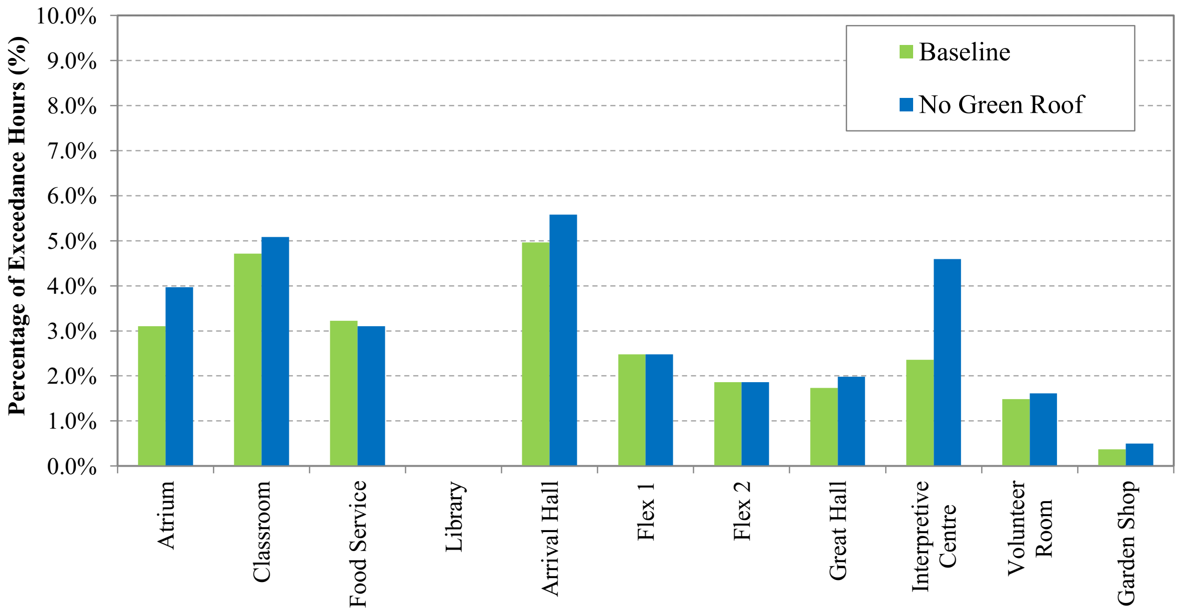

Figure 8.56 – Sensitivity analysis on the VanDusen's green roof (*EH* method)

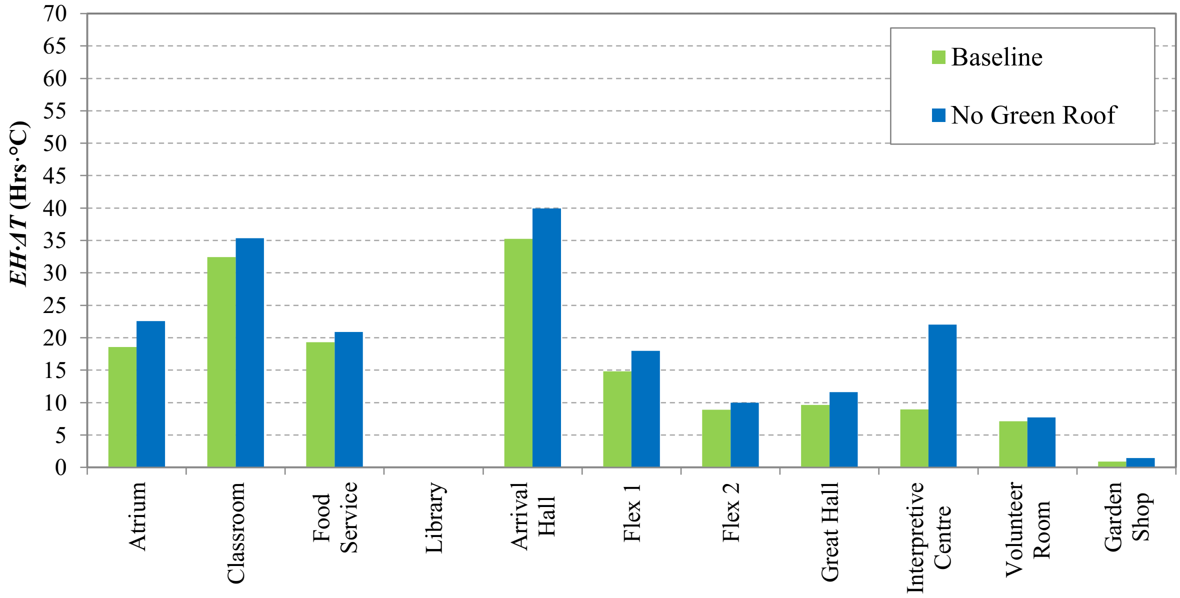

Figure 8.57 – Sensitivity analysis on the VanDusen's green roof (*EH·ΔT* method)

Except for the interpretive centre, the influence of the green roof is similar independent of the space. Given that the interpretive centre is at the core of the building and has no windows; from first principles, the construction performance has a higher impact on a space that is not properly ventilated. For all the other spaces the green roof slightly improves the natural ventilation effectiveness in the same degree. For the whole building, the *EH* is 2.39% for the baseline and 2.80% for the simulation without the green roof.

8.7.4 Solar Chimney

VanDusen's solar chimney is claimed to be one on the main features in the building's natural ventilation strategy and this sensitivity analysis might be able to endorse that claim. So, the baseline simulation shows the normal building with the solar chimney. In the other simulation there was no solar chimney at the building's roof, just a flat continuity of the building's roof. Figure 8.58 and 8.59 illustrates the percentage of *EH* and *EH·ΔT*, respectively

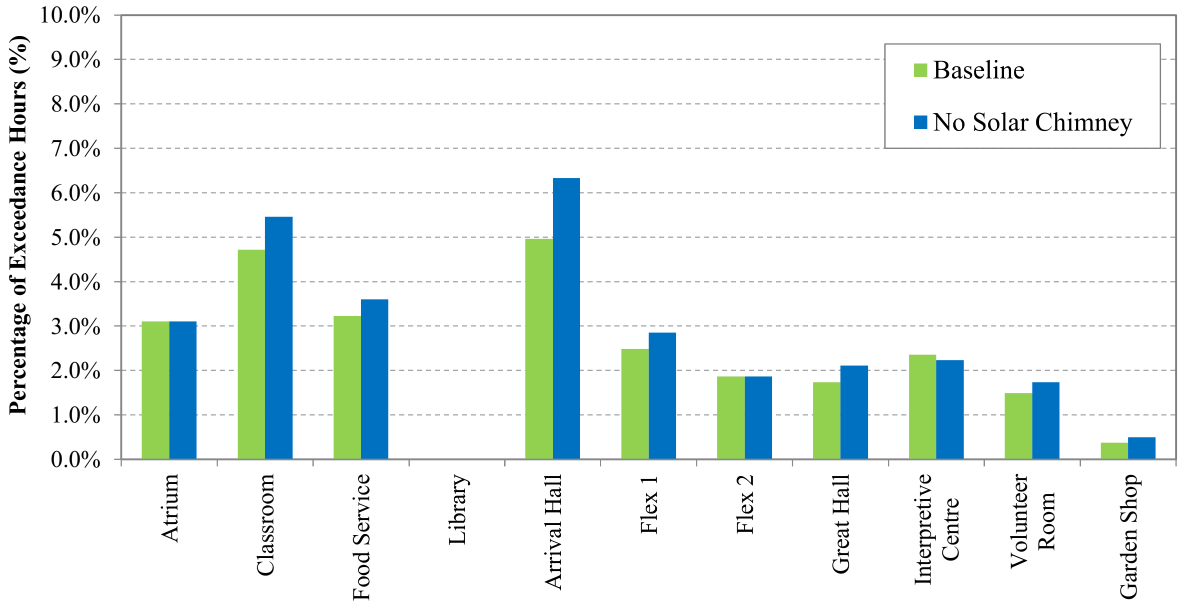

Figure 8.58 – Sensitivity analysis on the VanDusen's solar chimney (*EH* method)

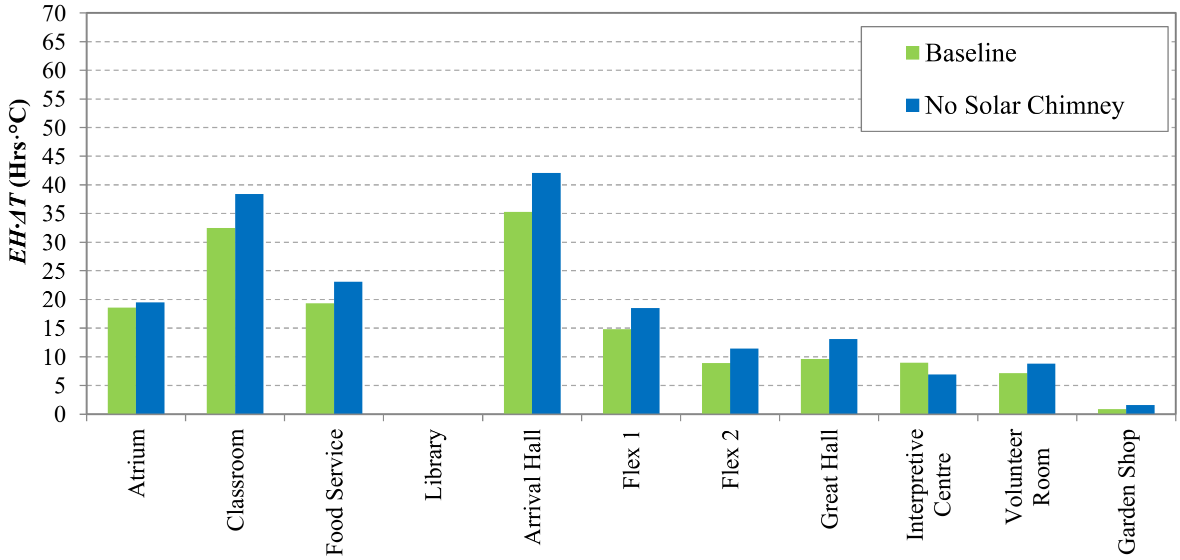

Figure 8.59 – Sensitivity analysis on the VanDusen's solar chimney ($EH{\cdot}\Delta T$ method)

The presence of the solar chimney improves the natural ventilation effectiveness for most of spaces. In the overall building, the *EH* was 2.39% for the baseline and 2.71% for the simulation without the solar chimney. Interestingly, the spaces directly connected with solar chimney (*i.e.* atrium) showed a lower impact to the solar chimney in comparison with the rest of spaces, like the classroom and rental spaces. The reason behind that is because the cross-ventilation (by opening the doors of the atrium and the arrival hall) is successfully delivering thermal comfort for the atrium. Moreover, in the simulation without the solar chimney, the warm air is trapped at the plenum (figure 8.60, b), affecting the spaces' thermal performance by decreasing the buoyancy-driven ventilation from the other spaces. Figure 8.60 illustrates the flow paths for the simulation with and without the solar chimney.

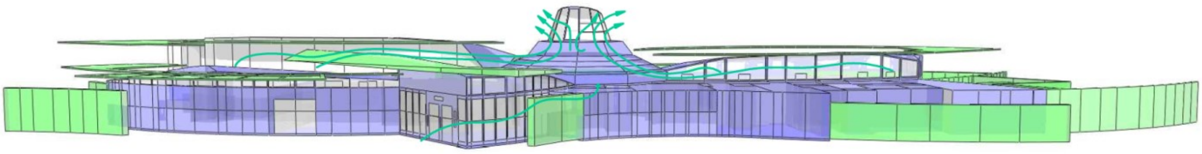

a) Baseline WBSM (with solar chimney)

b) WBSM without solar chimney

Figure 8.60 – Airflow paths for the simulation with and without solar chimney

Figure 8.61 illustrates the air temperatures for the atrium a solar chimney for a sunny and a cloudy day. It is observed that the sun is the main driving force to the spaces temperatures to the atrium and solar chimney. As expected, during sunny days with higher temperatures the solar chimney presents higher temperatures than the atrium. That temperature difference indicates that the solar chimney is successfully exhausting the air through its openings. This is observed by the constant exhaust airflow throughout the whole operation day. However, for cloudy days with mild temperatures, it is shown that the temperatures at the solar chimney are lower than the atrium, with the temperatures decreasing with the height. Furthermore, when the exhaust airflow is analyzed, it is detected that the solar chimney is successfully exhausting the airflow through its openings during the mornings and afternoon, but in the beginning of the evening the solar chimney, instead of exhaust the air, allows a small of air to flow into the building.

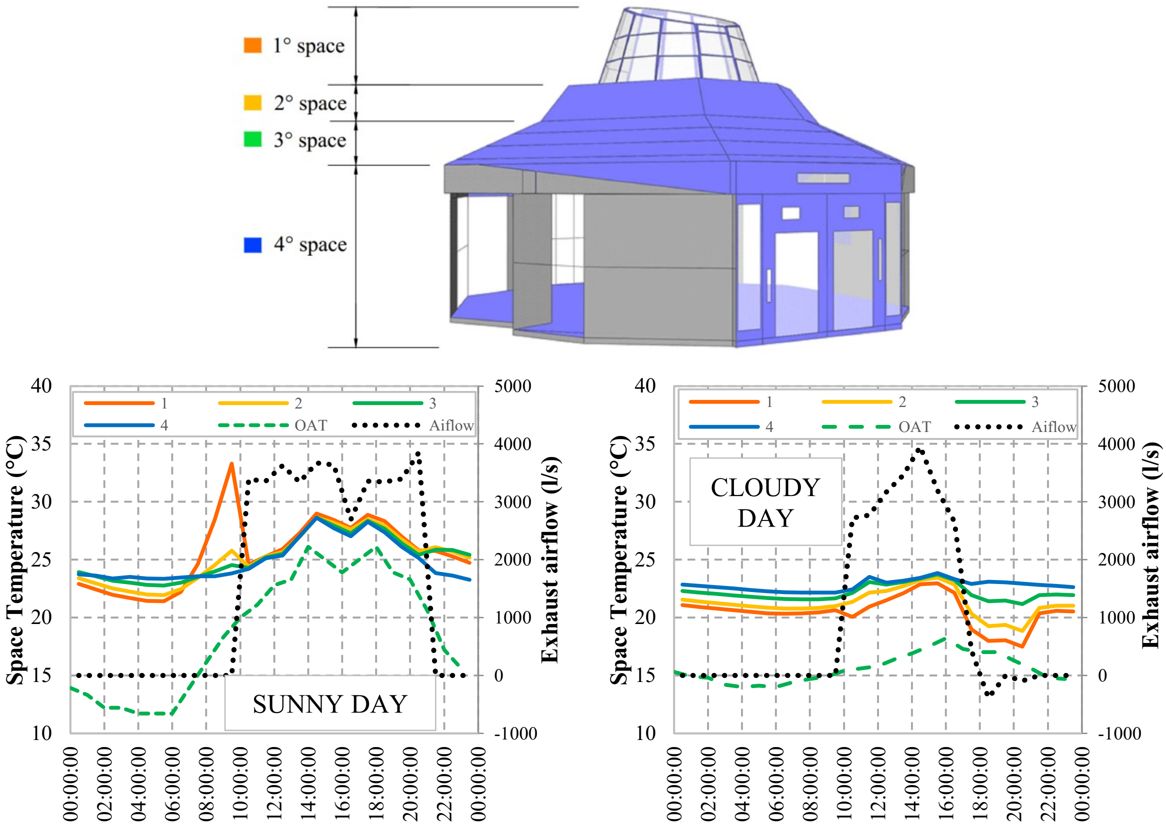

a) Atrium and solar chimney temperatures during a sunny day

b) Atrium and solar chimney temperatures during a cloudy day

Figure 8.61 – Solar chimney and atrium temperatures

Thus, it is possible to conclude that the optimum operation for the solar chimney is during sunny days. In these conditions, the exhaust airflow assumes stable and constant values throughout the whole day. For cloudy days, it is observed that airflow though the openings are more dynamic and unstable, even allowing inward airflow to the building. Regarding the solar chimney performance, further analysis is let for future research.

8.7.5 Sensitivity Analysis Results and Comparison

In summary, the results of the sensitivity analysis are presented in this section. Firstly, as expected, all the design features analyzed improve the natural ventilation effectiveness by cooling the spaces. Between the factors analysed, the more effective strategy is VanDusen's solar shading system. The second more effective factor is green roof, followed by the building's solar chimney in third and by the internal spaces connectivity in forth. However, the differences between the green roof, solar chimney and the internal connectivity are minimal. Differently from the shading system that showed substantially better results than the other features. Table 8.11 presents a summary for the results calculated in the analysis.

Table 8.11 – Final results on the sensitivity analysis

	EH (%)	*EH·ΔT* (°C·Hours)	*EH* (Hours)
Baseline	2.39	155.9	212
Reduced Internal Spaces Connection	2.63	173.8	233
No Solar Chimney	2.71	183.4	240
No Green Roof	2.80	189.5	248
No Solar Shading	3.82	271.3	339

Figure 8.60 illustrates the final results of the sensitivity analysis. The simulation with the current building design is added to this final analysis. With that, it is possible to observe the performance of the current building design in comparison with the other design configurations.

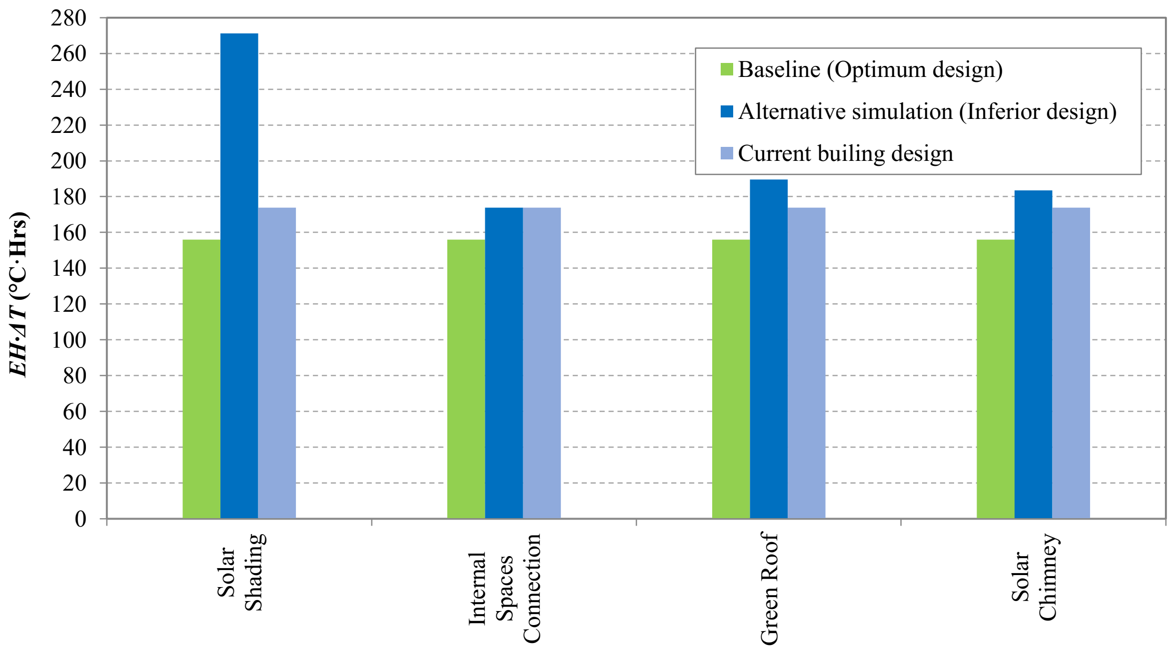

Figure 8.61 – Sensitivity analysis results

The results show the complexity of the natural ventilation strategy, which is composed by a number of different features. Besides the internal spaced connectively, all the other features are key architectural elements, which not necessarily is responsibility of the building designer. This endorses the idea of having a cooperative team working together in order to have efficient building, especially when involving a naturally ventilated building.

8.8 Comparison between Baseline (Optimum Design) and Current Building Performance under Natural Ventilation

Using the calibrated WBSM, this section presents a comparison between the improved and the current building performance for natural ventilation. The improved performance (baseline) is composed by all the features already presented in VanDusen but with the improved spaces connectivity and the mechanical ventilation throughout the night-time. Currently, the case study building does not have any type of ventilation during the night and there is no connection between key spaces, such as the great hall, Flex 1 and 2, classroom and volunteer room. To be able to have a fair comparison between the two models, the windows/doors operation for both simulations follow the same logic based on the building's opening hours, similar to the actual building performance. So, apart from the improved spaces connectivity and night-time mechanic ventilation, both building have the same features and windows operation. Figure 8.62 illustrates the percentage of *EH* for the internal spaces for the baseline and actual building performance.

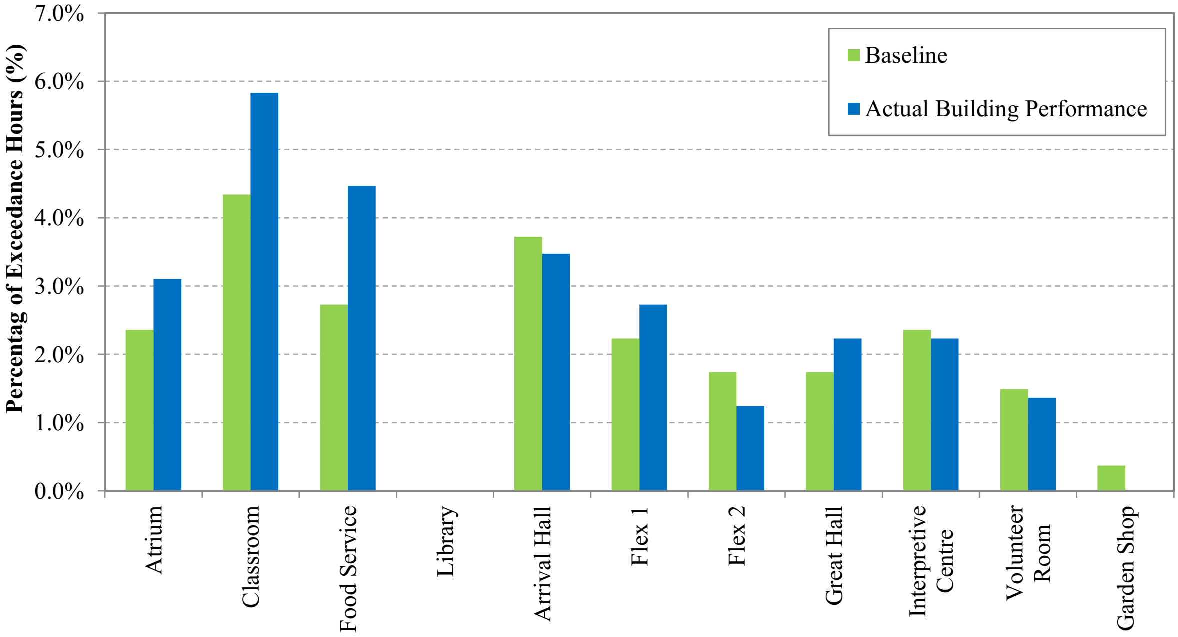

Figure 8.62 – Percentage of *EH* for baseline and actual building performance

As expected, the simulation of the actual building performance shows more hours of thermal discomfort than the optimum model. However, the difference between them is not significant. In terms of the overall building's thermal comfort, the baseline simulation has a *EH* of 2.10% and 2.42% for the actual building performance. The building's thermal mass plays a small role in keeping the operative temperatures lower during the occupied hours, consequently improving the building's thermal comfort. The improved connectivity between spaces has a small significance as well, as observed in section 8.7.2. In summary, the current building natural ventilation performance could be slightly improved with a better connectivity and night-time ventilation. However, no extreme enhancement in thermal comfort is expected with this improvement.

9. CONCLUSIONS

After studying the challenges and limitations for assessing natural ventilation using the Whole Building Simulation Model (WBSM), the thesis has presented a systematic methodological framework to assist the natural ventilation assessment. The framework has been successfully applied to an existing real landmark building in Vancouver.

The framework developed for WBSM (section 7.2) recognizes the key elements that compose the natural ventilation simulation, and provides the necessary feedback to the building designer in order to have a representative model. The flowchart for the field testing and monitoring is developed (section 7.3); it considers different levels of analysis and access to the building. In parallel, a methodology for the validation and calibration is suggested (section 7.5). In summary, the proposed framework gives the building designers the tools and methods needed in order to perform a systematic natural ventilation assessment.

Given the scarcity in the research literature in this specific topic, the proposed framework is a first step in the development of a systematic natural ventilation assessment. Further work is needed to develop a more comprehensive methodology. However, it is expected that the proposed framework serves as foundation for future work in the natural ventilation field.

The main challenges faced in the case study were the low quality of energy data, and the operational anomalies found in the building. These challenges are reflected in the level calibration achieved in the case study WBSM. Better quality data is needed in order to achieve a higher level of calibration following the proposed methodology for calibration (section 7.5). VanDusen is a particularly challenging building to model for natural ventilation because in addition to its unique shape, all its spaces have high ceilings, and this challenges the AFN fully-mixed room air principle. So, a software workaround was needed in order to address this limitation: representing each zone as a zonal model with spaces stacked vertically on top of each other.

Regarding the field testing performed in VanDusen from the August 10th to August 25th, it was shown that for the most spaces the temperature were in the comfort rage according to the

ASHRAE Standard 55 (2013) adaptive thermal comfort. The most comfortable space in VanDusen is the building's library, followed by the rental spaces (great hall, flex 1 and 2) and volunteer room. The atrium, garden shop, arrival hall and classroom presented temperatures outside the thermal comfort range for fair amount of time, with *EH* varying from 6 to 12% of the occupied hours. For two spaces, however, the amount of time that the spaces are outside the comfort range is too drastic and adjustments need to be considered. The food service showed a *EH* of 23% and the garden shop office a *EH* of 62%. It is possible to assume that the data sample was not significant for the whole summer operation but it indicates that the alternative measures need to be taken in order to provide comfort for these spaces during the summer. Moreover, the measured data was directly influenced by the anomalies found in the building operation (section 8.5). It is expected, after the adjustment in anomalies that the building performance under natural ventilation will likely to be improved.

On the strategies that compose the natural ventilation in the case study building (section 8.7), it is shown that the more effective strategy in delivering thermal comfort is provided by the solar shading system. Alongside that element, the internal spaces connectivity, solar chimney and green roof, come in that order of importance. The influence of the solar shading in the thermal comfort is perceived in all the spaces but is more evident in spaces that have exposure to solar radiation, in special rooms with south face fenestration. The influence of the spaces connectivity was more evident to the classroom and rental spaces, showing the dependence of those rooms to the others space connectivity. On the green roof influence, this feature affects all the spaces in a minor amount; for only a core room that does not have any purposely natural ventilation the green roof has a substantial influence in maintaining it cool. The solar chimney showed an influence in the overall thermal comfort provided by natural ventilation. Its influence was not observed in the spaces directly connected with the chimney, showing that the solar chimney is effectively drawing the warmer air from all different spaces and exhausting it through its openings.

The current natural ventilation operation was compared with an improved natural ventilation operation (section 8.8). The improvements include enhanced spaces connectivity in association with a plenum space and proper ventilation at night-time. Notwithstanding, these improvements did not drastically impact in the natural ventilation effectiveness in the building. Furthermore, the current single-sided ventilation strategy applied to several spaces (great hall, flex 1 and 2, classroom and volunteer room), though less effective than other strategies (*i.e.* buoyancy-driven and cross ventilation), is able to deliver thermal comfort for the occupants.

In conclusion, the effectiveness of natural ventilation is affected by the architectural design; but from the case study building, for Vancouver's mild summer season, there is no drastic influence of any specific design feature on the overall effectiveness of natural ventilation. For this case study, the major design feature was the solar shading system. However, it is important to put the results of this study in its climate context. Therefore, it can be hypothesized that the results from the sensitivity analyses would have been more dramatic in hot humid climate. Testing this hypothesis is left for future research. In summary, the effectiveness of natural ventilation is a result of an integrated effort of a number of design features. There is no silver bullet to improve the natural ventilation effectiveness.

Last but not least, the assessment of thermal comfort in naturally ventilated buildings need to consider a systematic feedback from occupants. Simulations and measurements indicate that occupants should in general be thermally satisfied in the building. However, informal surveys with staff indicated some level of dissatisfaction mainly due to a lack of control over the indoor thermal environment. They felt that the indoor environmental conditions were imposed on them, *i.e.* lack of perceived control on the environment, which is one of the bases of the adaptive model. This raises the question: is the adaptive thermal comfort model appropriate for all naturally ventilated buildings? Would a model that considers the level of control be more appropriate? Answering these questions is left for future research.

10. FURTHER WORK

Further work is recommended in the two aspects: 1) the natural ventilation assessment of the VanDusen case study; and 2) in research to support the assessment of natural ventilation:

1) Further work in the natural ventilation assessment of the VanDusen case study:

- Evaluation of different natural ventilation operational strategies to VanDusen. Using the case study's WBSM, the effectiveness of each operational strategy should be analyzed. To name a few operational strategies: night-ventilation, internal doors operation, occupant's behaviour, and etc. Furthermore, it is possible to propose an intelligent window control based on the WBSM to maximize the natural ventilation effectiveness.
- Improve the quality of the energy data used in the whole year calibration of the WBSM. Until the present time, there are few data available and a number of gaps in the energy data available to the authors of this research.
- The use of surveys to obtain feedback on occupants' satisfaction and behaviours during the building usage, and the development of an uncertainty analysis will allow us to achieve the highest level of calibration suggested by section 7.3.
- Measure the thermal stratification on the case study building. The high ceiling of the building spaces are a source of uncertainty to modelling the airflow through the spaces. By measuring the thermal stratification in the spaces a better characterization of the actual building airflow patterns is possible. This data could serve to a finer characterization of the airflow in the WBSM (zonal model) or in a CFD simulation.
- Development of CFD analysis of several internal building spaces. In special, the building's solar chimney could be modelled using CFD. After all, it was observed, from the sensitivity analysis, an important influence of the solar chimney in the overall building performance. The initial step would be mapping the temperatures at the atrium and at the top part of the solar chimney in order to serve as boundary conditions.
- Evaluate the use of PPD (Predicted Percentage of Dissatisfied) and PMV (Predicted Mean Vote) as metric to evaluate the natural ventilation effectiveness. Even though

these factors are design to determine the thermal comfort in mechanically ventilated buildings, as natural ventilation was imposed for most of the building's occupants and they normally do not have the option to interact with the building to achieve thermal comfort (*i.e.* lack of perceived control on the indoor environment), the use of Fanger model might be considered valid to evaluate the thermal comfort for provided.

- The use of C_p calculated by CFD simulation. Addressing the uncertainty inherent from the wind forces driving natural ventilation. In addition, a comparison between C_p generated by CFD simulation and the values adopted by the WBSM could be made. After all, the complexity in the building geometry is likely to be generating a discrepancy between real and simulated C_p values.

2) Further research work to support natural ventilation assessment:

- The use of the AFN mixed-model assumption to predict thermal comfort for naturally ventilated spaces. Natural ventilation imposes unstable and non-uniform airflows, possibly creating drafts, stagnant areas, and thermal stratification for the spaces, which may create thermal discomfort for some occupants. This is not taken into account by AFN, and the results of the simulation do not indicate those complexities.
- A rigorous climate and outdoor micro-climate analysis was out of the scope of this research. However, the outdoor climate and micro-climate is the main boundary condition for natural ventilation and deserves close study. There are existing tools to support climate analysis to some degree; however, these tools need to be tested, and models and methods for a comprehensive climate and site micro-climate analysis need to be integrated into the proposed methodology.
- As discussed in this thesis, the coupling of outdoor climate and indoor airflows in naturally ventilated buildings is still in need for research; particularly, as function of the type of openings in a building.
- Addressing uncertainty in natural ventilation design and assessment is another important topic that was out of the scope of this research. A rigorous study of the available literature needs to be conducted and a proper method be developed to address the uncertainty, due to the two main factors affecting natural ventilation: the wind, and the occupants' needs and behaviors.

- Analysis of the impact of occupants' behaviors on building performance, including the development of algorithms to simulate various occupants' behaviors. Results from the literature need to be studied and assessed their applicability to support the assessment of naturally ventilated buildings.
- Develop better approaches for the field assessment and measurement of naturally ventilated buildings and integrate its results in WBSM. In particular, integrate the complexities originate from the difficulty to measure air pressure differentials and air flows in the field; as well as integrating surveys' data into the assessments.

REFERENCES

1. Allocca, C. (2001). Single-sided Natural Ventilation: Design Analysis and General Guidelines. Master's Thesis. Massachusetts Institute of Technology, USA, 2001.
2. Allocca, C.; Chen, Q.; Glicksman, L. R. (2003). Design analysis of single-sided natural ventilation. Energy and Building 35, pp. 785–795, 2003.
3. Andersen, K. T. (2002). Friction and contraction by ventilation openings with movable flaps. Proceedings of Roomvent 2002, Copenhagen, Denmark, 2002.
4. ASHRAE 90.1 (2010) Energy Standard for Buildings Except Low-Rise Residential Buildings. American Society of Heating, Refrigeration and Air-Conditioning Engineers, Georgia, Atlanta 2010.
5. ASHRAE Fundamentals (2009). ASHRAE handbook: Fundamentals. American Society of Heating, Refrigeration and Air-Conditioning Engineers, Georgia, Atlanta 2013.
6. ASHRAE Guideline 10 (2016). ASHRAE Guideline 10 – Interactions affecting the achievement of acceptable indoor environments. American Society of Heating, Refrigeration and Air-Conditioning Engineers, Georgia, Atlanta 2016.
7. ASHRAE Guideline 14 (2014). ASHRAE Guideline 14 – Measurement of Energy and Demand Savings. American Society of Heating, Refrigeration and Air-Conditioning Engineers, Georgia, Atlanta 2014.
8. ASHRAE Standard 55 (2013). Thermal Environmental Conditions for Human Occupant. American Society of Heating, Refrigeration and Air-Conditioning Engineers, Georgia, Atlanta, 2013.
9. Atkinson, J.; Chartier, Y.; Pessoa Silva, C. (2009). Natural ventilation for infection control in health care settings. World Health Organization, 2009.
10. Balaras, A.; Bossaer, A.; Dascalaki, E.; Ducrame, D.; Santanouris, M. (1999). Modelling large openings with COMIS. Energy and Buildings 30, pp. 105–115, 1999.
11. Baumbach, G. (1990). Luftreinhaltung. Berlin, Heidelberg, New York, Springer, 1990.
12. Beizaee, A.; Firth, S. K.; Vadodaria, K.; Loveday, D. (2012). Assessing the ability of PMV model in predicting thermal comfort sensation in naturally ventilated buildings

in UK. Proceeding of 7th Windsor Conference: The changing context of comfort in a unpredictable world, London, 2012.

13. Belleri, A. (2013). Integrated Methods for Natural Ventilation. Phd Thesis, Universitá Degli Studi di Bergamo, Facoltà di Ingegneria Industriale, Italy, 2013.
14. Blondeau, P.; Spérandio, M.; Allard, F. (1997). Night ventilation for building cooling in summer. Solar Energy 61 (5), pp. 327–335, 1997.
15. Bradly, D. E.; Utzinger, D. M. (2007). Enhancement and Use of Combined Simulation Tools in the Assessment of Hybrid Natural/Mechanical Ventilation Systems. ASHRAE Transactions, v. 113, Part 2, 2007.
16. Breesch, H.; Janssens, A. (2007). Reliable Design of Natural Night Ventilation Using Building Simulation. 10th Thermal Performance of the Exterior Envelopes of Whole Buildings, Atlanta, USA, 2007.
17. BS 5925 (1991). Code of practice for ventilation principles and designing for natural ventilation. British Standard Institute, 1991.
18. Cable, M. (2009). An Evaluation of Turbulence Models for Numerical Study of Forced and Natural Convective Flow in Atria. Kingston, Ontario, 2009.
19. Caciolo, M.; Marchio, D.; Stabat, P. (2009). Survey of existing approaches to assess and design natural ventilation and need for further developments. 11th International IBPSA Conference, pp. 220–227, Glasgow, 2009.
20. CEN Standard EN15251 (2007) Indoor environmental input parameters for design and assessment of energy performance of buildings addressing indoor air quality, thermal environment, lighting and acoustics Bruxelles: European committee for Standardisation
21. Chen, Q. (1995). Comparison of Different k-e Models for Indoor Air Flow Computations. Numerical Heat Transfer Part B: Fundamentals: An International Journal of Computation and Methodology, pp. 353–369, 1995.
22. CIBSE AM10 (2005). Natural ventilation in non-domestic buildings. The Charted Institution of Building Services Engineers, London, 2005.
23. CIBSE TM52 (2013). The limits of thermal comfort: avoiding overheating in European buildings. Chartered Institution of Building Services Engineers, London, 2013.

24. Climate Suitability Tool (2017). NIST Multizone Modeling Website. Retrieved from: http://www.bfrl.nist.gov/IAQanalysis/software/CSTdesc.htm.
25. Coakley, D.; Raftery, P.; Keane, M. (2014). A review of methods to match building energy simulation models to measured data. Renewable and Sustainable Energy Reviews, v. 37 pp. 123–141, 2014.
26. Coakley, D; Raftery, P.; Molloy, P. (2012). Calibration of whole building energy simulation models: detailed case study of a naturally ventilated building using hourly measured data. Building Simulation and Optimization, Proceedings of the 2012 building simulation and optimization conference, pp. 57–64, 2012.
27. Cobalt (2009). VanDusen Gardens – Sustainable Design Report. Vancouver, Canada, 2009.
28. Cook, M.; Ji, Y.; Hunt, G. R. (2003). CFD Modelling of Natural Ventilation: Combined Wind and Buoyancy Forces. International Journal of Ventilation 1 (3), pp. 167–179, 2003.
29. CoolVent (2017). CoolVent – The Natural Ventilation Simulation Tool by MIT. Retrieved from: http://coolvent.mit.edu/.
30. Cóstola, D.; Alucci, M. (2007). Pressure Coefficient Simulated by CFD for Wind-driven Ventilation Analysis. Proceedings: Building Simulation 2007, pp. 999 – 1006, 2007.
31. Cóstola, D.; Blocken, B.; Hensen, J. L. M. (2009). Overview of pressure coefficient data in building energy simulation and airflow network programs. Building and Environment 44, pp. 2027–2036, 2009.
32. Cóstola, D.; Blocken, B.; Ohba, M.; Hensen, J. L. M. (2010). Uncertainty in airflow rate calculation due to the use of surface-averaged pressure coefficients. Energy and Building 42, pp. 881–888, 2010.
33. CRADLE-CFD (n.d). Products and Services, scSTREAM. Software Cradle Co. Ltd. Retrieved from: http://www.cradle-cfd.com/products/scstream/index.html/.
34. D'Aquilio, A.; Sileryte, R.; Yang, D.; Turrin, M. (2016). Simulating natural ventilation in large sports buildings – Prediction of temperature and airflow patterns in the early design stages. SimAUD, London, UK, 2016.

35. Dascalaki, E.; Santamouris, M.; Buant, M; Balaras, C. A.; Bossaer, A; Ducarme, D.; Wouters, P. (1999). Modeling large openings with COMIS. Energy and Buildings, v. 30, pp. 105–115, 1999.
36. DesignBuilder [Computer software] (2016). DesignBuilder v.5. Retrieved from: https://www.designbuilder.co.uk/.
37. Durrani, F.; Cook, M. J.; McGuirk, J. J. (2015). Evaluation of LES and RANS CFD modelling steady states in natural ventilation. Building and Environment 92, pp. 167–181, 2015.
38. Ellis, J. (2016). Assessment of Natural Ventilation Design and Efficacy in a Net-Zero Energy House – A Case Study of the Harmony House. Master's Thesis, British Columbia Institute of Technology, Canada, 2016.
39. Emmerich, S. J.; Dols, W. S.; Axley, J. M. (2001). Natural Ventilation Review and Plan for Design and Analysis Tools. National Institute of Standards and Technology, NISTIR 678, 2001.
40. Emmerich, S. J.; Nabinger, S. J.; Gupte, A.; Howard-Reed, C.; Wallace, L. (2003). NISTIR 7035. National Institute of Standards and Technology, Gaithersburg, MD, and National Exposure Research Laboratory, US Environmental Protection Agency, 2003.
41. EnergyPlus (2015). EnergyPlus Documentation – Engineering Reference, The Reference to EnergyPlus Calculations. 2015.
42. eQUEST [Computer software] (2016). Quick Energy Simulation Tool v.3.65. Retrieved from: http://www.doe2.com/equest/.
43. Etheridge, D. W.; Sandberg, M. (1996). Building ventilation: theory and measurements. John Wiley & Sons, Chischester, New York, 1996.
44. Evola, G.; Popov, V. (2006). Computational analysis of wind driven natural ventilation in buildings. Energy and Buildings 38, pp. 491–501, 2006.
45. Fabrizio, E.; Monetti, V. (2015) Methodologies and Advancements in the Calibration of Building Energy Models. Energies, v. 8, pp. 2548–2574, 2015.
46. Furbringer, J. M.; Roulet, C. A.; Borchiellini, R. (1999). An overview of the evaluation activities of IEA ECBCS Annex 23. Energy and Buildings, v. 30, pp. 19–33, 1999.

47. Geros, V.; Santamouris, M.; Tsangrasoulis, A.; Guarracino, G. (1999). Experimental evaluation of night ventilation phenomena. Energy and Buildings 29 (2), pp. 141–154, 1999.
48. Heiselberg, P. (2004). Builidng integarted ventilation systems-modelling and design challenges. Prceedings of CIB 2004, Toronto, Canada, 2004.
49. Heiselberg, P.; Sandberg, M. (2006). Evaluation of discharge coefficients for windows openings in wind driven natural ventilation. International Journal of Ventilation 5 (1), pp. 43– 52, 2006.
50. Hensen, J. L. M. (1991). On the thermal interaction of building structure and heating and ventilation system. PhD thesis, Eindhoven University of Technology, 1991.
51. Heo, Y. (2011). Bayesian calibration of building energy models for energy retrofit decision-making under uncertainty. Ph.D. Thesis, Georgia Institute of Technology, USA, 2011.
52. Humphreys, M.; McCartney, K.; Nicol, F.; Raja, I. (2001). Thermal comfort: use of controls in naturally ventilated buildings. Energy and Buildings 33, 235–244, 2001.
53. IEA-EBC (2017). IEA-EBC Annex 66 – Definition and Simulation of Occupant Behavior in Buildings. Retrieved from https://annex66.org/.
54. IES-VE – Integrated Environmental Solution (2012). MacroFlo Calculation Methods, IES Virtual Environment 6.5. United Kingdom, 2012.
55. IES-VE [Computer software] (2016). Integrated Environmental Solutions – Virtual Environment v.2016. Retrieved from: https://www.iesve.com/.
56. Integral Group (2013) Vandusen Botanical Gardens Visitor Centre – Net Zero Site Energy Use Report. Vancouver, BC, 2013.
57. International Energy Agency (2013). Transition to Sustainable Buildings Strategies and Opportunities to 2050. International Energy Agency (IEA), Paris, France, 2013.
58. Iqbal, A.; Afshari, A.; Wigo, H.; Heiselberg, P. (2015). Discharge coefficient of centre-pivot roof windows. Buildings and Environment 92, pp. 635–643, 2015.
59. Iqbal, A.; Nielsen, P. V.; Afshari, A.; Heiselberg, P. (2012). Numerical predictions of the discharge coefficient of a window with moveable flap. Healthy Buildings 2012: 10th International Conference. Queensland University of Technology, 2012.

60. Karava, P.; Stathopoulos, T.; Athienitis, A. K. (2003). Wind driven flow through openings – a review of discharge coefficients. International Journal of Ventilation 3 (3), pp. 255–266, 2003.
61. Karava, P.; Stathopoulos, T.; Athienitis, A. K. (2004).Wind Driven Flow through Openings – A Review of Discharge Coefficients. International Journal of Ventilation, v. 3 (3), pp. 255–266, 2004.
62. Karava, P.; Stathopoulos, T.; Athienitis, A. K. (2007). Wind-induced natural ventilation analysis. Solar Energy 81, pp. 20–30, 2007.
63. Karava, P.; Stathopoulos, T.; Athienitis, A. K. (2011). Airflow assessment in cross-ventilated buildings with operable façade elements. Building and Environment, v. 46 pp. 266–279, 2011.
64. Kato, S.; Murakami, S.; Mochida, A.; Akabayashi, S.; Tominaga, Y. (1992). Velocity-pressure field of cross ventilation with open windows analyzed by wind tunnel and numerical simulation. Journal of Wind Engineering and Industrial Aerodynamics 44, pp. 2575–2586, 1992.
65. Knoll, B.; Phaff, J.; de Gids, W. (1996). Pressure coefficient simulation program. Air infiltration Review 17, pp. 1–5, 1996.
66. Kobayashi, T.; Sandberg, M.; Kotani, H.; Claesson, L. (2010). Experimental investigation and CFD analysis of cross-ventilated flow through single room detached house model. Building and Environment 45, pp. 2723–2734, 2010.
67. Kukadia, V. (1998). Work Package 2: performance of naturally ventilated buildings–final monitoring preport. NatVent, Pan-European Project Encouraging the Use of Natural Ventilation in Office-type Buildings, 1998.
68. Larsen, T. S. (2006). Natural Ventilation Driven by Wind and Temperature Difference. PhD Thesis, Aalborg University, Department of Civil Engineering, 2006.
69. McDonough, J. M. (2013). Introductory Lectures on Turbulence – Physics, Mathematics and Modeling. Departments of Mechanical Engineering and Mathematics, University of Kentucky, 2013.
70. Mitterhofer, M.; Norrefeldt, V.; Stratbücker, S. (2016). Advanced modeling and simulation methods for assessment and optimization of indoor climate. IAQVEC

2016, 9th International Conference on Indoor Air Quality Ventilation & Energy Conservation in Buildings, 2016.

71. Mora, R. (2015). Climate Analysis 1: Scale in Climate & Weather Analysis. Research Methods – Class notes, British Columbia Institute of Technology, 2015.
72. Mora, R. (2016). Building Air Flow Principles. Building Science 1 – Class notes, British Columbia Institute of Technology, 2016.
73. Murakami, S.; Kato, S.; Akabayashi, S.; Muzutani, K.; Kim, Y. (1991). Wind tunnel test on velocity-pressure field of cross-ventilation with open windows. ASHRAE Transactions, v. 97, pp. 525–538, 1991.
74. National Resource Canada – NRC (2015). Advantages of Energy Efficiency. Web address: http://www.nrcan.gc.ca/energy/efficiency/buildings/eeb/3949, 2015.
75. Nielsen, P. V.; Allard, F.; Awbi, H. B.; Davidson, L.; Schalin A. (2007). Computational Fluid Dynamics in Ventilation Design. REHVA Guidebook No 10, Finland, 2007.
76. OpenStudio [Computer software] (2016). OpenStudio v.1.14. Retrieved from: https://www.openstudio.net/.
77. Paciuk, M. 1990. The Role of Personal Control of the Environment in Thermal Comfort and Satisfaction at the Workplace. Environmental Design Research Association (EDRA) 21:303-312.
78. Page, J.; Robinson, D.; Scartezzini, J-L. (2007). Stochastic Simulation of Occupant Presence and Behaviour in Buildings. Proceedings of Building Simulation 2007, 10th IBPSA Conference, 2007.
79. Perez-Lombard, L.; Ortiz, J.; and Pout, C. (2008). A review on buildings energy consumption information. Energy and Buildings, v. 40, pg. 394–398, 2008.
80. Pfafferott, J.; Herkel, S.; Jaschke, M. (2003). Design of passive cooling by night ventilation: evaluation of a parametric model and building simulation with measurements. Energy and Buildings, v. 35, no. 11, pp. 1129–1143, 2003.
81. Phaff, J. (1977). Model tests of the wind pressure distribution on some common building shapes. Delft University of Technology, Netherland, 1977.
82. Phaff, J. (1979). Continuation of model tests of the wind pressure distribution on some common building shapes. Delft University of Technology, Netherland, 1979.

83. Phaff, J. C.; de Gids, W. F.; Ton, D.V. van der Ree; Schijndel, L. L. M. (1980). The ventilation of buildings: Investigation of the consequences of opening one window on the internal climate of a room. Delft, Netherlands, 1980.
84. Pope, S. B. (2000). Turbulent flows. Cambridge University Press, 2000.
85. Price, K.; Storn, R. M.; Lampinen, J. A. (2005). Differential Evolution: A Practical Approach to Global Optimization. Springer-Verlag Berlin Heidelberg, 2005
86. Ramponi, R. (2014). Computational modeling of urban wind flow and natural ventilation potential of buildings. PhD Thesis, Technische Universiteit Eindhoven, 2014.
87. Rijal, H. B.; Humphreys, M. A.; Nicol, J. F. (2014). Development of a Window Opening Algorithm to Predict Occupant Behavior in Japanese Houses. 30th International PLEA Conference, 2014.
88. Sagaut, P. (2006). Large eddy simulation for incompressible flows: an introduction. 2nd Edition, Springer, 2006.
89. Sandberg, M (2004). An alternative View on Theory of Cross-Ventilation. International Journal of Ventilation, v. 2, no. 4, pp. 400–418, 2004.
90. Schulz, T.; Eicker, U. (2013). Controlled Natural Ventilation for Energy Efficient Buildings. Energy and Buildings 56, pp. 221–232, 2013.
91. Seifert, J.; Li, Y.; Axley, J. (2006). Calculation of wind-driven cross ventilation in buildings with large openings. Journal of Wind Engineering and Industrial Aerodynamics 94 (12), pp. 925–947, 2006.
92. Seifert, J.; Li, Y.; Axley, J.; Rosler, M. (2006). Calculation of wind-driven cross ventilation in buildings with large openings. Journal of Wind Engineering and Industrial Aerodynamics 94, pp. 925–947, 2006.
93. Swami, M. V.; Chandra, S. (1998). Correlations for pressure distribution on buildings and calculation of natural ventilation airflow. ASHRAE Transactions 94, pp. 243–266, 1998.
94. Tan, G.; Glicksman.; L. R. (2005). Application of integrating multi-zone model with CFD simulation to natural ventilation prediction. Energy and Buildings 37, pp. 1049-1057, 2005.

95. Teodosiu, C.; Kuznik, F.; Teodosiu, R. (2014). CFD modeling of buoyancy driven cavities with internal heat source – Application to heated rooms. Energy and Buildings 68, pp. 403–411, 2014.
96. TRNSYS [Computer software] (2015). Transient System Simulation Tool v.17. Retrieved from: http://www.trnsys.com/.
97. Tuohy, P. G; Rijal, H. B.; Humphreys, M. A.; Nicol, J. F.; Samuel, A.; Clarke, J. (2007). Comfort driven adaptive window opening behaviour and the influence of building design. Proceedings of Building Simulation 2007, 10th IBPSA Conference, 2007.
98. Tuomaala, P. (2002). Implementation and evaluation of air flow and heat transfer routines for building simulation tool. PhD thesis, Helsinki University of Technology, 2002.
99. Wachenfeldt, B. J. (2003). Natural ventilation in building – detailed prdeiction of energy performance. PhD Thesis, Department of Energy and Process Engineering, Norwegian University of Science and Technology, Trondheim, Norway, 2003.
100. Walton, G. N. (1982). Airflow and Multiroom Thermal Analysis. ASHRAE Transactions 88 (2), pp. 78–91, 1982.
101. Wang, L.; Chen, Q. Y. (2004). Using a coupled multizone and CFD program for natural ventilation studies. Proceedings of CIB 2004, Toronto, Canada, 2004.
102. Yamanaka, T.; Kotani, H.; Iwamoto, K. Kato, M. (2006). Natural, wind-forced ventilation caused by turbulence in a room with a single opening. International Journal of Ventilation, v. 5, no. 1, pg. 179–187, 2006.
103. Yang, C.; Shi, H.; Yang, X.; Zhao, B. (2010). Research on Flow Resistance Characteristics with Different Window/Door Openings Angles. HVAC&R Research 16, pp. 813–824, 2010.
104. Yuan, J.; Srebric, J. (2004). Transient prediction of contaminant distribution by introducing energy load calculations into multi-zone modelling. Proceedings of CIB 2004, Toronto, Canada, 2004.
105. Zhai, J.; Krarti, M.; Johnson, M. H. (2010). Assess and implement natural and hybrid ventilation models in whole-building energy simulation. ASHRAE TRP-1456:

Department of Civil, Environmental and Architectural Engineering, University of Colorado, 2010.

106. Zhaia, Z.; Mankibi, M. E.; Zoubir, A. (2015). Review of natural ventilation models. Energy Procedia, v. 78 pg. 2700–2705, 2015.

APPENDIX A – VANDUSEN ENVELOPE CONSRTRUCITION SETTINGS

Table A.1 shows the envelope construction applied to the WBSM.

Table A.1 – VanDusen's envelope construction characteristics [1]

<table>
<tr><th></th><th></th><th>Envelope description</th><th>Materials used on the Envelope (from internal to external surfaces)</th><th>Thermal resistance - m²K/W (h.ft².°F/Btu)</th><th>Baseline for climate zone 5 Vancouver, BC (ASHRAE 90.1)</th><th>Cross section</th></tr>
<tr><td rowspan="3">Roof Construction</td><td>Roof Type 1 (R1)</td><td>Typical timber framing roof condition</td><td>Green roof system C/W drainage mat, root barrier, protection board, roofing membrane, protection board, vapour barrier, 2 layers of plywood, wood joists with splay insulation (R-40), GWB, acoustic batt insulation, fabric liner, fir plywood in steel framing support system</td><td>7.91 (R-45)</td><td rowspan="3">3.66 (R-21)</td><td>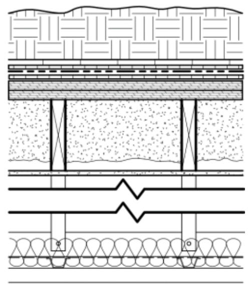</td></tr>
<tr><td>Roof Type 3 (R3)</td><td>Petal B/F roofing</td><td>Stone ballast, filter fabric, protection board, roofing membrane, overlay board, vapour barrier, 2 layer of plywood, wood joist with spray insulation (R-40), GWD, acoustic batt insulation, fabric liner, fir plywood in steel framing support system</td><td>7.91 (R-45)</td><td>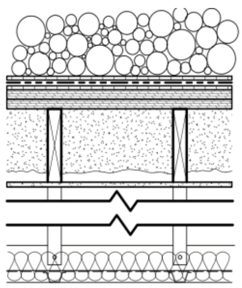</td></tr>
<tr><td>Roof Type 4 (R4)</td><td>Typical concrete roof condition</td><td>Green roof system C/W drainage mat, filter fabric, root barrier, protection board, roofing membrane, overlay board, 150 mm rigid insulation, vapour barrier, concrete roof, drywall ceiling in some location</td><td>7.74 (R-44)</td><td>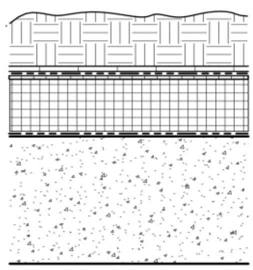</td></tr>
</table>

Table A.1 – VanDusen's envelope construction characteristics [2]

		Envelope description	Materials used on the Envelope (from internal to external surfaces)	Thermal resistance - m²K/W (h.ft².°F/Btu)	Baseline for climate zone 5 Vancouver, BC (ASHRAE 90.1)	Cross section
Wall Construction	Wall Type 2 (W2)	Concrete wall at mechanical rooms	Blackfill, gravel, drainage mat, 150 mm rigid insulation, below grade damp proofing, concrete wall	3.34 (R-19)	2.74 (R-15)	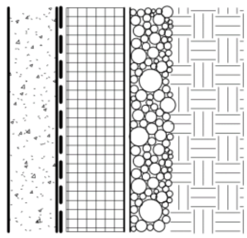
	Wall Type 3 (W3)	Concrete wall below grade	Concrete wall with waterproof admixture, drainage along outside of wall	0.08 (R-0.5)	2.74 (R-15)	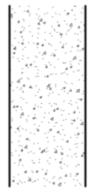
	Wall Type 4 (W4)	Typical rammed earth wall	Rammed earth wall, 150 mm rigid insulation, rammed earth wall	5.03 (R-28)		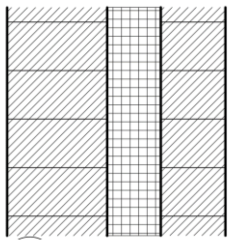
	Wall Type 4.2 (W4.2)	Typical concrete sandwich wall	Concrete wall, 150 mm rigid insulation, concrete wall	5.25 (R-30)		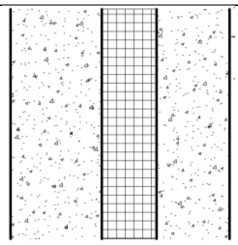
	Wall Type 7 (W7)	External clad wall	16 mm drywall, 2x4 studs, 155mm gap, 2x6 studs, spray insulation, 13 mm external wall board, 1x1" batt, wood siding	4.21 (R-24)		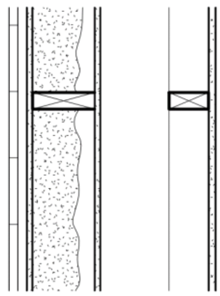

Table A.1 – VanDusen's envelope construction characteristics [3]

	Envelope description	Materials used on the Envelope (from internal to external surfaces)	Thermal resistance - m²K/W (h.ft².°F/Btu)	Baseline for climate zone 5 Vancouver, BC (ASHRAE 90.1)	Cross section
Floor/Slab Construction – Floor Type (F1)	Typical floor condition	Concrete slab with radiant piping, underslab vapour barrier, rigid insulation, structural fill	2.73 (R-15)	4.67 (R-27)	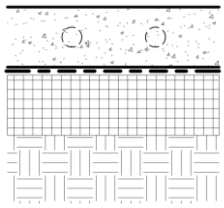
Glazing System	External 2SSG glazing	6" painted aluminum, low-e glazing	0.5 (U-2.0 W/m²K)	0.4 (U-2.6 W/m²K)	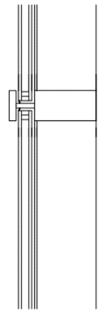

APPENDIX B – VANDUSEN EQUIPMENT LOADS

Table B.1 presents the list of the applied equipment loads.

Table B.1 – VanDusen's equipment loads (Integral Group, 2013)

Room Name	ASHRAE Space Type	Area (m²)	ASHRAE Equipment Density (W/m²)	ASHRAE Load (W)	Equipment type in the space (see table B.2)	Estimated Load (W)	Estimated Load per hour (kWh/hour)	Estimated equipment operating hours
Arrival Hall	Multipurpose	118.0	10.76	1271	9	550	0.55	1 hour per day
Atrium	Atrium	162.8	5.38	876	1,1,8,8,9	900	0.9	Building operating hours*
Garden Shop	Retail	129.6	5.38	697	1,1	200	0.2	
					9	550	0.55	Building operating hours*
Shop Office	Office	9.3	10.76	100	1	100	0.1	Building operating hours*
Shop Storage	Active Storage	20.4	2.15	44	-	-	-	-
Library	Library	139.9	16.15	2258	1	100	0.1	Libray Operating Hours*
					9	550	0.55	1 hour per day
Classroom	Classroom	90.9	10.76	978	1,2,3,4,9	1605	4.815	1 hour per day
Flex 1	Multipurpose	72.6	10.76	781	1,2,3,4,9	1605	4.815	1 hour per day
Flex 2	Multipurpose	75.5	10.76	812	1,2,3,4,9	1605	4.815	1 hour per day
Great Hall	Multipurpose	146.6	10.76	1578	1,2,3,4,9	1605	4.815	1 hour per day
Classroom Storage	Active Storage	17.8	2.15	38	-	-	-	-
Flex 2 Storage	Active Storage	4.7	2.15	10	-	-	-	-
South Corridor Storage	Active Storage	1.9	2.15	4	-	-	-	-
South Corridor	Corridor	58.2	2.15	125	9	550	0.55	1 hour per day
Food Service	Food preparation	132.7	16.15	2143	9	550	0.55	1 hour per day
Volunteer	Multipurpose	88.7	10.76	955	1,4,9	1450	4.35	1 hour per day
Food Prep/Servery	Food preparation	39.0	16.15	630	-	-	-	-
North Corridor	Corridor	68.5	2.15	148	9	550	0.55	-
Interpetative Centre	Multipurpose	55.5	10.76	597	1,3,8,8	320	0.32	1 hour per day
Men's W/C	WC	34.8	5.38	187	6,9	1950	5.85	-
Woman's W/C	WC	47.0	5.38	253	6,9	1950	5.85	-
Water	Mech/Elec	11.9	2.15	26	-	-	-	-
Electrical Room	Mech/Elec	14.5	2.15	31	-	-	-	-
Mechanical	Mech/Elec	81.6	2.15	176	-	-	-	-
Main Storage	Active Storage	21.7	2.15	47	1,10	700	0.7	Building operating hours*
Access W/C	WC	8.6	5.38	46	6,9	1950	5.85	1 hour per day
Office	Office	30.0	10.76	323	1,1,1	100	0.3	1 hour per day
Bike Room	Active Storage	13.8	2.15	30	-	-	-	-
Vestibule (from Bike room to Corridor to mechanical)	Corridor	5.2	2.15	11	9	550	0.55	1 hour per day
Corridor (to mechanical)	Corridor	26.6	2.15	57	9	550	0.55	1 hour per day
Flex 1 Storage	Active Storage	4.7	2.15	10	-	-	-	-
Library Storage	Active Storage	8.7	2.15	19	-	-	-	-
Vol Storage	Active Storage	13.4	2.15	29	-	-	-	-
Library Copy	Office	6.5	10.76	70	5,5,5	90	0.27	1 hour per day
Janitor	Active Storage	5.4	2.15	12	-	-	-	-
Locker	Active Storage	4.9	2.15	11	-	-	-	-
Office Storage	Active Storage	7.2	2.15	15	-	-	-	-
Vestibule	Corridor	6.2	2.15	13	-	-	-	-

*NOTE: Building Operating hours are shown in table B.3

The equipment applied to the WBSM is presented by table B.2.

Table B.2 –Equipment applied to the WBSM (Integral Group, 2013)

Equipment Type Tag	Equipment load	
	Types of equipment	Load (W)
1	Computer	100
2	Audio system	85
3	Video projector	70
4	Coffee Maker	800
5	Printer	90
6	Hand dryer	1400
7	Microwave	800
8	Monitors	75
9	Vacuum cleaner	550
10	Server	250

The building operation hours is presented by table B.3.

Table B.3 – VanDusen's operation hours (Integral Group, 2013)

Garden and Gift shop hours	
January and February	10 a.m. to 4 p.m.
March	11 a.m. to 5 p.m.
April	12 a.m. to 6 p.m.
May	13 a.m. to 8 p.m.
September	15 a.m. to 7 p.m.
October	16 a.m. to 5 p.m.
November and December	17 a.m. to 4 p.m.
Library Hours	
Tuesday through Friday	10 a.m. to 3 p.m.
Wednesday evenings	7 a.m. to 9 p.m.
Sunday	1 a.m. to 4 p.m.
Monday and Saturday	Closed

APPENDIX C – VANDUSEN LIGHTING LOADS

The lighting loads applied to the WBSM are presented by table C.1.

Table C.1 – VanDusen's lighting loads (Integral Group, 2013)

	Lighting Load (W)
Arrival Hall	1200
Atrium	1384
Garden Shop	1120
Garden Shop Office	33
Garden Shop Storage	29
Library	1305
Classroom	1088
Flex 1	1193
Flex 1 Storage	29
Flex 2	1193
Flex 2 Storage	29
Great Hall	1288
Classroom Storage	33
South Corridor	852
North Corridor	732
Food Service	855
Volunteer Room	1362
Volunteer Room Storage	33
Food Preparation	190
Interpretative Centre	276
Men's WC	689
Women's WC	1169
Service Corridor	257
Mechanical Room	605
Access WC	52
Office	99
Office Storage	33
Office Vestibule	52
Bike Room	112
Janitor's Closet	55
Locker Room	56

APPENDIX D – WBSM VALIDATION

The values for the CVRMSE and NMBE used to validate the WBSM are presented by table D.1.

Table D.1 – Values of CVRMSE and NMBE used to validate the WBSM [1]

		Atrium	Classroom	Arrival Hall	Flex 1	Flex 2	Food Service	Great Hall	Garden Shop Office	Garden Shop	Library	Volunteer
Day 1	CVRMSE (%)	24.4	18.5	24.1	16.3	15.7	45.3	15.5	42.1	19.8	12.6	15.0
	NMBE (%)	-2.2	2.3	3.9	1.1	0.8	8.4	-0.3	8.1	4.0	2.0	-1.0
Day 2	CVRMSE (%)	38.1	27.1	38.2	23.1	19.3	44.0	22.7	68.0	30.8	32.7	22.5
	NMBE (%)	-0.6	4.5	2.8	1.8	2.2	6.0	1.3	13.1	4.4	6.4	-0.1
Day 3	CVRMSE (%)	30.8	28.6	35.8	22.2	19.7	42.9	21.7	55.8	29.5	26.7	12.3
	NMBE (%)	0.3	4.8	3.1	2.0	2.7	6.3	1.0	10.4	4.1	4.2	0.8
Day 4	CVRMSE (%)	32.9	27.5	37.6	24.9	21.0	45.2	23.8	64.2	30.0	29.5	14.6
	NMBE (%)	-0.3	4.1	2.2	1.5	2.3	5.8	0.3	11.8	3.6	5.6	0.5
Day 5	CVRMSE (%)	31.7	43.3	37.1	28.1	29.5	46.8	28.5	65.8	36.2	35.6	17.7
	NMBE (%)	2.2	7.7	4.0	4.1	4.7	7.0	0.7	12.4	6.0	6.4	2.4
Day 6	CVRMSE (%)	38.9	51.9	46.2	29.6	33.9	56.0	29.4	64.0	45.8	44.8	29.1
	NMBE (%)	5.5	9.4	6.8	4.9	6.0	7.2	5.5	11.8	7.8	8.5	5.3

Table D.1 – Values of CVRMSE and NMBE used to validate the WBSM [2]

		Atrium	Classroom	Arrival Hall	Flex 1	Flex 2	Food Service	Great Hall	Garden Shop Office	Garden Shop	Library	Volunteer
Day 7	CVRMSE (%)	42.8	66.5	54.2	37.2	47.3	65.0	35.6	75.9	54.7	64.2	45.6
	NMBE (%)	7.1	13.1	9.9	7.2	9.3	12.1	7.0	14.5	10.5	13.0	9.0
Day 8	CVRMSE (%)	19.1	25.1	26.2	21.9	18.9	43.0	16.7	57.3	22.2	15.5	18.7
	NMBE (%)	-1.2	2.3	4.6	0.9	0.4	7.1	-0.1	11.1	4.4	2.5	25.2
Day 9	CVRMSE (%)	34.6	34.0	43.1	18.6	21.2	55.4	17.9	56.9	41.2	36.3	20.7
	NMBE (%)	3.3	6.3	7.4	3.0	3.9	8.3	2.4	10.3	7.2	6.6	3.6
Day 10	CVRMSE (%)	36.1	38.8	44.0	22.4	23.8	53.5	23.9	63.3	44.0	44.9	23.9
	NMBE (%)	4.1	7.1	5.4	3.5	4.4	8.8	3.7	11.5	7.2	8.5	4.0

APPENDIX E – COMPARISON BETWEEN STRATEGIES DURING A HOT DAY

Figure E.1 shows the comparison between the temperatures of the baseline and the model with no solar shading system, during the hottest day of the simulation.

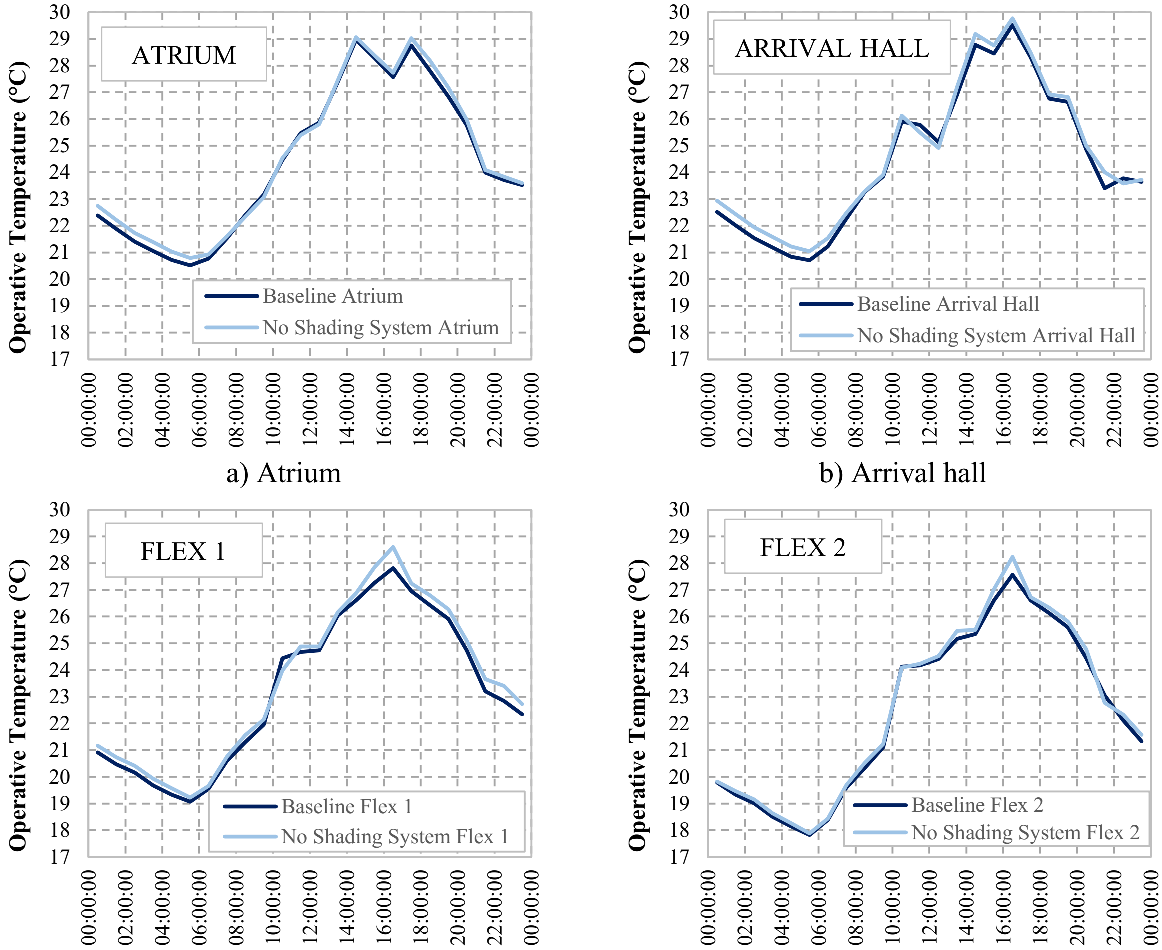

a) Atrium b) Arrival hall

c) Flex 1 d) Flex 2

Figure E.1 – Comparison of temperatures during a hot day for the solar shading simulation [1]

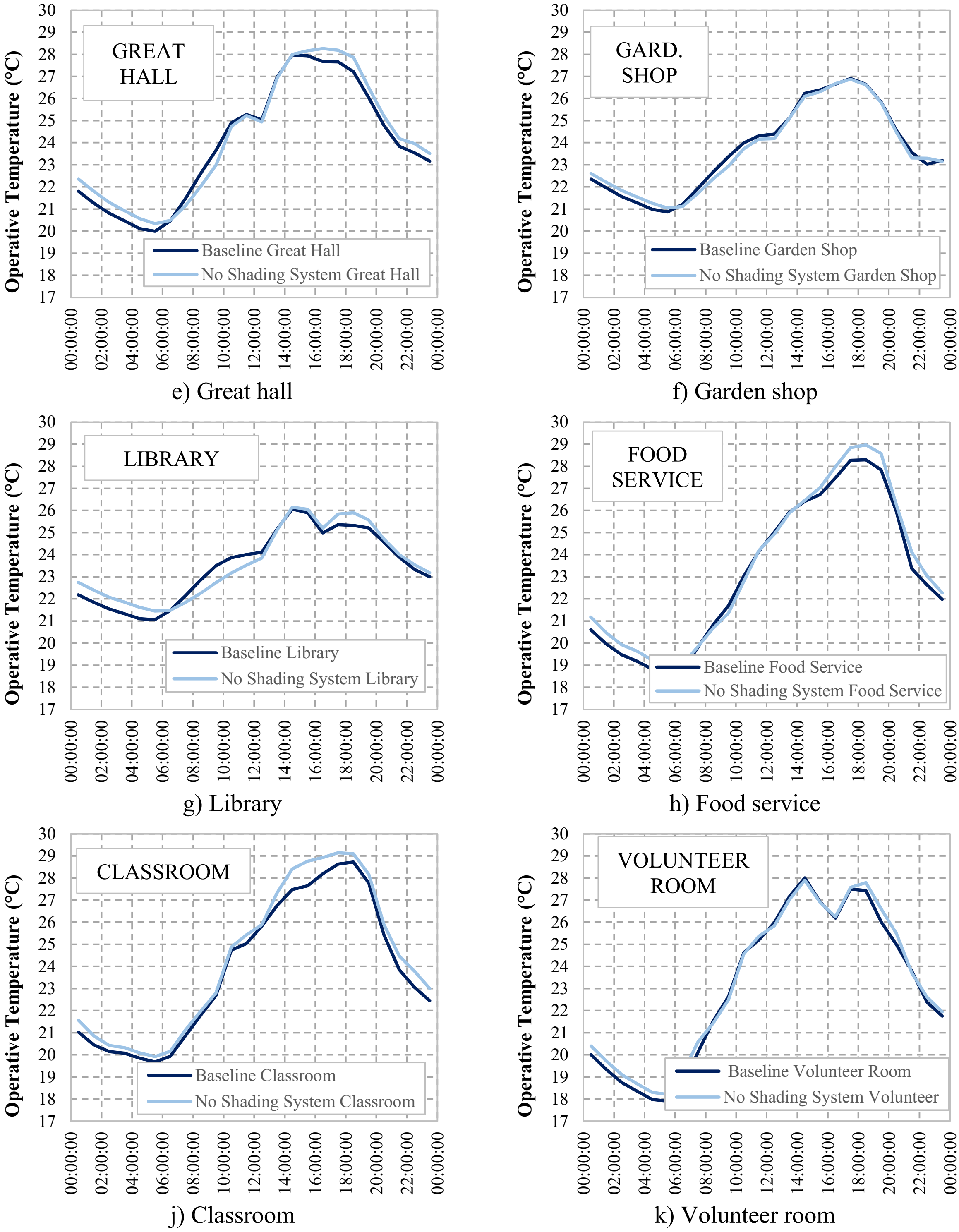

Figure E.1 – Comparison of temperatures during a hot day for the solar shading simulation [2]

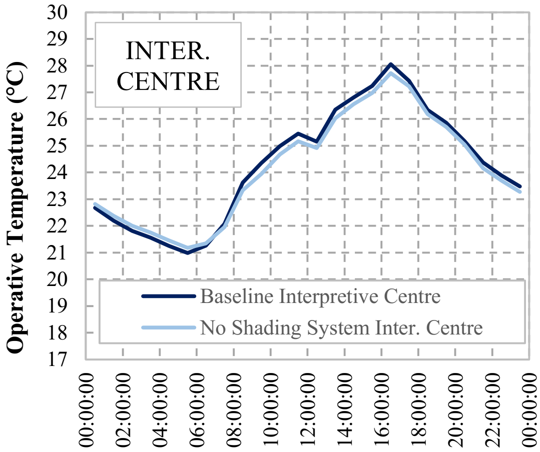

l) Interpretative Centre's hot days analysis

Figure E.1 – Comparison of temperatures during a hot day for the solar shading simulation [3]

Figure E.2 shows the comparison between the temperatures of the baseline and the model with reduced spaces connectivity, during the hottest day of the simulation.

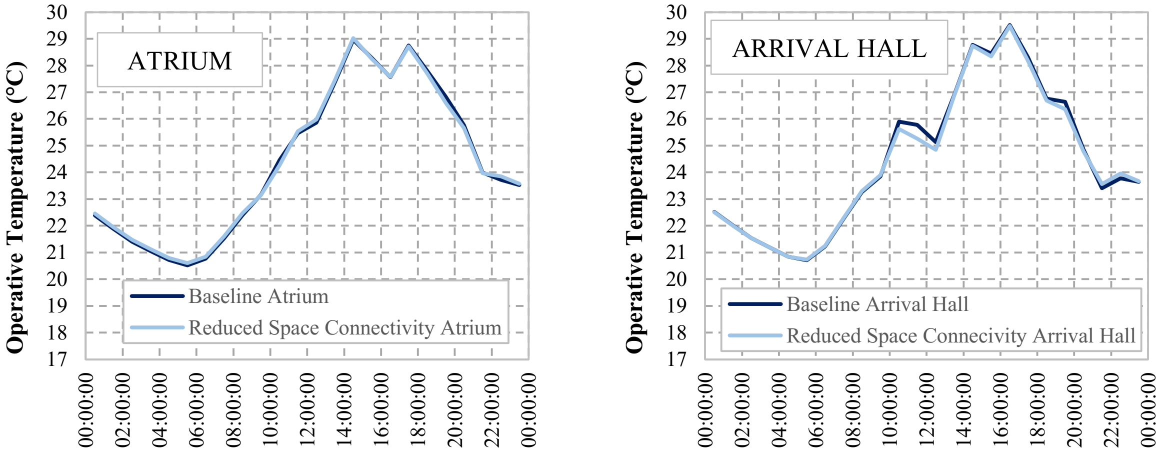

a) Atrium's hot days analysis

b) Arrival hall's hot days analysis

Figure E.2 – Comparison of temperatures during a hot day for the reduced space connectivity simulation [1]

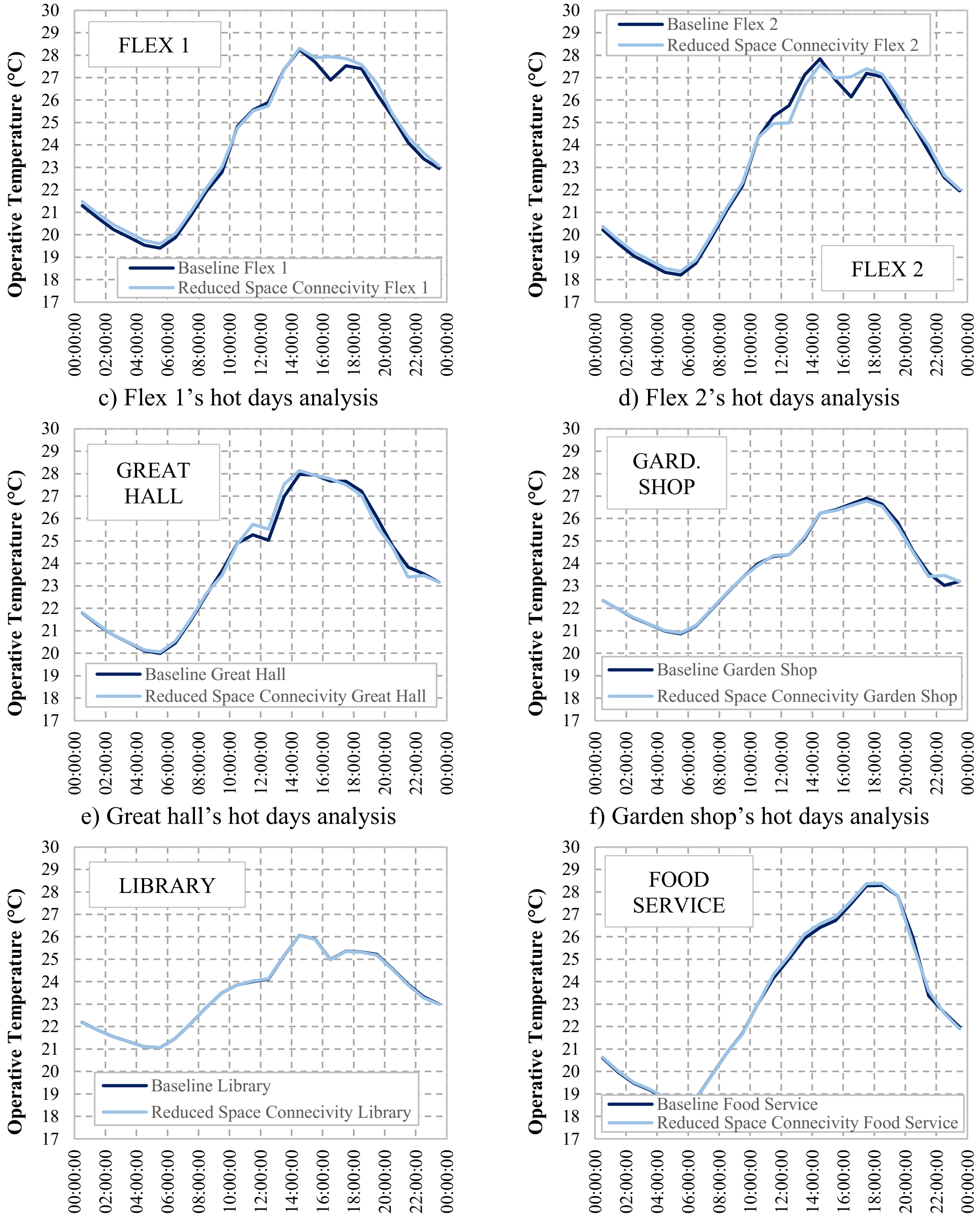

c) Flex 1's hot days analysis

d) Flex 2's hot days analysis

e) Great hall's hot days analysis

f) Garden shop's hot days analysis

g) Library's hot days analysis

h) Food service's hot days analysis

Figure E.2 – Comparison of temperatures during a hot day for the reduced space connectivity simulation [2]

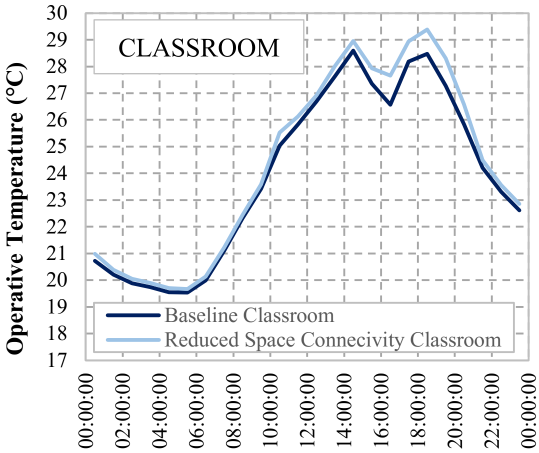

j) Classroom's hot days analysis

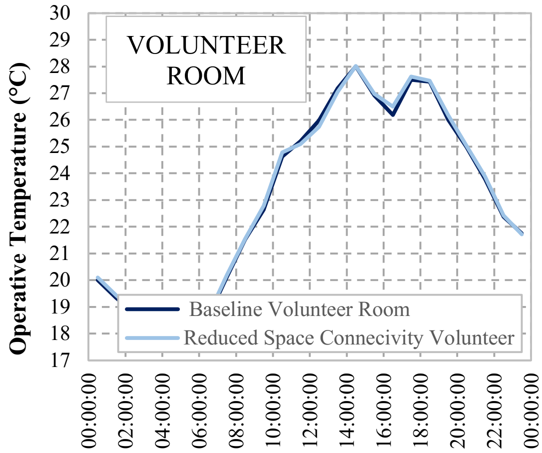

k) Volunteer room's hot days analysis

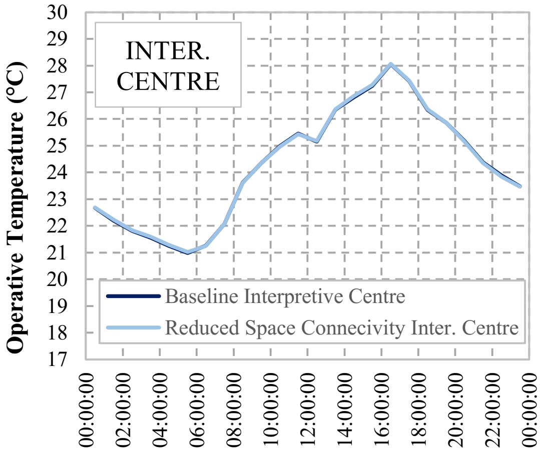

l) Interpretative Centre's hot days analysis

Figure E.2 – Comparison of temperatures during a hot day for the reduced space connectivity simulation [3]

Figure e.3 shows the comparison between the temperatures of the baseline and the model with no green roof, during the hottest day of the simulation.

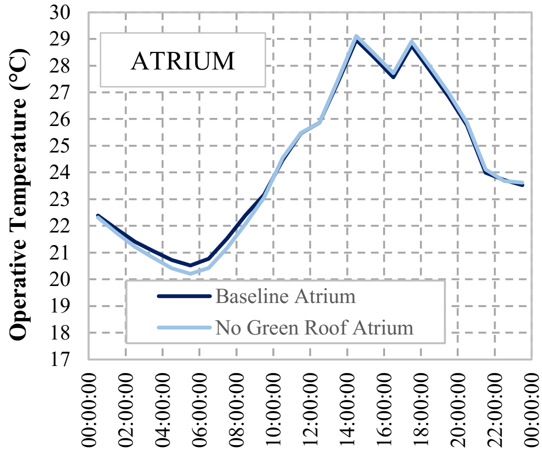

a) Atrium's hot days analysis

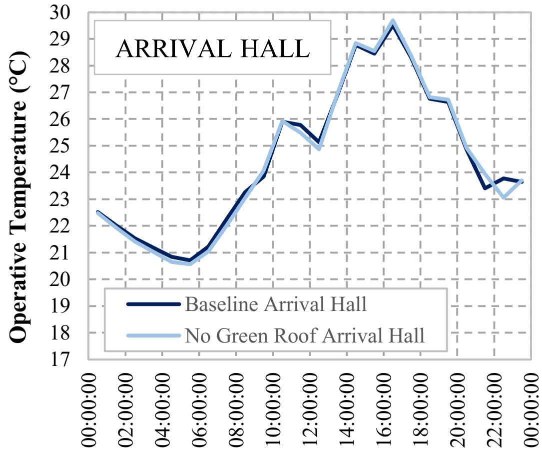

b) Arrival hall's hot days analysis

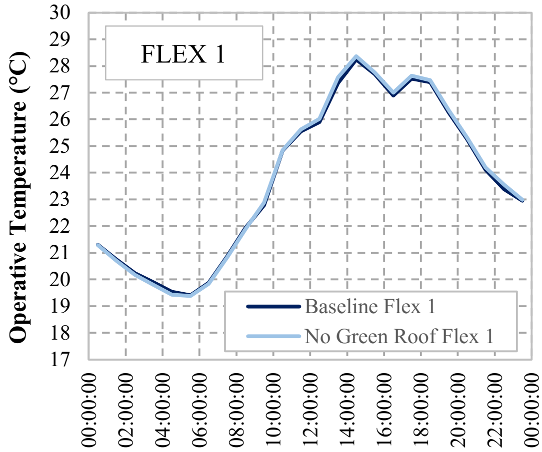

c) Flex 1's hot days analysis

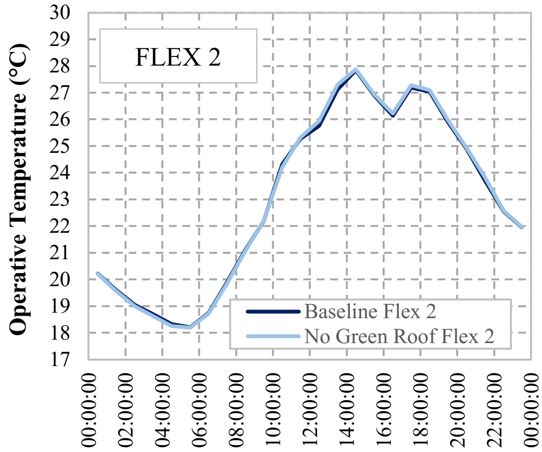

d) Flex 2's hot days analysis

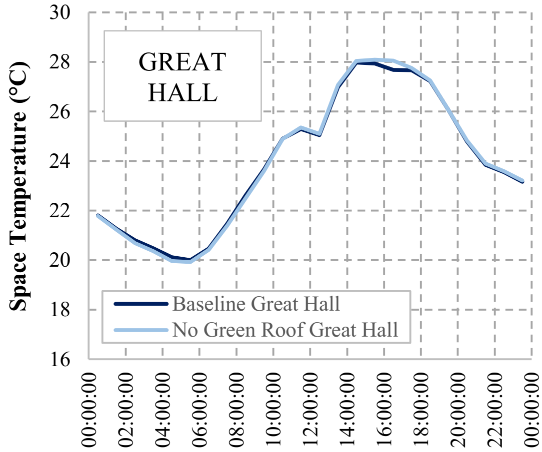

e) Great hall's hot days analysis

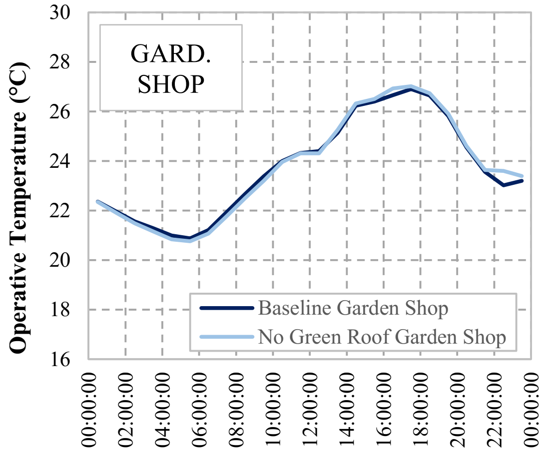

f) Garden shop's hot days analysis

Figure E.3 – Comparison of temperatures during a hot day for the green roof simulation [1]

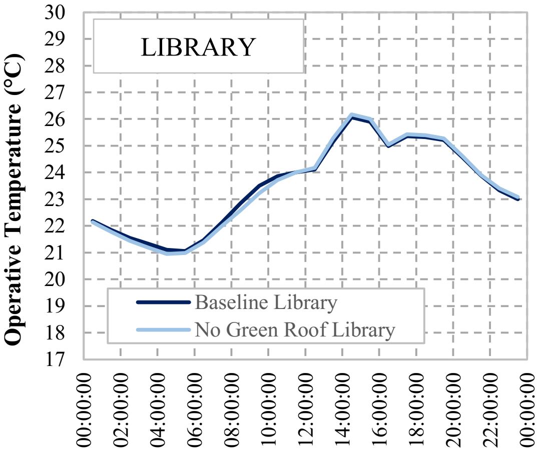

g) Library's hot days analysis

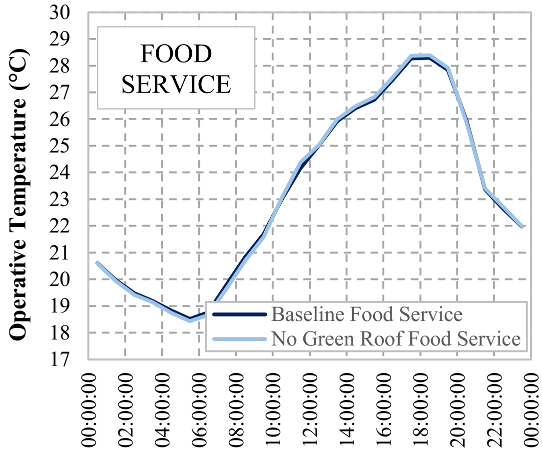

h) Food service's hot days analysis

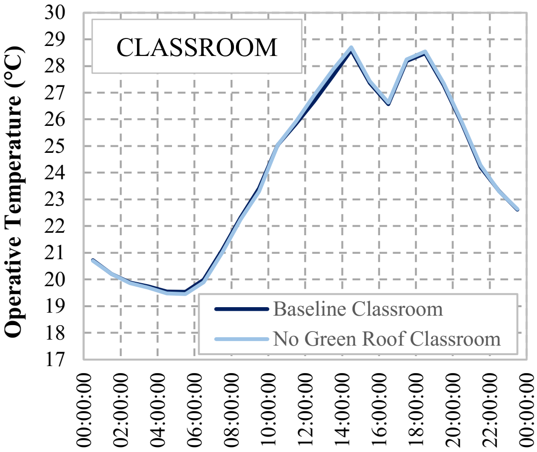

j) Classroom's hot days analysis

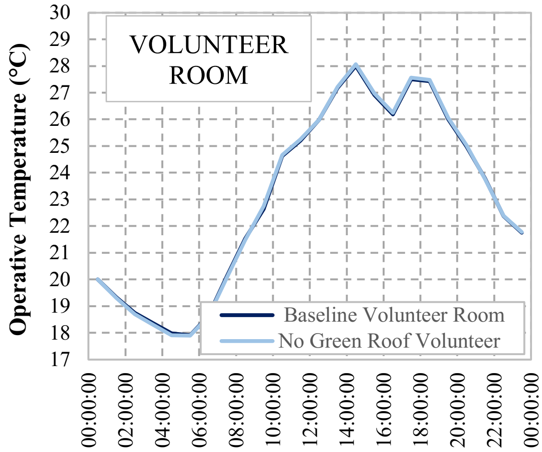

k) Volunteer room's hot days analysis

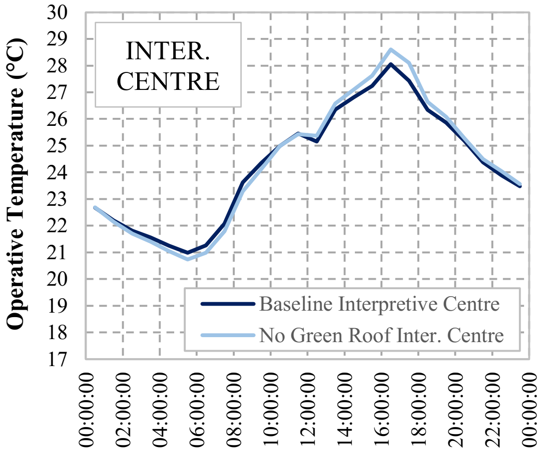

l) Interpretative Centre's hot days analysis

Figure E.3 – Comparison of temperatures during a hot day for the green roof simulation [2]

Figure E.4 shows the comparison between the temperatures of the baseline and the model with no solar chimney, during the hottest day of the simulation.

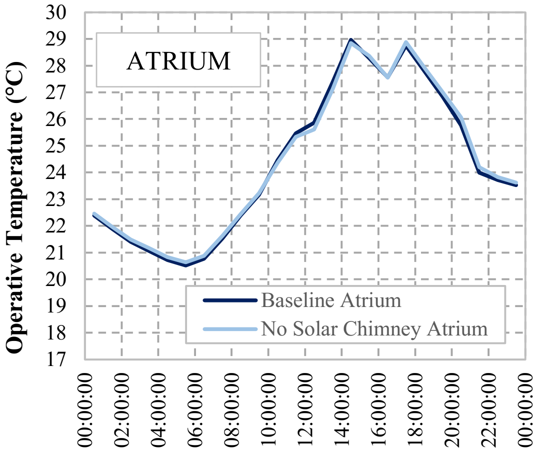

a) Atrium's hot days analysis

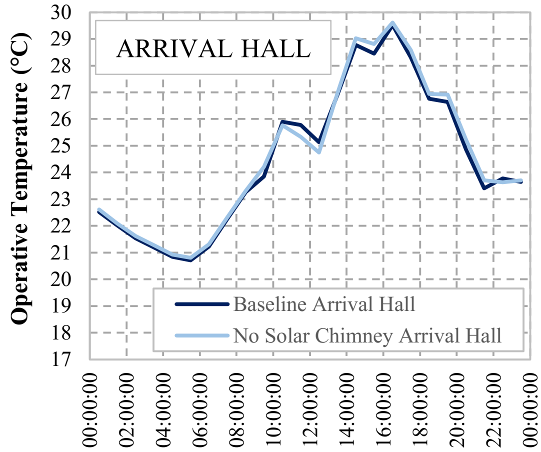

b) Arrival hall's hot days analysis

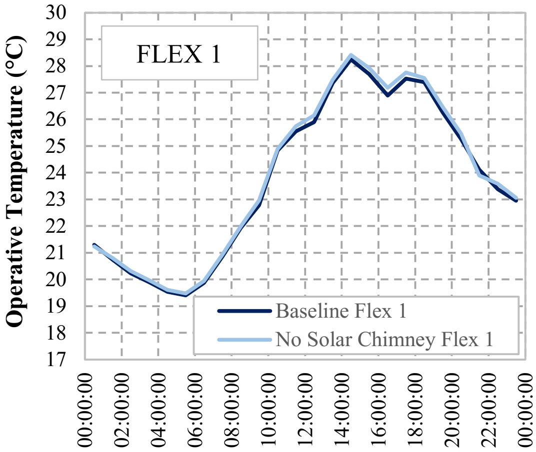

c) Flex 1's hot days analysis

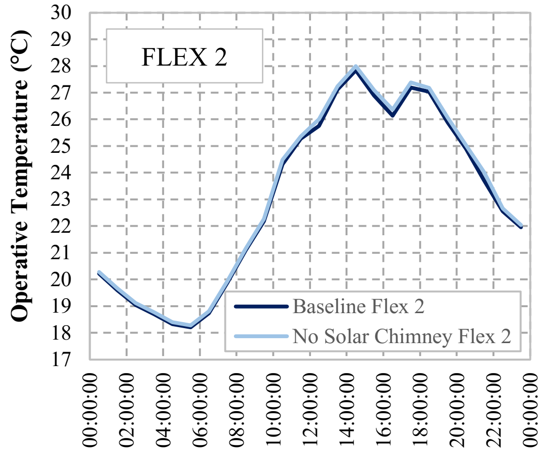

d) Flex 2's hot days analysis

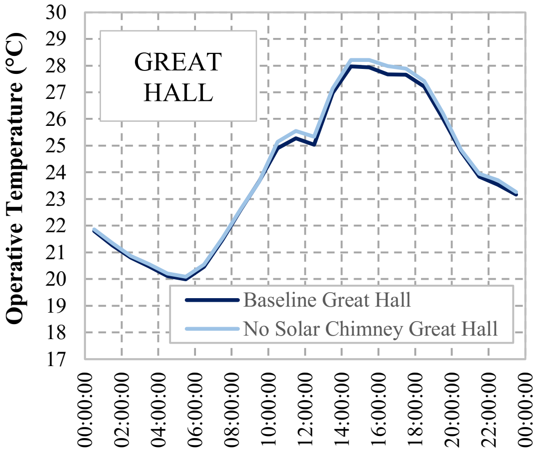

e) Great hall's hot days analysis

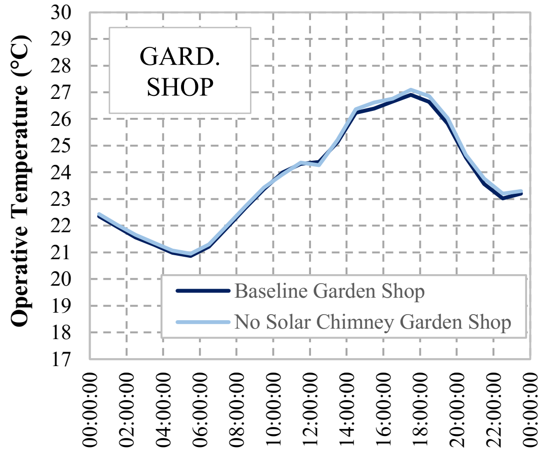

f) Garden shop's hot days analysis

Figure E.4 – Comparison of temperatures during a hot day for solar chimney simulation [1]

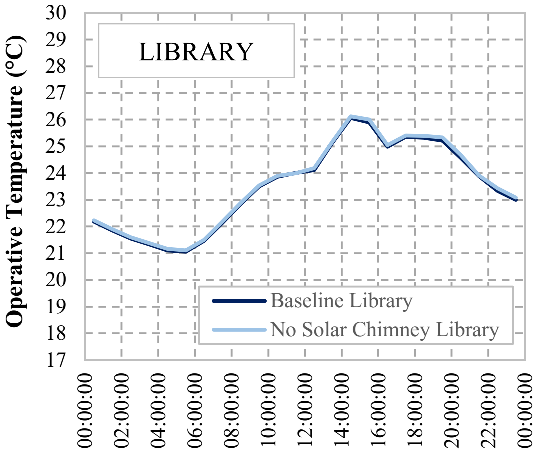

g) Library's hot days analysis

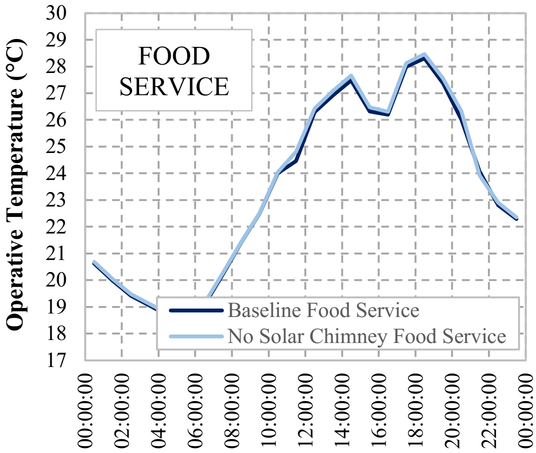

h) Food service's hot days analysis

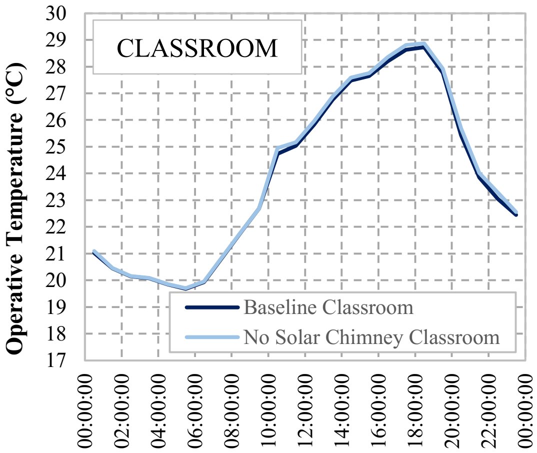

j) Classroom's hot days analysis

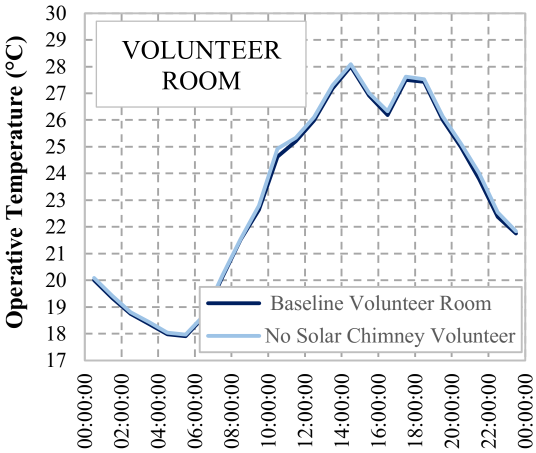

k) Volunteer room's hot days analysis

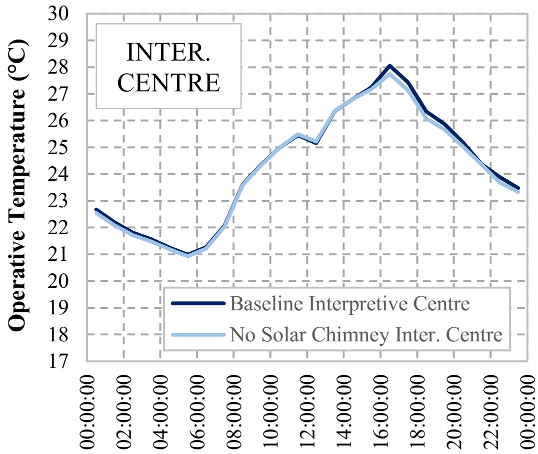

l) Interpretative Centre's hot days analysis

Figure E.4 – Comparison of temperatures during a hot day for solar chimney simulation [2]

APPENDIX F – NIGHT-TIME VENTILATION ANALYSIS

Figure F.1 illustrates the comparison between the baseline simulation, with night-time ventilation, and the simulation with no night-time ventilation. This first analysis includes the radiant floor system operation. The current slab setpoint temperature in the simulation is 21°C.

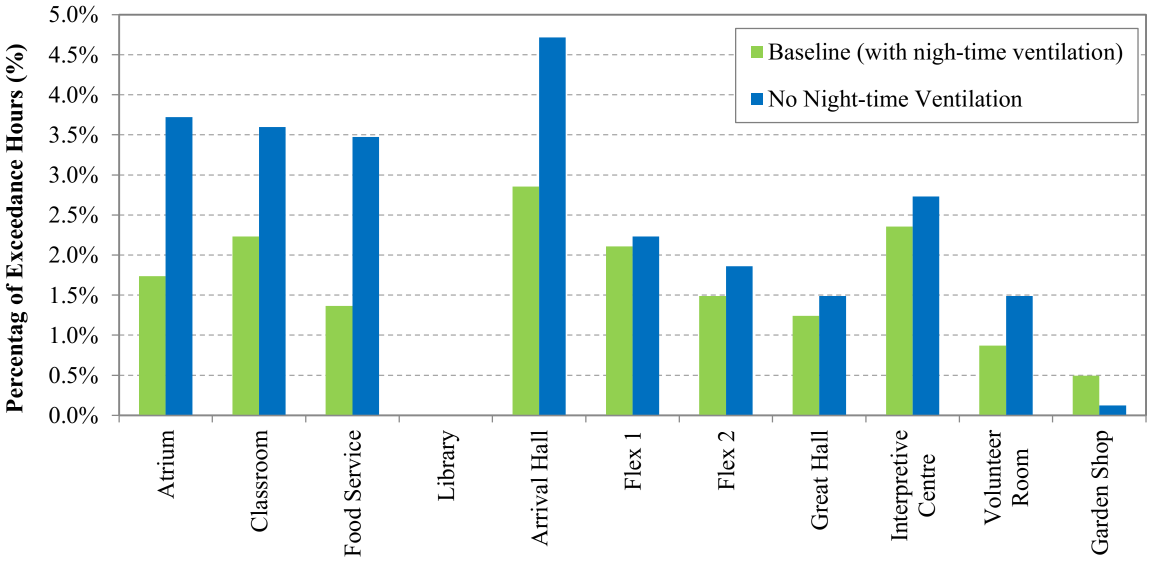

Figure F.1 – Percentage of *EH* for baseline and simulation with no night-time ventilation (radiant floor system on)

As expected, it is observed a decrease in thermal comfort in the simulation with no night-time ventilation. For the whole building, the baseline simulation has a *EH* of 2.10% and the simulation with no night-time ventilation has a *EH* of 2.31%. Moreover, it is detected that for the simulation with night-time ventilation (*i.e.* baseline model) the radiant floor slab operation is slightly affecting the natural ventilation effectiveness. Because of the lower temperatures at nigh-time, the radiant floor system is activated, slightly compromising the natural ventilation effectiveness for the baseline simulation. With that, the space does not use the full potential of the night-cooling in association with the space's thermal mass to avoid thermal discomfort in the next day. For the simulation with no night-time ventilation, on the other hand, the temperatures are higher at unoccupied hours and the radiant floor slab is not activated.

To analyse the radiant floor system, figure F.2 shows the comparison between the baseline and the simulation with no night-time ventilation, both with the radiant system turned off.

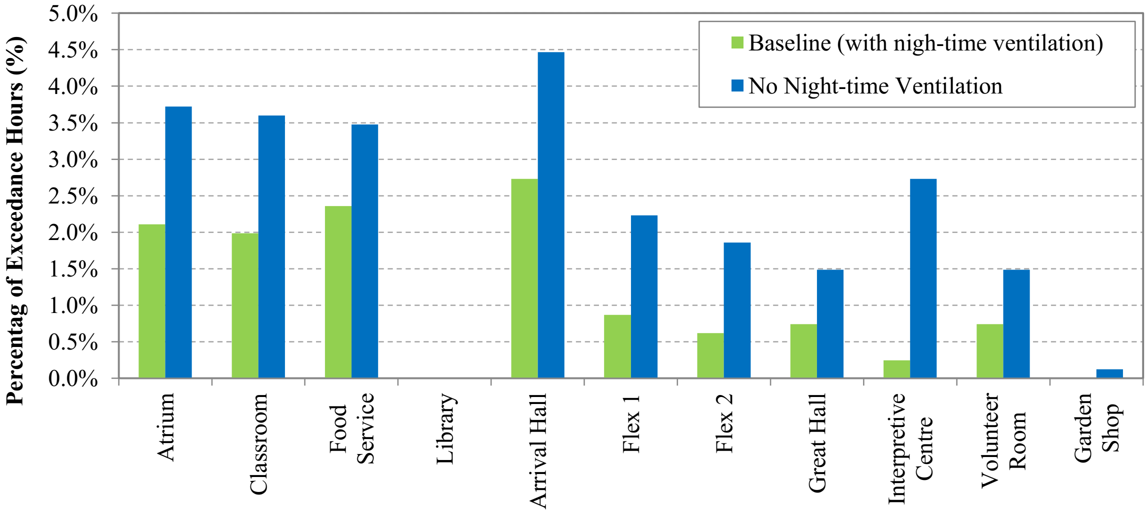

Figure F.2 – Percentage of *EH* for baseline and simulation with no night-time ventilation (radiant floor system off)

With the radiant floor off, the *EH* for the baseline is 1.52% and the simulation with no night-time ventilation has *EH* of 2.14%. Thus, comparing the baseline simulations with and without the radiant system, it is detected a slightly improvement in the natural ventilation effectiveness when the radiant slab is turned off. The baseline with radiant floor slab has a *EH* of 2.10% and with no radiant floor slab a *EH* of 1.52%. For the simulations with no night-time ventilation, it is also shown a little improvement in the natural ventilation effectiveness when the radiant floor is turned off, with a *EH* of 2.31% for the simulation with the radiant slab on and a *EH* of 2.14% when the radiant slab is off.

The daily temperatures are presented by figure F.3 to F.6. They are divided in mild and warm day temperatures, and with and without radiant floor system. It is observed that the night-time ventilation is more effective in cooling down the space during days with relative mild temperature, especially when the radiant slab is turned off. During the hot days, the nigh-time ventilation does not drastic change the indoor temperatures.

Figure F.3 illustrates the internal temperatures during a day with mild temperatures and with the radiant slab turned on.

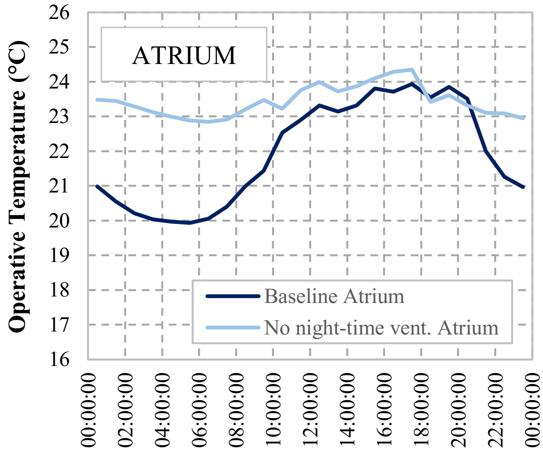

a) Atrium with radiant floor during a day with mild temperatures

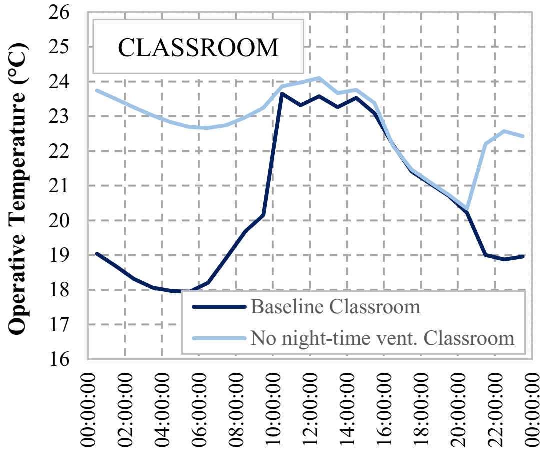

b) Classroom with radiant floor during a day with mild temperatures

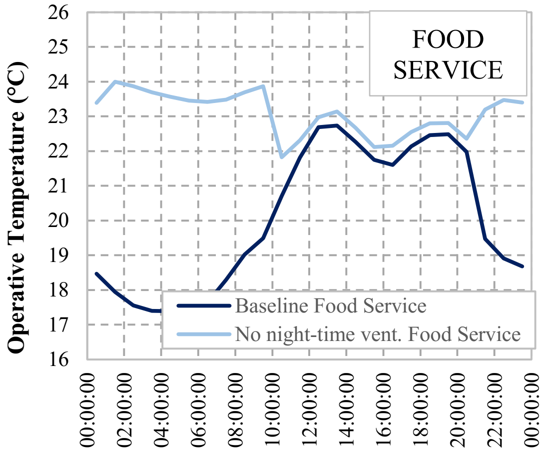

c) Food service with radiant floor during a day with mild temperatures

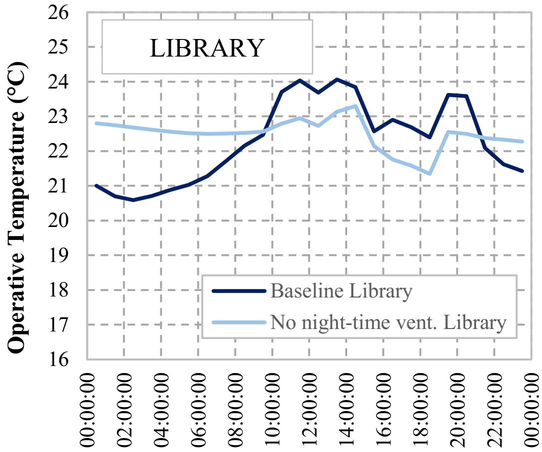

d) Library with radiant floor on during a day with mild temperatures

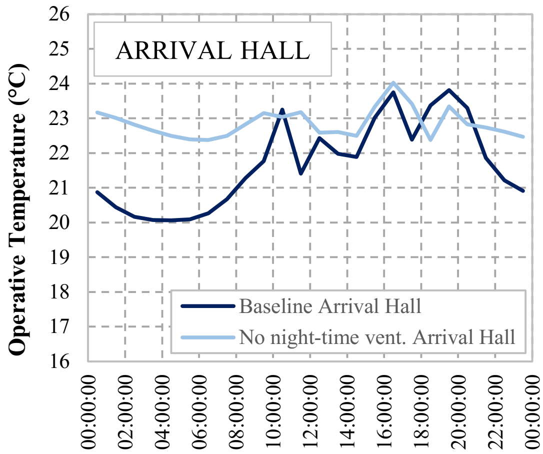

e) Food service with radiant floor on during a day with mild temperatures

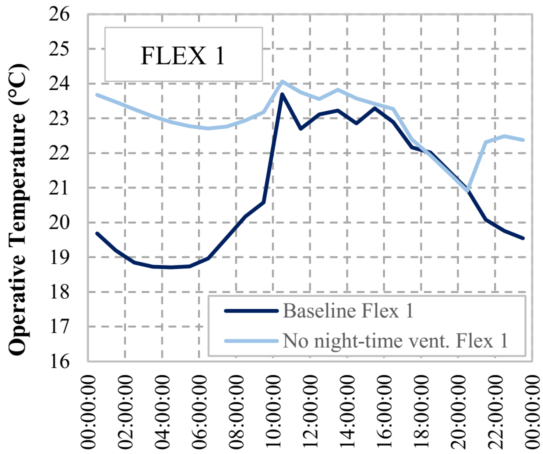

f) Flex 1 with radiant floor on during a day with mild temperatures

Figure F.3 – Daily temperatures for the simulation with radiant floor during a day with mild temperatures [1]

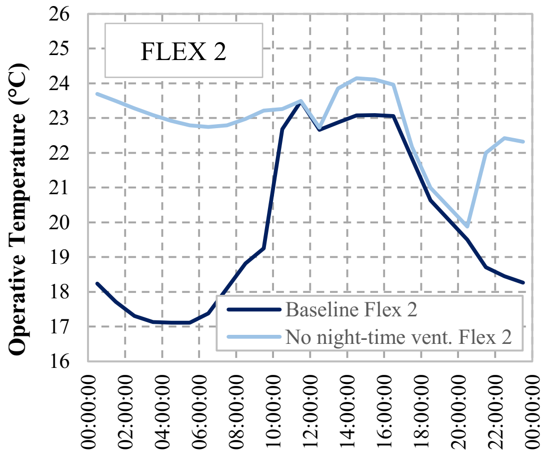

g) Flex 2 with radiant floor on during a day with mild temperatures

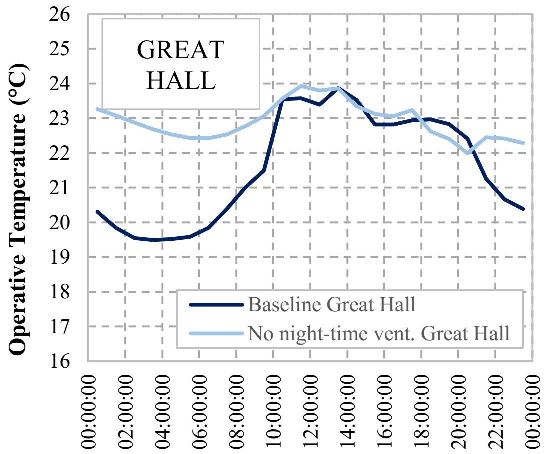

h) Great hall with radiant floor on during a day with mild temperatures

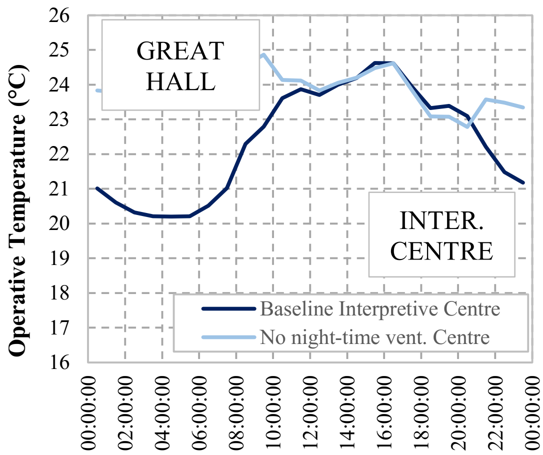

i) Interpretative centre with radiant floor on during a day with mild temperatures

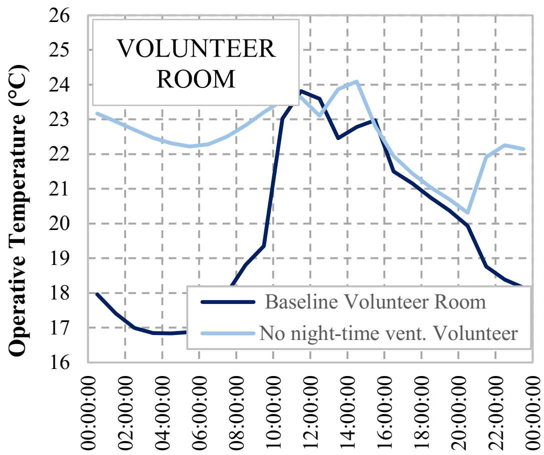

j) Volunteer room with radiant floor on during a day with mild temperatures

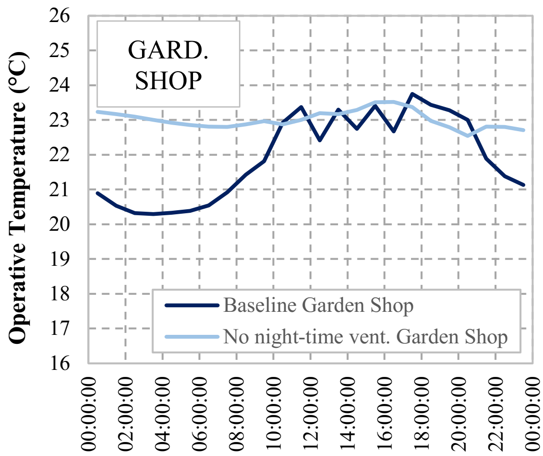

k) Garden shop with radiant floor on during a day with mild temperatures

Figure F.3 – Daily temperatures for the simulation with radiant floor during a day with mild temperatures [2]

Figure F.4 illustrates the internal temperatures during a day with warm temperatures and with the radiant slab turned on.

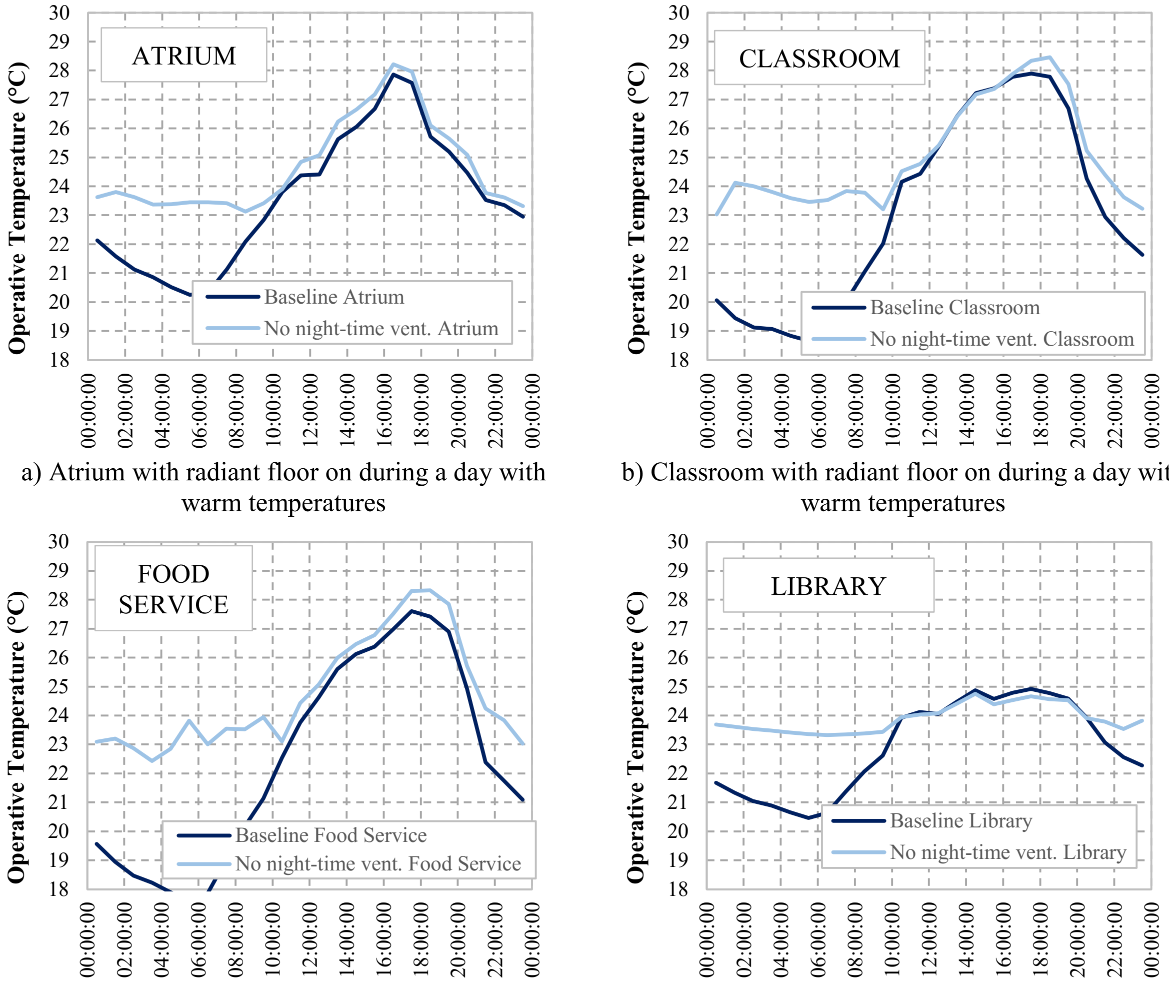

a) Atrium with radiant floor on during a day with warm temperatures

b) Classroom with radiant floor on during a day with warm temperatures

c) Food service with radiant floor on during a day with warm temperatures

d) Library with radiant floor on during a day with warm temperatures

Figure F.4 – Daily temperatures for the simulation with radiant floor on during a day with warm temperatures [1]

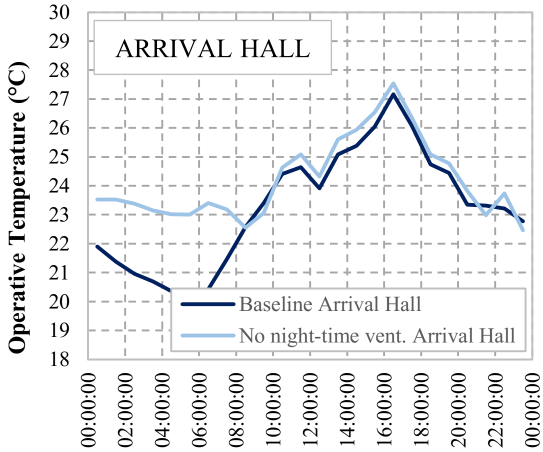

e) Arrival hall with radiant floor on during a day with warm temperatures

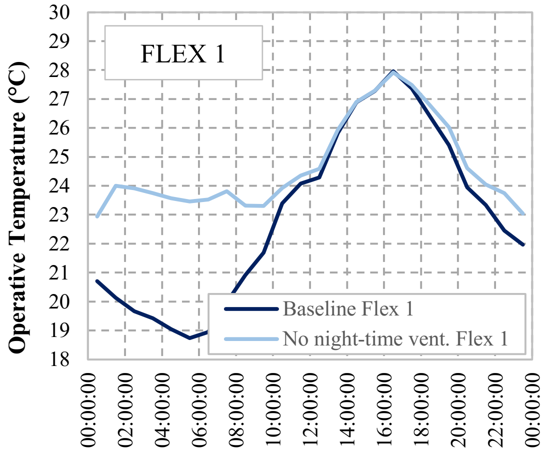

f) Flex 1 with radiant floor on during a day with warm temperatures

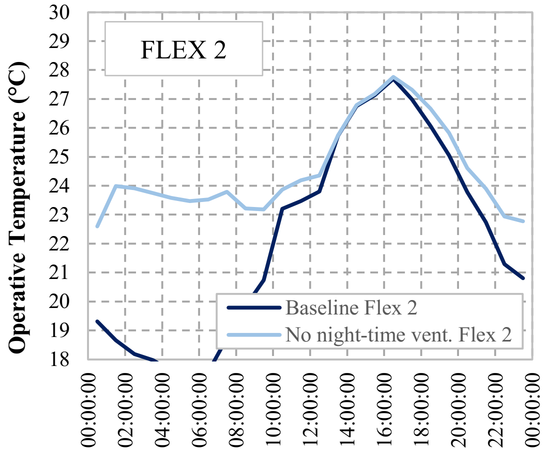

g) Flex 2 with radiant floor on during a day with warm temperatures

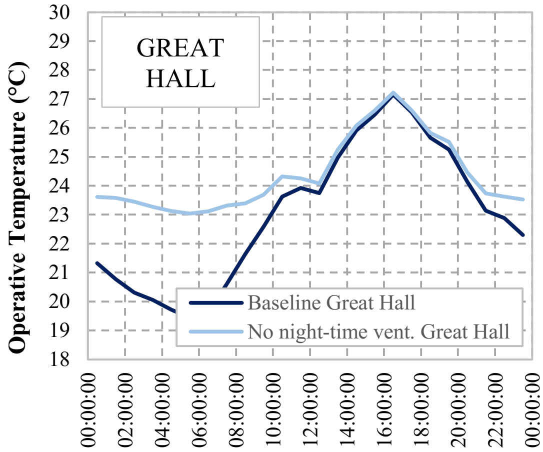

h) Great hall with radiant floor on during a day with warm temperatures

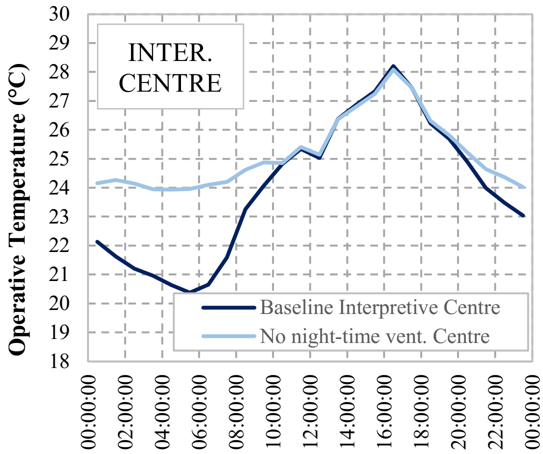

i) Interpretative centre with radiant floor on during a day with warm temperatures

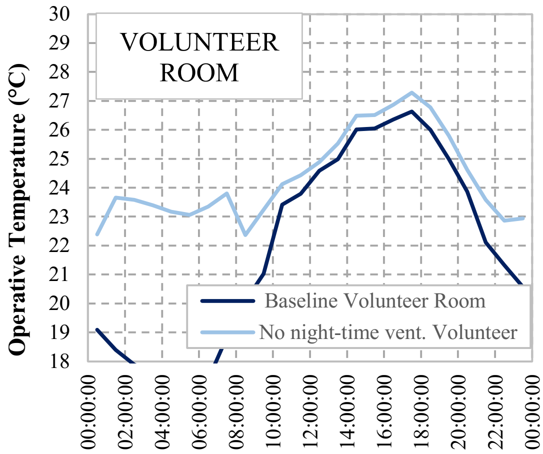

j) Volunteer room with radiant floor on during a day with warm temperatures

Figure F.4 – Daily temperatures for the simulation with radiant floor on during a day with warm temperatures [2]

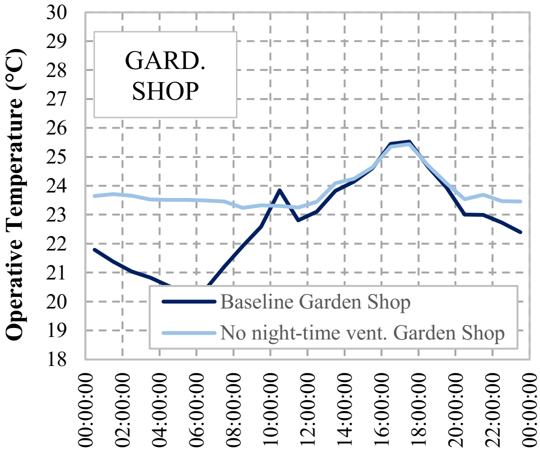

k) Garden shop with radiant floor on during a day with warm temperatures

Figure F.4 – Daily temperatures for the simulation with radiant floor on during a day with warm temperatures [3]

Figure F.5 illustrates the internal temperatures during a day with mild temperatures and with the radiant slab turned off.

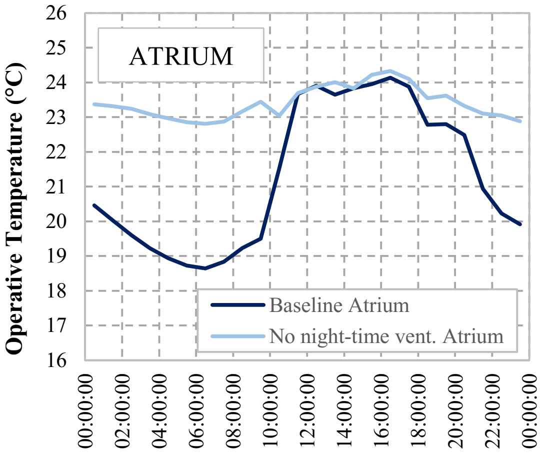

a) Atrium with radiant floor off during a day with mild temperatures

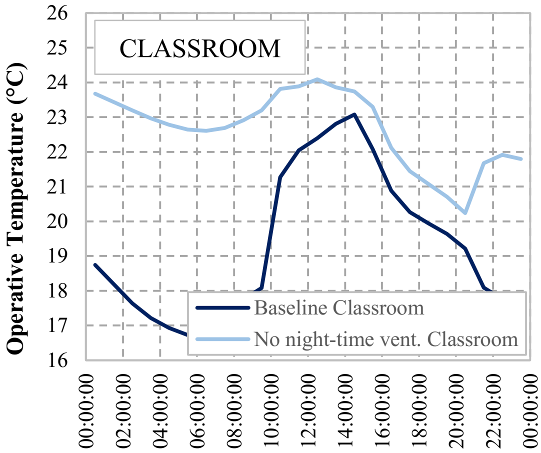

b) Classroom with radiant floor off during a day with mild temperatures

Figure F.5 – Daily temperatures for the simulation with radiant floor off during a day with mild temperatures [1]

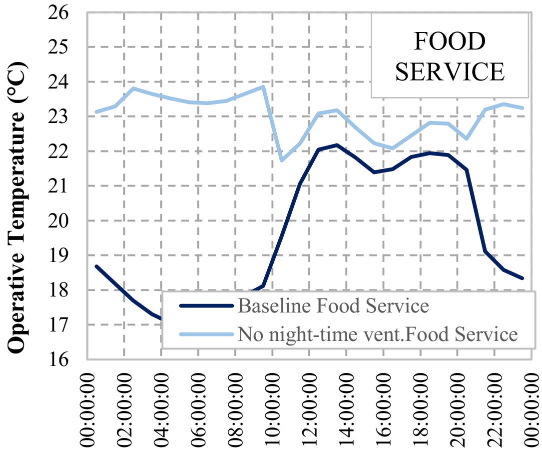

c) Food service with radiant floor off during a day with mild temperatures

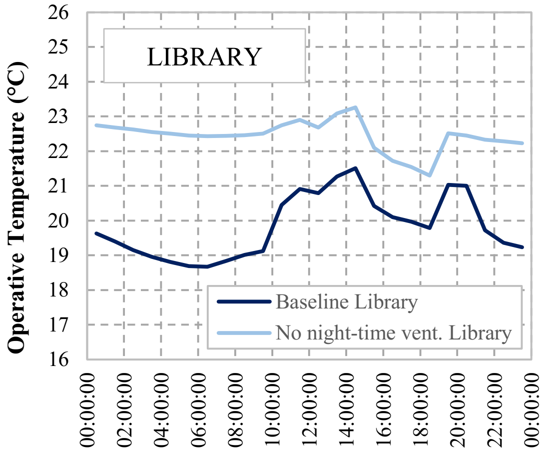

d) Library with radiant floor off during a day with mild temperatures

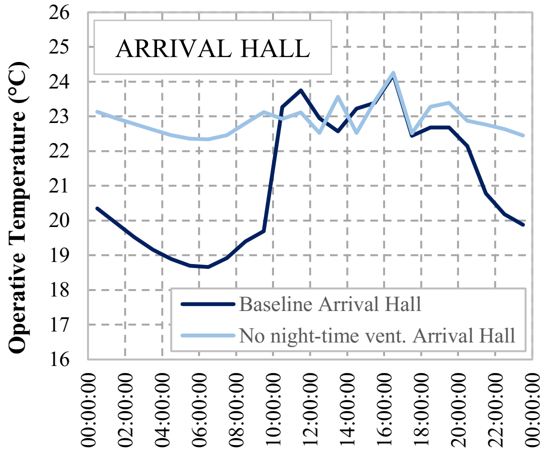

e) Arrival hall with radiant floor off during a day with warm temperatures

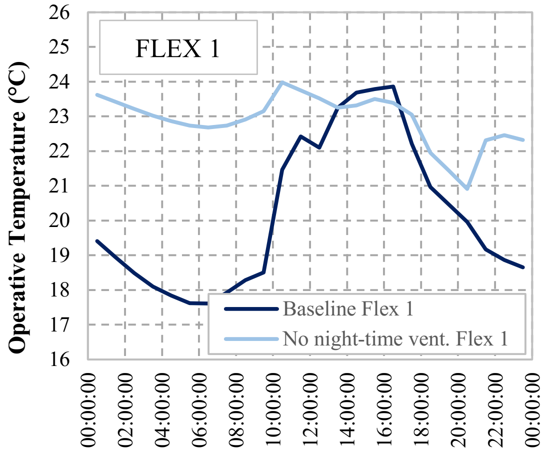

f) Flex 1 with radiant floor off during a day with warm temperatures

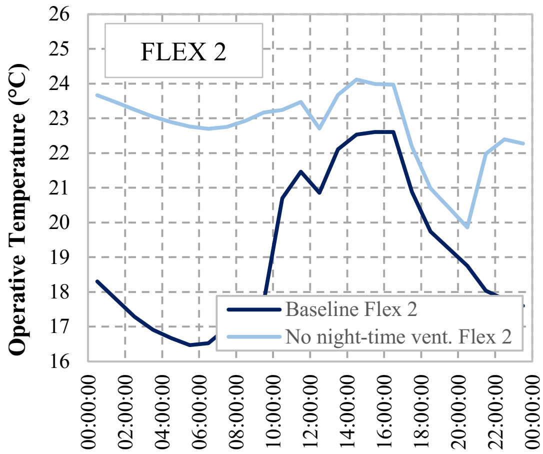

g) Flex 2 with radiant floor off during a day with mild temperatures

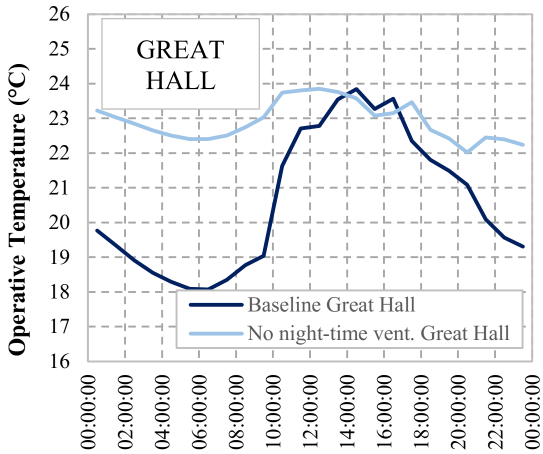

h) Great hall with radiant floor off during a day with mild temperatures

Figure F.5 – Daily temperatures for the simulation with radiant floor off during a day with mild temperatures [2]

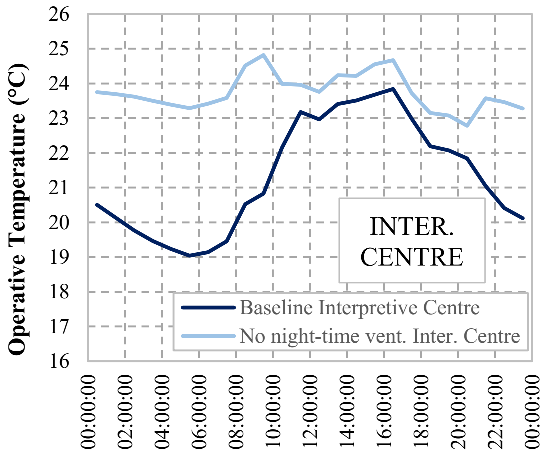

i) Interpretative centre with radiant floor off during a day with mild temperatures

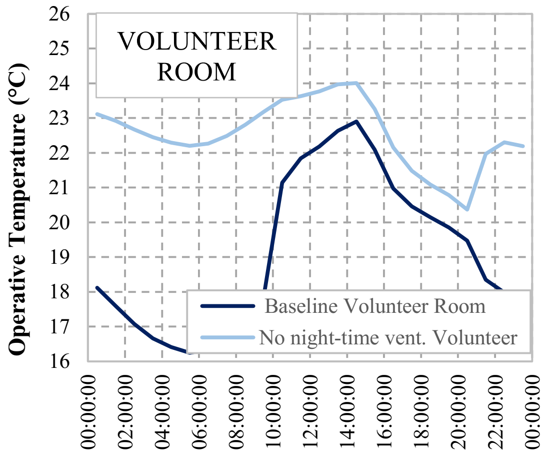

j) Volunteer room with radiant floor off during a day with mild temperatures

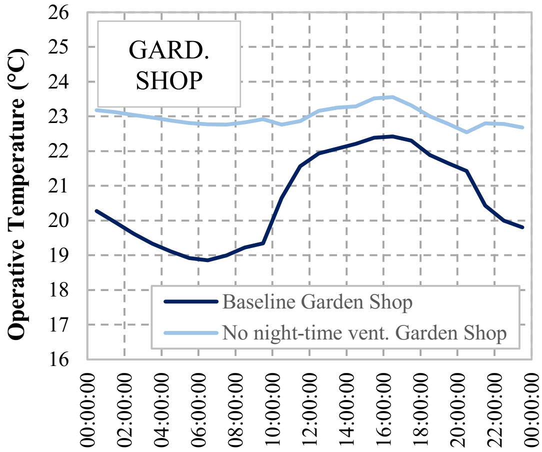

k) Garden shop with radiant floor off during a day with mild temperatures

Figure F.5 – Daily temperatures for the simulation with radiant floor off during a day with mild temperatures [3]

Figure F.6 illustrates the internal temperatures during a day with warm temperatures and with the radiant slab turned off.

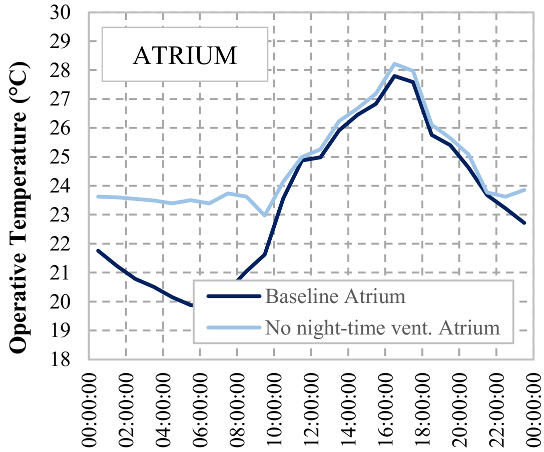

a) Atrium with radiant floor off during a day with warm temperatures

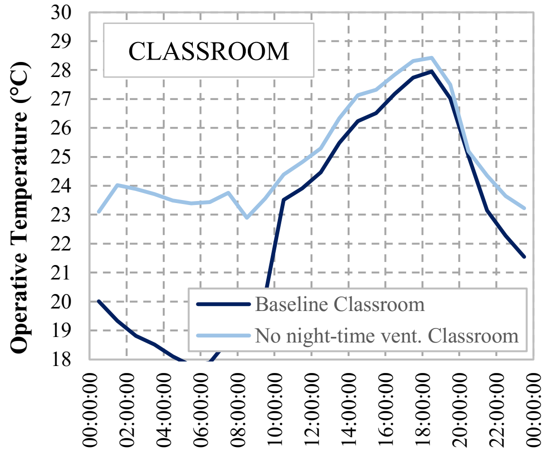

b) Classroom with radiant floor off during a day with warm temperatures

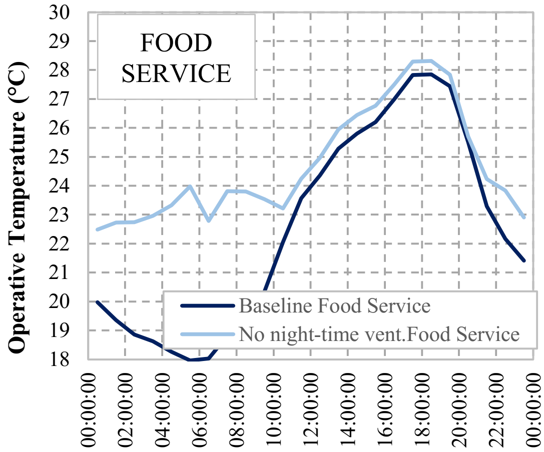

c) Food service with radiant floor off during a day with warm temperatures

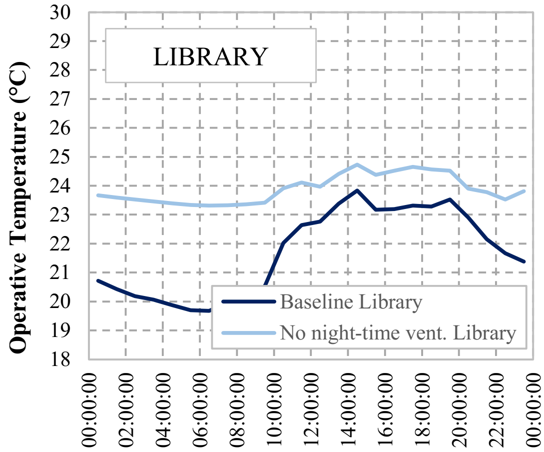

d) Library with radiant floor off during a day with warm temperatures

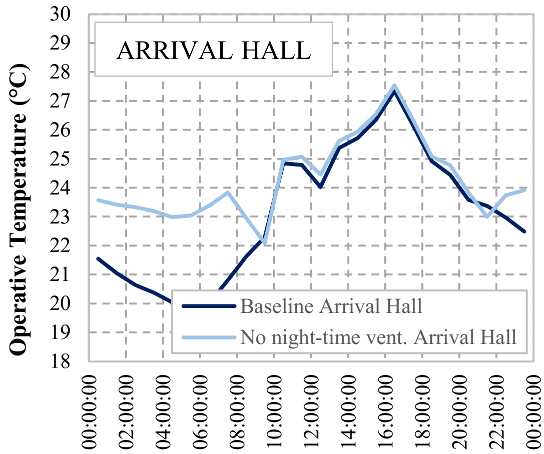

e) Arrival hall with radiant floor off during a day with warm temperatures

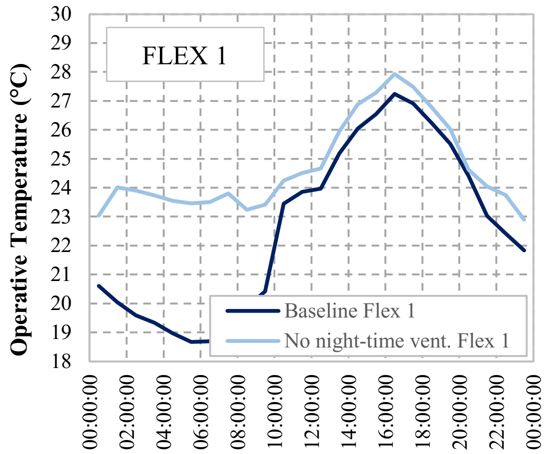

f) Flex 1 with radiant floor off during a day with warm temperatures

Figure F.6 – Daily temperatures for the simulation with radiant floor off during a day with warm temperatures [1]

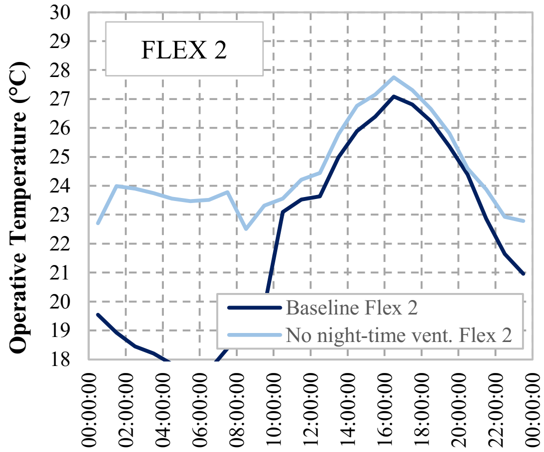

g) Flex 2 with radiant floor off during a day with warm temperatures

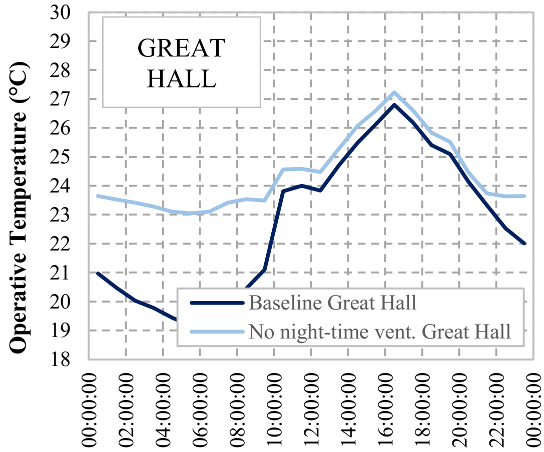

h) Great hall with radiant floor off during a day with warm temperatures

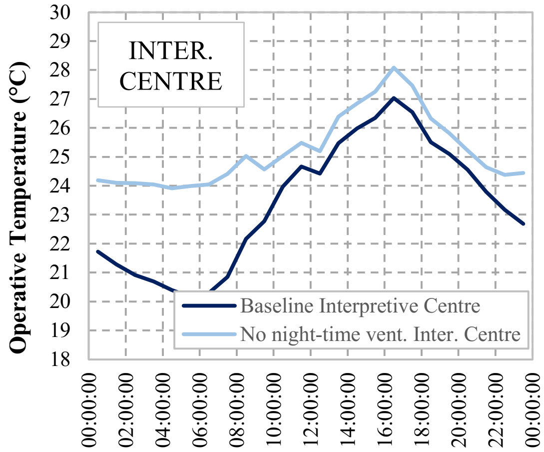

i) Interpretative centre with radiant floor off during a day with warm temperatures

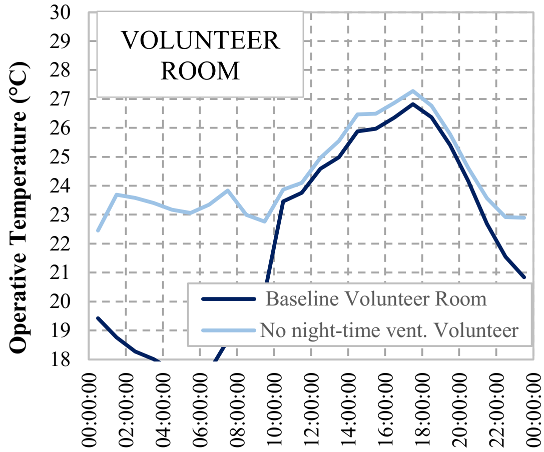

j) Volunteer room with radiant floor off during a day with warm temperatures

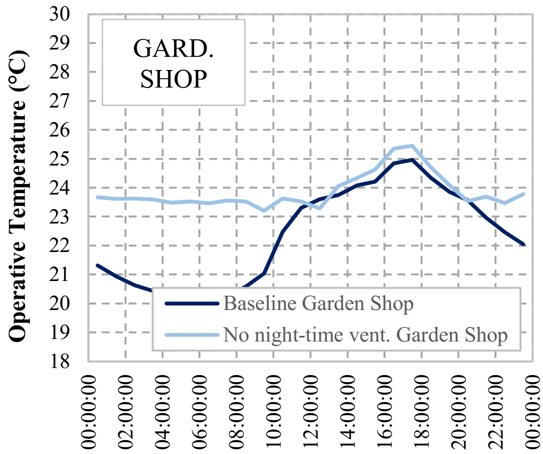

k) Garden shop with radiant floor off during a day with warm temperatures

Figure F.6 – Daily temperatures for the simulation with radiant floor off during a day with warm temperatures [2]